

# uCARE

You Can Always Reduce Emissions  
because you care

**GA 815002**

**Deliverable number:** D1.2  
**Deliverable title:** Augmented emission maps are an essential new tool to share and investigate detailed emission data

**Document ID:** uCARE-D1.2-v4.0  
**Dissemination level:** Public  
**Main Authors:** Jessica de Rooter, Armando Indrajuana, Mitch Elstgeest, René van Gijlswijk, Norbert Ligterink, Paul Tilanus (TNO)  
**Issue date:** October 2022  
**DOI** [10.5281/zenodo.3669985](https://doi.org/10.5281/zenodo.3669985)



## Disclaimer and acknowledgement



This project has received funding from the European Union's Horizon 2020 Programme Research and Innovation action under grant agreement No 815002

### Disclaimer

This document reflects the views of the author(s) and does not necessarily reflect the views or policy of the European Commission. Whilst efforts have been made to ensure the accuracy and completeness of this document, the uCARE consortium shall not be liable for any errors or omissions, however caused.

### uCARE consortium



## Document information

### Additional author(s) and contributing partners

Name	Organisation
Miriam Elser	Empa
Mats Gustafsson	VTI
Michal Vojtisek	CVUT
Thanasis Dimaratos	LAT
Stefan Hausberger (only sections 3.5.2 & 7.3)	TUG
Martin Opetnik (only sections 3.5.2 & 7.3)	TUG

### Document Change Log

Version	Date	Comments
V1.1	14-Jul-2020	First draft of version 2, based on D1.2-v1.0
V1.x	various	Revised versions based on the comments of Stefan, Uwe, Shaojun
V2.0	Oct-2020	Second final version, approved by Executive Board, (will be) submitted to EC.
V3.0	Aug-2021	Third final approved version; (will be) submitted to EC.
V4.0	Sept-2022	Addition of simplified cold start model and wear emission model

### Document Distribution Log

Version	Date	Distributed to
V2.0	2-11-2020	PO via e-mail, Zenodo
V3.0	19-8-2021	PO via e-mail, Zenodo

### Verification and approval

	Name	Date
Verification Final Draft by WP leader	Norbert Ligterink	19-8-2021
Check before upload by coordinator	Paul Tilanus	19-8-2021



## Executive summary

Vehicle emissions contribute substantially to worldwide pollutant emissions and poor local air quality. How people drive influences their car's pollutant emissions. However, the relationship between driving behaviour and emissions is also dependent on the vehicle. Detailed emission data is necessary to describe this relationship. The Horizon 2020 project uCARe has developed **a standard to publish and share detailed emission measurement data**. A range of different partners active in passenger car testing have already shared measurement data using this standard in the form of **augmented emission maps (AEMs)**. These AEMs contain emission data for either a specific vehicle (as defined by a few relevant parameters) or on a more general level. Using AEMs allows for data-driven analyses of the impact of behaviour on vehicle emissions, leading to scientific insights, tailored consumer advice and data-driven policy.

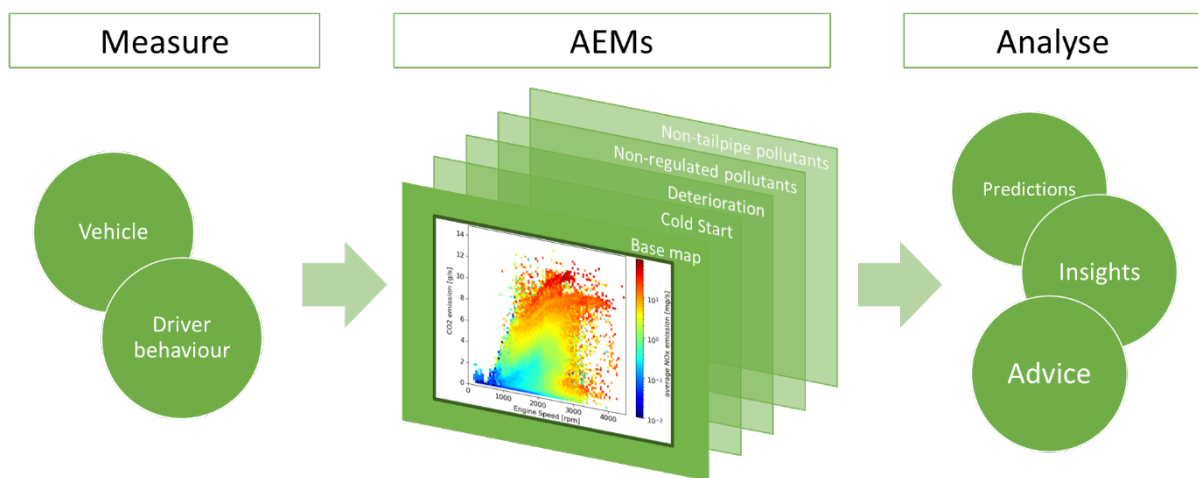


**Figure 0.1 – The vision of uCARe: sharing emission measurement data at a detailed level is important for scientific insight and individualised advice for consumers**

### AEMs are much more detailed than generalised emission factors

AEMs are a standardised way of presenting detailed measurement-based emission data.

- AEMs are **fact-based** – they contain only measurement data-backed values.
- AEMs can be **vehicle-specific** or generalised
- The accuracy and applicability of AEMs is ensured via the **significant amount of data** that is used to generate each map, which is noted in kilometres and hours of measurements in the metadata of each map.
- Data is **freely available** via the OpenAire platform Zenodo to which new data can and will continually be added as new measurements become available.
- Via AEMs and their surrounding framework, we facilitate **easy data sharing** of emission measurements.
- The **ready availability** of vehicle-specific and generalised AEMs, as well as the **supporting tools**, make this a solution that is ready for tool-builders and researchers to implement.
- AEMs are **flexible**: emission data can be shared in the form of maps dependent on any two variables, or in the form of a function. This allows for easy integration of new pollutants and relationships as they become available.

By openly sharing AEMs and their surrounding framework we intend to allow tool-builders, researchers, and policy makers to give data-driven advice, to engage and encourage drivers to modify their behaviour, and thereby reduce pollutant emissions

## Using the different layers within an AEM, emission analysis can be tailored to a specific individual vehicle and behaviour.

Using **only five vehicle parameters**, you can find (or generate) the relevant AEM(s) for a specific vehicle. They will either be vehicle-specific if the measurement data is available, or more generalised (e.g. per Euro class and fuel, or a related engine type). AEMs contain at least one base layer and/or augmentation layer (Figure 0.2). The base layer, or base map, contains tailpipe emissions under hot engine conditions for regulated and/or non-regulated pollutants. Current base maps are dependent on **either engine or vehicle speed**, and CO<sub>2</sub> emissions (where CO<sub>2</sub> is used as a proxy for power or engine load). The current augmentation layers allow for further specification of emissions, whether it is due to driving an older vehicle (deterioration) or driving with a cold engine (cold start). The AEM standard is flexible enough to allow for the addition of more layers, which ensures it is a future-proof way to support data-driven emission analysis.

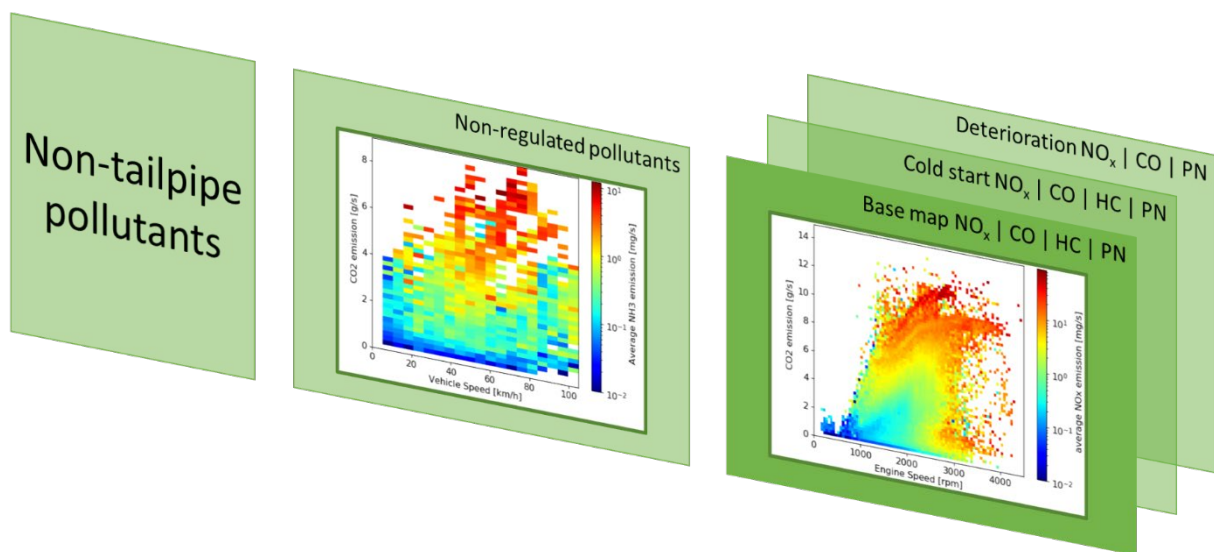


**Figure 0.2 – Graphical representation of the different layers that can be included within an augmented emission map (AEM). Note that this refers to the layers considered at this time: the AEM standard is flexible enough to allow for the addition of more layers in the future.**

In Part 1 of this document we introduce AEMs, how they can be used, and how they can be produced. In Part 2 we include reference information such as manuals for the provided tools, justification, and more in-depth discussion of the experiments performed within uCARE.

## Table of contents

<b>Executive summary .....</b>	<b>5</b>
<b>Table of contents .....</b>	<b>7</b>
<b>Part 1: Augmented emission maps are an essential new tool to share and investigate detailed emission data .....</b>	<b>10</b>
<b>1 Sharing detailed pollutant emission measurement data allows for data-driven analyses .....</b>	<b>10</b>
1.1 AEMs are a standard with which organisations can share detailed pollutant emission measurement data .....	10
1.2 Emissions are related to both the specific vehicle as well as driver behaviour...11	11
1.3 Analyses based on AEMs lead to scientific insight and tailored consumer advice ..	11
<b>2 What is an augmented emission map? .....</b>	<b>13</b>
2.1 AEMs are a standardised way of presenting measurement-based emission data ..	13
2.2 AEMs are fact-based .....	14
2.3 Each vehicle can be classified using the vehicle taxonomy– this will help you find or generate the right AEM.....14	14
2.4 Selecting or combining the right AEM.....20	20
2.5 AEMs are made up of base layers and augmentation layers .....	20
2.6 AEMs for non-tailpipe emissions are not yet available as they cannot yet be quantified explicitly across vehicles.....21	21
<b>3 I’m a tool-builder, how do I use AEMs? .....</b>	<b>23</b>
3.1 Interpreting base maps .....	23
3.2 Using base maps .....	23
3.3 Examples of base emission maps .....	23
3.4 Interpreting the cold start augmentation .....	26
3.5 Using the cold start augmentation .....	26
3.6 Examples of the cold start augmentation.....32	32
3.7 Interpreting the deterioration augmentation .....	36
3.8 Using the deterioration augmentation .....	36
3.9 Examples of the deterioration augmentation .....	39
<b>4 As a researcher or policy maker, how can AEMs give me insight into the relationship between driver behaviour and emissions? .....</b>	<b>40</b>
4.1 Low-CO <sub>2</sub> driving is not necessarily equivalent to low-NO <sub>x</sub> driving .....	40
4.2 Certain driving conditions have much lower relative emissions .....	40
4.3 Re-ordering trips can lead to lower emissions .....	41
<b>5 Contributing to uCARE emission data: the future of AEMs .....</b>	<b>43</b>
5.1 Determine the taxonomy code .....	43

5.2	Generate the AEM .....	45
5.3	Ensure consistent version control and name your files correctly .....	50
5.4	Upload the data to Zenodo .....	50
<b>6</b>	<b>Conclusions and recommendations .....</b>	<b>51</b>
<b>Part 2: Reference information.....</b>		<b>52</b>
<b>7</b>	<b>Cutting-edge non-tailpipe emission experiments form the foundation on which further AEM work can be built .....</b>	<b>52</b>
7.1	Non-tailpipe emissions – brake wear.....	52
7.2	Non-tailpipe emissions – tyre wear .....	56
<b>8</b>	<b>How ‘accurate’ are the base maps in AEMs? .....</b>	<b>79</b>
8.1	Sources of measurement data limitations .....	79
8.2	Quantity of measurement data limitations .....	80
8.3	Uncertainty from the chosen independent variables .....	82
8.4	Uncertainty from the data distribution.....	83
8.5	Uncertainty from vehicle dynamics .....	85
8.6	Uncertainty from vehicle specifications.....	88
8.7	Current conclusion on sources of uncertainty .....	88
<b>9</b>	<b>Generalising the cold start augmentation parameters does lead to increased uncertainty .....</b>	<b>89</b>
<b>10</b>	<b>Manuals for the available tools.....</b>	<b>95</b>
10.1	Selecting a base map.....	95
10.2	Combining a base map.....	98
10.3	Pseudocode cold start model.....	102
10.4	Generating a base map .....	106
<b>11</b>	<b>A formal explanation of the augmented emission map data exchange format .....</b>	<b>112</b>
11.1	Metadata.....	112
11.2	Emission base map data.....	114
11.3	Cold start .....	116
11.4	Deterioration .....	118
<b>12</b>	<b>Engine and vehicle deterioration leads to increased emissions .....</b>	<b>120</b>
12.1	Deterioration leads to increased emissions via several different mechanisms .	120
12.2	Deterioration influences cold start emissions.....	125
12.3	Comparison of data used to derive the applied tabulated deterioration factors	133
12.4	Investigation of the deterioration factors for NH <sub>3</sub> .....	137
12.5	Discussion on polynomial fits for vehicle mileage.....	138
12.6	Alternative approach for the implementation of the deterioration factors .....	143
<b>13</b>	<b>Background and project introduction .....</b>	<b>147</b>



13.1 Background uCARE ..... 147

13.2 Purpose of the document..... 148

13.3 Document Structure ..... 148

13.4 Deviations from original Description of Work (DoW)..... 148

**References ..... 150**

**Definitions & Abbreviations ..... 154**

# Part 1: Augmented emission maps are an essential new tool to share and investigate detailed emission data

## 1 Sharing detailed pollutant emission measurement data allows for data-driven analyses

### 1.1 AEMs are a standard with which organisations can share detailed pollutant emission measurement data

One of the observations made when writing the proposal for the uCARE project was that many organisations have measurement data on pollutant emissions available, and that sharing this data would be a significant step forward. Furthermore, it was noted that sharing this measurement data was done only at a limited scale. Data sharing was mainly hampered by the fact that the data format was usually the direct output of the measurement system(s) and specific tests executed, which make interpretation of someone else's data hard. Finally, if data was shared in e.g. scientific publications, it was mostly at an aggregate level.

The vision of uCARE is that data sharing of pollutant emission data *at a detailed level* is important

- for scientific purposes, e.g. enabling comparisons of vehicles;
- for building tools to provide car drivers (behavioural) advice on the use of *their* car, with the objective to reduce the pollutant emissions.

The Emission Maps are a concept, as well as the name and structure of the corresponding file format, to exchange the pollutant emission data at a more detailed level than just average test results in g/km. It is suitable for all regulated and non-regulated pollutant tail-pipe emissions. However, to cover also the brake and tyre wear emissions and the effects of e.g. cold start and deterioration, the concept was extended to Augmented Emission Maps (AEM).

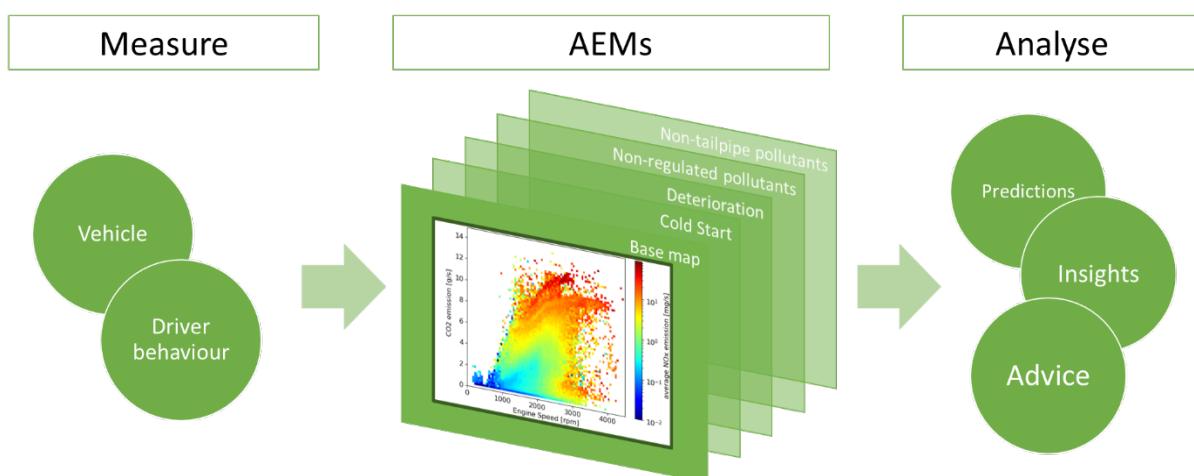


**Figure 1.1. The vision of uCARE is that the data sharing of emission measurement data *at a detailed level* is important for scientific insight and individualised advice for consumers**

## **1.2 Emissions are related to both the specific vehicle as well as driver behaviour**

The first step then is to understand how emissions are related to the use of the vehicle, caused by driver behaviour, which includes the use and maintenance of the vehicle *and* the on-road driving behaviour. The emissions of a vehicle are first and foremost linked to the characteristics of the vehicle: fuel type, emission standard, engine block, exhaust gas treatment technology, weight of the vehicle, and more. To characterise and categorise vehicles, a taxonomy has been developed (uCARE deliverable D1.1). Emission behaviour can be related to different levels in the taxonomy, e.g., euro class or engine block, and using the taxonomy, the empirical emission data can be attributed to groups of vehicles that share a taxonomy code (e.g., all vehicles fitted with a 1242 cc petrol engine of make X, or all Euro 6 petrol vehicles). Thereby it is assumed that all vehicles in the same taxonomy group have similar emission behaviour. Hence, it is important to wisely choose the level of the taxonomy that the uCARE insights in emissions are attached to. Emission data is in limited supply, but attributing the same emission behaviour to a group of technologies too diverse, can lead to large uncertainties. More about the link to the taxonomy can be found in Section 2.3.

Secondly, the emissions are linked to the state of the vehicle: deterioration of the vehicle over time leads to higher pollutant emissions, even with proper maintenance. Taking deterioration, and other effects like cold start into account, emissions of a specific vehicle might be significantly higher than can be calculated with the AEMs due to bad maintenance and/or tampering. This is discussed in Section 8.6.1.

Knowing the vehicle's characteristics and the state of the vehicle, a 'window' is left within which emissions can vary due to the way the vehicle is used. For each emission component the relation between emission level and use is different. For instance, nitrogen oxide levels are known to correlate well to the engine speed and the amount of power the engine must deliver. The emissions of tyre wear, on the other hand, are related to the weight of the vehicle, cornering speed, braking/acceleration, and external factors such as road surface types and weather conditions.

## **1.3 Analyses based on AEMs lead to scientific insight and tailored consumer advice**

With the AEMs for a large range of vehicles being available, one can study for instance:

- the difference in pollutant emissions of the same trip with different speed profiles;
- the difference in pollutant emissions of the same trip with different vehicles;
- the difference in pollutant emissions of the same shopping trip run clockwise and counterclockwise;
- etc.

In addition to this type of scientific results, a tool builder can

- build a generic tool,
- ask the driver for some inputs:
  - fuel type,
  - engine displacement,
  - engine power,
  - care make and model,
  - odometer reading,
- select the appropriate AEMs from the various points in the taxonomy and download these as input files to the tool.
- From that point onward, give advice on driver behaviour:
  - read the sensors of the vehicle to construct the trip in the AEM and report the emissions of the trip;
  - calculate the difference in pollutant emissions in case of different driver behaviour, e.g. driving the same trip with different speed profiles;
  - give a recommendation to the driver regarding optimal driver behaviour, e.g. the optimal speed profile of the trip and the gain in reduced pollutant emissions.

Note that this type of tool currently only exists and produces recommendations at a generic level. Drivers might easily consider the recommendations as 'not applicable to me/my car'. A tool that is individualised for their own specific car does not yet exist. uCARE WP2 will produce a prototype tool to show the potential of these individualised tools.

To enable the envisioned use as outlined above, the uCARE project has produced/is producing:

- A taxonomy in D1.1 (available).
- A tool to derive the manufacturer alliance, needed to find the car's taxonomy fully detailed identification (available).
- A range of AEMs uploaded to the open research data platform Zenodo (some AEMs available, growth of the collection will continue in the future).
- A tool that, based on the car's taxonomy leaf identification, lists all relevant AEMs, including all AEMs at higher levels in the taxonomy and their contents (available).

## 2 What is an augmented emission map?

### 2.1 AEMs are a standardised way of presenting measurement-based emission data

Based on measurement data of the key parameters, a map of the emission levels can be made. For nitrogen oxides (NO<sub>x</sub>), for example, the map can depict engine speed on the x-axis, CO<sub>2</sub> emissions on the y-axis, and the NO<sub>x</sub> emissions in mg/s as a colour. Figure 2.1 shows an example of such a map for a random vehicle/group of vehicles. Note that CO<sub>2</sub> emission is used here as a proxy for power or engine load<sup>1</sup>.

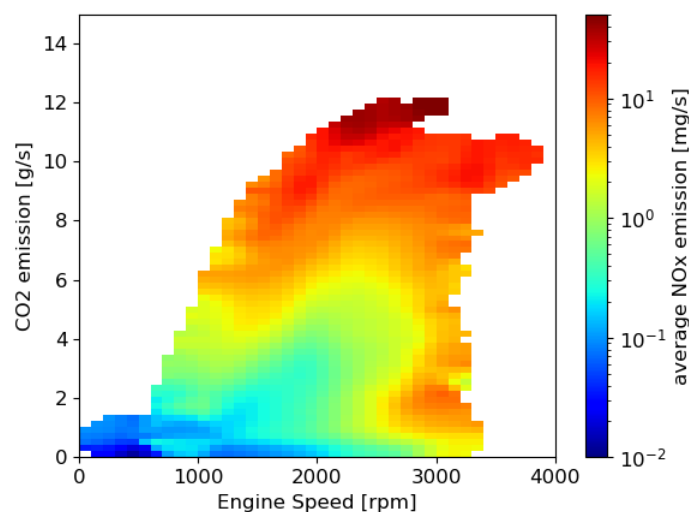


**Figure 2.1. Example emission map for average NO<sub>x</sub> emission from a Euro 6 diesel engine**

During driving, the engine speed and CO<sub>2</sub> output vary almost continuously. This means that the vehicle 'runs' across the map. Instantaneous emissions can thus be predicted on a second-by-second basis. High NO<sub>x</sub> emissions are often associated with high power demand and CO<sub>2</sub> emissions; Figure 2.1 shows a tenfold increase in average instantaneous NO<sub>x</sub> emissions coupled with a threefold increase in CO<sub>2</sub> emission rate (from 3 to 9 g/s of CO<sub>2</sub>).

The map shows that for this vehicle category, if a driver presses the accelerator pedal at mid to high engine speed, the emissions are high (top of the graph). Also driving with high engine speed and relatively low power, the emissions are high (right hand side of the graph).

To be able to create such a map, measurement data is needed for the entire spectrum of engine use, from at least one vehicle representative for the taxonomy code. Furthermore, interpolation algorithms are needed to fill the map if gaps occur. Also it may be necessary to reduce the map resolution if a limited amount of data is available. Boundary conditions should be set to warrant a minimum quality and usefulness of the emission maps produced. This is discussed in Chapter 5. Note that, maps can be generated not only for NO<sub>x</sub>. Chapter 5 contains a discussion of all envisaged emission map layers.

---

<sup>1</sup> The CO<sub>2</sub> flow in g/s is proportional to the fuel flow, i.e. energy delivered per time, i.e. the power content of the fuel.

## 2.2 AEMs are fact-based

Emission maps should be fact-based. It was agreed in the uCARE project to fill the distributable emission map files with data-backed values only. If gaps do occur in the emission map, the end-user has the freedom to choose a suitable interpolation method to fill in the gaps before further analysis or usage of the map.

For some map layers, it may be chosen to implement the emission maps as a continuous function instead. Parameter values to insert into the function can then be distributed per vehicle (class) in the same way maps are distributed. The function is then implemented on the tool side.

The descriptions below refer to the distributable, fact-based maps and functions. We note that, in this report, we focus primarily on the proposed structure of the AEMs.

## 2.3 Each vehicle can be classified using the vehicle taxonomy– this will help you find or generate the right AEM

The vehicle taxonomy is a controlled vocabulary and vehicle classification system for all passenger cars on the road. As described in D1.1 it has 11 levels; two parts can be distinguished: the vehicle part and the engine part. The engine is a child of the vehicle. The vehicle code contains the make and model, the transmission type, all-wheel drive capability and the battery capacity. An example of the first three levels is shown in Figure 2.2.

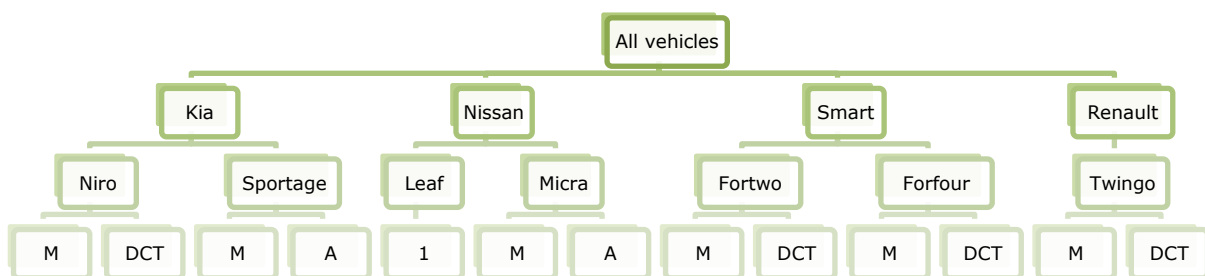


**Figure 2.2. Example of vehicle part of taxonomy: first three layers. Gearbox layer: M=manual, A=automatic, DCT=dual clutch transmission, 1=single speed**

Tyre and road wear characteristics, at least, can be linked to the vehicle code, because the vehicle code is related to the weight (and driver behaviour). Most emission characteristics are related to the drivetrain though. Each vehicle model/gearbox combination in the example can be fitted with one or more engine types (or traction motor types for electric vehicles). However, engines can be used across multiple manufacturers. In fact, of the seven vehicle models in Figure 2.2, the four rightmost ones can be fitted with the same “M281” engine, and should have similar NO<sub>x</sub> emissions at equal power demand and engine speed<sup>2</sup>.

Engines are characterised by the other six variables in the taxonomy:

<sup>2</sup> Provided the engine calibration and ECU parametrization is identical, for a given engine used in different vehicle models and furthermore that vehicles had timely maintenance and have similar mileage.

- Powertrain type (e.g. ICE, electric)
- Fuel type (e.g. petrol, electricity)
- Emission standard (e.g. Euro 6)
- Engine displacement (e.g. 1598 cm<sup>3</sup>)
- Engine power (e.g. 66 kW)
- Manufacturer alliance

The list of manufacturer alliances is provided in D1.1. It is intended to avoid having double entries of the same engine. The engine specifications (the combination of the first five variables) typify the alliance code in 95% of the cases; a lookup table will be provided. For the other 5%, the vehicle manufacturer provides a definitive answer; this list will also be provided.

Figure 2.3 shows an example of the hierarchy of engine specifications. The 1-liter versions of the four rightmost vehicles in Figure 2.2 share the same alliance code: RNM3 - Renault-Nissan-Dacia-Smart.

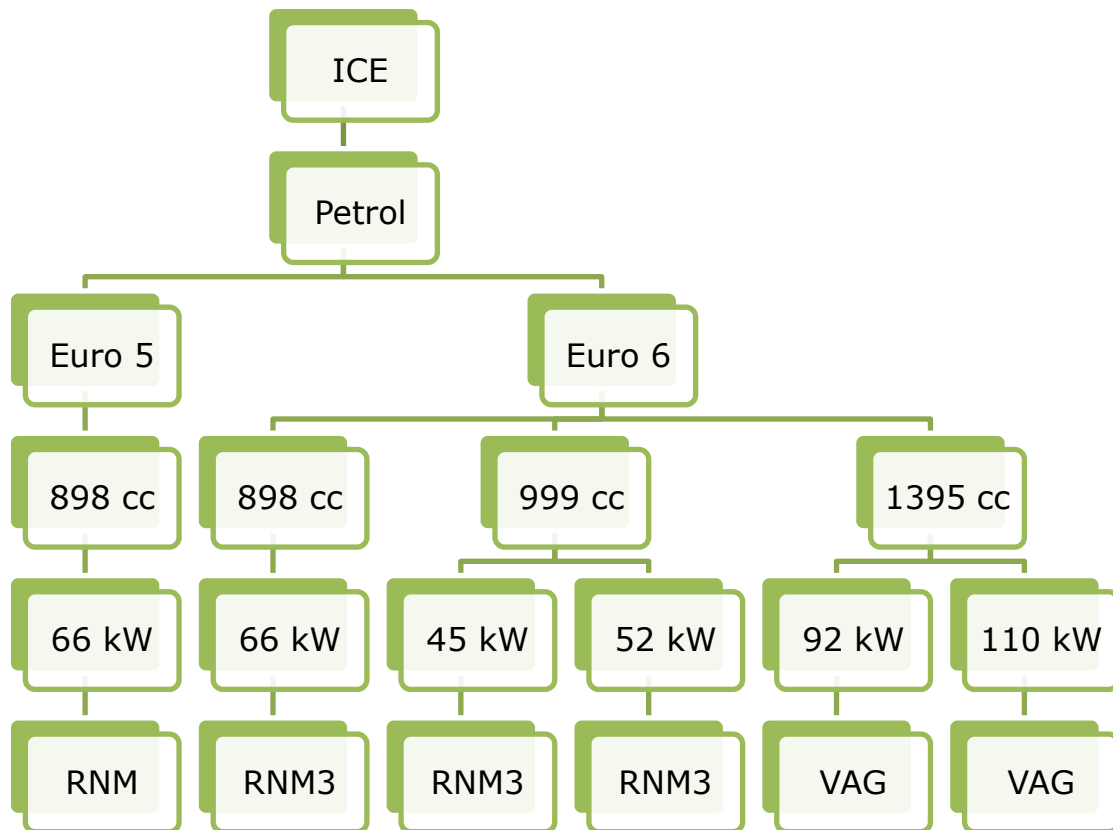


**Figure 2.3. Example of engine part of taxonomy**

### 2.3.1 Naming conventions used for AEMs

A data file structure was proposed to simplify the exchange of emission map data, see Chapter 9. At the moment, all map layers, except wear emissions, are related to the internal combustion engine of a vehicle (see Section 2.6). Therefore, the naming scheme of the emission map files will be related to the engine part of the taxonomy. Hereafter an abbreviation is proposed for practical reasons. Wear emissions are related to vehicle properties rather than engine properties. Wear emission maps will be distributed with their own naming scheme.

## 0. Powertrain types: not included in the name

The emission maps always refer to the internal combustion engine part of a vehicle, even if there is an electric drivetrain as well. The powertrain type as a variable is not needed to characterise the ICE, and in fact would create redundant data. Therefore, it is left out of the file name.

## 1. Fuel types

The following translation is made, see Table 2.1.

**Table 2.1. Fuel Type codes**

<b>Fuel type as D1.1</b>	<b>Fuel type abbreviation</b>
<b>Diesel</b>	D
<b>Petrol</b>	P
<b>Electricity</b>	E
<b>Ethanol (E85)</b>	A
<b>CNG</b>	C
<b>LPG</b>	LP
<b>Hydrogen</b>	H
<b>Biodiesel</b>	BD
<b>LNG</b>	LN
<b>LPG/Petrol</b>	LP--P
<b>CNG/Petrol</b>	C--P
<b>Ethanol/Petrol</b>	A--P
<b>Biodiesel/Diesel</b>	BD--D
<b>Electricity/Hydrogen</b>	E--H
<b>Electricity/Petrol</b>	E--P
<b>Electricity/Diesel</b>	D--E

We allow for bi-fuels/flexi-fuels by concatenating fuel types in alphabetical order, joining with a double hyphen (--).

## 2. Emission standards

The translation can be found in Table 2.2. A further breakdown of Euro 6 was done, especially for diesel vehicles, because real-world emissions have changed significantly in Euro 6d-Temp and Euro 6d. A similar breakdown can be implemented for Euro 5 (i.e. Euro 5a and 5b), but little evidence for the need for this with regards to emissions has been observed. Furthermore, the build year can also be included: `_6b-2015_`. This can be useful especially in the case of Euro 6b and 6c, to distinguish pre- and post-diesel gate engines,

where differences are observed in the same emission class. Lastly, although we do recommend using the further breakdown of Euro 6, we acknowledge that this is not always feasible. For this reason, 6 remains a valid emission standard abbreviation.

**Table 2.2. Emission standards coding**

<b>Emission standard as D1.1</b>	<b>Emission standard abbreviation</b>
<b>Euro 0</b>	0
<b>Euro 1</b>	1
<b>Euro 2</b>	2
<b>Euro 3</b>	3
<b>Euro 4</b>	4
<b>Euro 5</b>	5
<b>Euro 6a</b>	6a
<b>Euro 6b</b>	6b
<b>Euro 6c</b>	6c
<b>Euro 6d-Temp</b>	6dT
<b>Euro 6d</b>	6d

### 3. Engine displacement

The displacement is included without unit, in cubic centimetres.

### 4. Rated power

The rated power is included without unit, in kW.

### 5. Manufacturer alliance

The manufacturer alliance codes and the names of associated manufacturers are listed in Table 5.1.

The parts of the name are connected by underscores.

Example:

The engine block on the left-hand side of Figure 2.3 will have the following filename:

P\_5\_898\_66\_RNM

### 2.3.2 Naming conventions for AEMs that contain data of more than one vehicle type

For each vehicle type the procedure described in Section 2.3.1 results in a unique name. Emission data specific for that vehicle type will be provided in the AEM with that name. However, some data is not unique for a single vehicle type and it would be redundant to repeat that data in multiple AEMs.

The second main reasons to have an AEM at a higher level in the taxonomy is when there is not sufficient data available to produce an AEM with an acceptable level of detail, i.e. a reasonable number of bins (see Section 8.2).

For example, if the emission map of all Petrol Euro 6 vehicles with an engine displacement of 898 cc and 999 cc, as shown in Figure 2.3, have the same emission map for some pollutant emission, that emission can be recorded in P\_6\_898-999\_ALL\_RNM3.map.txt.

The following methods of placing an AEM at higher levels in the taxonomy are applicable within the AEM exchange format. Note that the examples given below are generically indicative, and not intended to be taken as actual examples of maps that can be combined.

- **Fuel Type**  
Multiple fuel types can be combined. The combined fuels are connected in the AEM name by a hyphen. An AEM that is independent of the fuel used, e.g. an AEM for wear emissions of brakes, can use ALL in the name.  
Example: A combined AEM for Diesel, Biodiesel and a bi-fuel Biodiesel/Diesel could have a name starting with "D-BD-BD--D\_".
- **Emission standard**  
Multiple emission standards can be combined. The combined emission standards are connected in the AEM name by a hyphen. An AEM that is independent of the emission standard, e.g. an AEM for wear emissions of tyres, can use ALL in the name.  
Example: A combined AEM for Euro 6 variants could have a name where the emission standard reads "\_6a-6b-6c-6dT-6d\_".
- **Engine displacement**  
Multiple engine displacements can be combined in a range. The combined engine displacements are connected in the AEM name by a hyphen and includes all displacements in the range, including the values in the name. An AEM that is independent of the engine displacement, can use ALL in the name.  
Example: P\_6\_898-999\_ALL\_RNM3.map.txt includes all engine displacements from 898 cc (inclusive) up to and including 999 cc.
- **Rated power**  
Multiple rated powers can be combined in a range. The combined rated powers are connected in the AEM name by a hyphen and includes all rated powers, including the values in the name. An AEM that is independent of the rated power, can use ALL in the name.  
Example: P\_6\_898-999\_ALL\_RNM3.map.txt in Figure 2.3 would be equivalent to P\_6\_898-999\_40-70\_RNM3.map.txt.
- **Manufacturer alliance**  
Multiple manufacturer alliances can be combined. The combined manufacturer alliances are connected in the AEM name by a hyphen. An AEM that is independent of the manufacturer alliance can use ALL in the name.

### 2.3.3 Almost every vehicle in the Netherlands vehicle fleet can be described by the vehicle taxonomy

In the Netherlands, as of 22 January 2020, around 9.7 million passenger vehicles are registered in the Dutch vehicles database. Analysing the composition of the passenger vehicle fleets, Volkswagen is the most common brand (11.4% share of the total fleet), with Volkswagen Golf and Polo as the most common models.

Based on the Open Data from the vehicles database of the Dutch type approval authority RDW (opendata.rdw.nl), the uCARE engine family code can be derived and assigned to (almost) every registered vehicle. For 6.5% of the vehicles one or more parameters are missing. Generating the engine code for these vehicles would require some additional work.

For the vehicles with complete information, uCARE engine codes are assigned and analysed. The most popular uCARE engine code in the Netherlands belongs to petrol vehicles with a 998 cc engine with a rated power of 50 kW from the Toyota-Citroën-Peugeot alliance. This uCARE engine code is associated with small passenger vehicles such as the Toyota Aygo. This engine code has two variants based on the emission standards coding, 1.9% has Euro 4 emission standards while 1.4% has Euro 5 emission standards.

Figure 2.4 shows the top 10 uCARE engine families registered in the Netherlands, which together are fitted in 8.3% of the passenger car fleet in the Netherlands.

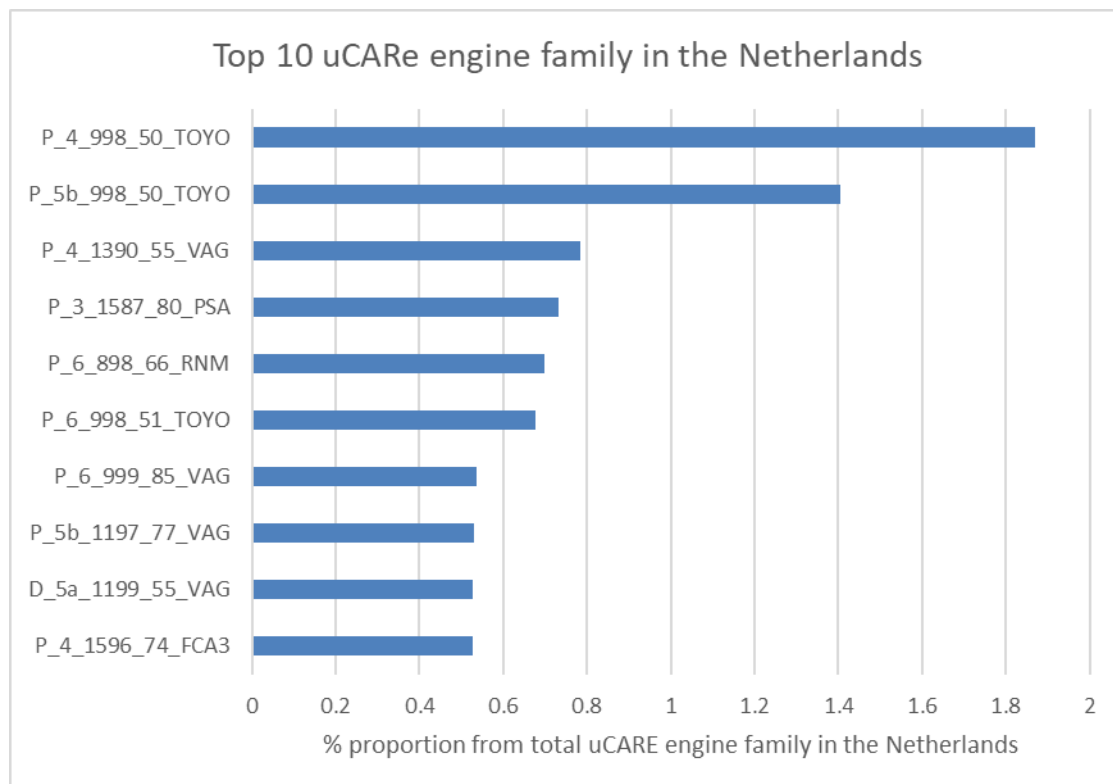


**Figure 2.4. Top 10 uCARE engine families for passenger vehicles registered in the Netherlands, together they cover 9% of the total fleet.**

## 2.4 Selecting or combining the right AEM

Over the last few years, AEMs have been created for many engines. **AEMs are freely available on the OpenAire platform Zenodo.**<sup>3</sup> However, given the vast number of engine types in use (including updates with newer Euro standard compliance), it has not been possible to create a vehicle-specific emission map for every single one of them. Fortunately, dependent on the map layer, there are similarities among certain maps that can be used to make extrapolations to other engines deemed similar in behaviour. Three tools were developed to help tool-builders: fallback maps, a selection tool, and a combining tool.

### *Fallback AEMs*

Though the uCARE consortium attempts to create as many AEMs as possible, starting with the most common vehicles currently on the road, it can't be excluded that by the end of the uCARE project not all vehicles are covered for all pollutant emissions by AEMs.

For that reason, *F\_E\_ALL\_ALL\_ALL.map.txt* (where F and E stand for the specific fuel type and euro class parameters, such as D and E6b respectively) AEMs will be available for all Fuel/Euro-class combinations, covering all regulated pollutant emissions. These fallback maps are generated by aggregating available data at the fuel and euro class level.

### *Selection tools*

The fallback maps ignore the possible differences in emissions caused by engine displacement, power, and make. Therefore, recently a more sophisticated tool (see also Section 10.1) was developed that, for any given untested car/engine, selects the best suitable one among the available maps. The selection tool can help to find a more representative NO<sub>x</sub> map than a generic fallback map. Further criteria to select the best map may be the amount of data (the second-best suitable map may have more detail), and engine manufacturer as opposed to alliance code; various collaborations of one manufacturer have different alliance codes, but may utilize the same exhaust gas treatment equipment.<sup>4</sup>

### *Combining tool*

A tool has also been developed to allow for the interpolation and combination of existing AEMs (see also Section 10.2). In this way, we facilitate the comparison and contrast of different AEMs, as well as allowing for the user to combine different AEMs. By combining different AEMs, emission data can be aggregated further to the specific application of the tool-builder or researcher.<sup>4</sup>

## 2.5 AEMs are made up of base layers and augmentation layers

Isolated effects of different conditions and emission sources are expressed in separate layers, together forming augmented emission maps: all layers characterize parts of the emission behaviour of the vehicle.

The tailpipe emissions under hot engine conditions are referred to as the **base layer** for the emission maps. Tailpipe emissions are used as the base layer for two main reasons. Firstly, and most importantly, tailpipe emissions are the emissions with the most impact on the environment. Secondly, with regards to the data-based nature of the emission maps, most tests and monitoring programs collect tailpipe emission data. Current base layers would describe NO<sub>x</sub> (primary focus), PN, CO, and HC emissions. Other base layers can include tailpipe emissions of non-regulated emissions: NO<sub>2</sub>, N<sub>2</sub>O, PAH, CH<sub>4</sub>, cyanides, and NH<sub>3</sub>.

---

<sup>3</sup> <https://zenodo.org/communities/ucare/>

<sup>4</sup> See also <https://github.com/Project-uCARE/>

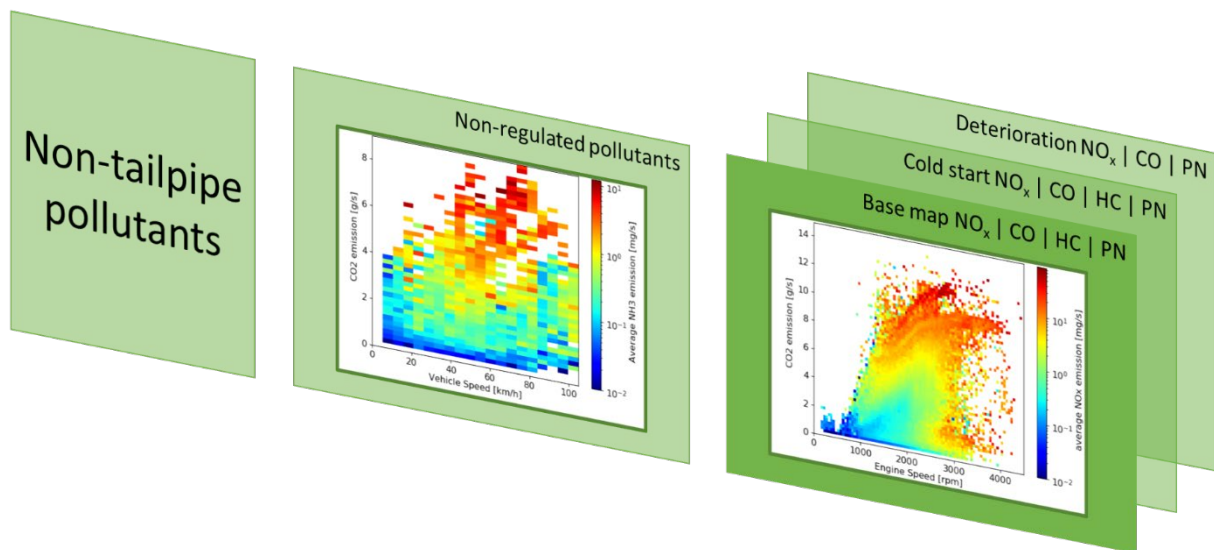


**Figure 2.5. Graphical representation of the different layers that can be included within an augmented emission map (AEM). Note that this refers to the layers considered at this time: the AEM standard is flexible enough to allow for the addition of more layers in the future.**

On top of the base layers, the following **augmentation layers** are currently available:

- Tailpipe emissions under cold start conditions: NO<sub>x</sub> (primary focus), PN, CO, HC
- Deterioration: additional tailpipe emissions as a result of ageing and/or poor maintenance: NO<sub>x</sub>, PN, CO, HC, NO<sub>2</sub>, N<sub>2</sub>O, PAH, CH<sub>4</sub>, cyanides, NH<sub>3</sub>

Augmentation layers are used to augment the data provided by the base layers. The initial proposals above address a range of conditions that are influenceable by the user which can affect vehicle emissions.

Each map layer can have a different x- and y-axis, a different resolution, and a different level in the taxonomy to be attached to. The layers are discussed separately in later chapters (e.g. Sections 3.1, 3.4 and 3.7).

## **2.6 AEMs for non-tailpipe emissions are not yet available as they cannot yet be quantified explicitly across vehicles**

As opposed to the detailed and standardised engine emission tests, the experimental data that is available for non-tailpipe emissions either describes very specific cases or does not result in conclusive relationships between uCARE-relevant parameters and non-tailpipe emissions. For this reason, we offer several general recommendations for emission reduction in this section, based on our findings. Cutting-edge non-tailpipe emission experiments have been performed, and the results of these (along with an overview of the current state of knowledge) are discussed in Chapter 7. These experiments highlight where more measurements are needed before the relationships between driver behaviour and non-tailpipe emissions can be quantified in the form of AEMs.

### **2.6.1 General recommendations for tyre wear reduction**

Based on what has been studied in uCARE and literature, at the current state of knowledge, only general advice to car owners about how to minimise tyre wear can be used. Three categories are suggested: choice, maintenance and driving behaviour. When it comes to the choice of tyres, there is not enough information available for recommendations concerning tyre wear. However, in regions where studded tyres are available, these will produce high road wear (contributing to PM10) and so recommendations do address this.

### Choice

- studded tyres - when choosing winter tyres, consider non-studded tyres to reduce emissions of road wear particle (e.g. references [1, 2])
- right tyres for right season – do not use winter tyres in summer or vice versa, this will increase the wear and is also a traffic safety risk (e.g.[3, 4])

### Maintenance

- wheel alignment – if your tyres wear unevenly, despite correct inflation pressure, check wheel alignment

### Pre-trip

- inflation pressure – check correct pressure regularly
- reduce unnecessary load

### During trip (behaviour)

- adaptive soft driving (slow acceleration and deceleration)
- use engine braking when possible
- keep speed limits (higher speeds will increase emissions)

## 2.6.2 General recommendations for brake wear reduction

All recommendations promoting gentle driving (i.e. free of abrupt movements, harsh accelerations, stops and cornering) are believed, in general, not only to lead to lower fuel consumption, higher safety, higher passenger comfort, and less tyre wear, but also to lower brake emissions.

Likewise, the general rules for lowering the fuel consumption are also believed to apply to reducing brake wear emissions:

- avoiding high speeds,
- limiting unnecessary stops by looking ahead and anticipating

These general rules are similar to the recommendations (well known by heavy vehicle operators) to prevent overheating of friction brakes (which results in a grave safety hazard):

- anticipating and looking ahead,
- avoiding excessive speeds,
- using the air drag and/or engine braking to slow down the vehicle.
- Note that the rule to use engine compression brakes and/or retarders is not relevant for most passenger cars.

When operating vehicles with electric drive train, whether dedicated or hybrid, mild braking at braking powers within the rating of the electric drive promotes the use of generally emissions-free electrodynamic braking. Electrodynamic braking also has the possibility to salvage portion of the kinetic energy as electric power in the vehicle battery.

## 3 I'm a tool-builder, how do I use AEMs?

### 3.1 Interpreting base maps

Base maps can be used to predict driver emissions. On a second-by-second basis, relevant driving parameters (e.g. engine load, vehicle speed, and/or RPM) can be used to look up the expected instantaneous emissions for a specific vehicle (see Figure 3.1). The instantaneous emissions can be used to approximate driver emissions over the duration of a trip. Different driving parameters lead to different emissions. In this way, advice can be given as to the driving parameters which can lead to lower emissions.

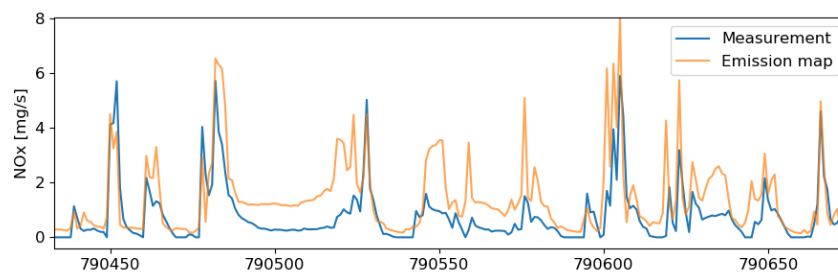


**Figure 3.1. Comparison of NO<sub>x</sub> emissions from measurement data and as calculated from an emission base map using vehicle speed and CO<sub>2</sub> emission**

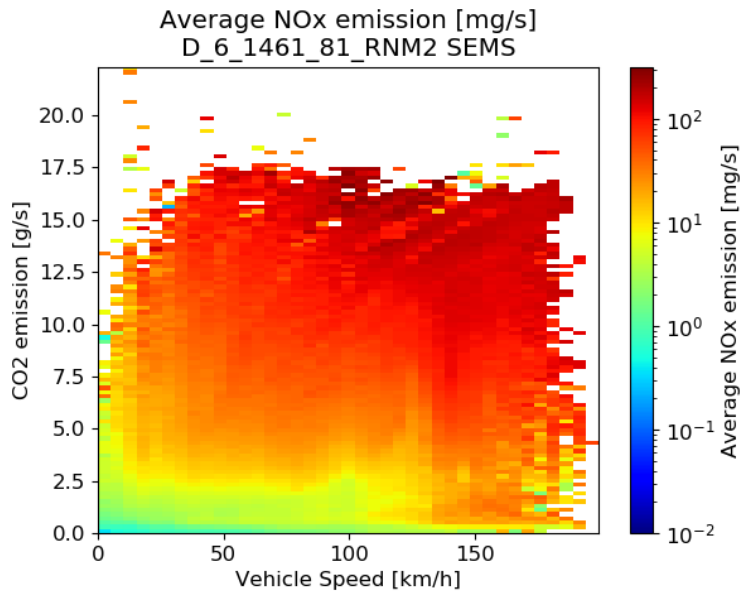
Note that in some cases, the average measured emissions may differ from the prediction due to unknown causes or causes that have not been included, such as maintenance. However, most relevant with regards to decreasing emissions is behaviour that leads to high emissions, i.e. the peaks in Figure 3.1, and these emission peaks are captured well by the emission maps.

### 3.2 Using base maps

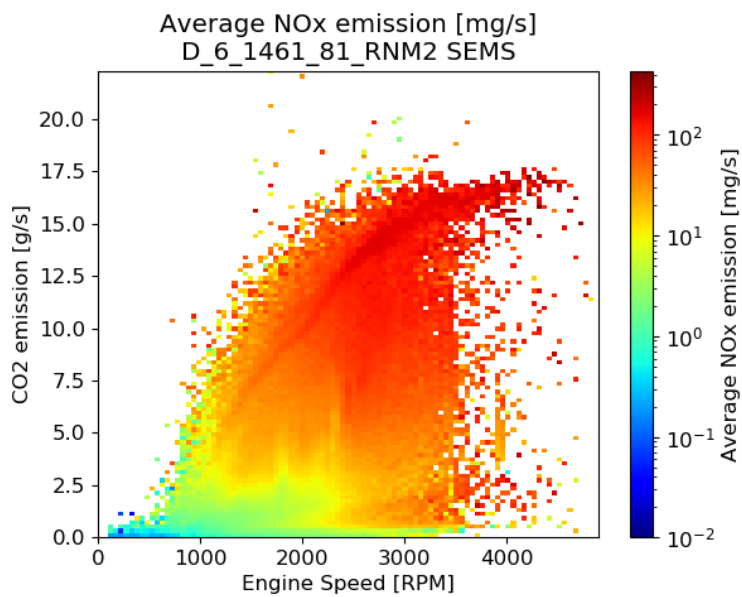
In a base map, emissions are described in a table-like format, where two input values (currently one for CO<sub>2</sub> emissions, and one for vehicle or engine speed) are used to determine a third value (the emissions per second). In this way, emissions can be calculated on a per second basis. This leads to an emissions profile that is specific to a specific trip. Note that this profile does contain a measure of uncertainty due to the nature of real-world driving, which we'll discuss in later sections (e.g. Chapter 8).

### 3.3 Examples of base emission maps

Monitoring the emissions of vehicles gives a good coverage of the whole operation spectrum of an engine. Figure 3.2 shows a graph of a NO<sub>x</sub> emission map which is based on more than 600 hours of on-road measurement data of a Euro 6 diesel car. The average NO<sub>x</sub> emission is shown per bin of vehicle speed and CO<sub>2</sub> emission. Figure 3.3 is based on the same data but shows the average NO<sub>x</sub> emissions per engine speed and CO<sub>2</sub> emission bin.

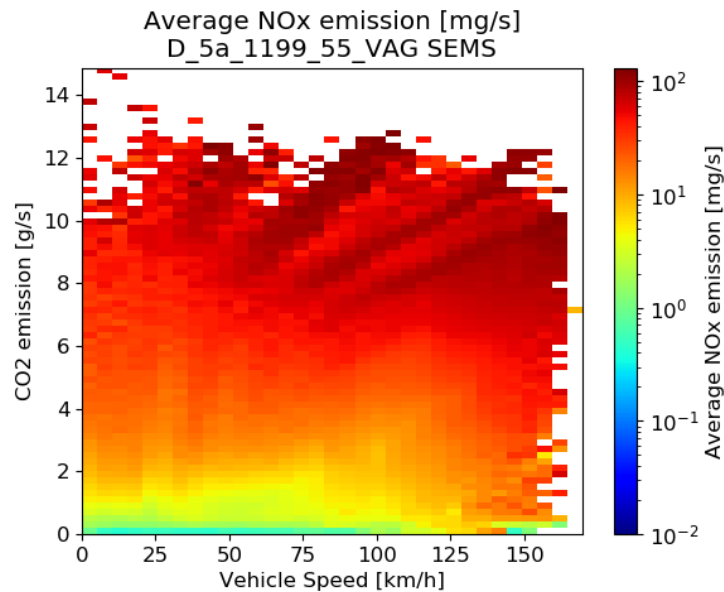


**Figure 3.2. Emission map graph of a 1461cc, 81kW Euro 6 Diesel engine with average NO<sub>x</sub> emission [mg/s] per vehicle speed [km/h] and CO<sub>2</sub> [g/s] bin.**



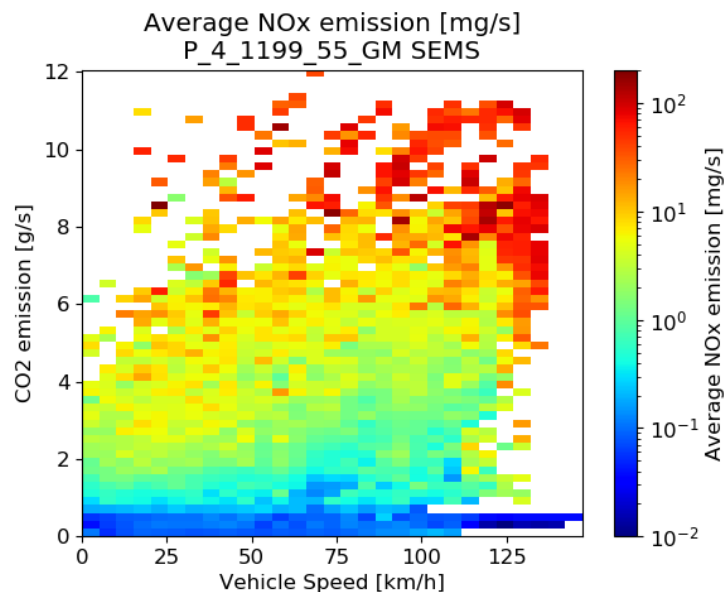
**Figure 3.3 Emission map graph of a 1461cc, 81kW Euro 6 Diesel engine with average NO<sub>x</sub> emission [mg/s] per engine speed [rpm] and CO<sub>2</sub> [g/s] bin.**

Figure 3.4 shows a NO<sub>x</sub> emission graph of a Euro 5a diesel engine with almost 330 hours of monitoring data. In the CO<sub>2</sub> emission range higher than 7 grams per second the effect of shifting gears is visible by the dark red lines.



**Figure 3.4. Emission map graph of a 1199cc, 55kW Euro 5a diesel engine with average NO<sub>x</sub> emission [mg/s] per vehicle speed [km/h] and CO<sub>2</sub> [g/s] bin.**

Figure 3.5 shows the emission plot for a Euro 4 petrol engine. In comparison with Figure 3.4 this engine emits less NO<sub>x</sub> over the whole spectrum. However, the amount of underlying data for Figure 3.5 is much less than Figure 3.4.



**Figure 3.5 Emission map graph of a 1199cc, 55kW Euro 4 petrol engine with average NO<sub>x</sub> emissions[mg/s] per vehicle speed [km/h] and CO<sub>2</sub>[g/s] bin.**

### 3.4 Interpreting the cold start augmentation

Cold start extra emissions (CSEE) occur at engine start mostly due to the inefficient functioning of the cold after-treatment system. Here we present a method to estimate the CSEE of NO<sub>x</sub>, CO, HC and PN for any given trip (i.e. engine speed, engine velocity and road gradient). The resulting CSEE are additional to the hot emissions and form a continuous function in time over the cold start period.

As for the hot emissions, the engine speed, velocity, and load have a significant influence on the CSEE. However, in this case we also have to consider the temperature of the after-treatment system, which depends in turn on the ambient temperature and the accumulated heating energy produced in the combustion process since the engine start. Because of these dependencies, the CSEE cannot be easily presented in a map format, so either a continuous function over time (the detailed model in Section 3.5.1) or characteristic polygons (the simplified model in Section 3.5.2) can be used to estimate the second-by-second CSEE.

The CSEE for any given trip can be estimated using the functions described in Section 3.5. The model parameters (represented in blue in the equations) are characteristic of the specific engine block code and are reported in the corresponding cold start augmentations. In Section 5.2.3 a method to estimate the model parameters from emission measurements is described. The pseudocodes to estimate the CSEE and to determine the model parameters are reported in Section 10.3. Chapter 9 discusses the validity and uncertainties connected to generalising the model parameters, as well as the simplified model.

### 3.5 Using the cold start augmentation

The model to estimate the CSEE reported in Section 3.5.1 is based on the detailed physical description of the warm-up process presented in [5], which was simplified and adapted to make it applicable to a larger number of vehicles. However this detailed model requires specific vehicle emission tests which are not always available, and so a simplified model has been developed and is reported in Section 3.5.2.

#### 3.5.1 Description of the detailed model

The cold start model requires the following input data: vehicle mass ( $m$ ), vehicle drag coefficients ( $f_0, f_1, f_2$ ), stop/parking time ( $t_{stop}$ ), ambient temperature ( $T_{amb}$ ), and the driving parameters including velocity ( $v(t)$ ), engine speed ( $n(t)$ ) and road gradient ( $\alpha(t)$ ).

The model is based on a set of seven parameters ( $w_p, w_n, w_0, Q_{in0}, n_0, q_1, q_2$ ) to describe the energy balance of the engine and the warm-up process of the after-treatment system, and additional six (to seven) parameters ( $t_{1X}, t_{2X}, t_{3X}, m_{1X}, m_{2X}, m_{3X}, (m_{4X})$ ) to model the cold start duration and the extra emissions for each pollutant ( $X = \text{CO, HC, NO}_x \text{ and PN}$ ). These parameters are determined from exhaust measurements of chassis dynamometer and real-world emission tests (see Section 5.2.3 for a detailed description). The cold start model parameters are vehicle specific (at an engine level) and are reported in the corresponding cold start augmentations.

The model consists of six subsequent sections:

#### 1) Cool down of vehicle during parking/engine off:

In a first step the temperature of the engine at the start of the test ( $T_{e0}$  [°C]) is estimated with euro class specific cool down curves using the oil temperature as a proxy:

$$\frac{dT_e}{dt} = \frac{T_{e0} - T_{e_{end}}}{t_{stop}} = -a * (T_{e_{end}} - T_{amb}) \quad [3.1]$$

where  $T_{e_{end}}$  [°C] is the temperature of the engine before it being turned off (i.e. at the end of the previous trip),  $t_{stop}$  [s] is the stop or cool down time, and  $T_{amb}$  [°C] is the ambient temperature. The fitting parameter ( $a$  [1/s]) is determined experimentally from cool down

measurements with vehicles from different euro classes. The currently available results are presented in Table 3.1, where  $n$  represents the number of vehicles tested. These results will be updated when additional cool down data (from diesel vehicles and missing euro classes) becomes available.

**Table 3.1. Cool down constant (a) for different euro classes**

Petrol	a [1/s]	n	Source
<b>Euro 4</b>	$2.8 \cdot 10^{-4}$	1	Weilenmann et al., 2013
<b>Euro 6</b>	$1.6 \cdot 10^{-4}$	1	uCARE

In case of longer stop times ( $t_{stop} > 10$  h) the initial engine temperature is set to ambient ( $T_{e0} = T_{amb}$ ) as less than 10% of the initial temperature increase has remained.

### 2) Model for vehicle motion:

The traction or wheel power ( $P$  [W]) is calculated from the vehicle and driving parameters as follows:

$$\begin{aligned}
 P &= v * F_{wheel} = v * (F_{acc} + F_{drag} + F_{roll}) \\
 &= v * \left( m * \frac{dv}{dt} + f_0 + f_1 * v + f_2 * v^2 + m * g * \sin(\alpha) \right)
 \end{aligned}
 \quad [3.2]$$

where  $v$  [m/s] is the engine velocity,  $F_{wheel}$  [N] is the force acting on the wheels and is given by the sum of the acceleration ( $F_{acc}$  [N]), drag ( $F_{drag}$  [N]) and rolling ( $F_{roll}$  [N]) forces,  $m$  [kg] is the inertial mass of the vehicle,  $f_0$  [N],  $f_1$  [N\*s/m] and  $f_2$  [N\*s<sup>2</sup>/m<sup>2</sup>] are the road load coefficients,  $g$  [m/s<sup>2</sup>] is the gravitational acceleration constant and  $\alpha$  [-] is the road gradient.

### 3) Engine model for hot running conditions:

The input power during hot running conditions ( $Q_{inhot}$  [W]) is calculated as a linear function of the mechanical power ( $P$  [W]) and the engine speed ( $n$  [rpm]):

$$Q_{inhot} = w_p * P + w_n * n + w_0 \quad [3.3]$$

For motoring ( $Q_{inhot} \leq 0.9 * Q_{ino}$ ) and idle ( $v < 0.5$  km/h) conditions,  $Q_{inhot}$  is corrected as follows:

$$Q_{inhot,motoring} = 0.9 * Q_{ino} * \frac{n}{n_0} \quad [3.4]$$

$$Q_{inhot,idle} = Q_{ino} * \frac{n}{n_0} \quad [3.5]$$

The heating power ( $Q_{hhot}$  [W]) is then calculated as the difference between the input power and the power delivered to the wheels:

$$Q_{hhot} = Q_{inhot} - P \quad [3.6]$$

A portion of this heat is transferred to the coolant, while the rest leaves the engine with the exhaust gas. A scheme of the energy balance for the hot running engine is presented in Figure 3.6.

### 4) Engine model for cold start

During the cold start, the input power ( $Q_{in,cold}$ ) is higher than during hot running conditions (i.e.  $\Delta Q_{in} = Q_{in,cold} - Q_{in,hot} > 0$ ), primarily to overcome the increased friction of the cold engine, or else as a result of a controller decision to have a faster warm-up. Because it is not possible to measure the temperature at all friction points within the engine, we assume that during the cold start the relevant temperature for the engine friction ( $T_{frict}$  [°C]) rises linearly with the heating energy:

$$T_{frict} = T_{e0} + q_2 * \int_0^t Q_{h,hot} * dt \quad [3.7]$$

where  $T_{e0}$  [°C] is the engine temperature at the test start.

Based on the correlation with measurement data, the cold start extra input power ( $\Delta Q_{in}$  [W]) is assumed to be proportional to the input power and to follow a second order law over temperature:

$$\Delta Q_{in} = Q_{in,hot} * (q_1 * (T_{e,hot} - T_{frict}))^2 = Q_{in,hot} * \left( q_1 * \left( T_{e,hot} - T_{e0} - q_2 * \int_0^t Q_{h,hot} * dt \right) \right)^2 \quad [3.8]$$

Note that  $\Delta Q_{in}$  becomes zero when  $T_{frict}$  reaches the hot running engine temperature ( $T_{e,hot}$ ).  $T_{e,hot}$  was initially treated as an additional model parameter, but it was found to be fairly constant and independent of the euro class. Therefore, it was set to 120 °C for all petrol cars and 110 °C for all diesel vehicles, which is slightly above the oil temperature for a hot running engine.

As shown in Figure 3.6 (b), the total heating power during the cold start ( $Q_{h,cold}$  [W], in the following denoted as  $Q_h$ ) can then be obtained from:

$$Q_h = Q_{h,cold} = Q_{h,hot} + \Delta Q_{in} \quad [3.9]$$

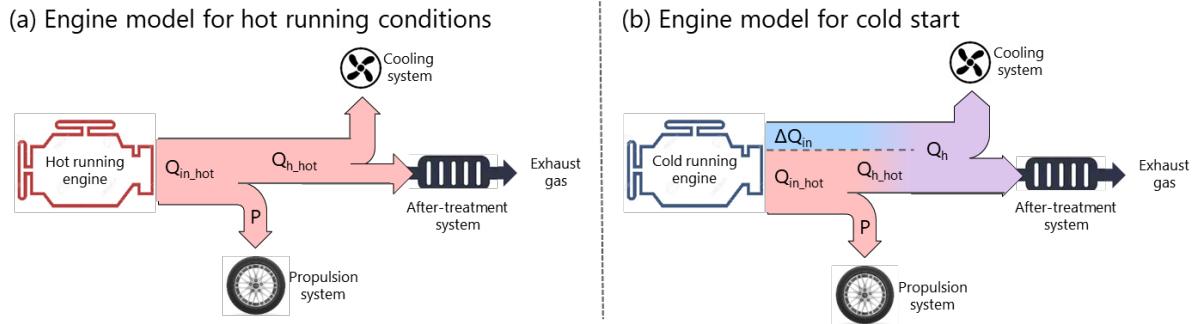


**Figure 3.6 Energy balance for a (a) hot running and (b) cold running engine**

To model short trip sequences, we need to determine the engine temperature at the end of each trip segment ( $T_{e,end}$  [°C]), which is used in the cool down model. As for the cool down process, the oil temperature is used as a proxy. From a series of dedicated measurements with different stop times, the engine temperature was found to increase exponentially with the integral of the cold start heating power ( $Q_h$  [W]):

$$T_e = T_{e,hot} - (T_{e,hot} - T_{e0}) * e^{-b * \int_0^t Q_h * dt} \quad [3.10]$$

To solve this equation, the engine temperature for hot running conditions ( $T_{e,hot}$  [°C]) and the exponential factor  $b$  [1/J] have to be defined. To investigate these parameters, we analysed data from IUFC tests from 30 petrol and 30 diesel passenger cars of various euro classes at different ambient temperatures. The results showed that the engine temperature during hot running conditions ( $T_{e,hot}$ ) varied between 80 and 120°C and was independent

of the fuel type and the euro class. Thus, a fixed value of  $T_{e_{hot}} = 100^\circ\text{C}$  is used in the uCARE emissions model. The exponential constant  $b$  [1/J] showed a slight dependency with the ambient temperature and was, on average, slightly higher for the petrol vehicles. However, the vehicle-to-vehicle variability was dominant and no influence from the euro class was observed. Therefore, an average value of  $b = 1.0 \cdot 10^{-7}$  1/J is used in the uCARE model.

### 5) Model for the cold start duration:

For each pollutant X (X=CO, HC, NO<sub>x</sub> or PN), the integrated heating power over the cold start period ( $Q_X$  [W]) is estimated as:

$$Q_X = t_{1X} * (T_{e_{hot}} - T_{e0}) + t_{2X} * (e^{t_{3X} * (T_{e_{hot}} - T_{e0})} - 1) \quad [3.11]$$

The end of the cold start ( $t_{endX}$ ) is then determined by minimizing the difference between the cumulated heating power and the cold start heating power for each pollutant:

$$t_{endX} \text{ so that: } \text{Min of } Q_{diff} = \text{abs} \left( \int_0^{t_{endX}} Q_h * dt - Q_X \right) \quad [3.12]$$

### 6) Pollutants model:

For each pollutant X, the CSEE ( $dmX$  [g/s]) are estimated as:

$$dmX = m_{exh} * (m_{1X} - m_{2X} * T_{e0})^3 * e^{-m_{3X} * (\int_0^{t_{endX}} Q_h * dt)^{1/2}}, \text{ for X= CO, HC \& PN} \quad [3.13]$$

$$dmX = m_{exh} * \left( (m_{1X} - m_{2X} * T_{e0}) * e^{-m_{3X} * (\int_0^{t_{endX}} Q_h * dt)^{1/2}} - m_{4X} \right), \text{ for X= NOx} \quad [3.14]$$

where  $m_{exh}$  [g/s] is the exhaust mass flow, which is approximated by:

$$m_{exh} = \frac{Q_h}{2538.7}, \text{ for petrol vehicles and} \quad [3.15]$$

$$m_{exh} = \frac{Q_h}{507.7}, \text{ for diesel vehicles} \quad [3.16]$$

The factor in the denominator of  $m_{exh}$  takes into account the heat capacity of the exhaust gas, the exhaust gas temperature and the percentage of the heating power that flows into the exhaust system. Because these two last factors can vary significantly for different vehicles, the estimated  $m_{exh}$  might deviate significantly from the measurements in some cases. However, any inaccuracy in  $m_{exh}$  will be absorbed by the model parameters in the equations for  $dmX$ , so that, even when the estimate of  $m_{exh}$  is imprecise, the extra emissions ( $dmX$ ) are still modeled accurately.

Note that for high  $T_{e0}$  (i.e. short cool down period), the term  $(m_{1X} - m_{2X} * T_{e0})$  in equations [3.13] and [3.14] might become negative, leading to negative CSEE. In such case the term  $(m_{1X} - m_{2X} * T_{e0})$  should be set to zero.

## **3.5.2 Simplified model approach for fleet averages and for cases with limited test data**

Since the detailed model for the cold start extra emissions needs special vehicle emission tests (ideally with the IUFC dynamometer cycle at three different start temperatures), and usually only test data for a limited number of vehicles is available, the uncertainty of representativeness for the vehicle fleet can be low (see also Chapter 9).

Many vehicle emission tests include on-board tests (PEMS tests) with cold starts. Chassis dyno tests typically include a WLTC<sup>5</sup> with cold start and maximum one or two additional cold start tests in real world cycles.

Due to the increasing share of cold start extra emissions on the overall vehicle emissions, we developed a simplified model approach which can use any cold start test as input to produce the necessary parameters for cold start simulation.

### 3.5.2.1 Basic assumptions for simplification

The detailed cold start model needs test-(sub-)cycles driven under both cold and hot conditions. The cold start extra emissions (CSEE) and their evolvment over time are calculated as difference between cold and hot emission levels.

For well-functioning modern cars, cold start related emissions are much higher than the hot emissions as demonstrated in Figure 3.7. In this test, 100% of the HC emissions occurred during the cold start phase, which lasts for about 100 seconds: 500 meters of the total test distance of 10km. For NO<sub>x</sub> the cold start contributes 80%, and for PN about 20%, of the total test emissions.

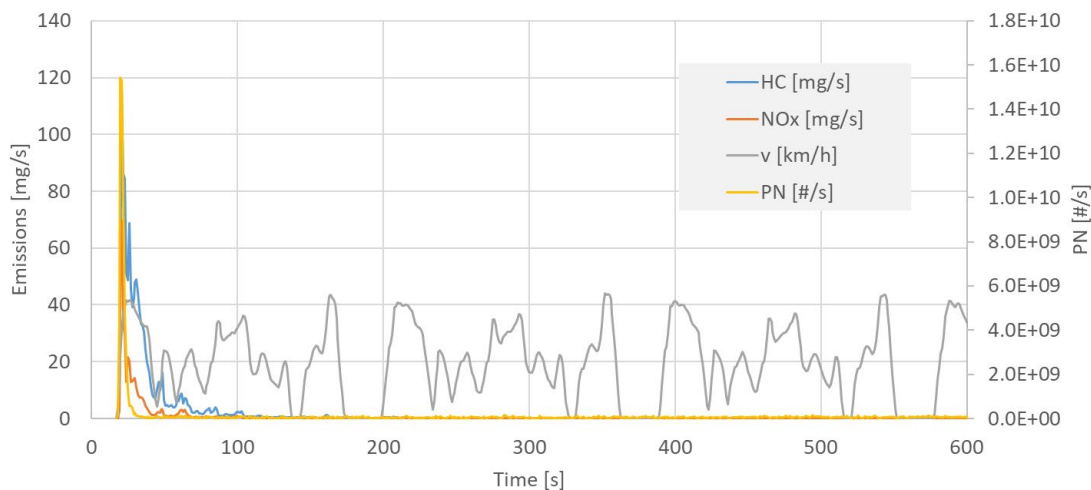


**Figure 3.7. IUFC test results on a Euro 6d petrol car for a cold start at 0°C**

We conclude that for exhaust gas components and/or vehicles with significant cold start extra emissions, we do not need a very accurate value for the hot emission level, we can use the simulated hot emissions (see Section 3.2 for hot emissions simulation approach using hot emission maps). Thus, we can calculate the CSEE as

$$CSEE = E_{cold_{measured}} - E_{hot_{simulated}} \quad [3.17]$$

where  $CSEE$  is the cold start extra emissions in [g/start] or in [g/s];  $E_{cold_{measured}}$  the emissions measured in any cycle after a cold or cool start in [g/start] or in [g/s]; and  $E_{hot_{simulated}}$  the emissions *simulated* for hot engine conditions (e.g., with the model PHEM) for the cycle used for  $E_{cold_{measured}}$  in [g/start] or in [g/s].

The CSEE can thus be calculated from the software automatically from any test data, which includes a cold or a cool start. Inaccuracies in the simulated hot emissions do not significantly affect the accuracy of CSEE for all components where cold start emissions are much higher than the hot emissions. For exhaust gas components with rather low cold start emission contribution, the subtraction of simulated hot emissions increases the

<sup>5</sup> We generally recommend not to use type approval cycles for parameterisation of real-world emission models since emission control strategies are likely be optimised for these test conditions. Thus, also for cold start emissions the WLTC data is rather fall-back option than a recommended standard.

uncertainty of the CSEE. However, the higher uncertainty has then rather low impact on the overall uncertainty of the sum of cold and hot emissions, due to the small contribution of cold starts.

As the main parameter explaining the CSEE over time, we use the cumulated energy losses of the combustion engine, like in the detailed model. This energy loss is the difference of energy provided to the engine by the fuel and the mechanical work delivered by the engine. This energy loss is heating the engine and exhaust gas aftertreatment components and the coolant during cold start and is partly also released via the exhaust as the Enthalpy of the gas at tailpipe. Thus, the CSEE should depend to a large extent on this energy loss.

$$\dot{Q}_{loss} = \dot{m}_{fuel} \cdot H_u - P_e \quad [3.18]$$

$$Q_{loss} = \int \dot{Q}_{loss} dt \quad [3.19]$$

where  $Q_{loss}$  is the cumulated energy loss integrated from engine start on,  $\dot{m}_{fuel}$  the fuel mass flow [kg/s],  $H_u$  the upper heating value of the fuel [kWh/kg], and  $P_e$  the effective power delivered by the engine.

In this simple version of the cold start model, we do not consider additional parameters affecting the CSEE level. In theory also the engine power during cold start has an impact, with increasing CSEE with increasing power level. However, the typically limited number of cold start tests per vehicle does not usually allow for the reliable quantification of this effect in an automated process. We may add a correction function later, when cold start test data for cycles leading to significantly different engine power levels (but with the same start temperatures) is available.

The analysis of the cold start emission data of petrol and diesel cars seemed to suggest to not fit the dependency of the CSEE on  $Q_{loss}$  into a function, since the cold start behavior can be quite different between vehicles. Instead of a function we therefore use a interpolating line between successive support points such that any cold start behaviour is covered (see Section 3.5.2.2).

### 3.5.2.2 Model description

The cold start extra emissions, calculated from the measured cold start emissions minus the simulated hot emissions, are plotted over  $Q_{loss}$ , as shown in Figure 3.8 (right). To produce the characteristic polygons,  $Q_{loss}$  is calculated from the measured fuel consumption and the heating value minus the effective engine power. The effective engine power can be measured or simulated by the software (in our case the vehicle model PHEM is used<sup>6</sup>).

Since each test may start at different ambient temperatures, we are using generic relations between temperature at start and the corresponding  $Q_{loss}$  (Figure 3.8 left). If a vehicle is measured at several different cold start temperatures, the  $Q_{loss} @ start to T_{start}$  function can be parametrized by shifting the measured CSEE polygons for each test until they match. The starting points of the individual curves then show the differences in  $Q_{loss}$  for the different start temperatures. If no tests at different start temperatures are available for a car, we use generic relations. The generic  $Q_{loss} @ start to T_{start}$  function are the averages per exhaust gas component and emission concept from the vehicles measured with significantly different start temperatures.

Both, the CSEE polygons and the  $Q_{loss} @ start to T_{start}$  function are different per exhaust gas component and for petrol, diesel, and Euro classes. The differences in the

---

<sup>6</sup> Without using the model PHEM, one can calculate the engine power demand in each second of the cycle from the equations of vehicle longitudinal dynamics as described in the description of PHEM.

$Q_{loss}$  @ start to  $T_{start}$  function for exhaust gas components results from the different light off temperatures (typically lowest for  $NO_x$ , highest for HC).

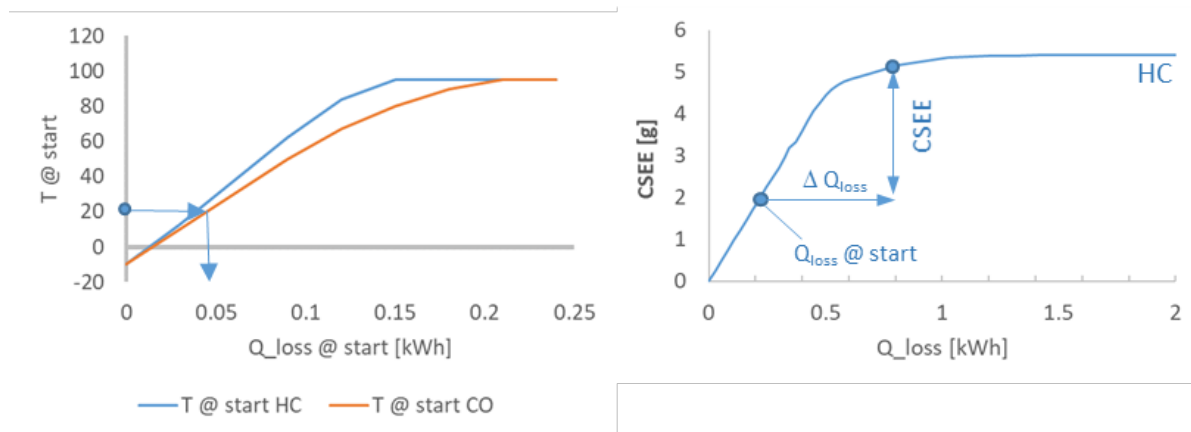


**Figure 3.8. Schematic picture of a polygon for the  $Q_{loss}$  @ start to  $T_{start}$  function (left) and for the HC cold start extra emissions over  $Q_{loss}$  (right)**

Having produced the characteristic curves, they can be used to simulate the CSEE in any driving cycle. To calculate the CSEE, the model takes for a given start temperature the corresponding  $Q_{loss}$  @ start as shown in Figure 3.8 on the left side. With this  $Q_{loss}$  value the CSEE polygon is entered. From this start value,  $Q_{loss}$  is increasing every second in the cycle according to the calculated  $\dot{Q}_{loss}$ . For the resulting  $Q_{loss}$ , the corresponding CSEE is interpolated from the CSEE polygon. The total CSEE in [g/start] is the CSEE value interpolated at the end of cold start phase, i.e. when the polygon is horizontal, minus the CSEE value interpolated for  $Q_{loss}$  @ start. The instantaneous CSEE in [g/s] can be gained from the differences of the total CSEEs in [g] interpolated for the  $Q_{loss}$  per second.

To simulate the start temperature for a trip with engine off phases, cool down curves, of the catalyst temperature are used, which provide the reduction of the difference of the coolant temperature to the ambient temperature as function of the engine off time.

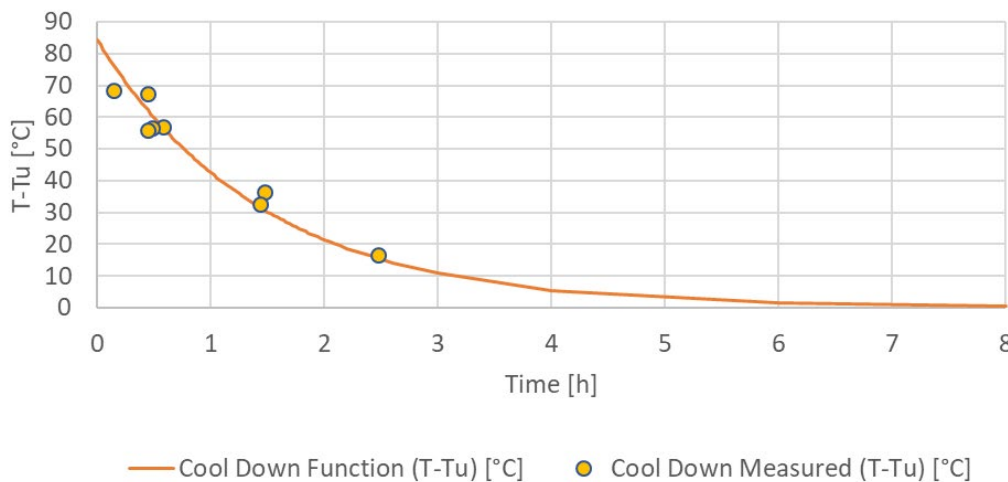


**Figure 3.9. Polygon for cool down curve for the coolant**

### 3.6 Examples of the cold start augmentation

In the following we show some examples of how the cold start augmentations can be used to estimate cold start extra emissions.

Figure 3.10 shows the results of the model parametrization using IUFC measurements at  $-7\text{ }^{\circ}\text{C}$  (top) and  $23\text{ }^{\circ}\text{C}$  (bottom) for a Euro 6c petrol vehicle. The left panels show the second-by-second cold start extra emissions and the right panels the corresponding integrated emissions. It can be seen, that, for all the measured pollutants, the CSEE occur mostly in the first sub-cycle (first 3 minutes) and are higher at lower ambient temperature. The total CSEE (in g/start or #/start) are determined by integrating the CSEE within the cold start period (i.e. until the cumulative becomes constant).

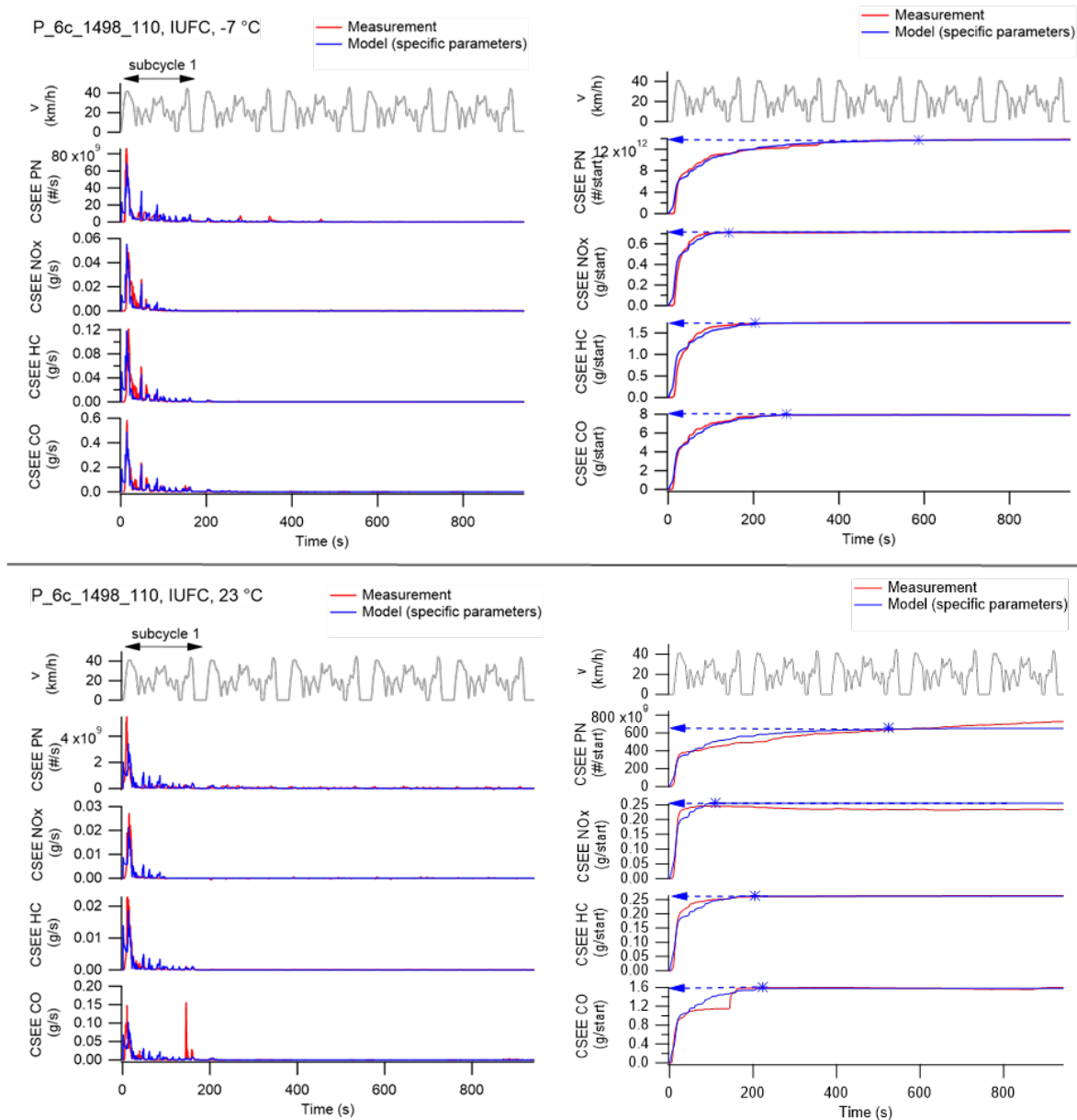


**Figure 3.10. Results from cold start model parametrization with IUFC cycles at  $-7\text{ }^{\circ}\text{C}$  (top) and  $23\text{ }^{\circ}\text{C}$  (bottom) for a Euro 6c petrol vehicle. The left panels show the second-by-second cold start extra emissions and the right panels the corresponding integrated emissions.**

Once the model specific parameters have been determined for a given vehicle with IUFC measurements, we can use the cold start model to determine the CSEE for any cycle or trip. For example, Figure 3.11 reports the modelled CSEE of a NEDC cycle, for the petrol vehicle in Figure 3.10, using the specific model parameters reported in the corresponding cold start augmentation. The measured CSEE for the NEDC cycle were obtained by subtracting the average emissions in the 4<sup>th</sup> sub-cycle from the total measured emissions, as described in Section 5.2.3. The comparison with the measured CSEE shows

that the model results are quite accurate for CO, HC, and NO<sub>x</sub>, while the model significantly overestimates the measured PN CSEE.

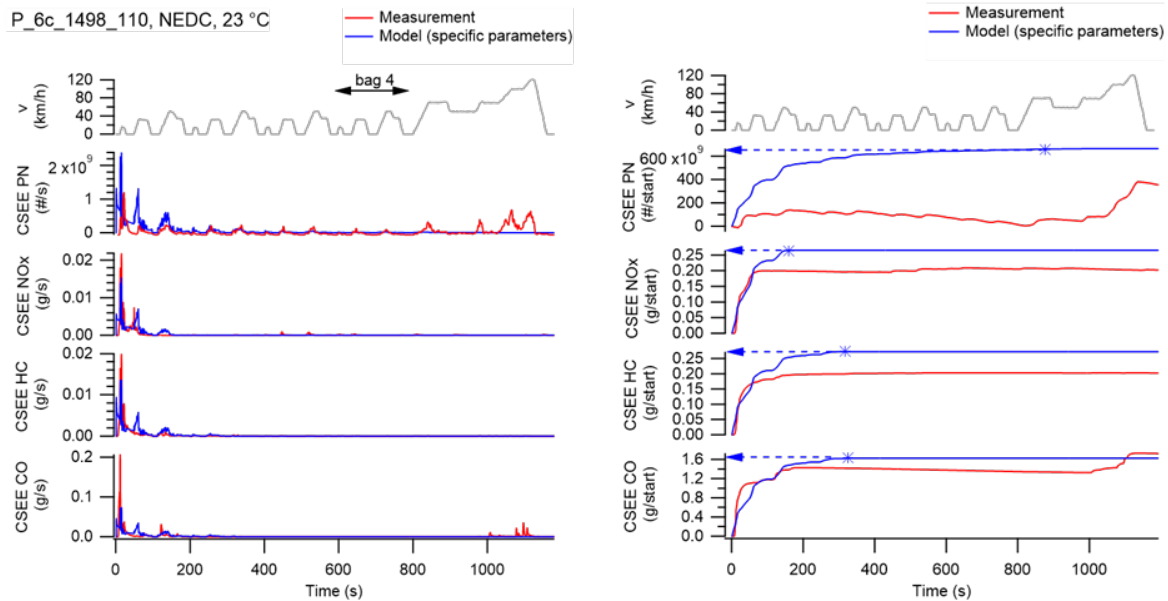


**Figure 3.11. Results from cold start model of a NEDC at 23°C for a Euro 6c petrol vehicle using vehicle specific model parameters**

The CSEE highly depend on the engine and after-treatment technologies of the single vehicle. In general, petrol vehicles are characterized by large CO and HC CSEE, while diesel vehicles have larger NO<sub>x</sub> CSEE. However, some diesel vehicles, show lower NO<sub>x</sub> emissions during the cold start period than during hot operation, which leads to negative NO<sub>x</sub> CSEE. As an example, in Figure 3.12 we present the model parametrization results from a Euro 6d-Temp diesel vehicle. As shown, the cold start model can also fit such negative NO<sub>x</sub> CSEE trends quite accurately.

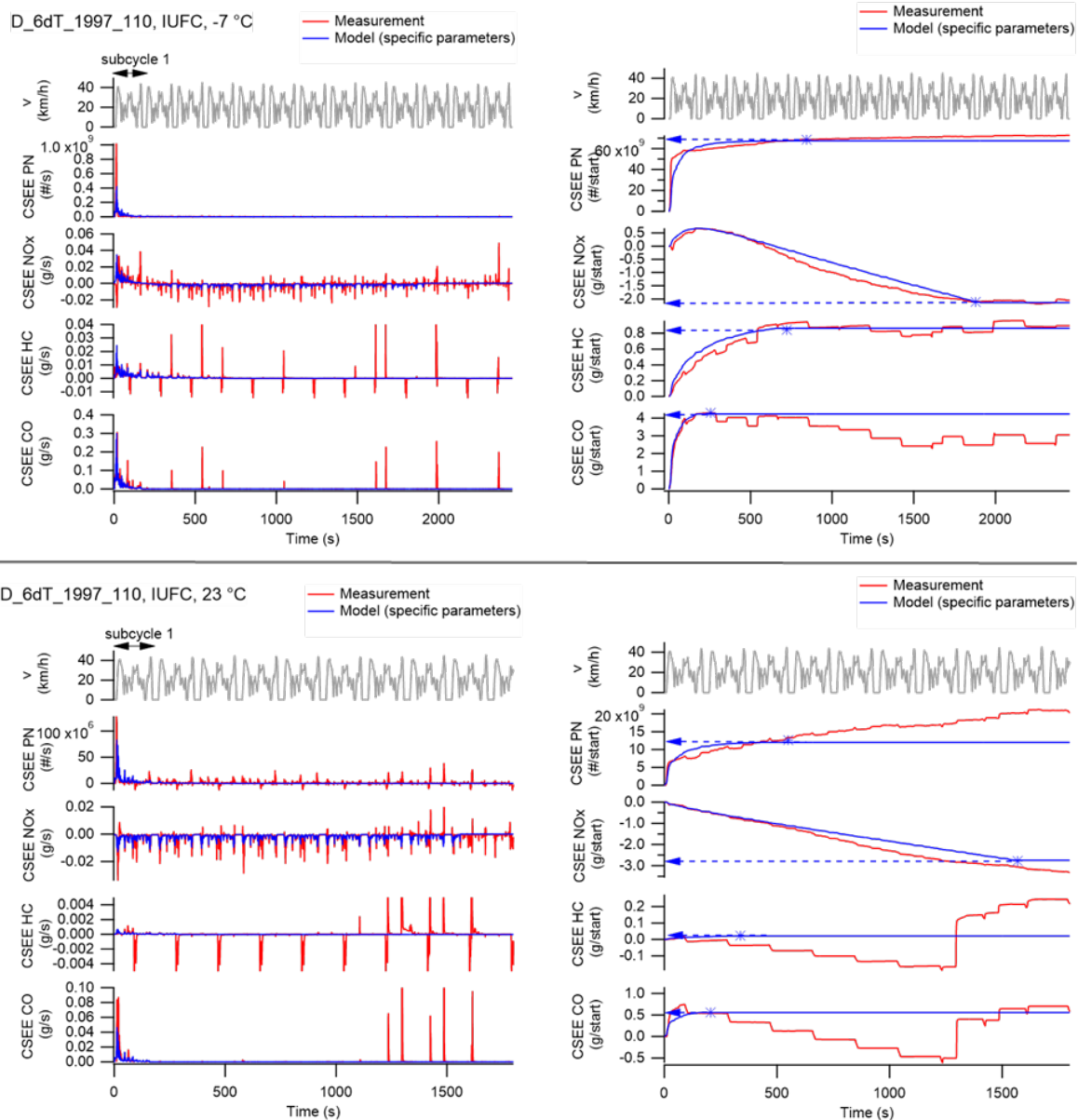


**Figure 3.12. Results from cold start model parametrization with IUFC cycles at -7°C (top) and 23°C (bottom) for a Euro 6d-Temp diesel vehicle**

If the specific model parameters cannot be determined for a certain vehicle (i.e. no IUFC data available), the CSEE can still be estimated using the optimized parameters (if NEDC/WLTP/RDE data available) or average fallback parameters. A comparison between the model results using specific, optimized, and average parameters is presented in Chapter 9.

Other two very important parameters influencing the CSEE are the ambient temperature and the vehicle technology (for simplicity represented here by the euro class and the fuel type). In Figure 3.13 we report the total CSEE estimated with the cold start model for a WLTP cycle using the fallback model parameters of different euro classes and fuel types and varying the ambient temperature from -15°C to 30°C. For CO, HC, and PN we observe a decrease of the CSEE for increasing ambient temperatures, and, in most cases, for increasing euro class. These trends are less pronounced for NO<sub>x</sub>, for which we observe rather small CSEE overall, that even become negative for certain diesel euro classes.

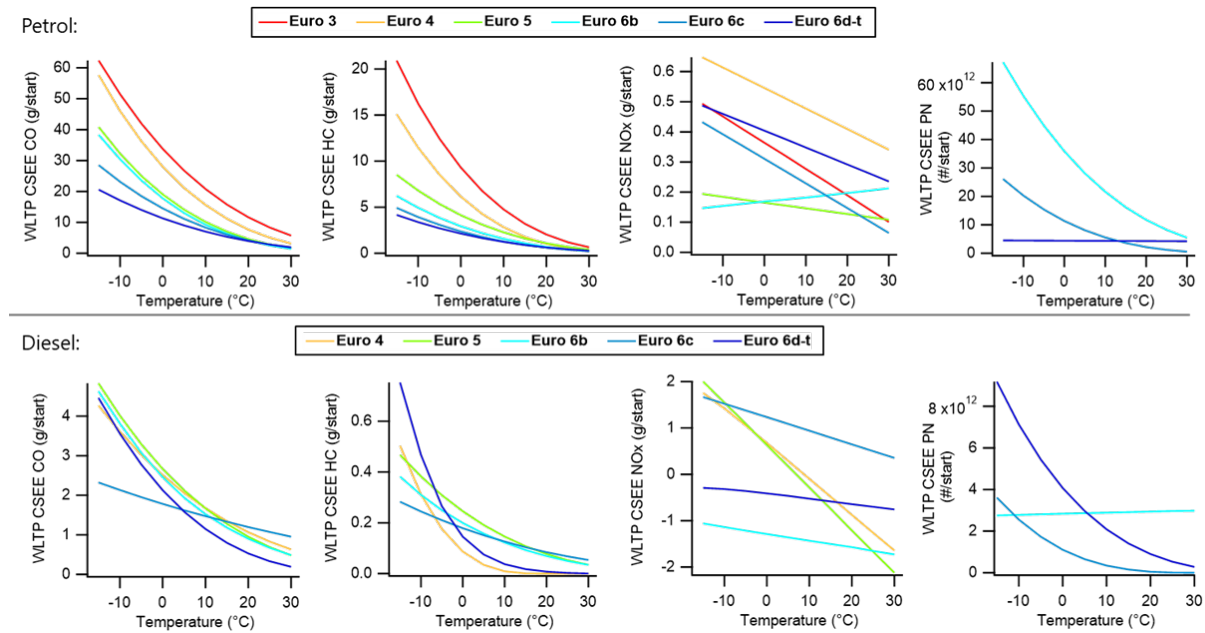


**Figure 3.13. Modelled CSEE for different pollutants for a WLTP cycle varying vehicle technology and ambient temperature**

### 3.7 Interpreting the deterioration augmentation

The approach taken to implement deterioration is through the so-called "deterioration factors". These factors indicate how emissions increase due to deterioration, as a function of mileage. Therefore, if a vehicle of interest is older has a different mileage than the vehicle which was used in the creation of a base map, the deterioration factors can be used to predict the relevant base map emissions for the vehicle of interest.

The deterioration factors are given in a tabulated format and are applied over the complete base emission map. The factors are defined according to the fuel type and the emission standard (Euro class) of the vehicle and are a function of vehicle mileage. Deterioration factors are provided for NO<sub>x</sub>, CO, HC emissions for both petrol and diesel vehicles from Euro 1 to Euro 6. The applied factors are over a span of 0 to 300,000 km.

### 3.8 Using the deterioration augmentation

#### 3.8.1 Deterioration factors

The deterioration augmentation is based on the deterioration factors that are given in tabulated format separately for NO<sub>x</sub>, CO, HC emissions for both petrol and diesel vehicles from Euro 1 to Euro 6. Practically, these factors represent the way emissions are affected over vehicle mileage increase. Deterioration factors are defined with respect to a reference mileage, 50,000 km. In other words, at this mileage all deterioration factors are 1. Apart from the 50,000km, the deterioration factor tables currently have three additional breakpoints, usually at 100,000, 200,000 and 300,000 km. Below 50,000 km all deterioration factors are assumed equal to 1. In order to calculate the deterioration factor value at an intermediate mileage, a linear interpolation is applied between two adjacent mileages. For example, the calculation of the deterioration factor at 160,000 km would be done by interpolating the corresponding deterioration factor values at 100,000 and 200,000 km. In this way, the deterioration factor at any intermediate mileage can be determined.

The calculation of the emission map at a certain mileage combines the base map with its mileage and the corresponding deterioration factors. Initially the deterioration factor values

for the mileage of the base map and the desired mileage are calculated, applying the linear interpolation procedure described above. Then the base map is multiplied by the ratio of the deterioration factor value at the desired mileage to the deterioration factor value at the mileage of the base map. For example, if the base NO<sub>x</sub> emission map of a Euro 5 petrol car corresponds to 60,000 km and the calculation of the emission map at 120,000 km is requested, then (with reference to Table 3.4):

Step 1: Calculation of NO<sub>x</sub> deterioration factor for Euro 5 petrol car at 60,000 km, by interpolating the values at 50,000 (NO<sub>x</sub> deterioration factor = 1) and 100,000 km (NO<sub>x</sub> deterioration factor = 1). Thus, at 60,000 km the NO<sub>x</sub> deterioration factor for Euro 5 petrol cars is 1.

Step 2: Calculation of NO<sub>x</sub> deterioration factor for Euro 5 petrol car at 120,000 km, by interpolating the values at 100,000 (NO<sub>x</sub> deterioration factor = 1) and 200,000 km (NO<sub>x</sub> deterioration factor = 2.5). Thus, at 120,000 km the NO<sub>x</sub> deterioration factor for Euro 5 petrol car is 1.3.

Step 3: Multiplication of the base NO<sub>x</sub> emission map with the ratio 1.3/1.

An alternative approach to the tabulated format, using equations, is given in Section 12.6.

### 3.8.2 Vehicle mileage

Deterioration factors are a function of vehicle mileage, which in some cases is not available. In such cases, an approximation can be made based on vehicle age. Below we present a collection of equations describing the correlation between vehicle mileage and age (Table 3.2 and Table 3.3). The equations are based on five different bodies of work: CONOX [6], RICARDO [7], TRL [8], APR [9] and TNO [10]. This work is also discussed and compared in Section 12.5.

Based on this data, correlations were derived, as summarised in the tables below for both petrol and diesel cars. For diesel cars it appears that the CONOX Sweden database has a large deviation compared to the other four. Dutch data from TNO report 2016 R11872 [10] also shows large deviations for diesel cars in the Netherlands due to the road and fuel tax system, as well as the fact that most diesel cars in the Netherlands are primarily for business use.

**Table 3.2. Polynomial fit equations for mileage estimation for petrol cars.  $x$  represents vehicle age and  $y$  the estimated mileage in km.**

Data Source	Polynomial fit equation
CONOX Sweden	$y = 12070 x + 8347.3$
CONOX Switzerland/UK	$y = -386.64 x^2 + 15852 x - 5244.7$
RICARDO	$y = -164.25 x^2 + 13672 x - 578.9$
TRL	$y = -537.38 x^2 + 18172 x$
APR	$y = (-0.4884 x^2 + 15.707 x) \cdot 1000$
TNO	$y = 9229 + 15769 * x - 371.59 * x^2$

**Table 3.3. Polynomial fit equations for mileage estimation for diesel cars.  $x$  represents vehicle age and  $y$  the estimated mileage in km.**

<b>Data Source</b>	<b>Polynomial fit equation</b>
<b>CONOX Sweden</b>	$y = 20038 x - 2291.2$
<b>CONOX Switzerland/UK</b>	$y = -538.29 x^2 + 23739 x - 7174.9$
<b>RICARDO</b>	$y = -585.78 x^2 + 23059 x + 8287.7$
<b>TRL</b>	$y = -746.21 x^2 + 24658 x$
<b>APR</b>	$y = -895.5 x^2 + 24862 x$
<b>TNO</b>	$y = 15710 + 32735 * x - 963.55 x^2$

### 3.8.3 Combining the cold start and deterioration augmentation

In real vehicle operation, both the deterioration of the aftertreatment system due to ageing and the cold start operation affect emissions. To improve model calculations, these two effects should be combined. It should be considered that passenger cars spend most of their operational time in warm/hot conditions. Furthermore, the deterioration factors have been determined using remote sensing (RS) data, which mostly corresponds to warm/hot conditions of the vehicle (only the vehicles parked very close to the RS equipment, i.e., a few hundred metres, will be measured while being still in the cold start phase). Thus, the deterioration factors largely depict the 'hot' emissions of the vehicle. This means that for an aged vehicle (i.e. aged catalyst), **the deterioration factor should be applied on the base (hot) emission map, followed by the cold start augmentation**. In a more detailed approach, the catalyst ageing effect on the light-off temperature (the temperature at which the conversion efficiency of the catalyst is 50%) can be incorporated. This is discussed further in Section 12.2.

### 3.9 Examples of the deterioration augmentation

A petrol Euro 5 vehicle is used to present the implementation of deterioration factors. An analysis on NO<sub>x</sub> and CO emissions has been made as an example. The map generating script was used with emissions being multiplied with their respective deterioration factors, as described above. Mean emission maps can be made for every available mileage, but here we show two extremes: 50,000 and 300,000 km (Figure 3.14). The deterioration factors used in this example are presented in Table 3.4. The legal durability requirements are up to 160,000 kilometres for components, and 100,000 kilometres in use, which may be the reason behind the increases beyond these mileages.

**Table 3.4. Deterioration factors as a function of cumulated mileage used in the example**

Pollutant	0 km	50,000 km	100,000 km	200,000 km	300,000 km
NO <sub>x</sub>	1.00	1.00	1.00	2.50	3.50
CO	1.00	1.00	1.30	2.00	3.00

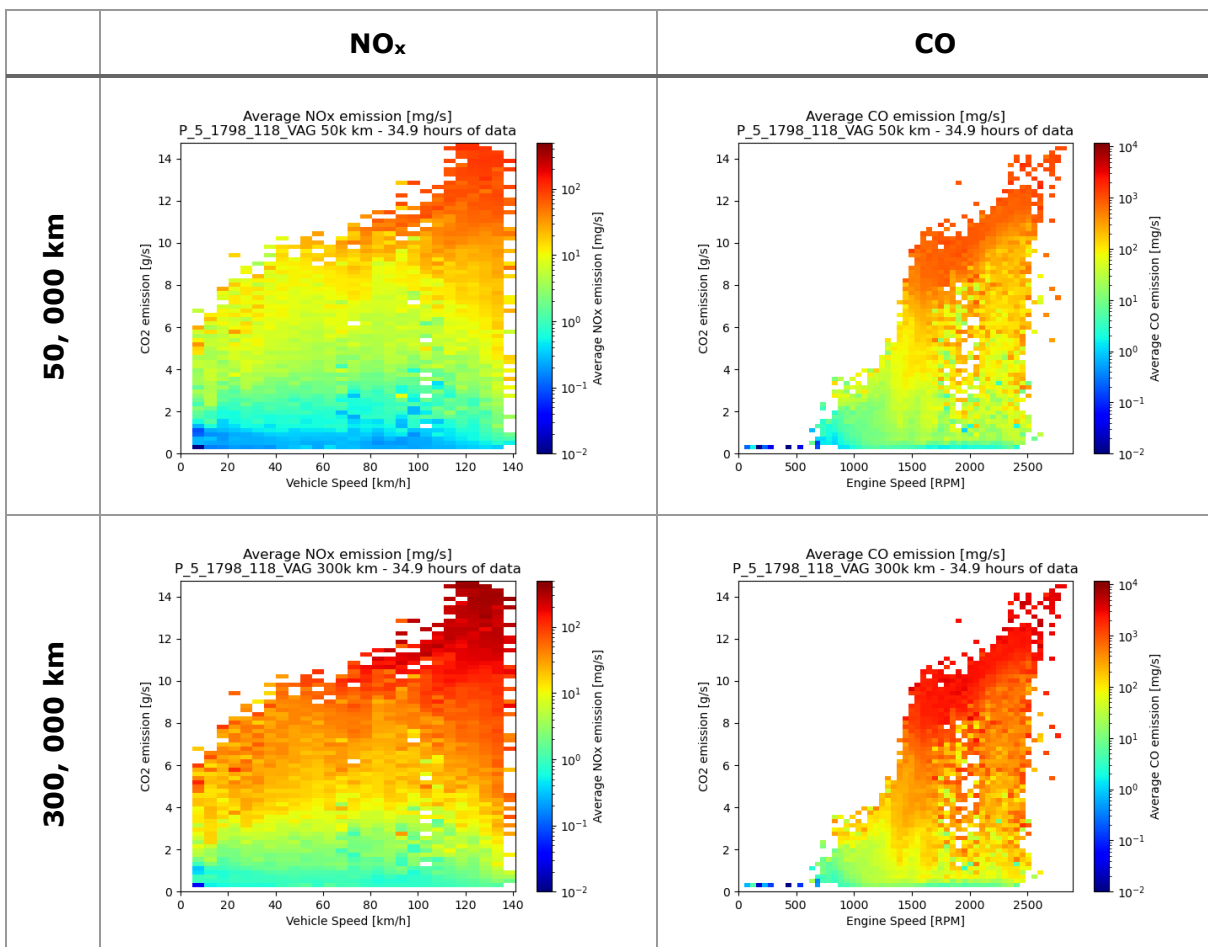


**Figure 3.14. The effect of applying deterioration factors on a base map for NO<sub>x</sub> (dependent on vehicle speed), and CO (dependent on engine speed), to compare emissions at mileages of 50, 000 and 300,000 km.**

## 4 As a researcher or policy maker, how can AEMs give me insight into the relationship between driver behaviour and emissions?

AEMs can also be used to gain additional insight into the relationship between driver behaviour and pollutant emissions. This can then be used to take specific legislative decisions or give concrete advice based on that insight. Here we provide some examples of insights that have been gained from the use of AEMs.

### 4.1 Low-CO<sub>2</sub> driving is not necessarily equivalent to low-NO<sub>x</sub> driving

One example is the advice given regarding drivers' gear choice. Conventional eco-driving instructions to reduce CO<sub>2</sub> suggest using a high gear to maintain low engine speeds (around 1500 RPM as demonstrated by the purple oval in Figure 4.1). However, we can use AEMs to see that for low NO<sub>x</sub> driving this advice may need to be modified.

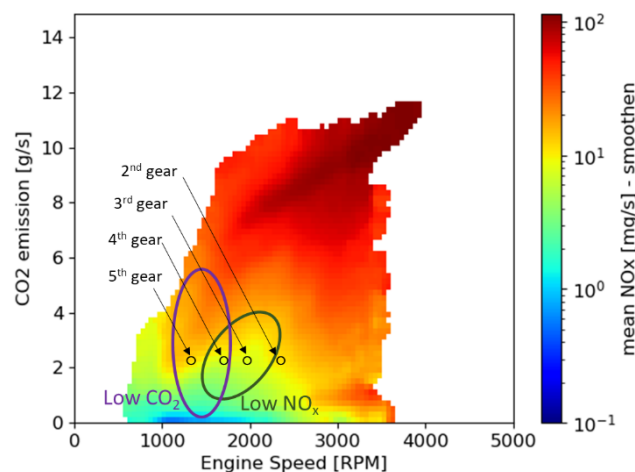


**Figure 4.1. Annotated NO<sub>x</sub> base map of a Euro 5 Volkswagen Polo with a 1199 cc 55 kW engine (D\_5a\_1199\_55\_VAG), based on over 400 hours of data. Annotations indicate the engine speed range recommended for low CO<sub>2</sub> emissions (purple), as well as the area of the base map with lower NO<sub>x</sub> (green). An indication is also given of where on the emission map driving at different gears would be while driving around 50 km/h with an CO<sub>2</sub> emission of approx. 150 g/km.**

Euro 5 diesel vehicles have high NO<sub>x</sub> emissions, which make them an excellent candidate for emission-decreasing behaviour-based advice. The base map in Figure 4.1 shows NO<sub>x</sub> emissions of a Euro 5 diesel vehicle, dependent on CO<sub>2</sub> and engine speed. If we compare the NO<sub>x</sub> emissions for different gears (as annotated in Figure 4.1) we see that for a CO<sub>2</sub> emission around 2 g/s, a lower gear would produce lower NO<sub>x</sub> emissions: 3<sup>rd</sup> gear has lower NO<sub>x</sub> emissions than 5<sup>th</sup>. Looking at the area in the map with lower NO<sub>x</sub> (the green oval in Figure 4.1), this advice for low NO<sub>x</sub> driving particularly holds when accelerating (i.e. when CO<sub>2</sub> emissions are higher).

### 4.2 Certain driving conditions have much lower relative emissions

Analyses in the past with Euro 6 vans have shown that each vehicle technology has its own particular emission map in terms of vehicle speed and CO<sub>2</sub> emission. These emission maps indicate optimisations and weak spots in the emission control strategy. High engine load and high CO<sub>2</sub> emission outside the optimized vehicle operation may lead to a

disproportional increase in NO<sub>x</sub> emission. One of the vehicles that demonstrates this is a Euro 6 Volkswagen Caddy, shown in Figure 4.2.

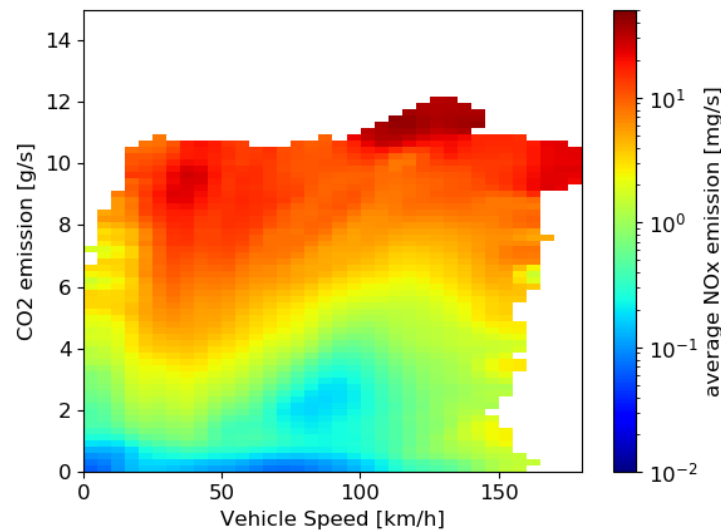


**Figure 4.2. Average NO<sub>x</sub> emission base map from Euro 6 Volkswagen Caddy (D\_6\_1968\_55\_VAG) as a function of vehicle speed and CO<sub>2</sub> emission based on monitoring data. A smoothing profile is applied to generate a continuous surface in the base map.**

The effect of constant vehicle operation on the motorway between 80 - 100 km/h is shown by an area of very low NO<sub>x</sub> emission in the emission map. At vehicle speed 100 km/h, the CO<sub>2</sub> emission is about 2.5 g/s. At this operational point for motorway driving, NO<sub>x</sub> emission is in the order of 0.2-0.4 mg/s, which is extremely low (around a factor 10 below the limit of 80 mg/km). In the cases of higher dynamics at 80-100 km/h (CO<sub>2</sub> emission outside the region 1-3 g/s), average NO<sub>x</sub> emission is higher.

On the other hand, the region with vehicle speed lower than 50 km/h and CO<sub>2</sub> emission higher than 3 g/s represents highly dynamic driving within the city. Clearly, this dynamic driving, possibly in combination with gear shifting, has the poorest performance of this vehicle. However, this relatively poor performance is still well below the type-approval limit for this vehicle.

### 4.3 Re-ordering trips can lead to lower emissions

With the cold start model we can estimate the CSEE not only for single trips/cycles, but also for trip sequences. Figure 4.3 shows the modelled CSEE for two inverted, but otherwise identical, trip sequences. Both trips consist of 3 short segments (each 850 m) and 1 long segment (~3.5km), with a break of 30 minutes between each of them. In this example we used the fallback model parameters of the Euro 6d-Temp petrol vehicles and an ambient temperature of 15°C. As shown in Figure 4.3, the order of the trip segments can significantly influence the total CSEE of the trip. Such analysis can be used to provide input for the drivers to decrease their cold start emissions, for example by planning the longest distances at the beginning of the trip. While in this example we only analysed the effect from changing the order of the trip segments, similar analysis can be done to investigate the result of varying breaks duration, average trip velocity, etc.

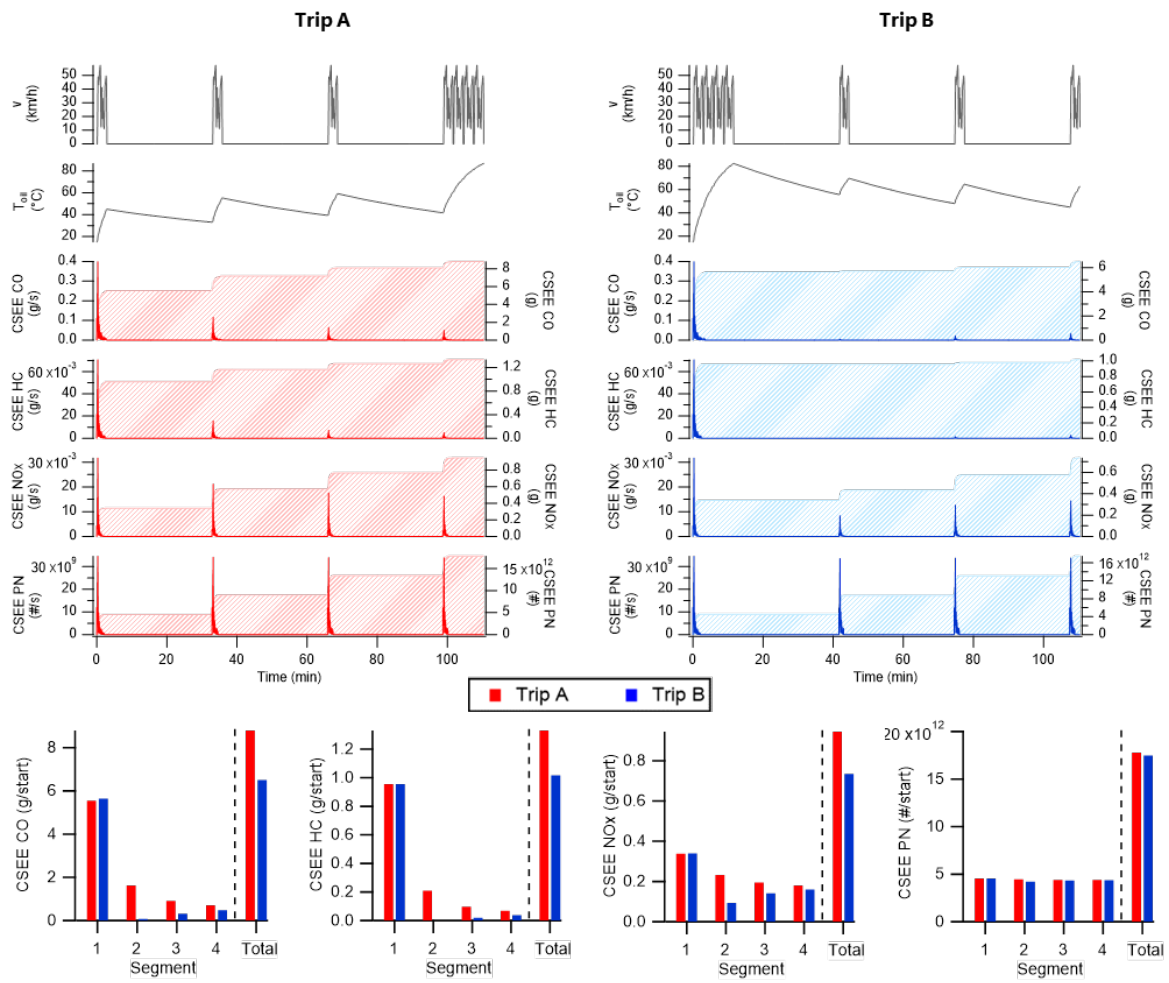


**Figure 4.3. Results from cold start model of inverted trip segments**

---

## 5 Contributing to uCARE emission data: the future of AEMs

Do you have emission measurement data that you would like to make available to other researchers or tool-builders? Great! Contribute by uploading your generated AEMs to the Zenodo uCARE community. You'll need to take the following steps:

- 1) Determine the taxonomy codes for the vehicles you've measured
- 2) Generate the AEM
- 3) Ensure consistent version control and name your files correctly
- 4) Upload the data to the Zenodo uCARE community

### 5.1 Determine the taxonomy code

To determine the taxonomy code, you'll need fuel type, Euro class, engine size/displacement (in cc), engine power (kW) and vehicle manufacturer. For Euro 6 diesel vehicles, a build year can also be useful. To generate the relevant engine code, please refer to the outline provided in Section 2.3. An alliance code tool is available to generate the alliance code. In 95% of the cases the alliance code can be determined using the engine code is alone, for the other 5% the vehicle manufacturer provides a definitive answer.

## 5.1.1 Manufacturer Alliances

**Table 5.1. Alliances of manufacturers**

ALFA	Alfa Romeo								
AUDI	Audi								
BENT	Bentley								
BMW	BMW	Mini	Rolls-Royce						
BMW2	BMW	Toyota							
CHRY	Chrysler	Dodge	Jeep	Ram					
FCA	Fiat	Alfa Romeo	Lancia	Jeep	Chrysler				
FCA2	Fiat	Alfa Romeo	Lancia	Jeep	Chrysler	Suzuki			
FCA3	Fiat	Ford	Lancia						
FCA4	Fiat	Alfa Romeo	Lancia	Opel/Vauxhall	Chevrolet	Cadillac	Saab	Suzuki	
FCA5	Fiat	Opel/Vauxhall	Lancia	Alfa Romeo					
FIAT	Fiat	Alfa Romeo	Lancia	Ferrari	Iveco				
FORD	Ford	Lincoln							
FORD2	Ford	Mazda	Volvo						
FP	Ford	Peugeot	Citroen	Jaguar	Land Rover				
GM	Opel/Vauxhall	Chevrolet	Opel/Vauxhall	Cadillac					
GM2	Opel/Vauxhall	Chevrolet	Opel/Vauxhall	Cadillac	Saab				
GM3	Opel/Vauxhall	Opel/Vauxhall	Suzuki						
HOND	Honda								
HOND2	Honda	Rover							
HYUN	Hyundai	Kia							
JEEP	Jeep								
JLR	Jaguar	Land Rover							
LADA	Lada								
MAZD	Mazda	Xedos							
MCLA	McLaren								
MERC	Mercedes								
MERC2	Mercedes	Infiniti							
MERC3	Smart	Renault							
MERC4	Mercedes	Jeep							
MGR	Micro	Rover							
MIT5	Mitsubishi	Kia	Hyundai						
MIT52	Mitsubishi	Smart							
MIT53	Mitsubishi	SsangYong							
MIT54	Mitsubishi	Citroen	Peugeot						
NISS	Nissan	Infiniti							
PAG	Ford	Volvo	Jaguar	Land Rover					
PAG2	Ford	Volvo	Jaguar	Mazda	BMW				
PAG3	Ford	Jaguar	Land Rover	Fiat					
PORS	Porsche								
PSA	Peugeot	Citroen	DS Automobiles						
PSA2	Peugeot	Citroen	DS Automobiles	Opel/Vauxhall					
PSA3	Peugeot	Citroen	Volvo						
PSA4	Peugeot	Citroen	DS Automobiles	Mini					
PSA5	Peugeot	Citroen	Ford	Opel/Vauxhall	Toyota	DS Automobiles			
PSAF	Peugeot	Citroen	Ford	Mini	Volvo	Mazda	Suzuki	Fiat	
PSAV	Peugeot	Citroen	Fiat						
RENA	Renault								
RNM	Renault	Nissan	Mitsubishi	Dacia	Datsun	Lada			
RNM2	Renault	Nissan	Mercedes	Dacia					
RNM3	Renault	Nissan	Dacia	Smart					
RNM4	Renault	Nissan	Opel/Vauxhall						
RNM5	Renault	Nissan	Opel/Vauxhall	Fiat					
SAAB	Saab								
SUBA	Subaru								
SUZU	Suzuki	Suzuki							
SUZU2	Suzuki	Nissan	Opel/Vauxhall						
SUZU3	Suzuki	Fiat							
TOYO	Toyota								
TOYO2	Toyota	Daihatsu	Lexus	Subaru					
TOYO3	Toyota	Peugeot	Citroen	Daihatsu	Subaru				
TOYO4	Toyota	Nissan							
TOYO5	Toyota	Aston-Martin							
TRIT	Chrysler	Mini							
VAG	VW	Audi	SEAT	Skoda	Lamborghini	Porsche			
VAG2	VW	Audi	SEAT	Skoda	Jeep	Dodge			
VAG3	VW	Man							
VOLV	Volvo								
VARI									

The association of alliance codes and particular engines will be regularly updated as new vehicles come to market.

## 5.2 Generate the AEM

The method of AEM generation is dependent on the data available. A manual for the generation of base maps based on CO<sub>2</sub> and vehicle speed (and RPM if available) is given in Section 10.4, while an outline is given below. Outlines for generating the cold start extra emissions and deterioration augmentations are given in Sections 5.2.3 and 5.2.4.

### 5.2.1 Generating the base layer - hot engine tailpipe emissions

Tailpipe emissions for a given vehicle can generally be related to engine speed and engine load, and (related to the aftertreatment for most Euro 6 diesel vehicles) a historic component describing the temperature level of the SCR system. Vehicles with the same engine/exhaust gas aftertreatment combination should have similar emission behaviour with respect to the hot emissions layer. Therefore, the full engine block code is chosen as the distinguishing identifier. Note that aftertreatment behaviour is highly software dependent which would require further investigation.

The emission maps are intended to be used in tools that simulate emissions of trips, e.g. to evaluate the improvement potential by changing driver behaviour. Vehicle speed profiles can be produced in many ways, without the necessity to read data from the vehicle's CAN bus. In order to also be able to share this data, a second design option is also available for the hot emissions layer, based on vehicle speed instead of engine speed. Note that the actual emissions at a given speed depend on the selected gear, which means that the map based on vehicle speed cannot represent all situations but only driving with "average" gear shift behaviour, where "average" is related to the gear shifting used in the measurement data with which the AEMs were generated.

Engine load, the second parameter to which tailpipe emissions can generally be related, is not always available. The CO<sub>2</sub> emission rate is chosen as the y-axis for NO<sub>x</sub> AEMs, as CO<sub>2</sub> is a good proxy for the engine power demand which will vary with acceleration, payload, road slope and wind. In the case of limited data (test cycle data only), the CO<sub>2</sub> emission can be estimated by estimating 'power' using payload and test cycle characteristics such as velocity profile with the equations of vehicle longitudinal dynamics.

The first maps depict NO<sub>x</sub> and are based on the TNO monitoring program<sup>7</sup> of a Volkswagen Caddy (2018), see Figure 5.1. The graph on the left-hand side has engine speed as an x-axis, the one to the right is based on vehicle speed.

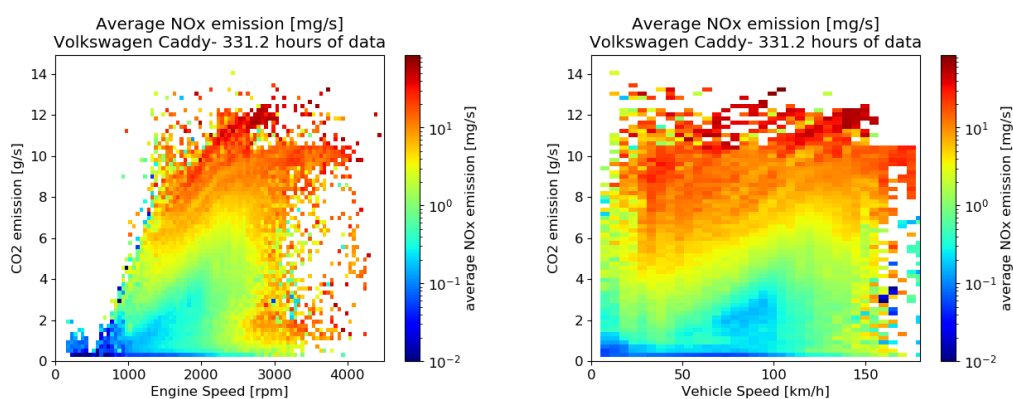


**Figure 5.1. Emission map of average NO<sub>x</sub> mass flow of a Euro 6 Volkswagen Caddy with a 1968 cc 55kW engine(D\_6\_1968\_55\_VAG), based on over 300 hours of driving data**

The explanation of how to use the map was given in Section 3.2.

<sup>7</sup> Measurements were done using the Smart Emissions Monitoring System (SEMS) [11]

Similar maps can be made for PN, CO and HC. Figure 5.2 shows an example of a CO map.

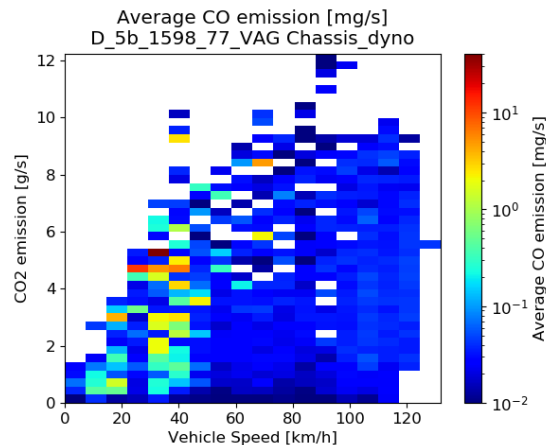


**Figure 5.2. Emission map of average CO emission mass flow of Euro 5b Ford Fiesta with a 1598 cm<sup>3</sup> 77 kW engine**

Emission maps of this design can be created for each engine block. However, for most engine blocks less than 300 hours of data is available. This does not have to hamper the usability of the emission maps, as long as map coverage is warranted, and the resolution is adjusted in an appropriate way. Mathematical solutions to this end are described in Section 8.1.

### 5.2.2 Non-regulated tailpipe emissions

Emissions of NO<sub>2</sub>, N<sub>2</sub>O, PAH, CH<sub>4</sub>, cyanides and NH<sub>3</sub> can be mapped over the most suitable variables, based on chassis dynamometer tests where more extensive analyser equipment is used (e.g. FTIR). PEMS tests usually record, additionally to NO<sub>x</sub>, also NO and NO<sub>2</sub> separately. An example NH<sub>3</sub> map (based on CO<sub>2</sub> and vehicle speed) is shown in Figure 5.3. Note that the independent variables for other emissions can still change as more information becomes available.

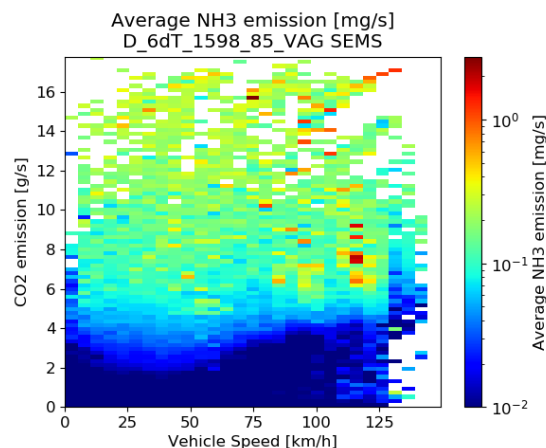


**Figure 5.3. Emission map of average NH<sub>3</sub> mass flow of a Euro 6 diesel vehicle with 1598 cc 85 kW VAG engine, based on 67 hours of driving data**

### 5.2.3 Generating the cold start augmentation

The cold start augmentations contain the vehicle parameters ( $m, f_0, f_1, f_2$ ) and the model parameters ( $w_p, w_n, w_0, Q_{in0}, n_0, q_1, q_2, t_{1X}, t_{2X}, t_{3X}, m_{1X}, m_{2X}, m_{3X}, m_{4X}$ ) needed to solve the equations of the cold start model.

It is important to note that the vehicle parameters reported in the cold start augmentations are characteristic to the specific vehicle make and model used to parametrize the model (not to the engine code) and are only reported for transparency purposes. If the specific vehicle parameters are unknown, we suggest using the average vehicle parameters reported in the corresponding fallback maps.

In the following we describe how the model parameters can be determined from emissions measurement data (model parametrization).

Within the uCARE project we explored several approaches to generate the model parameters based on the availability of measurement data. As shown in Figure 5.4, depending on their origin we differentiate between three types of model parameters: specific parameters, optimized parameters, and fallback parameters.

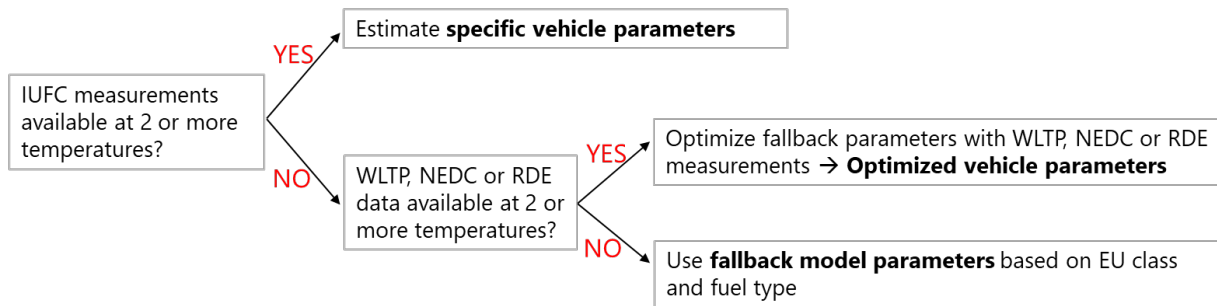


**Figure 5.4. Model parametrization paths**

#### *Specific model parameters*

Vehicle specific parameters can be obtained using chassis dynamometer emission measurements of repetitive cycles, following the approach described by Weilenmann et al. [5]. The repetitive test cycles consist of a short driving pattern (sub-cycle) that is repeated several times, so that the first repetitions characterize the cold start, while the last repetitions represent the hot running conditions. In the following we will describe the model parametrization using the IUFC driving cycle, which consists of 15 repetitions of the same sub-cycle, and for which we consider the sub-cycles 10 to 15 to be representative of the hot running conditions.

The chemical input power released in the combustion process ( $Q_{in}$  [W]) can be estimated from the measured  $CO_2$  and  $CO$  exhaust mass flows ( $m_{CO_2}$  [g/s] and  $m_{CO}$  [g/s], respectively):

$$Q_{in} = m_{CO_2} * \left( LHV_{fuel} \frac{MM_{fuel}}{MM_{CO_2}} \right) + m_{CO} * \left( LHV_{fuel} \frac{MM_{fuel}}{MM_{CO_2}} - LHV_{CO} \right) \quad [5.1]$$

where  $LHV_{fuel}$  [J/g] and  $LHV_{CO}$  [J/g] are the lower heating values of the fuel and  $CO$ , and  $MM_{fuel}$  [g/mol] and  $MM_{CO_2}$  [g/mol] are the molar mass of the fuel and  $CO_2$ .

Next, using only the results from the sub-cycles 10 to 15 (i.e.  $Q_{in_{hot}}$  [W]), we can estimate the model parameters  $w_p, w_n, w_0, Q_{in0}, n_0$  by solving the corresponding functions reported in the engine model for hot running conditions. Once these parameters have been calculated, the same functions can be used to calculate  $Q_{in_{hot}}$  over the full cycle.  $\Delta Q_{in}$  [W] can then be calculated as the difference between  $Q_{in}$  and  $Q_{in_{hot}}$  and can be used to

determine the model parameters  $q_1$  and  $q_2$  by solving the equations from the engine model for cold start.

Thanks to the repetitive nature of the test cycles, the cold start duration can then be determined experimentally for each pollutant using the so-called "gradient method", in which the cold start end is set to the point for which the gradient (growth) of the cumulated emissions becomes constant. Once the end of the cold start is set, the cold start extra emissions of the measured pollutants can be determined by subtracting the average hot emissions (from the sub-cycles 10 to 15) from the total measured emissions. The measured cold start duration and cold start extra emissions are then used to fit the model parameters of the cold start duration model ( $t_{1X}$ ,  $t_{2X}$ ,  $t_{3X}$ ) and the pollutants model ( $m_{1X}$ ,  $m_{2X}$ ,  $m_{3X}$ ,  $m_{4X}$ ).

A least-squares optimization method can be used in all cases to solve the model equations and determine the model parameters. In addition, in the engine model for the cold start and in the pollutants model the integrated signals ( $\int Q_{in}$  and  $\int dmX$ , respectively) can be used to increase the solution robustness.

Due to the strong dependence of the extra emissions with the ambient temperature, measurements of a repetitive cycle at, at least, two different ambient temperatures are required to parametrize the model with this method.

This procedure was applied to parametrize the model for 30 petrol and 30 diesel passenger cars of various euro classes for which IUFC measurements at 2 or 3 temperatures have been performed at Empa within the emission factors measurement program commissioned by the federal agency of environment (BAFU). For these 60 cars the vehicle specific parameters are reported in their respective augmented emission maps. In addition, these IUFC measurements were also used to compute the fallback model parameters based on the euro class and the fuel type that are used in the following.

#### *Optimized parameters*

The main drawback of the method described above, is the limited availability of measurements of repetitive cycles, especially at different ambient temperatures. Because the goal of the uCARe project is to estimate the emissions for a large number of vehicles, an approach to parametrize the model with more readily available measurements was developed. This approach includes the possibility to use more extensively used chassis dynamometer cycles, such as the New European Driving Cycle (NEDC) or the Worldwide Harmonized Light Vehicles Test Cycle (WLTC), as well as real driving emission measurements (RDE). The main idea behind this approach is to use the fallback model parameters for the engine models (for hot running conditions and cold start) and for the cold start duration model, and only optimize the parameters of the pollutants model, as those were found to vary the most between different vehicles in the same category (euro class and fuel type). To do so, we solve again the equations of the pollutants model using the fallback parameters as the initial guess and letting them vary within certain limits. The optimized parameters are obtained by minimizing the difference between the measured and modelled cumulated extra emissions. The measured cold start extra emissions are estimated by subtracting the average hot emissions from the total measured emissions. The hot emissions can be approximated, depending on the measurement type, as:

- NEDC: average emissions in the 4<sup>th</sup> repetition of the ECE-15 sub-cycle (between 585 and 780 seconds from test start)
- WLTC: average emissions in the 2<sup>nd</sup> sub-cycle (between 589 and 1022 seconds from test start)
- RDE: average emissions between 600 and 1000 seconds from test start (which corresponds to the IUFC sub-cycles 4 to 6) including only urban driving conditions (i.e.  $v < 60$  km/h)

Note that, as for the specific vehicle parameters, to obtain optimized vehicle parameters we need measurements at, at least, two different ambient temperatures.

In this case the cold start augmentations contain the fallback parameters from the euro class and fuel type for the two engine models and the cold start duration model, and the optimized parameters for the pollutants model.

#### *Fallback parameters*

When test data to parametrize the cold start model for single engine families is not available or is insufficient, we can still estimate the cold start extra emissions using the fallback parameters from the corresponding euro class and fuel type, which are reported in the fallback cold start augmentations. The fallback cold start augmentations were computed using the average of the IUFC measurements of all the vehicles within a given category (euro class and fuel type) and applying the standard procedure described earlier for specific model parameters.

However, our results show a high variability between the cold start extra emissions of different cars within the same euro class, especially at low ambient temperatures.

**Therefore, results obtained using the average model parameters need to be evaluated with caution and should only be considered as indicative.**

#### **5.2.4 Generating the deterioration augmentation**

Emission deterioration data is difficult to obtain since repetitive measurements on the same vehicle for long periods of time are needed with big intervals of accumulated vehicle mileage, for example every 50,000 km a vehicle needs to be measured. Remote sensing is a solution that has the potential to dissolve this problem, since it can provide both emission and registration information for a large car fleet. This gives the opportunity to categorize each vehicle according to fuel type and Euro class and acquire information for the vehicle mileage (or age).

Remote sensing technology is, in certain respects, the opposite of PEMS testing. Although limited data is collected on each vehicle, emissions from thousands of vehicles can be measured in a single day. The snapshot of the exhaust plume content collected from a passing vehicle is equivalent to about one second's worth of emissions data for a single operating condition, but over time many hundreds or thousands of such snapshots can be collected for a given vehicle model. The aggregate result is a quite accurate picture of the exhaust emissions of that vehicle model over time and over a range of operating conditions. Combined with the non-intrusive nature of remote sensing, as the vehicle does not "know" it is being tested, remote sensing is a particularly good solution for market surveillance. It can quantify the emissions of individual vehicle models, evaluate the impacts of environmental and driving conditions, and track emissions deterioration over time [12].

The key information of deterioration is from remote sensing. Within the CONOX project the remote sensing data of multiple projects has been analysed for deterioration effects. These results from CONOX have been used to update the HBEFA emission factors. This data was deemed the most reliable (see also Section 12.3) and was chosen for the current set of deterioration factors. The implemented data includes information from Euro 1 to Euro 6, mileages up to 300,000 km and includes the CONOX data. Graphs are provided in Figure 12.16 to Figure 12.21 for visualisation of the comparison.

Petrol and diesel NH<sub>3</sub> emissions were also examined via remote sensing data, as shown in Figure 12.22 and Figure 12.23. All diesel values have either a negative value or a peculiar trend. As for the petrol values, with exception of Euro 6, the trend appears to fluctuate. Even the Euro 6 values which appear to display a somehow consistent trend, have limited values as they correspond to only 5 years of data, with the fifth year exhibiting large dispersion.

### 5.3 Ensure consistent version control and name your files correctly

Correctly naming your AEM includes the engine code, as well as the organisation generating it: *Engine.Org-vx.map.txt*, where *Org* is your organisation and *x* is the version number. Examples of this include:

- D\_5a\_2231\_110\_TOYO2.Empa-v1.map.txt
- P\_3\_ALL\_ALL\_ALL.TNO-v2.map.txt
- E--P\_6\_1998\_135\_BMW.LAT-v1.map.txt
- P\_6dT\_1591\_97\_HYUN.TUG-v1.map.txt

It is your responsibility to ensure consistent version control. As the selection tool scans available AEMs, it will print several metadata fields including the notes. For this reason, we suggest that the notes field can be used to describe the measurement conditions (e.g. temperature range), measurement source, or changes/differences with other versions. For example, in the case of bi-fuels, v1 may contain maps related to one fuel, while v2 contains maps related to the other fuel. You can also take Zenodo versioning into account when assigning file names (see also <https://help.zenodo.org/#versioning> ). An organisation can decide if an update is worth just a new Zenodo version, or a new entry with v+1.

### 5.4 Upload the data to Zenodo

The OpenAire platform Zenodo facilitates the sharing of open scientific data. AEMs should be uploaded to the uCARE community:

- If you have not already done so, you will need to sign up for a Zenodo account.
- You can choose to upload your data together in one go, or as several different uploads.
- When uploading your data, type and select uCARE in the 'Communities' field.
- There is a range of metadata corresponding to the upload you are required to fill in. This includes author(s), a title, and a description.
- Make sure to select the 'Open Access' option for the 'Access right' under the 'License' heading.
- Once uploaded, you can upload a new version of an uploaded file (to do this you'd need to create a new version of the associated record, see also <https://help.zenodo.org>).

## 6 Conclusions and recommendations

To characterise, store and distribute emission data of vehicles, an emission map concept has been proposed. Experiment-based understanding of the relationship between the use of a vehicle and the emissions are described in a logical and structured way, be it in the form of a map or in the form of a function. Maps or functions can be created on any level of the vehicle taxonomy (D1.1), dependent on distinctiveness and availability of data.

A strict separation of factual data and interpretation has been pursued. Interpolation and smoothing of maps, as well as the implementation of the functions in the AEM, is considered part of the tools that use the maps/functions.

A file exchange format known as an augmented emission map (AEM) was developed, that can hold meta-information about a vehicle or engine, emission maps and functions. The naming of the files is laid down in this deliverable and is based on an abbreviation of the taxonomy variables.

The AEM concept currently distinguishes the following layers:

- Tailpipe emissions under hot engine conditions: NO<sub>x</sub>, PN, CO, HC
- Tailpipe emissions of non-regulated emissions: NO<sub>2</sub>, N<sub>2</sub>O, PAH, CH<sub>4</sub>, cyanides, NH<sub>3</sub>
- Tailpipe emissions under cold start conditions: NO<sub>x</sub>, PN, CO, HC
- Deterioration: additional tailpipe emissions because of ageing and/or poor maintenance: NO<sub>x</sub>, PN, CO, HC, NO<sub>2</sub>, N<sub>2</sub>O, PAH, CH<sub>4</sub>, cyanides, NH<sub>3</sub>

The dimensions of maps can vary for each layer, dependent on which parameters describe the emission behaviour best. For hot engine tailpipe emissions, vehicle or engine speed, and CO<sub>2</sub> emission mass flow (as a proxy for engine power) were selected. The maps are produced on an engine code level: vehicles sharing the same engine code are modelled in the same way. To handle a varying data availability among vehicle types or engine types, maps have a flexible resolution. The map resolution that is selected, complies to minimum standards in terms of coverage.

New findings from experiments may give insights not yet incorporated in the present description. We do note the following:

- Non-tailpipe emissions experiments highlight the need for more experiments and measurements to quantify the relationships between driver behaviour and non-tailpipe emissions.
- Independent variables for (non-regulated) pollutant emissions can still change as more information becomes available.
- The relationship between recent driving and current emissions is still unclear.
- Incidentally high emissions remain difficult to predict as their cause is often not discernible.

---

## Part 2: Reference information

### 7 Cutting-edge non-tailpipe emission experiments form the foundation on which further AEM work can be built

As opposed to the detailed, standardised *engine* emission tests, the experimental data that is available for *non-tailpipe* emissions either describes very specific cases or does not report conclusive relationships between uCARE-relevant parameters and non-tailpipe emissions. For this reason, we have supplied general recommendations in Section 2.6. Here we present an overview of the current state of knowledge on brake and tyre wear, as well as new results of the cutting-edge non-tailpipe emission experiments that were performed.<sup>8</sup> The overview and experiments further highlight the need for more experiments and measurements to quantify the relationships between driver behaviour and non-tailpipe emissions.

#### 7.1 Non-tailpipe emissions – brake wear

##### 7.1.1 Introduction

Friction brakes are currently the most common way to decelerate and stop road vehicles. Two common designs are used

- disc brakes, where brake pads are pressed against a cast iron, or steel, disc connected to the rotating wheel,
- drum brakes, where brake shoes are pressed against the inner surface of a rotating cast iron drum.

Brake pads and shoes comprise of a steel structural element, to which a friction lining is attached. The lining material is a complex mixture of binders, fibres, fillers, lubricants and abrasives [14]. During application of brakes, the kinetic energy of the vehicle is transformed to heat. For safety reasons, the brakes are designed with sufficient reserve capacity, so that the main factor limiting the deceleration rate is the adhesion of the tyre to the road surface. Both friction surfaces wear with use and are replaced periodically, with frequency depending primarily on the operating patterns of the vehicle.

The wear particles comprise of larger particles generated by physical abrasion of the material, and smaller particles formed by condensation of vapours resulting from high temperatures at friction surfaces (material volatilized at high temperature and newly formed compounds). The larger particles originating from mechanical processes are of diameters of several micrometres and higher. The smaller particles are typically nanoparticles with a diameter on the order of 10 nm formed by nucleation, with larger particles formed by condensation, coagulation and other processes (see [15] for a review for aerosol physics).

##### 7.1.2 Overview current knowledge on brake particle emissions

###### *Literature*

Until recently, there has been only a small number of studies evaluating the brake particle emissions. Approximately 40% of the particle mass was reported to be particles with an aerodynamic diameter smaller than 10  $\mu\text{m}$  ([14, 16] and references therein). Particle size distributions reported by Zum Hagen et al. [17], show peaks around 10 nm and 2-3  $\mu\text{m}$ ,

---

<sup>8</sup> The brake wear experiments have also been described in detail in [13].

suggesting that these are the most frequent sizes of particles from high temperature and mechanical processes, respectively.

On one set of brake pads and rotor studies by Zum Hagen et al. [17], the total number of particles emitted remained relatively very low below a certain threshold brake pad temperature, beyond which the particle number per stop increased exponentially with increasing temperature. No relationship between the particle number and either the total energy dissipated was observed. The total particle mass, on the other hand, did not correlate to the brake pad temperature, but increased (not linearly) with the total energy dissipated during the stop. The threshold temperature varied from 140 to 170 °C and gradually increased with consecutive tests. [16] report a similar observation, but with the higher temperature at which low metallic pads emit large quantities of nano-size particles, around 300 °C. Also, when milled sample of the pad material was heated to 300 °C, ignition of carbonaceous material was observed.

Mathissen et al. [18] report observations from two braking cycles developed to mimic real-world operation, a short, 3-hour version of the Los Angeles City Traffic cycle, and a newly developed WLTP braking cycle based on the collection of driving patterns used for the development of the World Harmonized Light Vehicle Test Procedure. Over the 3h-LACT cycle, the particle number stays relatively low below brake pad temperature of about 170 °C and increases exponentially with temperature for higher temperatures. For the entire WLTP cycle, the brake pad temperature is below 170 °C and no increase in particle number emissions is observed.

#### *New insights from uCARE*

In the uCARE project, a larger set of brake tests conducted within the Czech Science Foundation project focused on the production of antimony containing compounds during friction braking and their subsequent fate in the environment was analysed for the effect of braking conditions on particle production. As an example, data are presented from tests of two sets of brake pads for a popular (by frequency of vehicle registration) mid-range passenger car in the Czech Republic. One set is an "OEM" pad (original equipment manufacturer, pads supplied by the manufacturer-associated dealer as original replacement part), the other set is a typical aftermarket set of brake pads, representing the middle price range (neither low-cost nor premium or performance pads). (Note: A total of three aftermarket pads were tested.)

All data represent the total number of particles, including semi-volatiles, measured by an electric mobility classifier (Engine Exhaust Particle Sizer).

The relationship between the brake rotor temperature, both average over the braking event and final at the end of the braking, and particle production for stops from 40, 80 and 120 km/h is shown in Figure 7.1 for the OEM pads and in Figure 7.2 for the aftermarket pads, more or less confirming the general exponential relationship observed in [18].

The situation is not, however, straightforward. Figure 7.3 shows that during braking from 80 km/h to 40 km/h and from 80 km/h to 30 km/h, particle production starts increasing once a threshold braking power is reached, despite (see Figure 4.1) not much effect on average or final rotor temperature. The situation is far less clear for 120 to 80 km/h braking sequence, run with increasing intensity of braking.

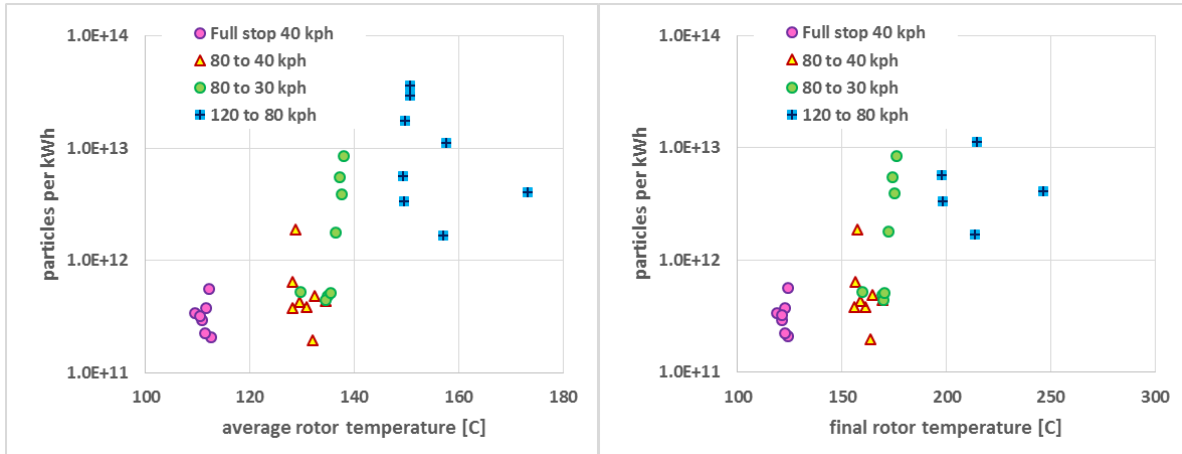


**Figure 7.1. Effect of average (left) and final (right) rotor temperature on particle production (normalized per kWh of braking power dissipated) – OEM pads**

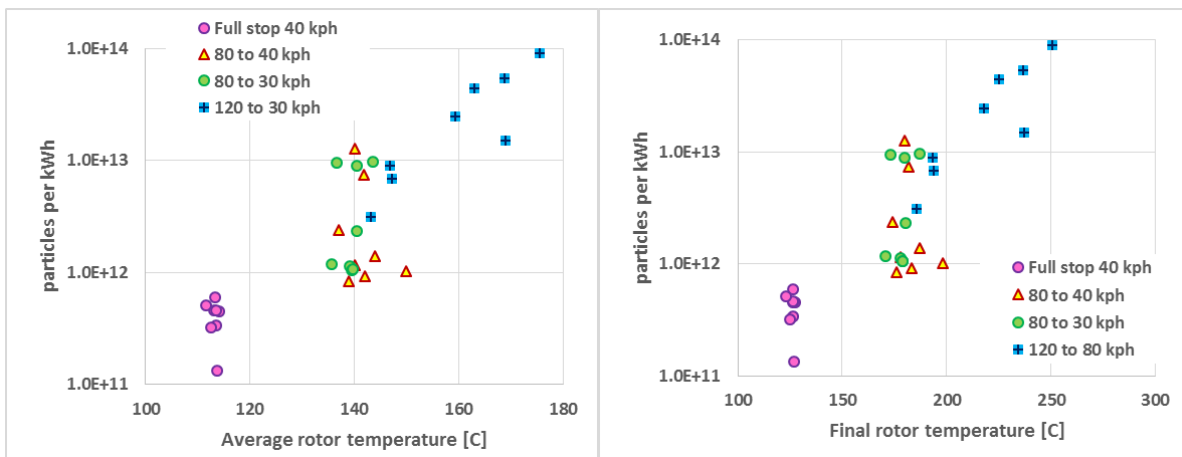


**Figure 7.2. Effect of average (left) and final (right) rotor temperature on particle production (normalized per kWh of braking power dissipated) – aftermarket pads**

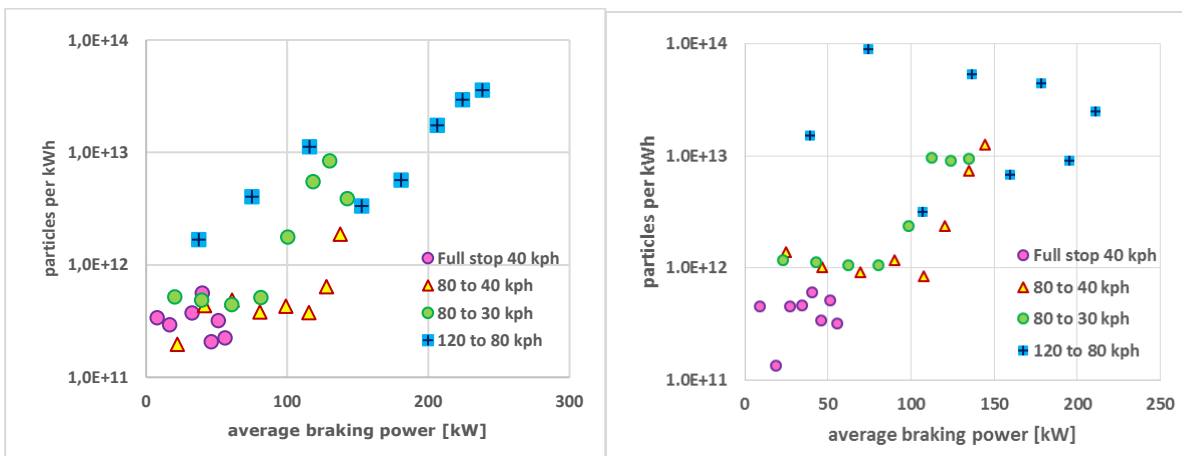


**Figure 7.3. Effect of average braking power on particle production (normalized per kWh of braking power dissipated) – left: OEM pads, right: aftermarket pads**

Likewise, aggregate data from a wider range of braking events, typically more intensive than braking in WLTP and LATC cycles, but still considered reasonably realistic for everyday driving, shown in Figure 7.3, suggests that the particle production is generally higher at both higher average braking powers and higher rotor temperatures at the end of the braking event. However, a range of braking events with final rotor temperature well over 200 °C is not associated with extreme particle production.

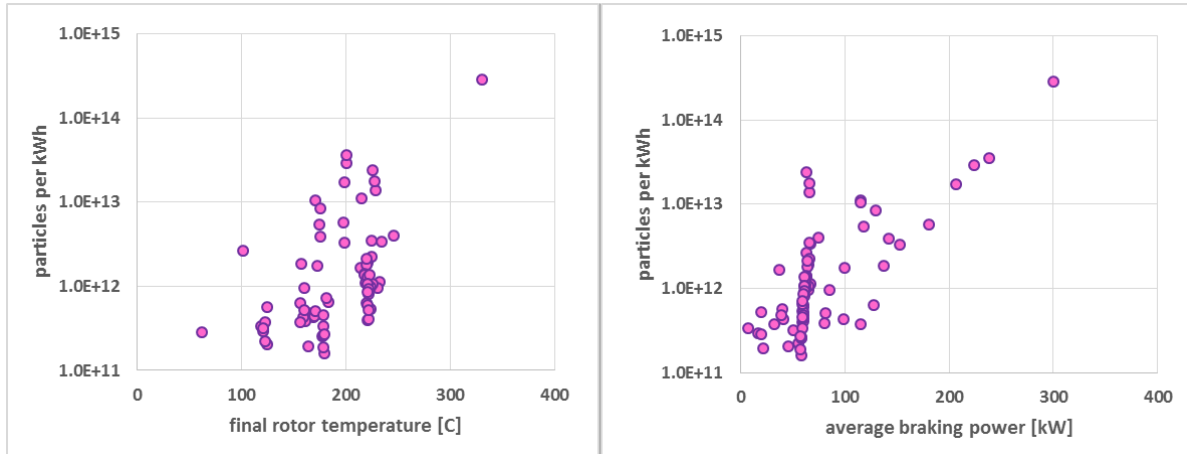


**Figure 7.4. Effect of average braking power (left) and final rotor temperature (right) on particle production (normalized per kWh of braking power dissipated) – a range of conditions – OEM pads**

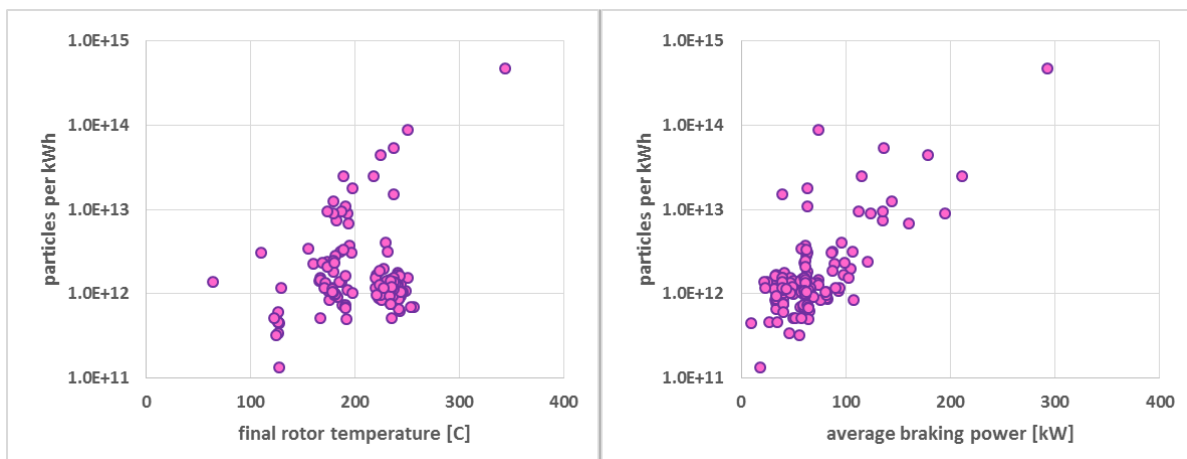


**Figure 7.5. Effect of average braking power (left) and final rotor temperature (right) on particle production (normalized per kWh of braking power dissipated) – a range of conditions – aftermarket pads**

### 7.1.3 Summary

Overall, it appears that when brake temperatures or braking power exceed certain threshold (which likely varies among vehicles, brake designs and brake pad materials), the total number of particles produced increases exponentially with brake temperature.

It also appears that during easy to moderate driving of passenger cars, brake emissions typically remain below  $10^9$ - $10^{10}$  solid particles per stop [18] or, when expressed in kWh, below or around the particle number limit applicable to exhaust emissions.

In this study, the total number includes semi-volatile particles from about 5 nm diameter, hence the number is higher than the number of non-volatile particles measured under the PMP protocol. It should be noted that the aggregate braking power, in kWh, cannot be higher, and is considerably smaller, than the aggregate engine power in kWh over a cycle/route.

## 7.2 Non-tailpipe emissions – tyre wear

### 7.2.1 Tyre wear influencing parameters

Vehicle tyres are complex products both regarding construction and materials. Material composition is highly variable and adapted to the expected use of the tyre. Factors ranging from vehicle class, weight, performance, climate and factors connected to tyre marking (wet grip, noise and rolling resistance) influence the chosen composition of tyre models [19, 20]. All these factors also influence the wear of the tyres and might also influence the ratio of the airborne particles emitted from tyres and their properties. In addition to tyre specific properties, their mounting, maintenance, and use affects the wear through factors like load, inflation pressure and wheel alignment (toe-in/toe-out, camber) [21, 22]. Drivers also influence the tyre wear by their behaviour. High speeds, fast acceleration and retardation, and frequent cornering lead to increased tyre wear [23].

There are also factors outside the influence of the driver's choice or actions that are important for tyre wear, including road surface properties and conditions as well as traffic and infrastructure design and planning. Micro and macro texture, state of maintenance and conditions related to meteorology (dry, wet, snow, ice) all have an influence (e.g. [24–26]). The design of the infrastructure and the traffic composition influence the wear by providing the conditions in which vehicles are driven. Large numbers of traffic lights and congestion can cause frequent acceleration and retardation, and a winding road, or many crossings, results in a lot of cornering. Total tyre wear factors are therefore often reported for urban, rural and motorway conditions, where urban conditions result in higher wear factors and motorway in lower (e.g. [27, 28]).

### 7.2.2 Estimating tyre wear and PM emissions from tyre wear – a uCARE perspective

To measure or estimate the PM emission from tyres involve several difficulties. The total wear can be estimated simply by weighing a tyre before and after having driven a certain distance and divide the weight loss by the distance. Since the weight loss will not only be dependent on the distance driven, but also on the vehicle properties, road alignment, surface conditions and driving behaviour, the estimated wear is only representative for the specific road, vehicle, conditions and driver.

To estimate the PM<sub>10</sub> emission from tyre wear involves multiplication with a percentage of the total wear or measuring it directly in the air under controlled conditions. The percentage can be estimated by collecting the total amount of wear particles and performing a size distribution analysis. Collection of tyre wear in realistic conditions involves sampling behind a wheel while driving. Tyre wear will not be emitted as a separate component but will be mixed with road wear and whatever dust that is already deposited on the road. Due to its sticky properties, tyre wear particles will form aggregates with other particles and form TRWP (tyre and road wear particles). To separate TWP (tyre wear particles) from TWP within PM<sub>10</sub> involves further separation and analyses. Compilations made in e.g. [19, 29] regarding tyre wear emission factors reflects the high variability resulting from different estimation or measurement approaches. Referring to an earlier compilation by Grigoratos and Martini [30], the variability of the PM<sub>10</sub> fraction is 0.1 – 10 %.

The main interests in uCARE are how choice, maintenance and driving behaviour affects the emissions from tyres and, if possible, to use emission maps or functions to implement any observed relations in the uCARE model. **Literature reporting experimental data that can serve as basis for this is very scarce.** Most information is instead to be found within modelling studies. There are a number of numerical models simulating tyre and vehicle dynamics, like e.g. FTire [31] and T.R.I.C.K. [32]. Wear is normally handled in a certain wear model but is seldom in focus in literature. An exception is Wang et al. [33], where numerical simulations of tyre wear were made for a range of tyre parameters. The parameters' relative impact on tyre wear from changes of 25 and 40 % can be seen in Figure 7.6, revealing that vertical load, inflation pressure and rolling velocity are the three

main influencing parameters. While higher vertical load and rolling velocity increases wear, higher inflation pressure reduces wear. Even though higher inflation pressure reduces wear, the authors mention that both too low and too high inflation pressure will increase wear due to abnormal wear or the tyre. These three parameters are possible for a driver to control and affect, which makes them interesting from uCARE's point of view.

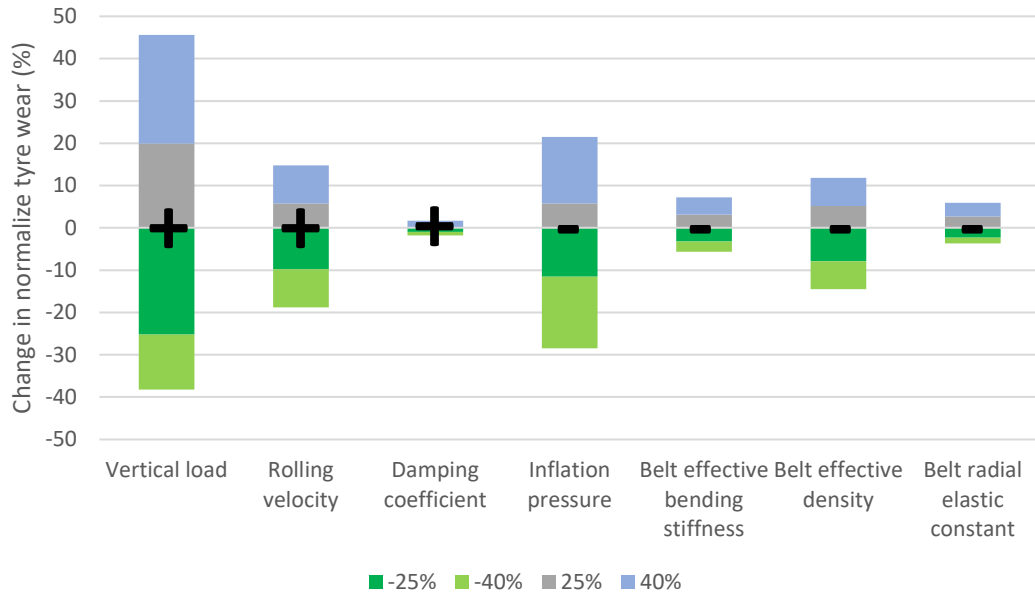


**Figure 7.6. Sensitivity analysis of the effect of tyre parameters on the tyre wear from a  $\pm 25\%$  and  $\pm 40\%$  change in the parameters. Plus and minus signs indicate the sign of the effect of each parameter. After [33].**

In another modelling study by Li et al. [34], the resulting sensitivity analysis indicated that the side slip angle was the most wear-influencing parameter followed by speed, sprung mass, ambient temperature and tyre inflation pressure (see Table 7.1).

**Table 7.1. Parameters sensitivity of tyre wear [34]**

Parameters	$ k_q _{q_0}$	$ k_q _{q_0}$	Orders
Tire pressure	-0.34757	0.34757	5
Ambient temperature	0.44423	0.44423	4
Speed	1.0233	1.0233	2
Sprung mass	0.95291	0.95291	3
Unsprung mass	0.12777	0.12777	7
Suspension stiffness	0.0129	0.0129	10
Suspension damping	-0.03219	0.03219	8
Side slip angle	1.41376	1.41376	1
Tread stiffness	-0.00012724	0.00012724	12
Tread damping	0.000144422	0.000144422	11
Sidewall stiffness	-0.0000884224	0.0000884224	13
Sidewall damping	0.0000050214	0.0000050214	14
Road roughness	0.02477	0.02477	9

Experimental data concerning influence of different tyre and driver parameters on specifically airborne PM emissions is even more rare in literature. Kwak et al [35] used an instrumented car to measure particles behind a front wheel. When on a test track, the emissions were defined as roadway particles (RWP, a mix of tyre wear, road wear, brake wear and suspended dust) and found increasing concentrations at increasing constant speeds up to about 110 km/h, after which the concentration decreased slightly. At a lateral

acceleration of  $3.1 \text{ m/s}^2$ , concentration of PM10 and PM2.5 were about 2 times higher than at 110 km/h constant speed, but at  $5.1 \text{ m/s}^2$  it was 18-23 times higher (Figure 7.7). In a chassis dynamometer, the influence of road dust could be excluded, and it was found that tyre wear particles also here increase with speeds up to 110 km/h but then the increase levels off (Figure 7.7).

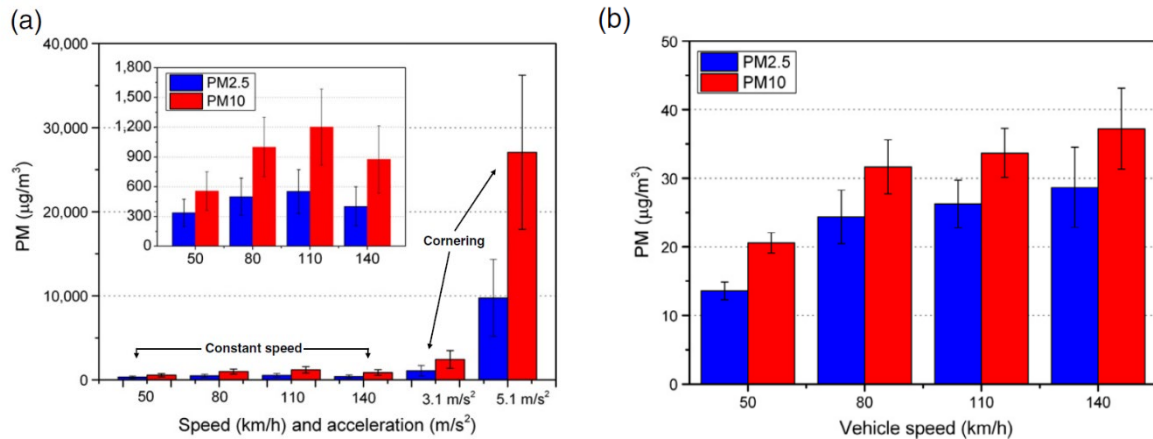


**Figure 7.7. Average PM10 and PM2.5 concentrations of (a) roadway particles under constant speed and cornering conditions, and (b) tyre wear particles during constant speed conditions (n=5, error bars are standard deviation). From [35].**

Cornering induces lateral acceleration, which has been studied by Tonegawa & Sasaki [36]. Using a truck equipped with an extra measurement tyre, they sampled PM10 and PM2.5 emissions from the tyre during different speeds up to 40 km/h and with lateral acceleration up to 0.4 G. Within this speed range they did not notice any emission dependency, while an increasing emission with acceleration was obvious and was fitted using a quadratic equation and considered valid for acceleration in general. The particle emission within a standard driving cycle (JC08) was calculated.

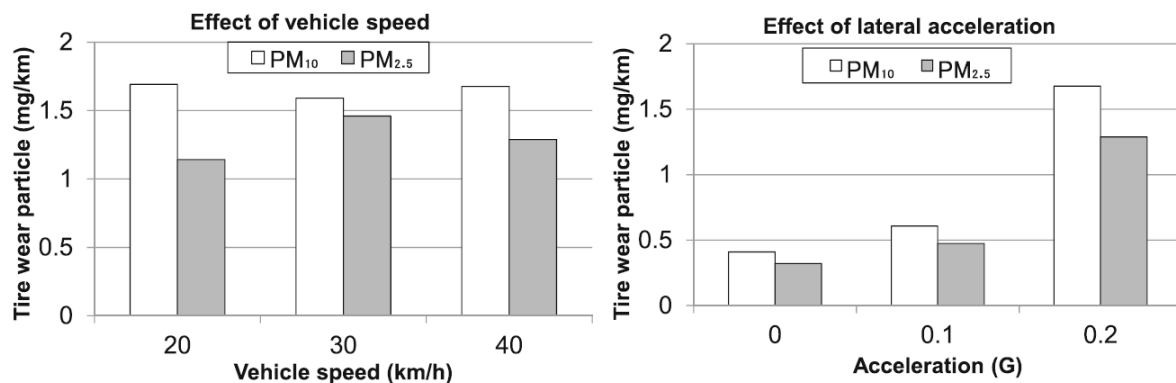


**Figure 7.8. Effect of vehicle speed and lateral acceleration of the tyre on tyre-wear particle generation. From [36].**

Experimental data on effects of load is also rare. Simons [37] suggested, based on data from Ntziachristos and Boulter [38], to combine the parameter  $5,73\text{E}-8 \text{ kg tyre wear/kg vehicle} \times \text{km}$  with gross vehicle weight (GVW) into vehicle specific tyre wear emissions in ecoinvent v3. One of few studies that actually have measured mass loss of tyres during driving was by Luhana et al. [39]. The authors conclude that the tyre weight loss is reduced with increasing mean trip speed, which is likely to reflect that trips at lower speeds involves more stop-and-go traffic and cornering (Figure 7.9). For advising individual drivers in uCARE this information is not useful, since higher speed actually increases emissions of his/her car while driving.

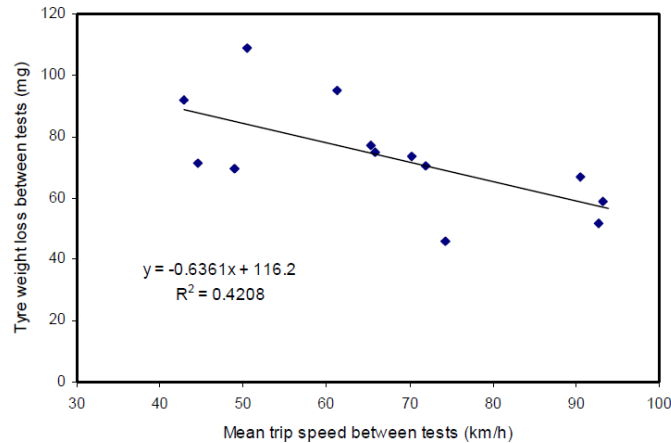


**Figure 7.9. Relationship between tyre weight loss and mean trip speed [39]**

In the EMEP/EEA air pollutant emission inventory guidebook [38], the Luhana et al. [39] results are implemented when calculating tyre wear emissions in a speed correction factor. A load correction factor is also used for HDV's. This factor is multiplied with the emission factor for personal cars and half the number of axles to generate a tyre wear emission factor for HDV tyres. As such, it is not applicable to personal cars and therefore not relevant for uCARe purposes.

### 7.2.3 Tyre wear emission investigations in uCARe

#### *Road simulator study*

To add more to the knowledge on tyre wear influencing parameters, some of the most important parameters possible to study experimentally using the VTI road simulator (Figure 7.10) were investigated in relation to PM10 emission. Speeds ranging from 30 to 70 km/h, loads from 1400 kg to 2200 kg and inflation pressures from 1.5 to 3.5 bars were investigated. The experiments were performed using two sets of tyres, one summer and one winter set. Concentrations were measured and emission factors calculated (see also Gustafsson & Svensson, VTI Memo [40]).



**Figure 7.10. The VTI circular road simulator.**

The results showed that speed increased the emission factors markedly (Figure 7.11), while load only had a small and inconclusive effect (Figure 7.12) and tyre inflation pressure no obvious effect at all (Figure 7.13).

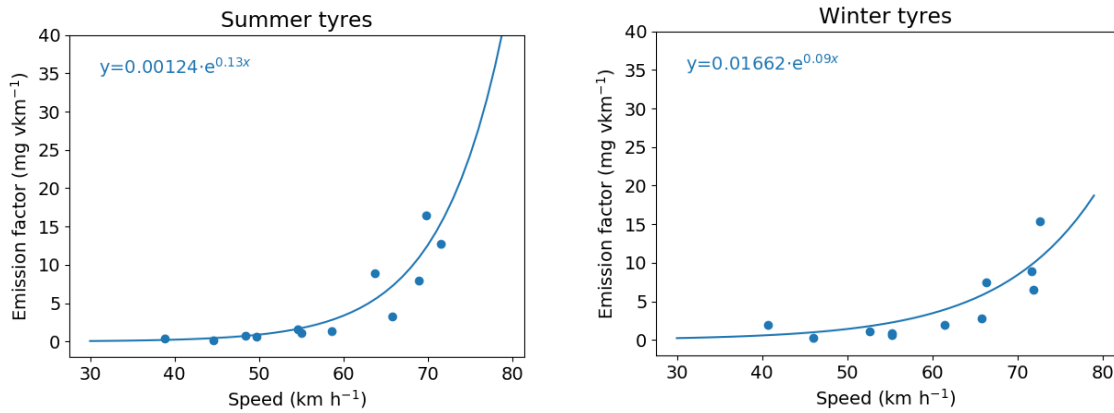


**Figure 7.11. Emission factors calculated for different speeds for a) summer tyres and b) winter tyres. An exponential curve is fitted to the points, with the equation given in the upper left corner.**

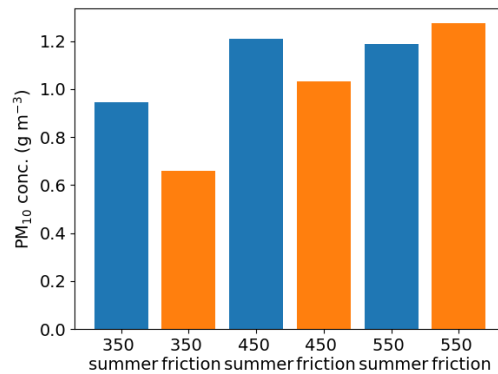


**Figure 7.12. Total, summed PM10 concentration during the experiment for summer and winter (friction) tyres at different loads.**

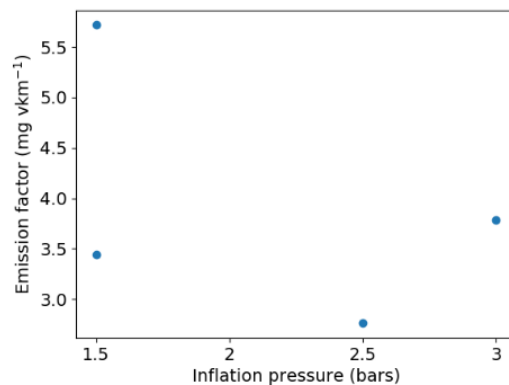


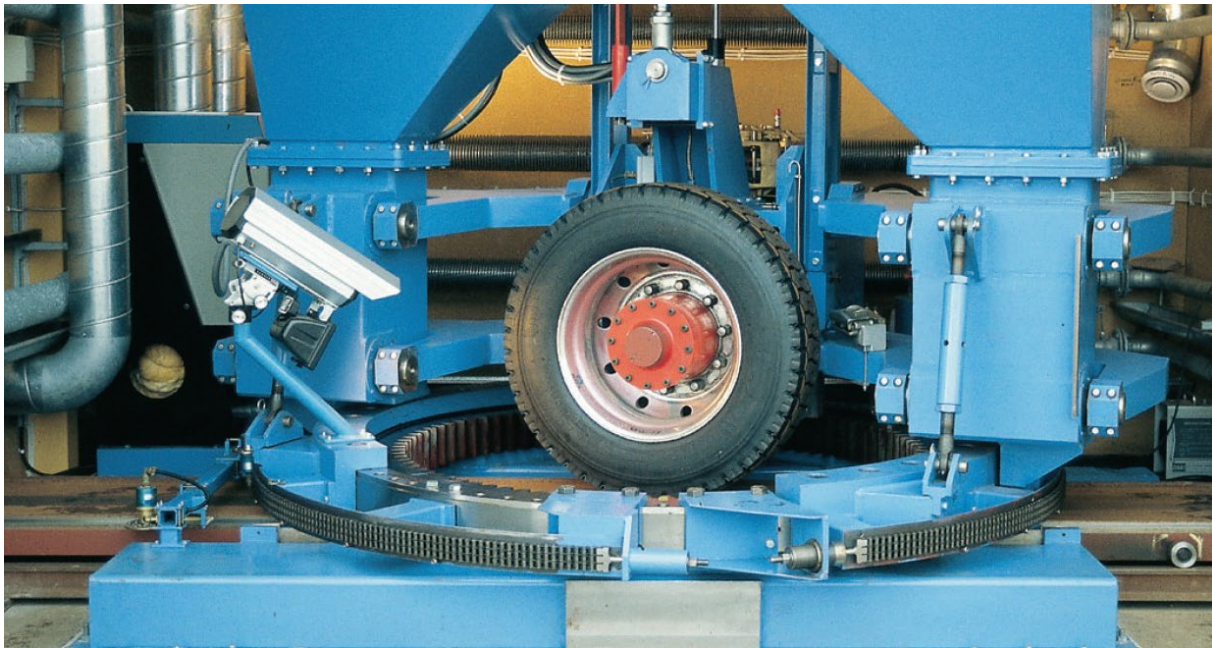
**Figure 7.13. Emission factors calculated for summer tyres for different inflation pressures.**

The reasons for these results can be manifold. The experiments were designed with PM10 emissions in focus: the total wear of the tyres (through loss of mass or tread depth) could therefore not be followed in an optimal way and so it cannot be excluded that the total tyre wear is affected as the models and literature suggest. In that case, the size distribution

must be affected accordingly: a higher total wear means a higher contribution of coarser particles, not contributing to PM<sub>10</sub>. However, support for this has not been found in literature. Another explanation can be that the simplified tyre models used in modelling approaches do not properly model the behaviour of modern tyres' wearing courses. E.g. the lateral deflection resulting from too high or too low inflation pressure, might be much smaller in reality than in models.

#### *Complementing tyre test rig study*

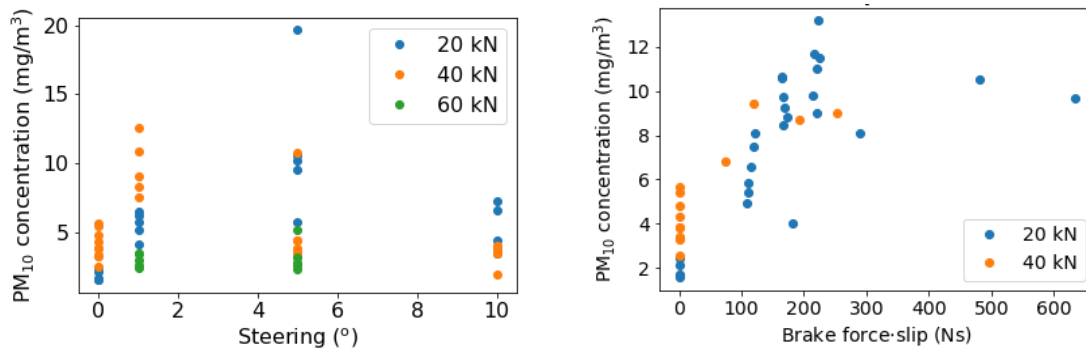
Continued tests in uCARE involved tests in the VTI tyre test rig (Figure 7.14), where a tyre is rolled over a moving surface. The tyre can be braked and steered during the tests, which gives the possibility to measure PM emissions at different braking forces and at different tyre angles. An advantage with this test rig is also the possibility to measure the forces acting on the tyre in three dimensions, which might enable implementation in the uCARE model.



**Figure 7.14. The VTI tyre test rig.**

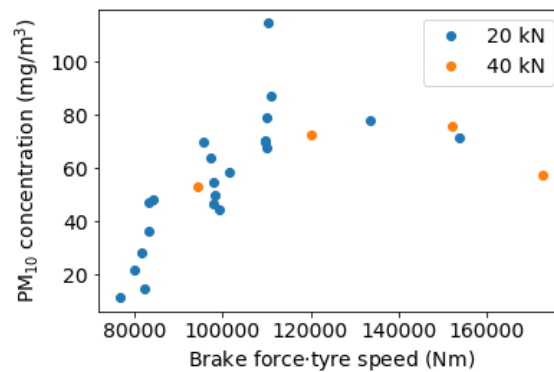
A series of tests were made on a truck tyre with different steering angles, brake force and with and without heating of the tyres. Each event produced a short pulse of particle emissions, which was measured by one DustTrak placed just behind the lower part of the tyre and one next to the brake discs. Each individual event created a pulse of short duration, and the resulting concentration was obtained by summing the concentrations over the duration of the pulse.

Figure 7.15 shows the PM<sub>10</sub> concentration measured by the tyre as a function of steering angle and as a function of brake force times slip. The slip was usually low, i.e. a few percent. The results indicate that the concentrations increase for a small increase in steering angle or brake force, but for higher angles or brake forces the increase levels off or even decreases. One reason for the levelling off may be that heavy steering or braking creates a larger number of particles with sizes larger than 10  $\mu\text{m}$  and are thus not monitored by the instrument. Another possibility could be to the contrary, i.e. that increasing friction heat could result in a shift towards finer fractions, which could also result in a level-off of the PM<sub>10</sub> concentration. Size distribution studies are needed to support or discard these theories.



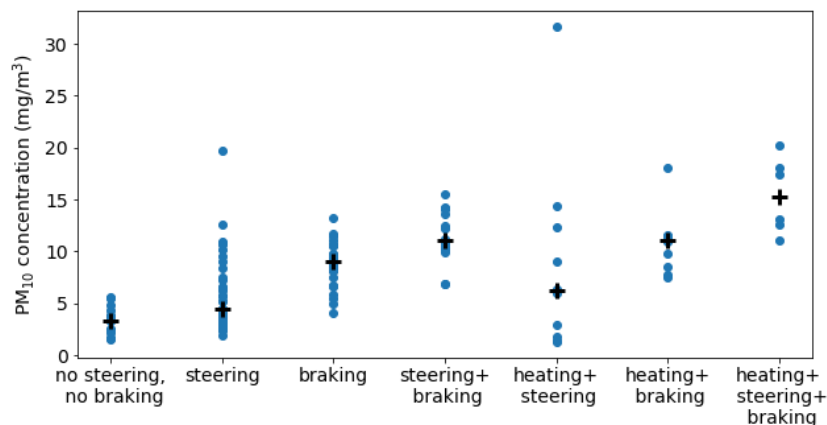
**Figure 7.15. PM10 concentration measured by the tyre as a function of a) tyre angle and b) brake force times slip. The colours denote different loads.**

Figure 7.16 shows the PM<sub>10</sub> concentration measured by the brake discs as a function of brake force times wheel speed. The concentrations are much higher than by the tyre, on average nine times higher. The trend is similar as for the measurements by the tyre. The concentrations increase sharply with small increases in brake force but levels off for higher values.



**Figure 7.16. PM10 concentration as a function of brake force times tyre speed. The colours denote different loads.**

Figure 7.17 shows the PM<sub>10</sub> concentration for all the tests for the DustTrak placed close to the tyre. The steering angle varied between 1 and 10 degrees, the brake force between 3000 and 7000 N and the load between 20 and 40 kN, so variation of concentrations is expected within each group. Nonetheless, it can be seen that the concentrations (and thereby the emissions) increase with steering and with braking compared to no steering or braking, and the increase is highest for a combination of both. The highest overall concentrations are obtained with a combination of heating, steering and braking. The average concentrations measured by the brake discs are also higher for a combination of steering and braking compared to only braking (not shown).



**Figure 7.17. PM<sub>10</sub> concentration by the tyre for a series of tests. The plus sign shows the median of each of the groups.**

The tests in the tyre test rig show some promising results. The effect of steering, braking, heating and load can be measured. As expected, the highest concentrations are found for a combination of heating, steering and braking. However, the trends are most clear for changes in the lower range of the variables, and in order to derive more conclusive results measurements of the size distribution of particles are also needed.

#### 7.2.4 How can current knowledge be implemented in uCARE?

To build relevant emission maps needed for the uCARE model from literature and the experiments performed in uCARE so far, is a challenge. The aim in uCARE is to advise car owners regarding choice and maintenance of tyres as well as on how driving style will influence wear emissions. Since tyre models in use amounts to thousands with no regulations regarding wear marking, and these tyre models then are used on hundreds of different car models with properties that will affect tyre wear, **it is not possible to get individual estimates of wear particle emissions**. The treadwear rate (TWR) marking, found on some tyres, might be a help in choosing tyres for lower emission, but tests have shown that the marking might not be reliable [41]. Tyres sold globally might also wear differently depending on differences in climate and road conditions.

As opposed to the detailed, standardised engine emission tests, the experimental data that could be used (both from uCARE and in literature) differ in methodology and calculation approaches and do not report conclusive relationships between uCARE-relevant parameters and PM emissions. Even though available data suggest that speed and acceleration (see above) affect emissions and model data also that load and inflation pressure affect emissions, some report linear relationships, while others, like in the uCARE tests, report non-linear relationships.

##### *Tentative tyre emission maps*

The following describes an attempt to use the data from simulator tests in uCARE in combination with other sources to produce tentative emission maps where emission is related to speed and vehicle weight.

The best fit to the speed dependency in the road simulator tests showed an exponential relation between PM<sub>10</sub> emission factor and speed, which results in very high emission factors if extrapolated to motorway speeds. This might be an effect of the tight turning in the simulator, also incorporating centripetal acceleration and a slip between tyres and pavement. Furthermore, this relationship seems not to be in accordance with literature. Instead, a power dependence is suggested, which is used in modelling studies by e.g. Salminen [42]. If a power function is used on the road simulator data, the resulting curve fit R<sup>2</sup> are about 0.1 lower than for an exponential fit but are likely to be more realistic. Resulting curve fits from the two tyres tested are seen in Figure 7.18.

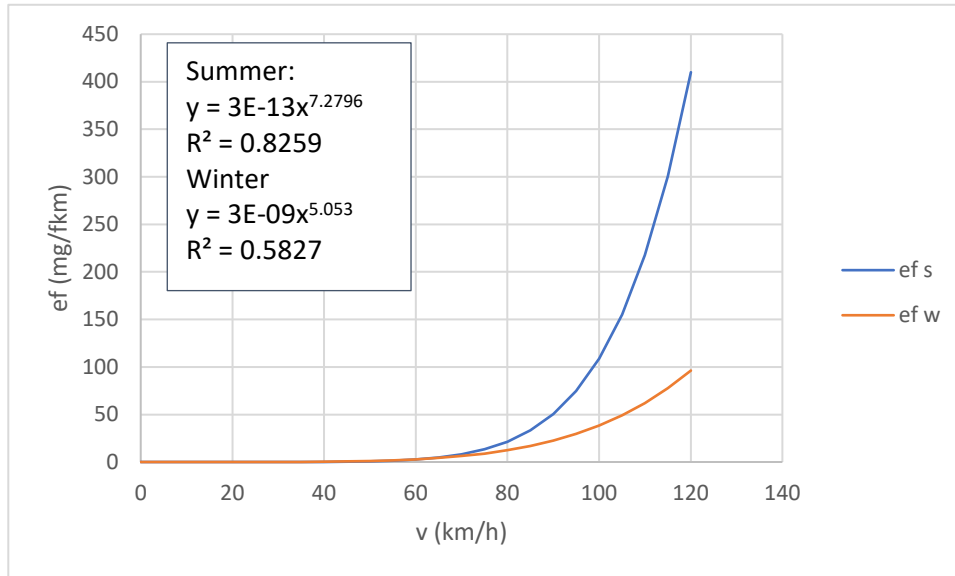


**Figure 7.18. Power law curve fits for data for summer and winter tyres.**

This data is for the standard mass used in the simulator which is 1800 kg. If we use a reference speed and a reference vehicle mass that we connect to an emission factor from the simulator and then use our simulator speed function and a mass function, a speed and vehicle mass emission map could be produced. A suggested tyre wear PM10 emission factor in emission databases is 0.0064 g/vkm [38]. This emission factor is independent of vehicle speed, weight etc. due to the scarcity of data.

Since the emission factor to load relationship in uCARE measurements were inconclusive, we suggest using the function used for the PM10 emission factor relation to load in OECD [43] based on work by Argonne National Laboratory [44]:

$$ef_{tyre} = 4 \cdot 10^{-7} \cdot mass^{1.326}$$

This equation is valid for a reference mass of 1453 kg. If we use the simulator mass of 1800 kg, the resulting reference emission factor is 0.0081 g/vkm. The reference speed is set to 70 km/h and speed function in Figure 7.11 is used to calculate emission factors from 30 to 120 km/h. These are then scaled using the ratio between the emission factor calculated for 1800 kg and ten other weights from 1200 to 2200 kg.

This procedure results in the mass-speed maps in Figure 7.19. The logarithm of the emission factor data has been plotted for better resolution in lower mass and speed ranges. It should be reminded that **these are maps for two specific sets of tyres** and cannot be regarded representative for all summer and winter tyres, but **merely serves as an illustration of possible tyre emission maps**. As can be seen, the speed equation for the summer tyres is steeper than that for winter tyres and generates both lower emission factors at low speeds and higher emission factors at high speeds.

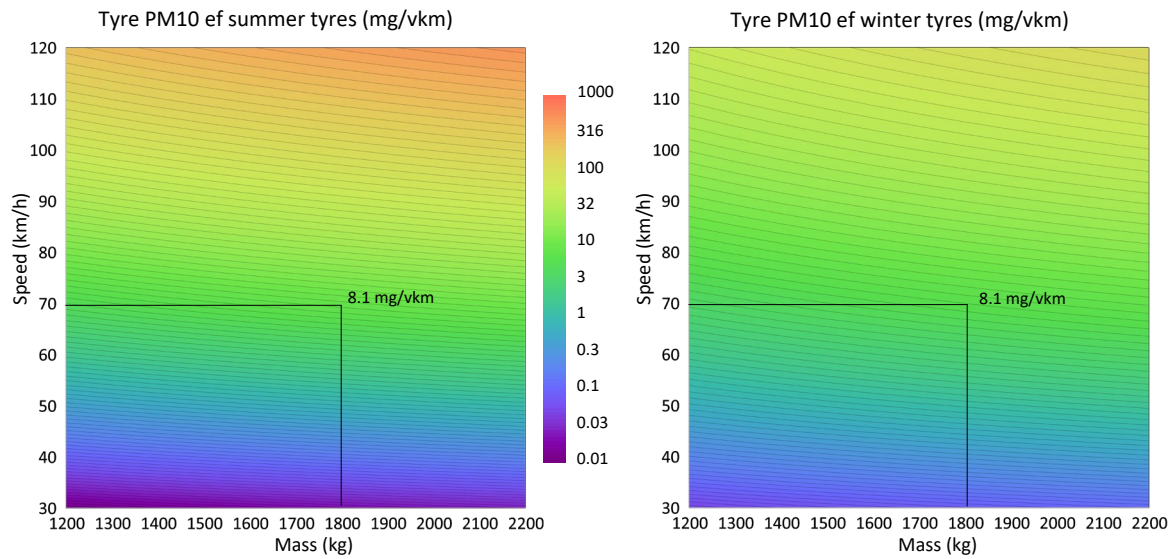


**Figure 7.19. Tentative emission maps for two specific tyre sets tested in uCARE, a summer tyre and a non-studded winter tyre. Maps are based on speed-emission factor relationships from uCARE tests and mass-emission factor function from OECD [43].**

**7.2.5 Comparison with tyre wear in emission inventories**

HBEFA 3.3 [45] uses fixed emission factors for non-exhaust PM for urban, rural and motorway traffic situations including a specific speed range for each road type. These include tyre and brake wear, but not suspension. Since tyre emissions are not specified, the emission factors are not comparable to the emission factors calculated in uCARE experiments.

VERSIT emission factors for the Netherlands distinguishes wear emission on the basis of the forces at the wheel: driving and braking for tyres and road, and braking only for brake emissions. The emissions are distinguished for vehicle categories, and recently they have been made proportional to vehicle weight, as a proxy for differences in power and wear. The data is limited, but comparison with roadside air quality, with attribution to the source, shows it is reasonable.

Also, emission factors do not change with traffic situation speed, but only for traffic situation. The speed influence on emission factor here depends on the traffic situation, i.e. on driving patterns like frequency of stop and go traffic, turning etc, why emission factors rather increase with slower speeds, which is typical for urban driving and vice versa. This approach is not useful from a uCARE perspective, where effect on emissions of individual drivers’ choices and behaviours are in focus.

**Table 7.2. Non-exhaust emission factors used in HBEFA 3.3 [45].**

Vehcat	Unit	EFA_Urban	EFA_Rural	EFA_MW
pass. car	mg/vehkm	54,00	22,00	47,00
LCV	mg/vehkm	54,00	22,00	47,00
coach	mg/vehkm	540,00	144,00	74,00
urban bus	mg/vehkm	540,00	144,00	74,00
motorcycle	mg/vehkm	13,50	5,50	11,75
HGV	mg/vehkm	540,00	144,00	74,00

In the EMEP/EEA handbook Tier II approach [38], the emission factor is valid for 80 km/h and a speed correction factor is used to adjust the emission factor according to mean trip speed. The factor is 1 at 80 km/h. The use of mean trip speed, as in HBEFA, adjusts the emission factor to driving behaviour connected to specific traffic situations rather than to

individual drivers' behaviour. To calculate the emission factors for size fractions of TSP, fixed mass fractions are used. For PM<sub>10</sub>, this is 0.6.

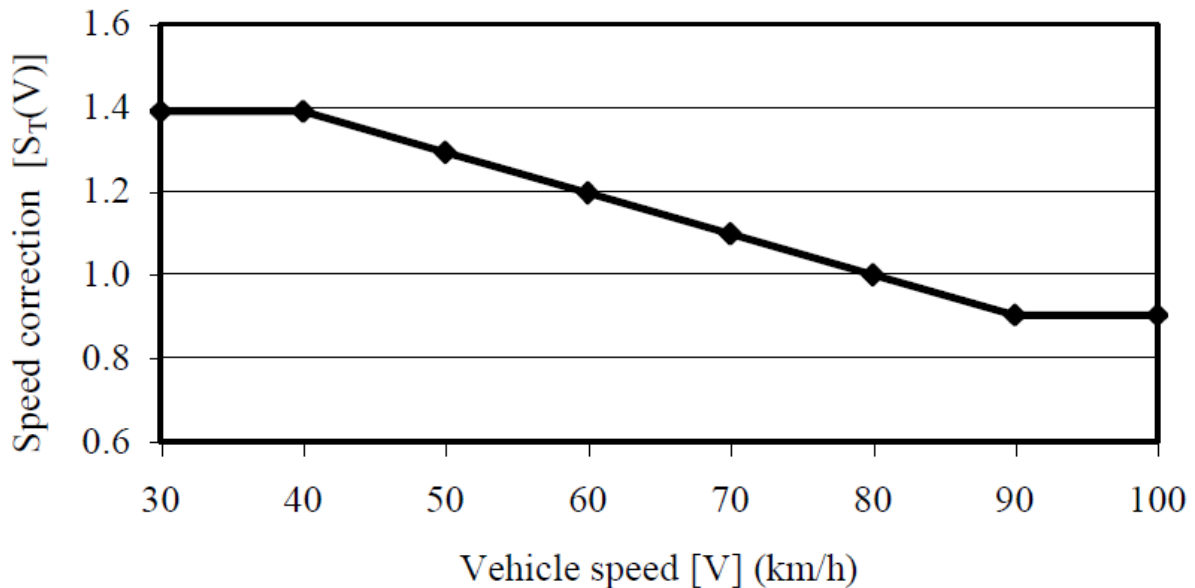


**Figure 7.20. Speed correction factor used in Ntzaichristos & Boulter [38].**

The EMEP/EEA handbook also has a load correction factor (LCF), which is only applied to heavy duty vehicles. The factor scales the emission factors linearly using a load factor (LF) ranging from 0 for an empty truck to 1 for a fully laden truck. Also, the number of axles of HDV's are used in the equation.

The MOVES 2014 model is partially based on one of the very few experimental works available, performed by Luhana [39]. This also shows a (weak) negative correlation between mean trip speed and tyre wear (Figure 7.9).

The decrease in emission rates with increasing mean trip speed in models like the ones above, indicates that the increasing emission with speed valid for individual cars, is overshadowed by the emissions related to acceleration, deceleration, and steering, which is inducing slip in the contact between tyre and pavement. The tyre test rig measurements in uCARE, show a clear increase in TWP generation with increasing brake force and slip, but also the complicating fact that particle emission within PM<sub>10</sub> levels off, indicating that the particles formed change in size distribution, which would affect all particle-fraction-defined emission factors. This hypothesis remains to be tested. If proven correct, tyre particle emissions at all slip inducing manoeuvres will vary in size distribution, so that the fraction of PM<sub>10</sub> and PM<sub>2.5</sub> (relevant from an air quality perspective) of the total tyre wear varies depending on the slip. This would further complicate how to define tyre wear emission factors in emission inventories.

At TNO there is a keen interest in source attribution of aerosols. The aerosols from wear emissions have distinct characteristics, like metals in brake wear, bitumen in road wear, and plastics and rubber in tyre wear. Therefore, it has been possible to validate the emission factors of wear emissions via road-side air sampling [46]. The emission factors are partly based on this source attribution.

**Table 7.3. The table of the Dutch emission factors of wear emissions from different sources. [47]**

Table 3.20A Emission factors for particles from tyres, brakes and road surfaces									3)		
	Unit	Passenger cars	Motorcycles	Mopeds	Delivery vans	Lorries	Road tractors	Busses	Share of PM10	Share of coarse particles	Remains on the vehicle
									%		
<b>Urban areas</b>											
Wear particles per tyre	mgs/km	33	30	7	40	77	60	52	5	95	-
Number of tyres per vehicle		4	2	2	4	11	11	8			
tyre wear particles per vehicle	mgs/km	132	60	13	159	850	658	415	5	95	-
Particles from break linings	"	21	8	0	23	69	63	52	49	20	31
Particles from asphalt road surfaces <sup>1)2)</sup>	"	180	74	50	180	922	922	922	5	95	-
Particles from stone road surfaces <sup>1)</sup>	"	180	74	50	180	922	922	922	5	95	-
<b>Rural roads</b>											
Wear particles per tyre	mgs/km	21	19	4	26	50	38	33	5	95	-
Number of tyres per vehicle		4	2	2	4	11	11	8			
tyre wear particles per vehicle	mgs/km	85	39	9	102	546	423	267	5	95	-
Particles from break linings	"	6	2	0	7	21	19	16	49	20	31
Particles from asphalt road surfaces <sup>1)2)</sup>	"	116	48	32	116	592	592	592	5	95	-
Particles from stone road surfaces <sup>1)</sup>	"	116	48	32	116	592	592	592	5	95	-
<b>Motorways</b>											
Wear particles per tyre	mgs/km	26	24	5	31	61	47	41	5	95	-
Number of tyres per vehicle		4	2	2	4	11	11	8			
tyre wear particles per vehicle	mgs/km	104	47	10	125	668	517	326	5	95	-
Particles from break linings	"	3	1	0	4	11	10	8	49	20	31
Particles from asphalt road surfaces <sup>1)2)</sup>	"	141	58	39	141	724	724	724	5	95	-
Particles from stone road surfaces <sup>1)</sup>	"	141	58	39	141	724	724	724	5	95	-

<sup>1)</sup> Urban areas: 67% asphalt, 33% stone; rural roads: 75% asphalt, 25 % stone; motorways: 100% asphalt. The emission factors are identical due to the lack of reliable data.  
<sup>2)</sup> See Table 3.25A for share of porous asphalt on motorways and the resulting emission reductions.  
<sup>3)</sup> Profiles for heavy metals in wear debris: see Table 3.23B  
N.B. WT1 = urban areas; WT2 = rural roads; WT3 = motorways  
Source: see Table 3.20B

## 7.3 An initial attempt has been made to model tyre and brake wear

From the data available from the measurement campaigns performed within the uCARe project and from the literature review, we set up models for tyre wear and for brake wear. Road abrasion and re-suspension are certainly also relevant non-exhaust particle sources but are not addressed here due to a lack of new data.<sup>9</sup>

### 7.3.1 Brake wear

Our target for the model development was to get in the position to assess the main impacts from the driving style and vehicle set up on the brake wear emission levels. Consequently, simple emission factor as function of road category or average speed were not adequate. Instead, we developed a model using brake power and brake disc speed as main parameters. Drivers can influence the brake power by the driving style and by reduced vehicle loading. E.g. the model should be able to predict effects of look ahead coasting instead of sharp braking before a stop.

#### 7.3.1.1 Basic correlations

Literature analysing emission factors, e.g. (Monks, 2019), (OECD, 2020) provide either simple average emissions in mg/km or speed dependent emission factors. Since we want to quantify the options to reduce emissions by an eco-friendly driving style, by vehicle settings (removal of load not needed, correct tyre pressure etc.) we produced a more physics-based model. We want to note, that this first attempt may have high uncertainties and may not consider all dependencies correctly, since the available data is quite limited and inhomogeneous.

<sup>9</sup> For road abrasion and re-suspension related particles one may use emission factors reported in various literature.

### Main physical background of brake wear emissions:

The wear of brake pads and rotors generate particles of various sizes and morphology, and each combination of speed, pressure, and temperature leads to a different amount of wear (OECD, 2020). Small particles below ca. 30 nm are produced especially by decomposition of binders. In case of organic pads the decomposition is reported to start at ca. 160°C (ranges from ca 150 to 200°C are reported). With inorganic pads decomposition starts not below 210°C, e.g. (Niemann, 2021). Above these temperatures particle number emissions increase exponentially due to nucleation. The quantity of binder being decomposed seems to depend on the history with decreasing quantity per event at repeated brake event at higher temperature. Larger particles are produced by abrasion of material from the pads and the disc.

A part of the particles created by abrasion during brake events is apparently stored in cavities of the coating. These particles may be released when the brake opens again with higher quantities released at high disk speeds compared to lower disk speeds. (Niemann, 2021) found this effect in brake wear measurements and validated the storage effect on brake pads via electron microscope analysis of the pads. Also the emissions of these stored particles are assumed to drop with repeated brake events at high rotational speeds of the brake.

### Correlations assumed:

Main impacts for the quantity of brake wear emissions seem to be:

- We assumed the brake energy [Ws] as main impact of brake wear in [mg]. Thus, brake emissions [mg/s] and [#s] shall correlate with the brake power [W]. This assumption is supported by several literature data, e.g. (OECD, 2020), (Niemann, 2021), (Sang-Hee Woo, 2021) as well as by the measurements performed within uCARE. In addition, emission factors reported show typically increasing trends with vehicle weight and thus higher brake power needed.

We calculate the brake power with the model PHEM from the equations of longitudinal dynamics from the difference of all driving forces at the wheel (deceleration, air and rolling resistance, gradient and the braking power provided by the drive train, Equation [7.1]). The calculation is done in 1Hz.

$$P_b = P_{wheel}^- - P_e = F_b \cdot r \cdot \omega \quad [7.1]$$

with

- $P_b$  .....brake power [W]
- $P_e$  .....power from the drive train, i.e. from engine motoring
- $F_b$  .....brake force [N]
- $\omega$  .....rotational speed of the discs [ $s^{-1}$ ]
- $P_{wheel}^-$  .....wheel power (relevant only if negative)

- ✓ The brake pressure is assumed to have a linear correlation to both, PM and PN emission quantities, e.g. (Niemann, 2021). The pressure defines the torque and the brake force.
- ✓ Since particles stored in cavities of the pads are rather released at higher speed, we assumed a higher than linear dependency to the rotational speed of the discs. (Niemann, 2021) found quadratic to cubic dependencies. The vehicle speed is proportional to the rotational speed of the disc.
- The temperature is an important parameter with exponential increasing emissions above ca 180°C to 210°C. However, since we have no data to simulate the brake temperature for representative installation situations in the

vehicle yet, we did not consider the temperature as separate parameter in this first attempt<sup>10</sup>.

- The type of brake pads seems to have a high impact on emission levels. Nevertheless, we did not yet consider a representative mix of different brake pads (organic, inorganic, different manufacturers) since the mix is unknown and the test data from literature is too inhomogeneous for splitting it into different brake pad types. If more data on brake wear tests is available in future, e.g. from the PMP programme, we may use a weighted set of test data as basis for the model parameterisation.
- The expected influence of brake history as a result of decreasing emissions of binders and particles attached in cavities is not considered explicitly to keep the model simple. We used all test results from multiple brake events from representative cycles for model parameterisation. Brake wear emitted after the brake opens again is attributed to the brake event before<sup>11</sup>. Thus, the model should represent average emissions as function of brake power and speed independent of the history. The history effect may explain a (large?) part of the spread in the test data<sup>12</sup>.
- In case literature provided only PM<sub>10</sub>, PM<sub>2.5</sub> or total PM and/or no information on the size range of PN, we used following default values for conversion:
  - 45% of the PM<sub>10</sub> emissions to be PM<sub>2.5</sub> (average of literature values)
  - 35% of total brake wear being PM<sub>10</sub> (average of values found in (Niemann, 2021) and (Hesse, 2021))
  - For PN the peak is assumed at ca. 80 nm with almost 100% PN below 1 micron. Thus, we define all PN to be below 2.5 µm. Larger particles contribute to particle mass emissions but not significantly to particle number emissions. Relevant number emissions from LN>2.5 µm may exist from a possible bimodal distribution, but these are not measured by typical condensation particle counters.
  - 50% of the brake PM emissions measured on brake test stands are emitted to ambient, the remaining is deposited on rim and wheel housing. Own tests on the chassis dyno suggest, that some of the deposited particles are released under vibrations. Neither the amount deposited, nor the remitted share is known today. The value is a placeholder until test data on entire vehicles is available to make a more robust assessment. For PN, we assume that 100% is emitted into the environment, as rather large particles can be captured that have almost no share in the PN.

---

<sup>10</sup> The temperatures measured on the brake test stand most likely differ from the ones to be expected in the vehicle due to quite different airflow situations. The temperature of brakes is implicitly considered by the brake power for short brake events. The effect of longer and/or very frequent brake events like in downhill driving is not considered in the current model.

<sup>11</sup> It seems, that emissions of brake wear stored in cavities need some minimum rotational speed, which could explain the over proportional impact of the disc speed on measured emissions reported in some studies. This effect should be reflected to some extent in the model by the rotational speed being a separate parameter beside the brake power. To which extent the test data used provides representative storage effects is open yet.

<sup>12</sup> The history effects as well as emissions of nucleation particles may be especially high for new brakes. Unfortunately, the information on preconditioning procedures for the brakes was not given in most literature data.

### 7.3.1.2 The Model

The brake wear PN emissions in [#s] are simply interpolated from a characteristic line, which can be defined via a polygon according to the brake power and disc speed calculated in 1 Hz.

$$E_{bn} = C_{(P_b \cdot \omega)} \tag{7.2}$$

$$\omega = \frac{v}{r_w} \tag{7.3}$$

$$E_b = E_b \cdot 0.5 \cdot D_{(\omega)} \tag{7.4}$$

- With:  $E_{bn}$  .....brake wear emissions PN [#s]
- $E_b$  .....brake wear emissions PM [mg/s]
- $C_{(P_b \cdot \omega)}$ .....Characteristic curve as polygon gained from the test data
- $r_w$ .....dynamic wheel radius [m]
- $v$ .....vehicle speed in [m/s]
- ..... $D_{(\omega)}$  PM/PN ratio for brake wear particles as function of the disc speed according to Figure 7.22

The characteristic polygon for PN was computed for  $(P_b \cdot \omega^z)$  bins from the average PN emissions per bin from all test data. The best regression coefficient for a fitting function was found for  $z=0.5$ . Thus, we used  $(P_b \cdot \omega^{0.5})$  on the x-axis. This supports the over-linear impact of the rotating disc speed but is a lower impact than reported in (Niemann, 2021). The polygon's supporting points were plotted over  $(P_b \cdot \omega^{0.5})$  and then smoothed to remove outliers in sections with few measured values. Figure 7.21 shows the resulting curve for PN.

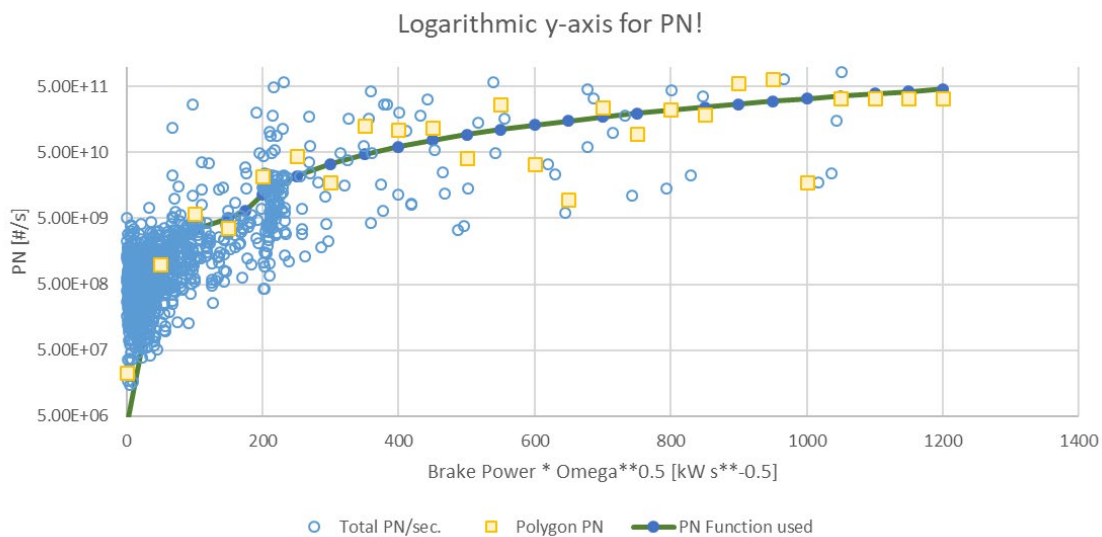


**Figure 7.21. Characteristic curve used in the PN model for brake wear per brake**

The PM10 emissions are computed from the PN emissions using a density function depending on the rotational disc speed. This reflects a trend reported e.g. in (Niemann, 2021) based on systematic tests on a brake dynamometer, that the density of particles [mg/#] drops with increasing disc speed. Figure 7.22 shows the density function used in the model. In (Niemann, 2021) as well as in (Hesse, 2021) somewhat lower values for PN/PM10 ratios are reported. The function used here was adjusted to meet the average of measured PM10 brake wear emissions for 50% release as airborne PM10.

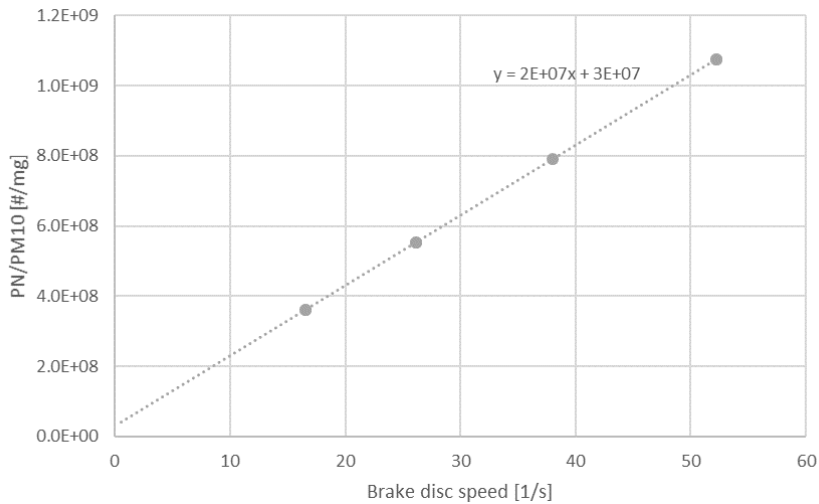


**Figure 7.22: PN/PM ratio used to convert PN into PM10 in the uCARE model**

Examples for model results are shown later together with the tyre wear.

### 7.3.2 Tyre wear

Like brake wear emissions, the significant impact tyre wear emissions on air quality have been known for several decades, due to their contribution to particulate matter concentrations, from their chemical composition near roads. Tyre wear emissions are generated by tread abrasion due to contact with the road surface. Consequently, particles formed from the interaction of tyres and pavement consist of a complex mixture of tread rubber and encrusted mineral particles from pavement (OECD, 2020). Tyre wear particles are composed of plasticisers and oils, polymers, carbon blacks and minerals as well as elemental content (mainly zinc and sulphur), (OECD, 2020). Approx. 50% of the tyre wear is rubber (Rausch, 2020), (Baensch-Baltruschat, 2020), (Steiner, 2021).

Only a small mass fraction of the total tyre wear is PM10, most wear has diameters above 10  $\mu\text{m}$ . (OECD, 2020) states, e.g., from a literature review, that only 1% of the wear is PM10 while (Hüglin, 2021) measured ca. 23% from PM as PM10. The measurements in (Hüglin, 2021) however, analysed only PM which arrived at kerb side on the sampling filters. Obviously a high mass share of tyre wear are not airborne due to their large size.

In on-road tests as well as in kerbside particle sampling, a differentiation between tyre wear, road wear and re-suspended particles is difficult and needs chemical analysis of the particles, which usually is only possible for larger particles since small ones hardly contribute to the sampled mass. (Beji, 2021) measured PM and PN in size classes behind the vehicle on a trailer. The ratio of total particle mass to PM from tyre and road wear was ca. 1.4 with high dependency on the road section. A separation between tyre and road wear was not given in (Beji, 2021).

To elaborate the emission model for tyre wear, the total mass loss of tyres over lifetime seems to be a robust base data, since no road wear and re-suspended particles need to be considered. From this data however, no dependencies on wheel power, vehicle speed, etc. can be gained. Consequently, we used data available from the tests in the uCARE project and available from literature to set up the detailed model and calibrated the model with data on total tyre wear with information from literature on the size ranges.

#### 7.3.2.1 Basic correlations

Literature reports correlations with vehicle mass, vehicle speed, brake force and steering angle). We assume the most significant parameter influencing the tyre wear [mg] to be

the energy [kWh] transmitted by the tyres to the road. Consequently, the emission factor in [mg/h] should depend on the power transmitted by the wheel [kW], see Equation 7.5.

$$E_t = C_{(P_t)} \tag{Equation 7.5}$$

- With:  $P_t$ .....Power transmitted per tyre [kW]
- $E_t$  Tyre wear emissions PM10 [mg/s]
- $E_{tn}$  Tyre wear emissions PN [#s]
- $C_{(pt)}$ .....Characteristic curve as polygon gained from the test data providing PM10 [mg/h] as function of the wheel power

A power dependency could explain the aforementioned dependencies, since speed, brake force and steering angle are related to the power at the wheels. Up to now, only (Steiner, 2021) calculated the total tyre wear emissions based on wheel work using a constant factor of 0.62 g/kWh. In order to bring a passenger car of 1300 kg to a stop from 100 km/h will require 0.14 kWh. Hence per stop from 100 km/h, the associated tyre wear emissions are about 90 mg.

### 7.3.2.2 The Model

The main issue to parametrise the characteristic curve  $C_{(P_t)}$  was, to translate existing data from literature into wheel power dependent emission data. For this translation, we used the equations of longitudinal dynamics applied in the model PHEM, e.g. (Matzer, 2019) to calculate the power at the wheels. The power per tyre is calculated as 25% of the total propulsion power for a vehicle with four wheels, Equation 7.6. We used the absolute value of the computed wheel power assuming that braking (negative power) has the same effect on tyre wear as positive power transmission.

$$P_t = 0.25 \cdot Abs ( P_{air} + P_{grad} + P_{acc} + P_{roll} ) \tag{Equation 7.6}$$

- With:  $P_{air}$  .....Power to overcome air resistance [kW]
- $P_{grad}$  .....Power to overcome air road gradients [kW]
- $P_{acc}$ .....Power for ac- an deceleration (+ and -) [kW]
- $P_{roll}$ .....Power to overcome rolling resistance<sup>13</sup> [kW]

The methods we used to calculate the wheel power for various test conditions from literature are listed in Table 4.

**Table 4: Methods applied to assess the wheel power for various emission data from literature**

Source	Method for calculation of tyre power
Average emission factors provided as function of average speed, such as e.g. in (EPA, 2021)	Speed dependency of the wheel work [kWh/km] according to all HBEFA 4.2 traffic situations for average car data.
Emission data from VTI test stand (the tyres move circularly on asphalt plate) 	$P_t = P_{roll} + P_{cornering}$ . (remark: if no torque transmitted on the wheel axle by the test stand)

<sup>13</sup> This power contribution is calculated as  $P_{roll} = v \cdot (r_0 + r_1 \cdot v)$ . We discussed if this power should be considered as reason for wear. Since we found test set ups, where obviously only rolling resistance occurred where also tyre wear was reported, we decided to consider the rolling resistance also as contributing to tyre wear.

<p>On vehicle tests with separate tyre holder as used e.g. in (Tongawa, 2021)</p>	<p>Via longitudinal dynamics using the vertical load on the wheel and speed reported in the literature.</p>
<p>Constant emission factors for average driving situations.</p>	<p>Not used to set up the characteristic emission curves. Data used only for calibration of final model.</p>

Figure 7.23 shows the data from different literature sources and from the uCARE test program plotted over the calculated wheel power. The MOVES 3 model data was obtained from weighting tyres from vehicles and sorted to speed bins in MOVES3 according to the predominant use of the cars. The other data results from direct tyre measurements on vehicles or on tyre test equipment. Having in mind the very different test methods and the uncertainties in the measurement of particle size dependent tyre wear emissions as well as in the assessment of the wheel power, the agreement between the data is very good.

Consequently we produced the characteristic curve “uCARE Model Proposal”, shown also in Figure 7.23, for the simulation of the PM10 tyre wear emissions in [mg/kWh] per tyre. As mentioned before, the wheel power is simulated by the model PHEM. The power per tyre is simply assumed as 25% of the total wheel power as mentioned above, ignoring different power distributions for front and rear wheel driven cars and during brake events. The overall uncertainty of the characteristic curve seems to be too high to gain any accuracy by splitting the power calculation into more details.

Obviously, there is a lack of test data for higher wheel power values. This is due to the test methods, which mostly do not test with high wheel torque or even without torque transmitted or use average trip data, where the total power at all wheels is usually below 25 kW. The flattening of the curve above ca. 4kW/tyre is a result of model calibration to total test results reported in literature on one hand and on the assumption that the diameter of tyre wear increases with increasing power. Thus, an increasing mass fraction is above the PM10 size.

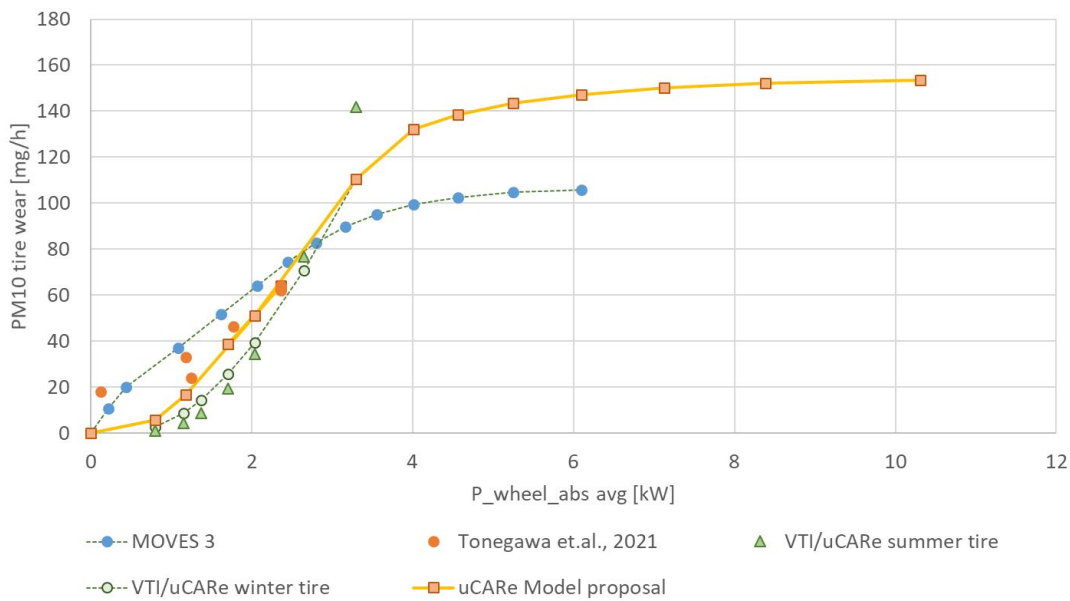


**Figure 7.23. Compilation of PM10 tyre wear data (values refer to one single wheel)**

**7.3.2.3 Plausibility check of the tyre model**

For average normal driving of a passenger cars, the model results in ca 5 mg PM10/veh.-km (see Figure 7.24), i.e. 1.25 mg/km per tyre.

The total tyre wear per tyre can be assessed from the profile depth difference of new and end of life tyres. On average we assume ca. 1.5 kg total tyre wear for a life time of 50 000 km<sup>14</sup>, i.e. 30mg/km per tyre as total tyre wear. Thus the PM10 fraction is ca. 5% of the total tyre wear. If we assume ca. 50% of the PM 10 to remain on the rims and in the wheel housing, 10% of total wear may be PM10 but only half released as airborne PM10. A much smaller fraction is reported to be PM2.5, with an average of data found in literature of ca. 30% from PM10. To calculate PN emissions from tyre wear, we found only one data source, namely (Beji, 2021) where the number and mass emissions for PM10 was measured with an ELPI impactor. Unless we find different data, we use this number to convert PM10 into PN emissions. The total number of particles above 10 µm most likely can be neglected.

**Table 5: Ratios of PM10 and PM2.5 to total tyre wear to meet the total mass loss of a tyre life time and PN emission density found in literature**

	Average per tyre	% of total PM <sup>(1)</sup>
Total PM	30 mg/km	100%
PM10	1.5 mg/km	5.0%
PM2.5	0.45 mg/km	1.5%
PN [# /mg <sub>PM10</sub> ]	9.1E+03 #/mg	

<sup>14</sup> Tyre dimension 215/60 R16 has ca 2 m circumference and 20 cm width with a new profile depth ca 6-8mm, end of life ca 3mm (minimum EU legislation = 1.6mm) with max. 80% profile area-- > 2 x 0.2 x 0.005 x 0.8 x 940kg/m<sup>3</sup> = 1.5 kg.

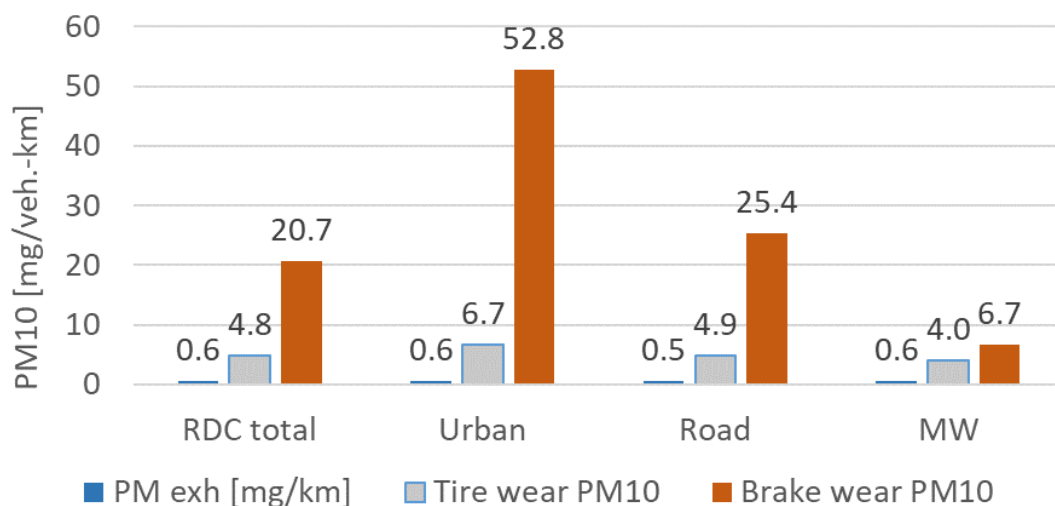
- (1) These ratios most likely is not constant. We expect higher % of larger particles at higher wheel power. A quantification of the change of the share of the size fractions is yet not possible, thus we use constant shares per size fraction in the first model version.

### 7.3.3 Model Results

Figure 7.24 shows the model results for PM<sub>10</sub> from tyre wear and brake wear compared to the exhaust gas emissions.

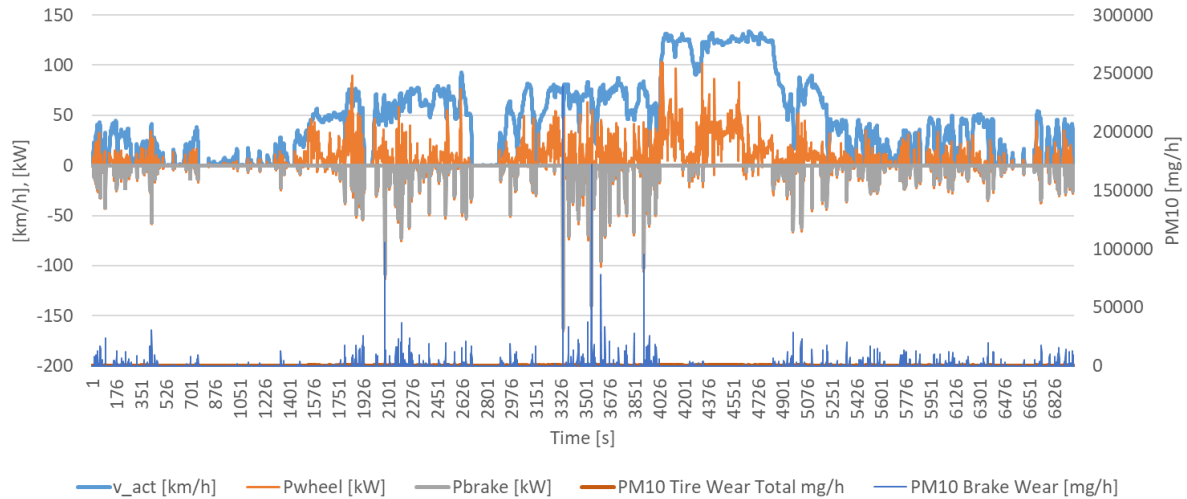
An average tyre wear of ca 5 mg PM<sub>10</sub>/veh.km is in line with most literature, which ranges from ca. 3.5 to 9 mg/km for passenger cars. We found also much higher values in literature, but these may refer to total tyre wear.

For brake wear the model calculates on average ca. 21 mg/veh.-km for a normal RDE test trip. The average of data found in literature is around ca 10 to 15 mg/veh.-km. (OICA, 2021) reports on average ca 20.4 mg/veh.-km in the WLTP brake test with a range between 4 and 43 mg/km depending on brake pad types. (Hesse, 2021) reports 19 to 50 mg/veh.-km for the WLTP brake test cycle. Thus, the order of magnitude provided by the model seems to be in line with recent test data. Including more brake pad type test data when available and using weighted averages of these tests to set up a characteristic curve for a "representative pad/disc combination" could be a next step to improve the model representativeness for average cars. The much higher brake emissions in urban driving compared to highway are also reported in literature, e.g. (Monks, 2019).



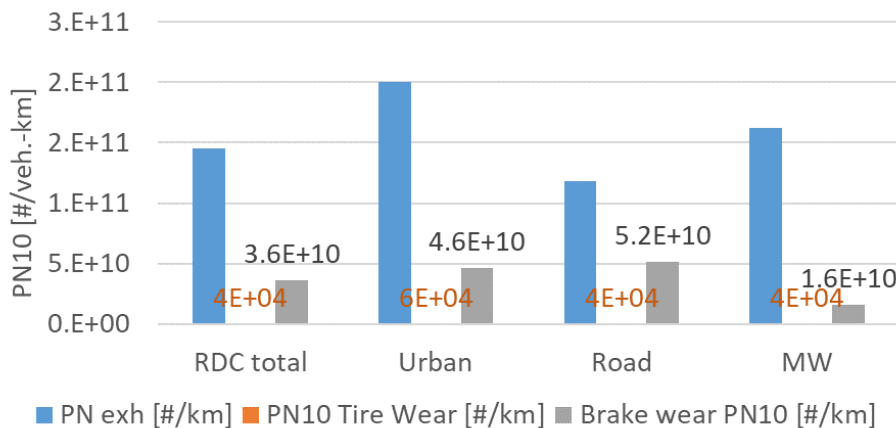
**Figure 7.24. PM<sub>10</sub> emissions calculated for a EURO 6d D-class diesel car for the speed and gradient trajectory from an average RDE test in the area of Graz**

Figure 7.25 shows the simulation results in 1Hz resolution. The high dependency on driving situations is obvious and as expected, when using brake and wheel power as main model parameters. Since the data analysed supports the strong dependency on these parameters, the new model should depicture the real emission behaviour much better than average speed dependent models or the use of simple average emission factors.



**Figure 7.25. Wheel and brake power and PM10 emissions calculated for a EURO 6d D-class diesel car for the speed and gradient trajectory from an average RDE test in the area of Graz**

Figure 7.26 shows the average PN emissions for the RDE test trajectory. Figure 7.27 shows the corresponding 1 Hz resolved data. In case of PN, the brake wear is lower than average exhaust PN (Euro 6 diesel cars have lower exhaust PN, petrol higher than the average shown here). Tyre wear is lower than brake wear PN by 6 orders of magnitude, if the source used for the (constant) PN density [# /mg] provides a reasonable order of magnitude.



**Figure 7.26. PN emissions calculated for a EURO 6d D-class car (average diesel + petrol for PN exhaust) for the speed and gradient trajectory from an average RDE test in the area of Graz**

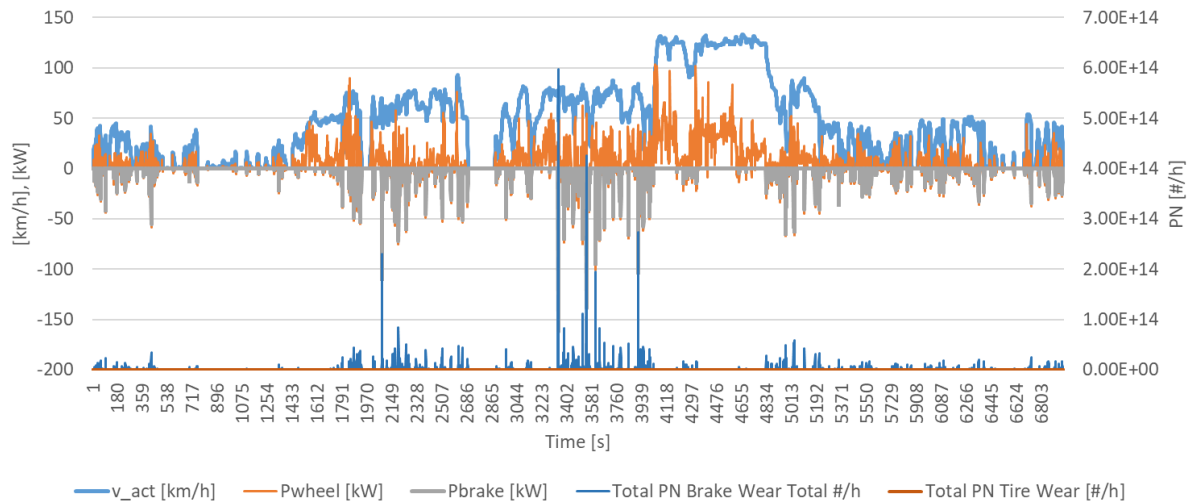


**Figure 7.27: Wheel and brake power and PN emissions calculated for a EURO 6d D-class car (average diesel + petrol) for the speed and gradient trajectory from an average RDE test in the area of Graz**

To validate the dependency on wheel and brake power, we performed tests on the chassis dynamometer at TU Graz where a partial flow of the air after the driven wheel was measured for PN concentrations. In addition the total PN concentration in the dynamometer room was measured. From the latter we can calculate total emissions over the tests by the room volume and concentration changes. From the partial flow we get relative PN emission levels in high time resolution. An extension by PM measurement is suggested to elaborate reliable rates for total PM / PM 10 / PM 2.5 as well as PN/PM 2.5 or PN / PM10 ratios. Since no resources are left in the uCARE project, such validation tests remain for possible follow up projects.

The tests performed so far, support the assumption of the wheel and brake power as main parameter to explain the corresponding PM and PN emissions. Figure 7.28 shows test result for tyre wear with three different constant speeds where the power at the wheel was varied by the chassis dyno brake setting. High PN are found in high power phases. Higher power at same speed levels lead to higher PN emissions. Same tests with positive power from the dynamometer machine, where the vehicle brake is active, give the sum of brake and wheel wear PN emissions.

With increased attention for brake and tyre wear, also in the new Euro-7 regulation, the topic remains of interest and study.

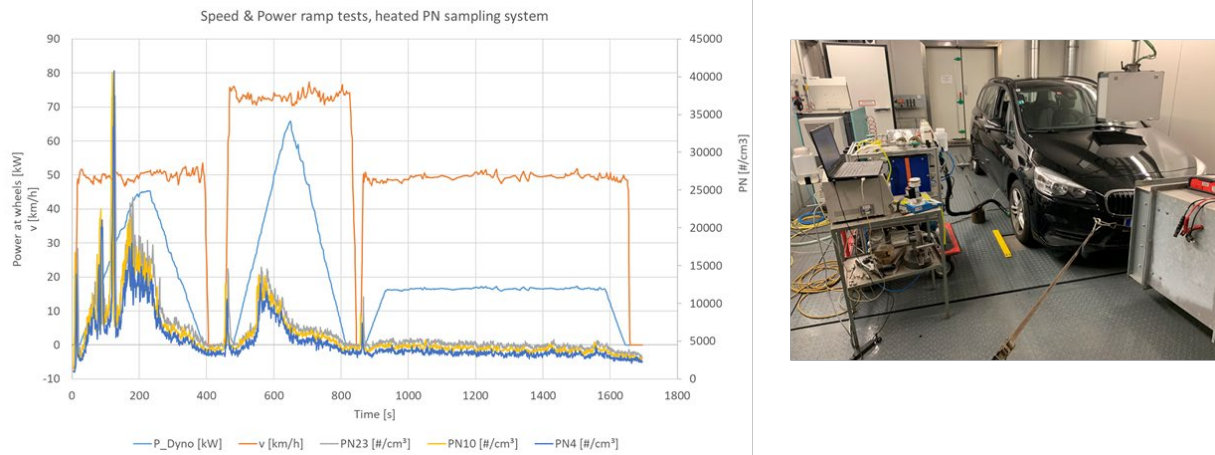


**Figure 7.28: Example for PN emissions measured for constant speed tests with different wheel power settings on the TUG chassis dyno with the sample probe set up shown in the figure right.**

To which extent the characteristic curves for tyre and brake wear can be applied also to HDVs is open yet.

## 8 How 'accurate' are the base maps in AEMs?

AEMs are a standard with which organisations can share detailed pollutant emission measurement data. All data that is used to produce base maps is data that has been measured for a vehicle with that specific engine code. To generate the emission base map, the second-by-second tailpipe emission measurement data are allocated according to the x-axis variable (vehicle speed or engine speed) and y-axis variable (CO<sub>2</sub> mass flow rate). The allocation procedure is dependent on the "bin size" of chosen x-variable and y-variable. For example, a bin can be designed to contain tailpipe emission from 45-50 km/h and 4 – 4.2 g/s CO<sub>2</sub> mass flow rate. For each bin in the emission base map, the average of the tailpipe emission is calculated and used as representative value per bin, as visualized in Figure 2.1.

When the emission map is used as tailpipe emission prediction tool (for example, as shown in Section 3.1), prediction error is expected due to various sources of uncertainties, ranging from limitation of measurement data availability to the limited information from the vehicle specifications. AEMs are not yet able to predict emission outliers but can still offer insights at a more detailed level than generalised emission factors.

### 8.1 Sources of measurement data limitations

Emission map layers rely on test data. Extensive real-world test data is not available for all engines or vehicles. The goal is to produce maps for as many vehicles/engines as possible, also for those for which limited data is available. Five levels of data availability can be distinguished:

Level 1: On-board emission measurement or monitoring data of real-world driving (ca. several hours up to several years). Data can be binned and averaged and converted into a map. In this conversion it is important that enough data is available for all the situations (combinations of variable values) that occur in real-world driving. Monitoring data can be collected using PEMS, SEMS or OBD-loggers using vehicle sensor data.

Level 2: Chassis dynamometer modal mass data from real world cycles (CADC, ERMES, WLTP up to EURO 6b<sup>15</sup>). Second-by-second exhaust mass flow data is available for many engine types. Test cycles generally provide a lower coverage of the vehicle/engine use area but may cover a broader range of exhaust gas components than Level 1 data. Representative real-world cycles, however, should cover most of the relevant engine operation areas. Maps may have to be reduced in resolution, due to the shorter test duration compared to Level 1 and the resulting smaller amount of instantaneous data available to fill the maps.

Level 3: Average emissions calculated over portions of tests, either on chassis dynamometer or on-road. These averages could be bag data from chassis dynamometer, from manufacturer test cycle data, or averages per road type. For engines for which only this data is available, the emission maps will hold only a few data points (e.g. urban, rural and motorway driving). In some occasions it is necessary to revert to such a simplified map to be able to give an indication of emission levels.

Level 4: Experiment based models. If test data is not readily available, it may be an option to base emission level estimations on models/functions determined during experimental research. For instance, to convert tyre test data to vehicle use related wear, the relation between e.g. speed and wear can be determined by experiments and in-lab simulations.

Level 5: Physics based models. Emissions can be predicted by modelling the behaviour of e.g. engine, aftertreatment, tyres and brakes. These models should be validated by

---

<sup>15</sup> It is intended not to use data from type approval tests (NEDC up to Euro 6c and WLTP from Euro 6d-Temp on). Engines are usually optimised for low emissions in type approval tests and thus maps from such cycles are not necessarily representative for real driving.

measurements but may predict behaviours in various operation points which have not been measured.

## 8.2 Quantity of measurement data limitations

To be able to create emission maps for (nearly) all vehicles/engines, we need to deal with the varying quantity of available measurement data. At the moment, the required minimum data inside each bin is set at 5 data points per bin. Bins with less than 5 seconds of data are not considered as valid data points and will not be included in the emission base map generation. The threshold of 5 seconds can be adjusted during the base map generation, depending on the end-user's preferences and source of data.

If quantity of valid data is still limiting despite lowering the threshold value, another approach is needed. One option is to determine the bin size during emission map generation depending on the amount of available data. By enlarging the bin size, variability within a bin can indeed be interpreted as such. Note that this currently holds for the base emission maps. Details about the algorithm for adjusting the bin size during the base map generation can be found in 10.4.4.

AEMs are all complemented by the datapoint count per bin and, for example, the standard deviation per bin. Figure 8.1 for example shows the datapoint count per bin and Figure 8.2 shows the standard deviation per bin. Figure 8.1 to Figure 8.4 complement the emission graph of Figure 3.2.

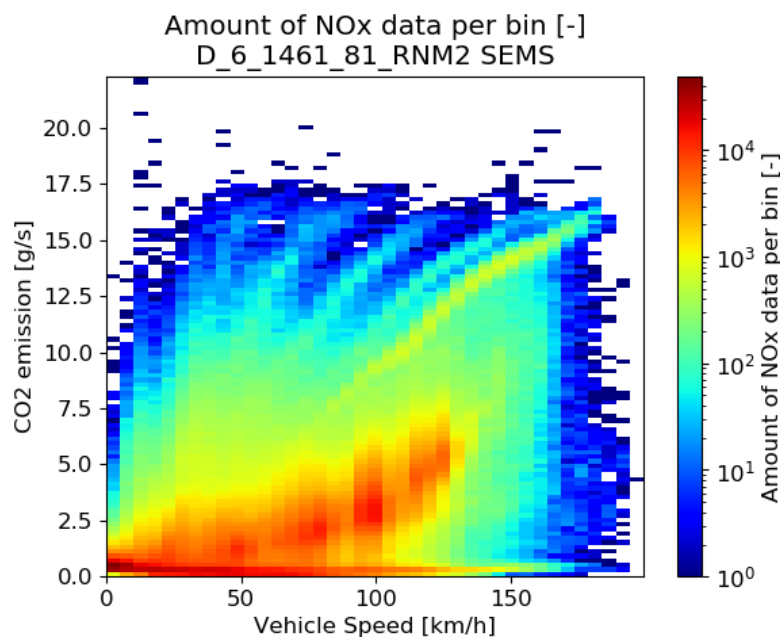


**Figure 8.1. Visualisation of the datapoint count per bin of a Euro 6, 1461cc, 81kW diesel engine.**

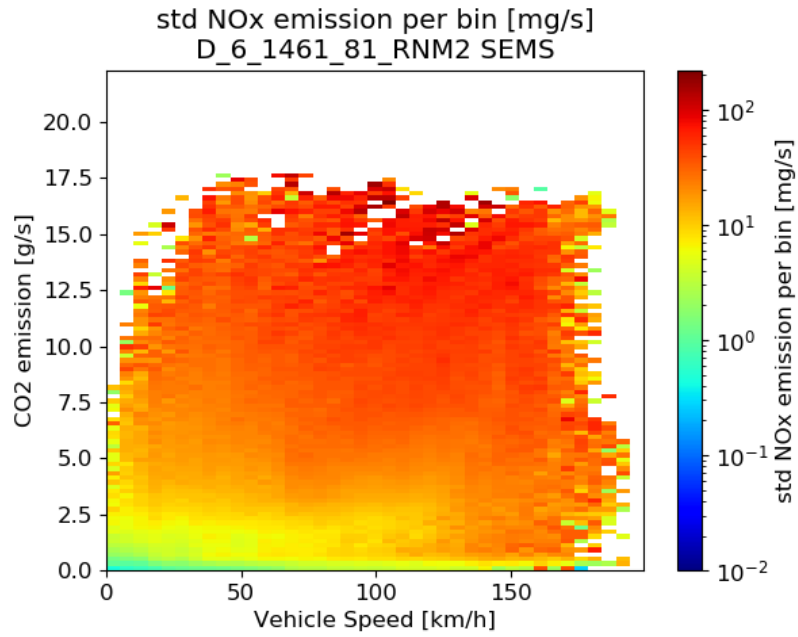


**Figure 8.2. Visualisation of the standard deviation of NO<sub>x</sub> per bin of a Euro 6, 1461cc, 81kW diesel engine.**

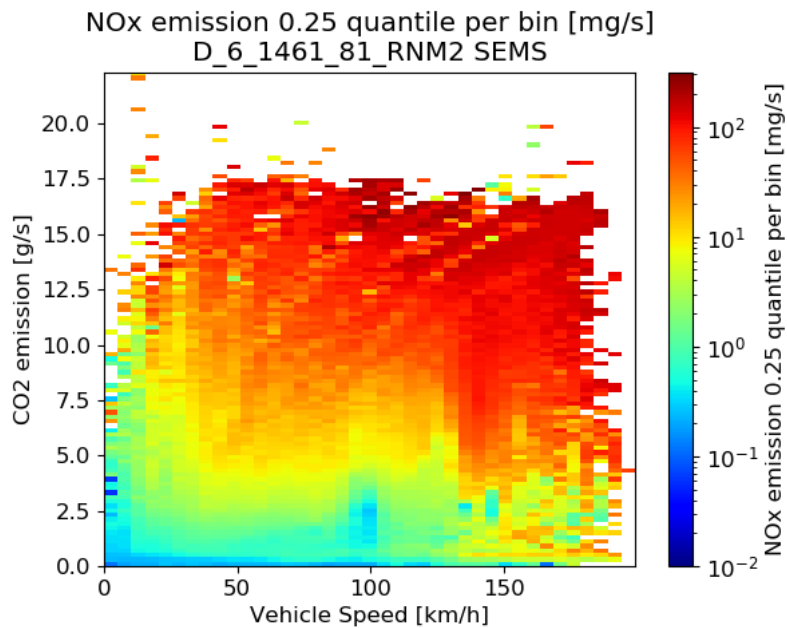


**Figure 8.3. Visualisation of the 25th quantile of NO<sub>x</sub> per bin of a Euro 6, 1461cc, 81 kW diesel engine**

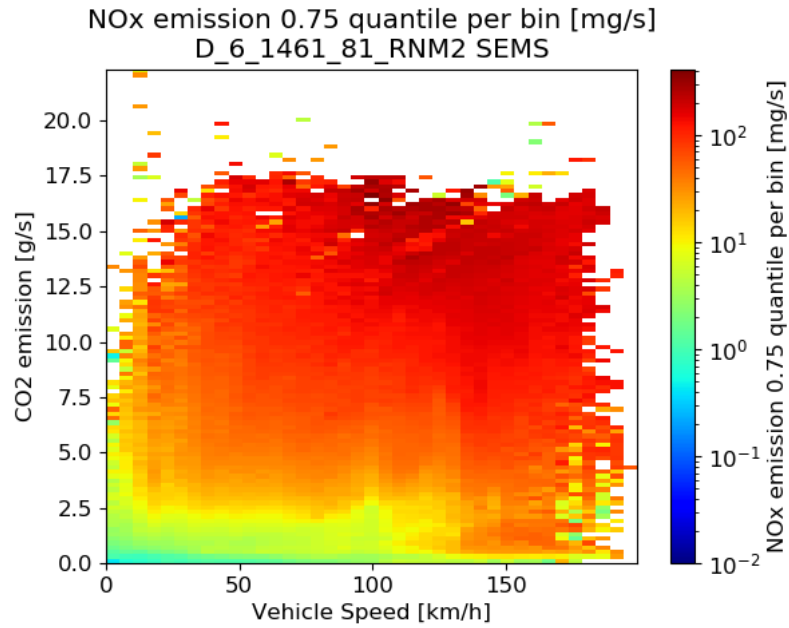


**Figure 8.4. Visualisation of the 75th quantile of NO<sub>x</sub> per bin of a Euro 6, 1461cc, 81 kW diesel engine**

### 8.3 Uncertainty from the chosen independent variables

In generating the base map, vehicle speed or the engine speed is chosen as one of the independent variables, depending on the available signals. When both signals are available, two base maps from the same vehicle can be generated, as shown in Figure 5.1.

The vehicle speed signal and the CO<sub>2</sub> mass flow rate signals are the basic independent variables for base map generation. Choosing the vehicle speed signal, however, will include an underlying uncertainty from the gear change behaviour which will affect the data distribution. Figure 8.5 shows a distribution of NO<sub>x</sub> emission from a Volkswagen Caddy, which is taken from vehicle speed and CO<sub>2</sub> combination around 50 km/h constant driving in the urban area.

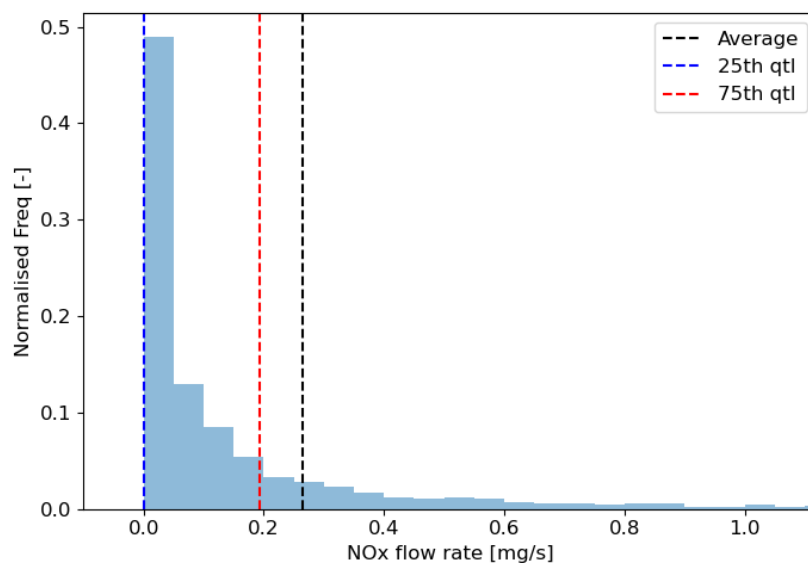


**Figure 8.5. Distribution of NO<sub>x</sub> emission from Volkswagen Caddy Euro 6, at vehicle speed around 50 km/h and CO<sub>2</sub> flow rate around 1 g/s**

The figure shows a non-normal distribution of NO<sub>x</sub> emission, in which the calculated NO<sub>x</sub> average ( $0.27 \pm 0.86$  mg/s) is higher than the 75<sup>th</sup> percentile quantile. This dataset can be further filtered based on the engine speed range, which resulted in different NO<sub>x</sub> emission subsets, visualized in Figure 8.6.

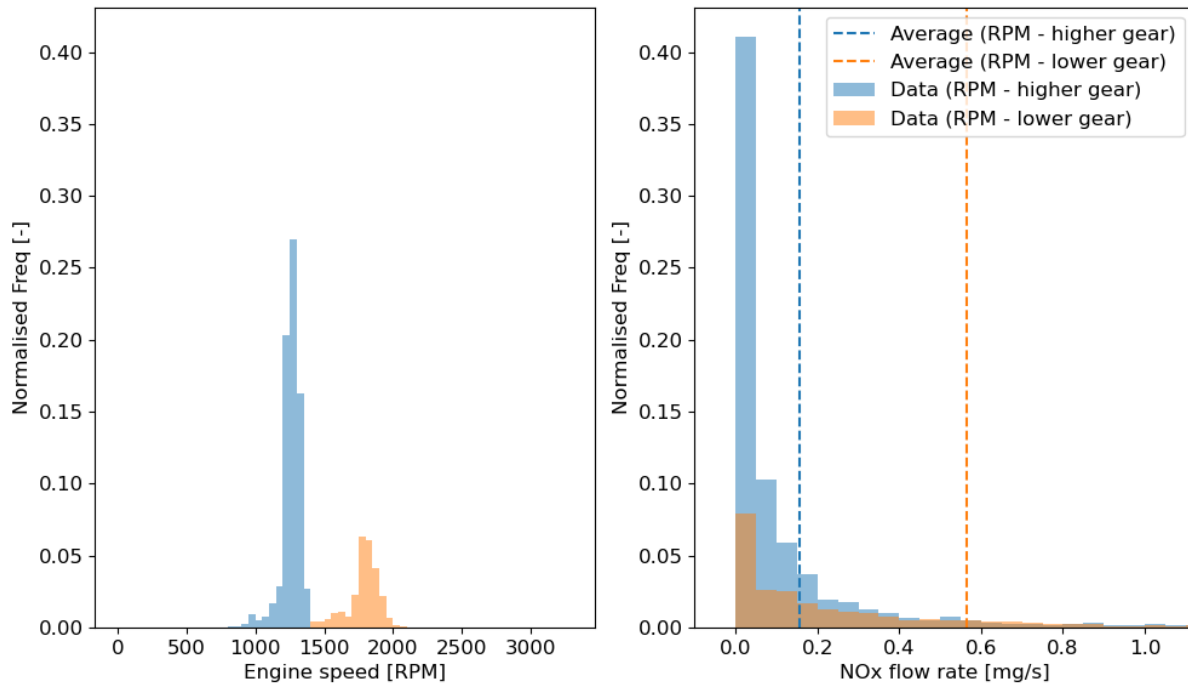


**Figure 8.6. Subset data from Figure 8.5, distribution of NO<sub>x</sub> flow rate as a function on engine speed and CO<sub>2</sub> mass flow rate, based on vehicle speed around 50 km/h**

The data subset with label "RPM - higher gear" is associated with constant driving at speed limit, while the "RPM - lower gear" subset is associated with a changing gear event. Note that the quantity of data in the higher gear is larger compared in the lower gear. These subsets have average NO<sub>x</sub> emission of  $0.16 \pm 0.47$  mg/s for higher gear, and  $0.57 \pm 1.43$  mg/s for the lower gear subset.

The average NO<sub>x</sub> emission based on this vehicle speed is therefore a combination of the two subsets from different engine speed range during driving. It is also observed that the average NO<sub>x</sub> based on engine speed at higher gear has a lower standard deviation compared to that based on vehicle speed or engine speed at lower gear.

It is therefore recommended to generate the base map using the engine speed signal as one of the independent variables, compared to using the vehicle speed signal. However, it is acknowledged that there will be measurement campaigns where the engine speed signal is not available, and the vehicle speed signal becomes the only available signal to be used as an independent variable.

## 8.4 Uncertainty from the data distribution

In addition of calculating average of the measurement data per bin for each emission map, the standard deviation, 25<sup>th</sup> and 75<sup>th</sup> quantile are also provided in the emission base map. These parameters give an indication of the variation of data inside each bin in the emission map.

However, as shown in Figure 8.5, the shape of the data distribution is not a normal distribution. The long tail from distribution results in occurrences of NO<sub>x</sub> emission higher than the calculated average value. For this example, the aftertreatment catalyst is able to reduce NO<sub>x</sub> tailpipe emission such that the NO<sub>x</sub> distribution is skewed toward 0 mg/s.

This skewed distribution is not universal in vehicles with different technology. Figure 8.7 shows the distribution of NO<sub>x</sub> emission of a Volkswagen Polo Euro 5 as a function of engine speed and CO<sub>2</sub> flow rate associated with driving on motorway around 100 km/h.

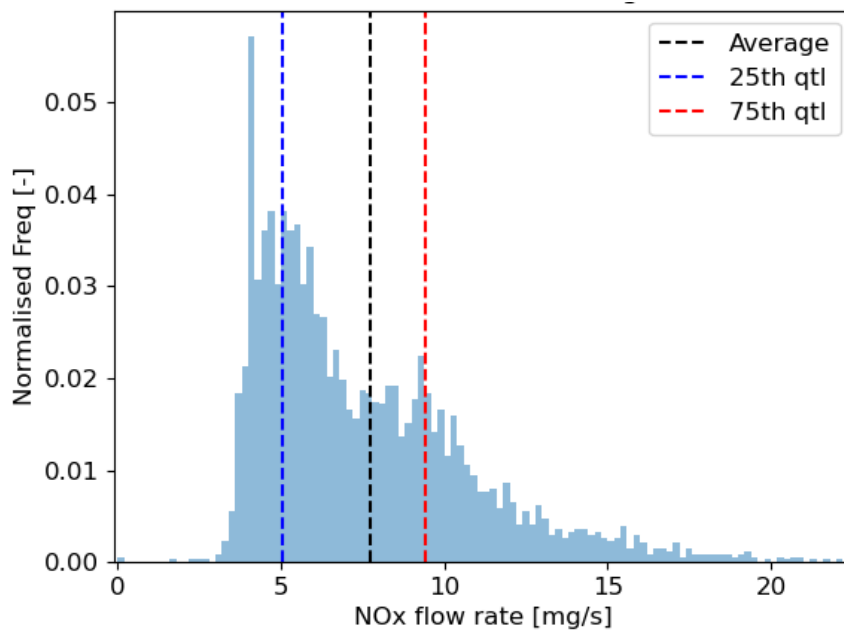


**Figure 8.7. Distribution of NO<sub>x</sub> emission of Volkswagen Polo Euro 5 at engine speed around 2000 RPM and CO<sub>2</sub> flow rate around 2.6 g/s**

In this example, the shape of the distribution is similar to a beta-prime distribution, however, with distinct peaks around 5 mg/s and around 10 mg/s. Further investigation shows that distribution can be further filtered depending on the air-to-fuel ratio, as shown in Figure 8.8, even though there are no distinct peaks in the air-to-fuel ratio distribution. No additional information can be found on why the air-fuel-ratio is controlled this manner.

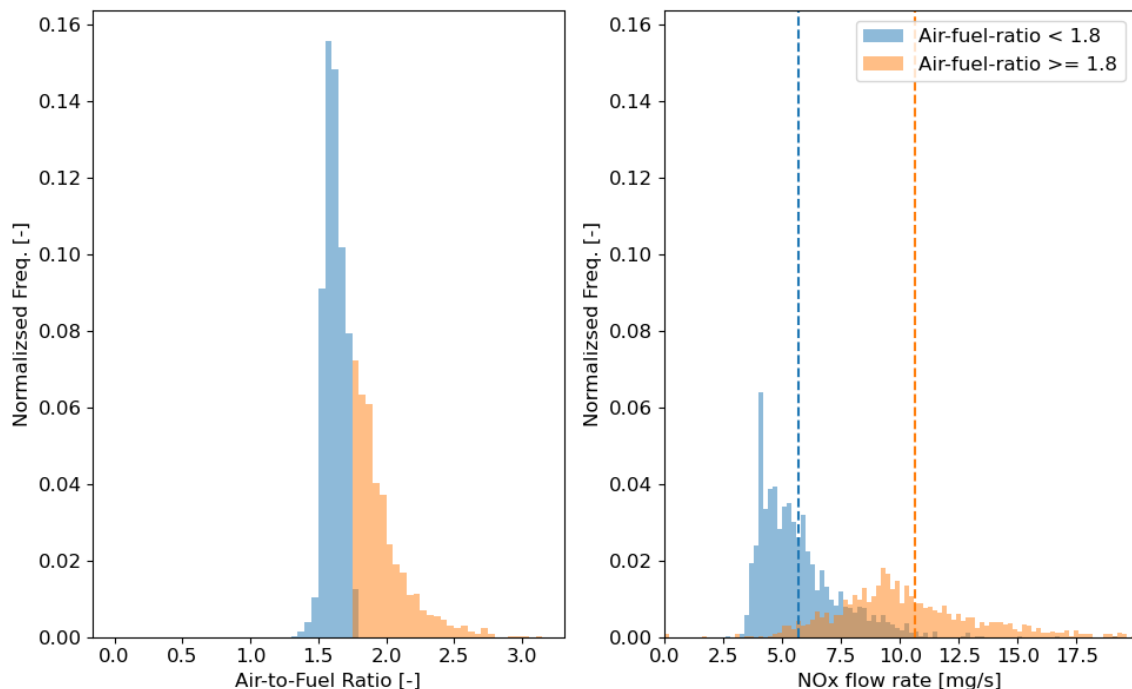


**Figure 8.8. Distribution of NO<sub>x</sub> emission from Figure 8.7, with further filtering based on air-fuel-ratio**

Ideally each distribution shape should be identified and formulated for a better accurate representative of the emission behaviour for vehicles with different technology. However,

as more measurement data from different vehicles will be collated based on taxonomy code specification, the resulting distribution shape may no longer be accurately formulated. As such, the average value of the emission is still chosen to be the best representative value for each bin in the emission base map.

## 8.5 Uncertainty from vehicle dynamics

The emission base map is designed based on instantaneous measurement data. However, the vehicle state is a time-variant system that is affected by the physical state of the vehicle leading to that measurement instant.

For example, the tailpipe NO<sub>x</sub> emission from vehicles installed with SCR aftertreatment is expected to differ depending on the temperature of the exhaust gas in the SCR. The temperature of the exhaust gas is dependent on how the vehicle speed and engine load develops during driving.

At the moment of writing, the calculated average values of each bin will diminish the historical effect from vehicle dynamics towards a steady-state vehicle state. Predicting the tailpipe emission of vehicles with constant speed, therefore, is expected to yield higher prediction accuracy compared to the dynamic behaviour of the vehicles (e.g. during acceleration or sudden braking).

An effort to incorporate the vehicle dynamics effect onto the engine base map design has been attempted and documented in 8.5.1. As the investigation is still ongoing, the result of this effort is not yet included in the delivered engine base map.

### 8.5.1 Historical effects on the NO<sub>x</sub> emission base map

A proposal has been made to describe the influence of dynamic behaviour on the NO<sub>x</sub> emissions of passenger cars, based on the AEM base map as a function of vehicle speed and CO<sub>2</sub> mass flow. The implementation will be further elaborated by means of an example from existing measurement data.

#### 8.5.1.1 Effect of vehicle dynamics on variation in NO<sub>x</sub> emission

The vehicle dynamics can be formulated utilizing the CO<sub>2</sub> emission flowrate. The CO<sub>2</sub> emission is a proxy of the engine load, therefore variation of the CO<sub>2</sub> emission rate can be used to describe the variation of engine load that is usually correlated to the vehicle dynamics.

The variation of the CO<sub>2</sub> emission is defined as the difference between the CO<sub>2</sub> emission flowrate and the moving average of the CO<sub>2</sub> emission.

The variation of the NO<sub>x</sub> emission is defined as the residuals between the measured NO<sub>x</sub> and the average NO<sub>x</sub> emission from the augmented emission map as a function of vehicle speed and CO<sub>2</sub> emission. Determination of the window size used to calculate the moving average of CO<sub>2</sub> is based on the autocorrelation of the NO<sub>x</sub> residual.

The effect of the variation of the CO<sub>2</sub> emission towards the NO<sub>x</sub> variation is defined as the gradient of the linear regression of the NO<sub>x</sub> residuals and squared CO<sub>2</sub> variation in each bin of the generated average NO<sub>x</sub> emission map:

$$CO_{2,variation} = CO_{2,measurement} - CO_{2,rolling\ mean}$$

$$\left. \frac{NO_{x,residual}}{(CO_{2,variation})^2} \right|_{@(vehicle\ speed, CO_2)_{bin}}$$

An example test case is used to illustrate the formulation step by step.

### 8.5.1.2 Example test case: Volkswagen Caddy

Referring to the generated NO<sub>x</sub> emission map as a function of vehicle speed and CO mass flow of the Volkswagen Caddy 2018 in Figure 5.1, the calculation of NO<sub>x</sub> residuals is shown in Figure 8.9 and the autocorrelation of NO<sub>x</sub> residuals is shown in Figure 8.10.

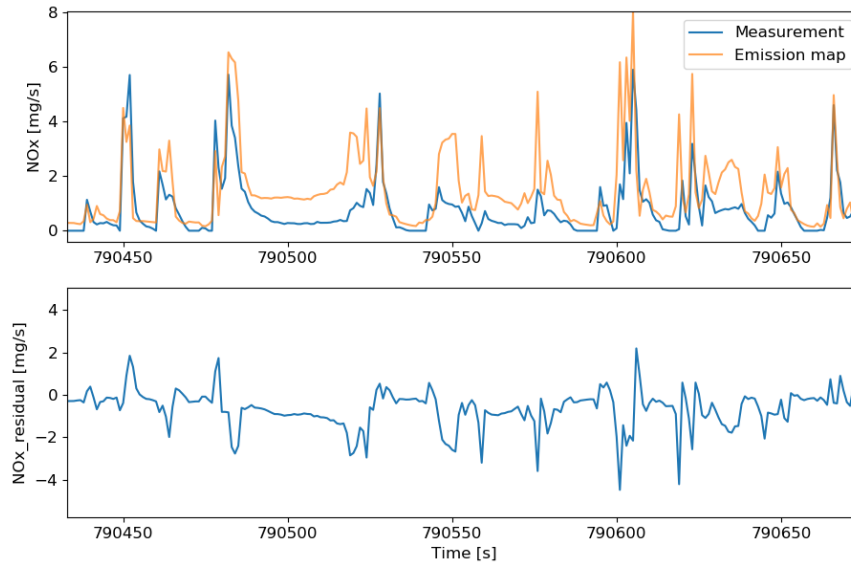


**Figure 8.9. Comparison of NO<sub>x</sub> emissions from measurement data and augmented emission map as a function of vehicle speed and CO<sub>2</sub> emission**

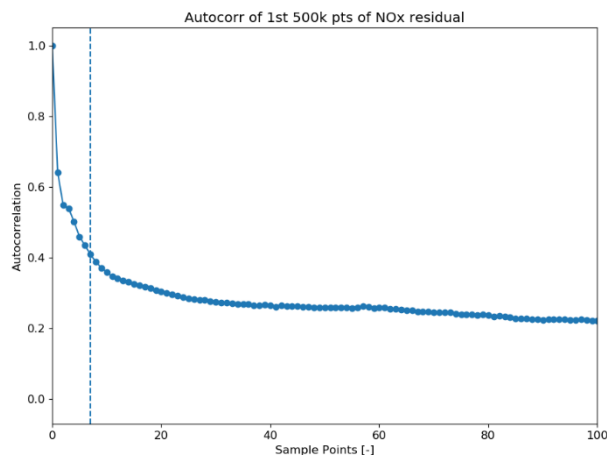


**Figure 8.10. Autocorrelation of residual NO<sub>x</sub>. The vertical line shows the sample point where the autocorrelation value reaches 0.4**

The duration of the moving average window of CO<sub>2</sub> values is selected at the point that the autocorrelation value reaches 0.4. In this example, the vertical line indicates that the window size is 7 seconds.

Once the moving average of the measured CO<sub>2</sub> is calculated, the NO<sub>x</sub> residuals and the squared CO<sub>2</sub> variation are binned by vehicle speed and CO<sub>2</sub> mass flow, similar to the way the emission maps are designed. The gradient of the linear regression of the NO<sub>x</sub> residuals and squared CO<sub>2</sub> variation is then calculated and plotted, as visualized in Figure 8.11.

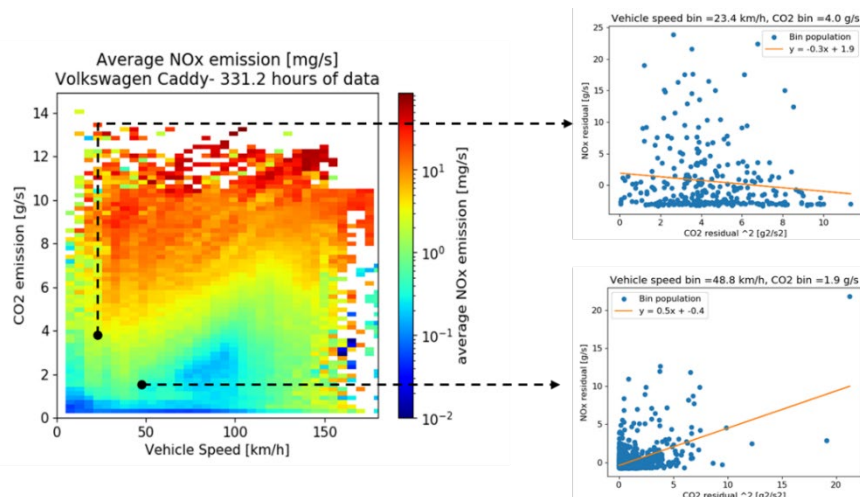


**Figure 8.11. Calculation of the effect of dynamics on NO<sub>x</sub> variation, visualized in the emission map. The small windows visualize the calculation of the gradient of the linear regression of the NO<sub>x</sub> residual as function of squared CO<sub>2</sub> variation.**

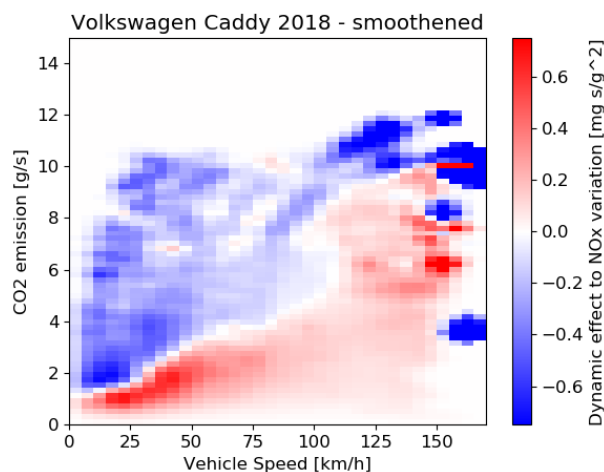


**Figure 8.12. Effect of vehicle dynamics on NO<sub>x</sub> variation (emission map design)**

The resulting gradients are then plotted similarly as the emission map and smoothed to show consistent trend, as shown in Figure 8.12.

The red area shows the driving profile that is associated with constant speed driving. For example, driving at a constant speed of 50 km/h will have an average CO<sub>2</sub> emission of around 2 g/s. Introducing dynamic driving in this area will result in NO<sub>x</sub> emission variation up to 0.5 mg/s per squared CO<sub>2</sub> variance.

The blue area is associated with acceleration, during which the engine load temporarily increases. The NO<sub>x</sub> emission in the blue area is already high as it represents the acceleration period during driving rather than constant speed driving. Any change in dynamics in this area (for example, more constant speed driving) would result in a negative NO<sub>x</sub> variation from the already high NO<sub>x</sub> average.

While Figure 8.12 adequately visualizes the effect of vehicle dynamics on NO<sub>x</sub> emission variation, the validation of this effect for NO<sub>x</sub> emission prediction is still ongoing. Specifically, whether the result from Figure 8.12 can be used along with the base emission map Figure 8.11 for a more accurate NO<sub>x</sub> emission prediction.

---

## 8.6 Uncertainty from vehicle specifications

### 8.6.1 Maintenance and tampering

Poor maintenance or tampering of vehicles can lead to very high pollutant emissions. The impact of tampering especially was discussed thoroughly in 'uCARE Deliverable D1.3 Tampering' [48]. If vehicle emissions are significantly higher than those predicted by the uCARE emission maps, then the possibility exists that this is due to poor maintenance or tampering.

### 8.6.2 OEM software configurations

Vehicles with the same taxonomy code may have different software configuration settings depending on the OEM. The difference in data distribution shown in Figure 8.8, for example, may be due to the control strategy coded in the OEM software. However, the method which this OEM software determines the air-fuel ratio is not open to public, and therefore impossible to unravel. With limited amount of measurement data and limited transparency on the software, therefore, there will be uncertainties resulting from the black-box nature of the OEM software that cannot be addressed.

## 8.7 Current conclusion on sources of uncertainty

The uncertainties from the emission base map affect the prediction accuracy when estimating the instantaneous tailpipe emission from vehicles. Because base maps only contain measured data, this data will reflect the circumstances in which it has been collected. If the measurement data was collected in limited circumstances, then the generated base map would be biased towards these circumstances, giving a narrower scope. This can lead to larger uncertainties when trying to predict emissions in other, highly different, situations. Furthermore, with a limited amount of data, large spread and uncertainties are unavoidable and should be considered when trying to predict a specific vehicle performance using the generated base maps.

However, if the data in a base map has been collected in diverse driving situations, and with significant amounts of measurement data, the emission base map will sufficiently represent the average emission performance of the vehicle across driving conditions. In this way, the prediction error from these uncertainties can be reduced. We do note that instances of incidentally high emissions remain difficult to predict as their cause is often not discernible. Metadata such as notes, the number of vehicles, amount of data, and average mileages used to generate the base maps are included in the AEM file to give an indication of the statistical significance of the data in the emission base maps.

## 9 Generalising the cold start augmentation parameters does lead to increased uncertainty

Because of the large number of dependencies, the cold start extra emissions (CSEE) cannot be easily represented in a map format. Instead, we use continuous functions over time to estimate the second-by-second CSEE. The parameters needed to solve the model equations are derived from measurement data and are reported in the corresponding cold start augmentations, which, as the base maps, are specific to the engine block code.

The cold start model is based on the physical description of the warm-up process developed by Weilenmann [5]. Within uCARe, the original model was simplified in some parts and extended in others in order to make it applicable to a larger number of vehicles, technologies and situations. In particular, we extended the model to make it applicable to diesel vehicles, included particulate number as an additional modelled pollutant, developed a parametrization method using WLTP, NEDC and RDE data to parametrize the model when no IUFC data is available, and computed the fallback model parameters for cases in which no emissions measurement data is available. Furthermore, we have reported Euro-class based cool-down curves (and model parameters) and have developed a function to fit the engine temperature during any trip, which enables the modelling of short trip sequences.

In the following we will briefly discuss the main uncertainty sources of the cold start model. First, we have to consider the standard model uncertainties deriving from the imperfections and idealizations made during the formulation of the physical model. Even in the best case in which we use the IUFC cycles for the model parametrization, these approximations lead to slight deviations between the measurements and the model results (see Figure 3.10. Results from cold start model parametrization with IUFC cycles at -7°C (top) and 23°C (bottom) for a Euro 6c petrol vehicle. The left panels show the second-by-second cold start extra emissions and the right panels the corresponding integrated emissions.). The model uncertainty further increases when we use model parameters determined from fitting specific cycles (e.g. IUFC/WLTP) that only contain limited driving situations to model any given trip or cycle. As an example, in Figure 9.1 we compare the cold start model results for a NEDC cycle at 23 °C using specific, optimized and fallback model parameters. As shown, in this particular example, the specific and optimized model parameters give fairly accurate results for CO, HC, and NO<sub>x</sub>, while the PN emissions are overestimated with the specific model parameters. In contrast, the fallback parameters largely overestimate the CSEE for CO, HC and PN, and underestimate the CSEE of NO<sub>x</sub>. Large errors are expected when using the fallback parameters, as we observed a large variability in the cold start behaviour of vehicles in the same euro class. This is because the CSEE depend much more on the specific vehicle technology than on the euro class itself. Thus, the model results obtained with fallback model parameters should only be considered as indicative.

Although it is suspected that many engines might be optimized to produce lower emissions in type approval tests (i.e. NEDC and WLTP) with a cold start, from our analysis we could not disentangle such effects in the cold start extra emissions. In fact, as shown in the example above, the model results using specific model parameters (from IUFC cycles, supposedly not optimized) and optimized parameters (from WLTP cycles, supposedly optimized) are very similar. However, in order to fully rule-out such effects, the best would be to repeat the analysis in Figure 9.1 for an RDE cycle, but such data is currently not available.

Finally, there are some additional uncertainties when modelling trip sequences derived from the use of average parameters in the modelling of the engine cool down and warm-up processes.

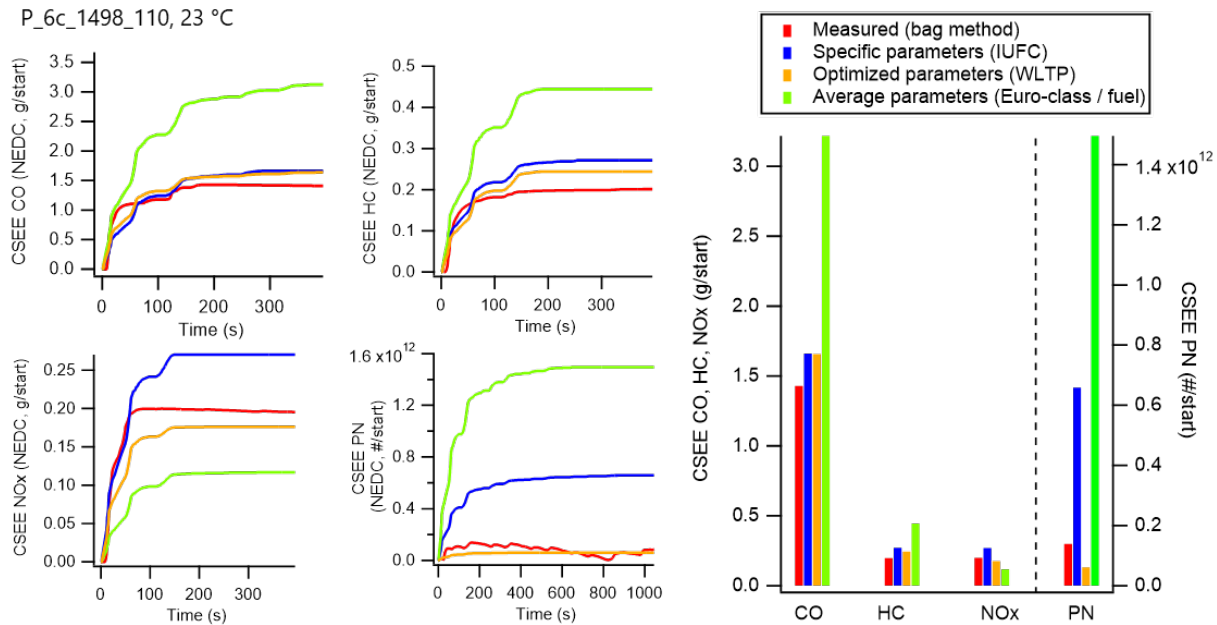


**Figure 9.1. Comparison of the cold start model results of a NEDC cycle at 23°C for a Euro 6c petrol vehicle using vehicle specific, optimized and average fallback model parameters**

### 9.1.1 Comparison and validation of the simplified cold start model

To validate the simplified model, several vehicles were measured on the dynamometer in the cold start cycle IUFC. To be able to investigate the cold start effects accurately, measurements were done with various standstill times between the test starts.

The simulation model was then set up from these measurements. For validation purposes, the simulation was carried out in two stages.

- Simulation with individual map and individual CSEE curve
- Simulation with average map and average CSEE curve incl. temperature function

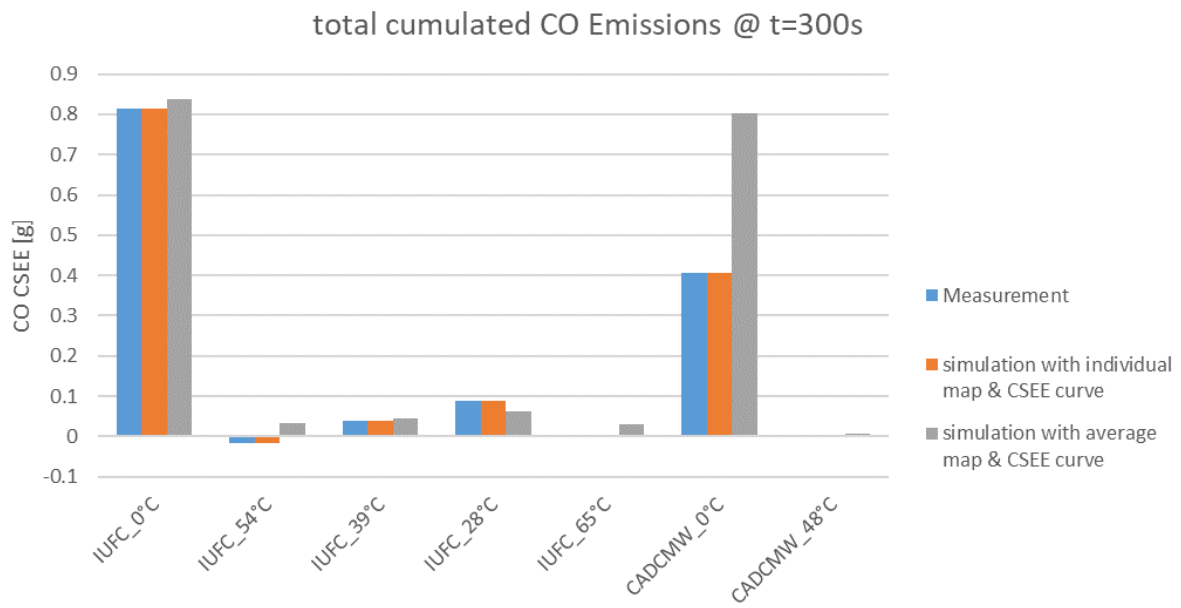
#### Simulation with individual map and individual CSEE curve

The simulation followed the method described above for each test cycle separately. I.e., for each measurement, a "warm" map was created from measurement data from the "warm" part of the measurement. In addition, a CSEE curve was created for each measurement. This data set was then used to simulate the measured cycles.

#### Simulation with average map and average CSEE curve incl. temperature function

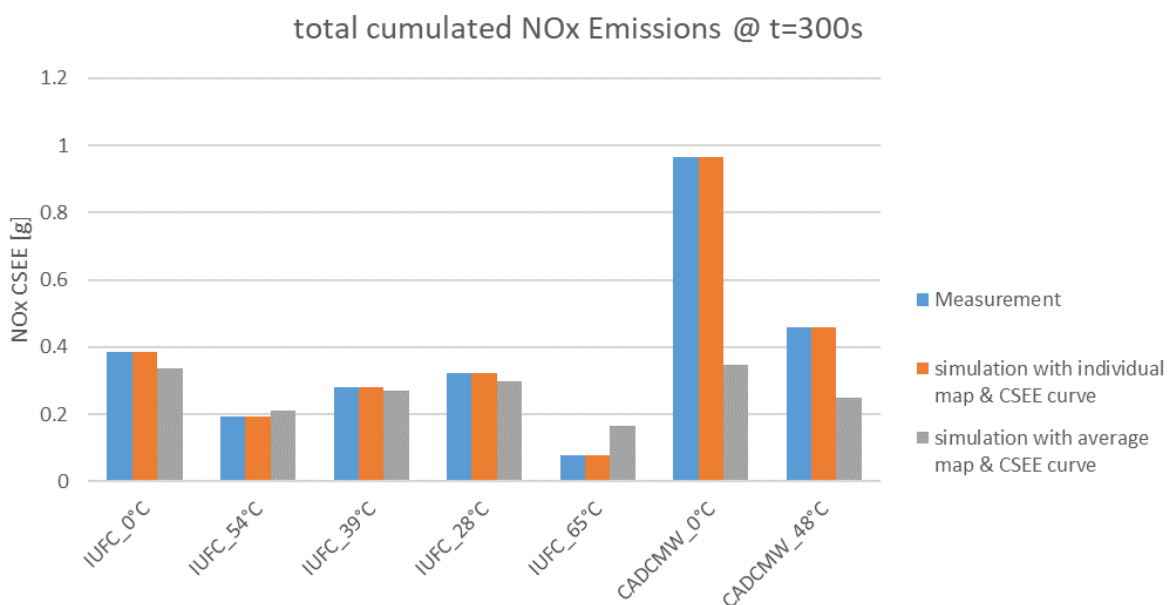
In this variant, an average cold start curve was created from all single tests and the  $Q_{loss} @ start to T_{start}$  function was derived by analysing all CSEE curves with the corresponding start temperatures of the individual measurements. In addition, an average engine hot-emission map was created from all tests.

Figure 9.2 shows the cumulated hot and cold CO emissions at  $t=300s$  for all measurements. The reason for showing the sum of cold and hot emissions is that is that one cannot distinguish hot emissions from cold emissions from the measured data. At 300 seconds, the cold start is likely to be finished so this time for comparisons makes sense. The simulation results of the first variant (individual simulation) show that the model is capable of reproducing measured cycles accurately. The simulation with average data, which would be used for the simulation of independent cycles, shows higher deviations as expected, since we compare the results to a single measured cycle.

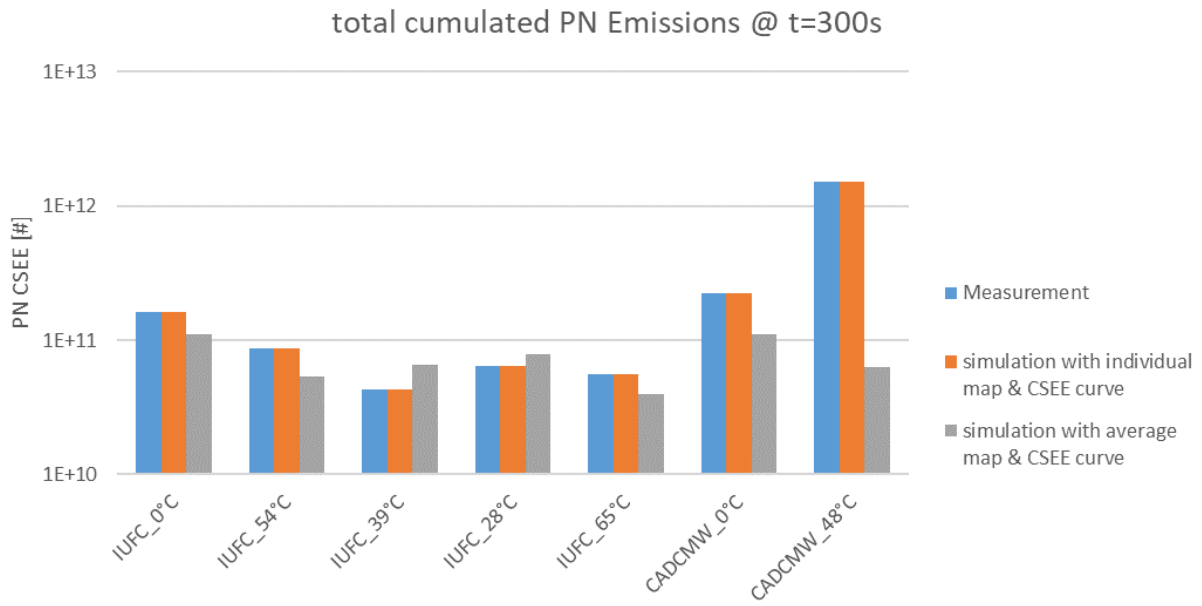


**Figure 9.2. Comparison of measured and simulated CO emissions in the first 300 seconds of an IUFC cycle for a diesel Euro 6d car**

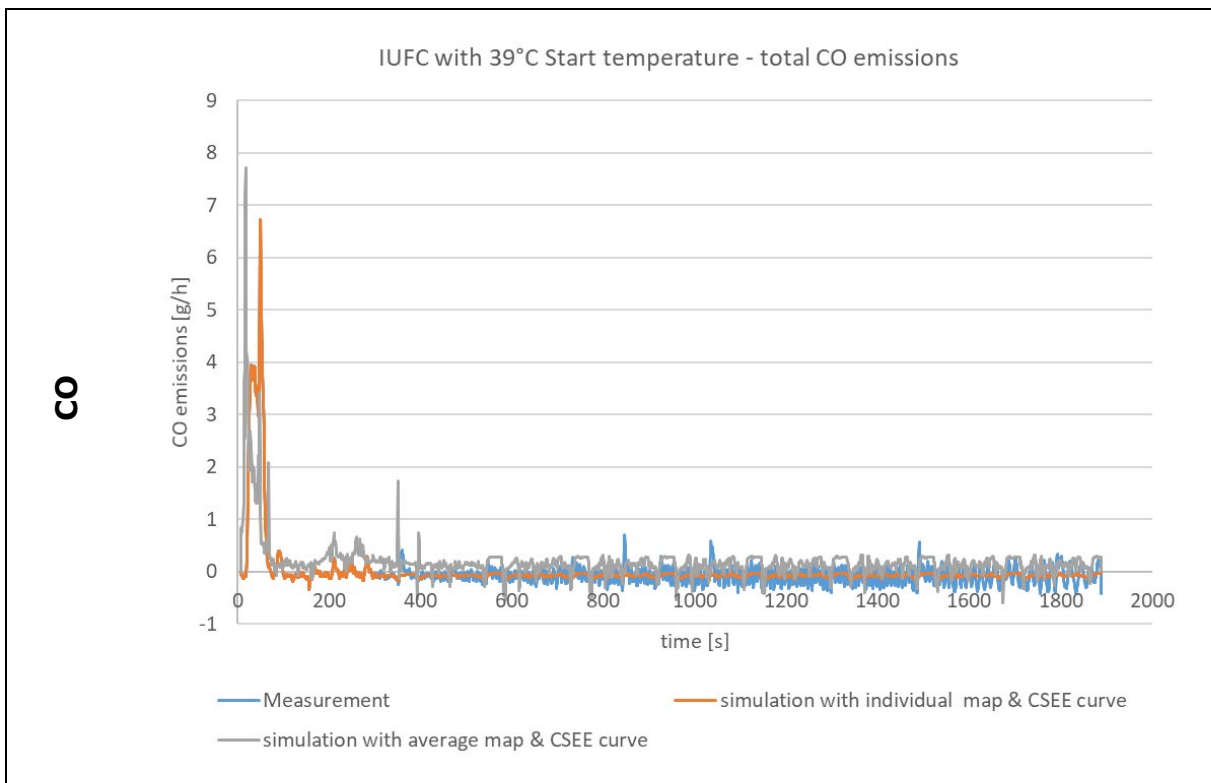
The deviations in the simulation of the CADC motorway cycle (CADCMW) at 0° start temperature show quite high deviations. Why the measured CSEE are much lower in the CADCMW compared to the ones in the IUFC for this vehicle may be explained by a more lean operation in the motorway test, since the measured NO<sub>x</sub> CSEE in this test are rather high (see Figure 9.3). Figure 9.3 and Figure 9.4 show the results for NO<sub>x</sub> and PN in the same formats as Figure 9.2, while Figure 9.5 shows the second-by-second results for a selected cycle for illustration.



**Figure 9.3. Comparison of measured and simulated NO<sub>x</sub> emissions in the first 300 seconds of an IUFC cycle for a diesel Euro 6d car**



**Figure 9.4. Comparison of measured and simulated PN emissions in the first 300 seconds of an IUFC cycle for a diesel Euro 6d car**



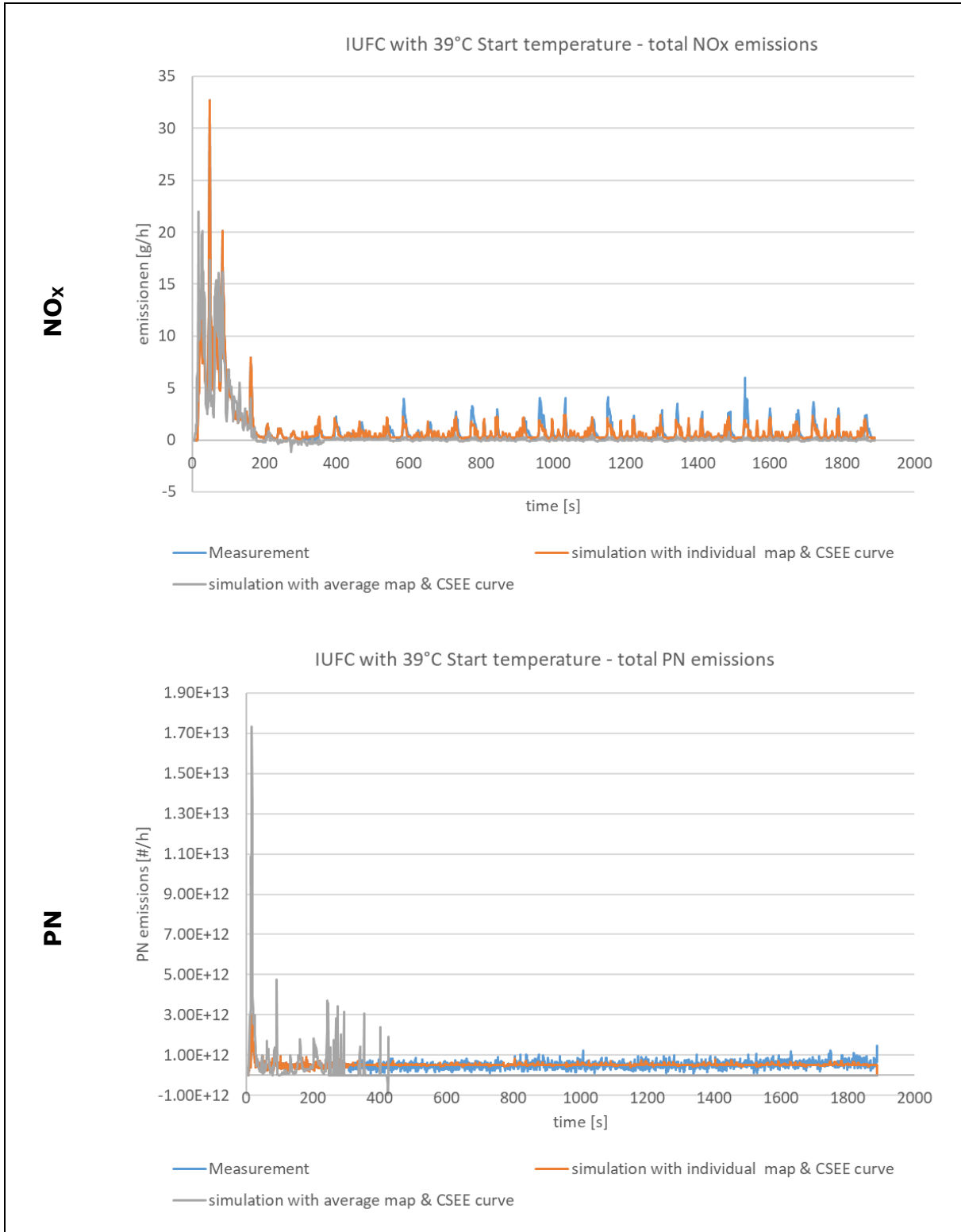


**Figure 9.5. Second-by-second emission results for a IUFC cycle with 39°C start temperature for (from top to bottom) CO, NO<sub>x</sub>, and PN**



## 10 Manuals for the available tools

### 10.1 Selecting a base map

The selection tool scans the AEMs in uCARe community on the open research platform Zenodo for the AEM(s) relevant to your specific vehicle. The tool provides a clear overview of which maps (base + augmentation layers) are available for the supplied engine code. The script will print the download link of the latest versions of the requested maps. The working procedure is visualized in Figure 10.1.

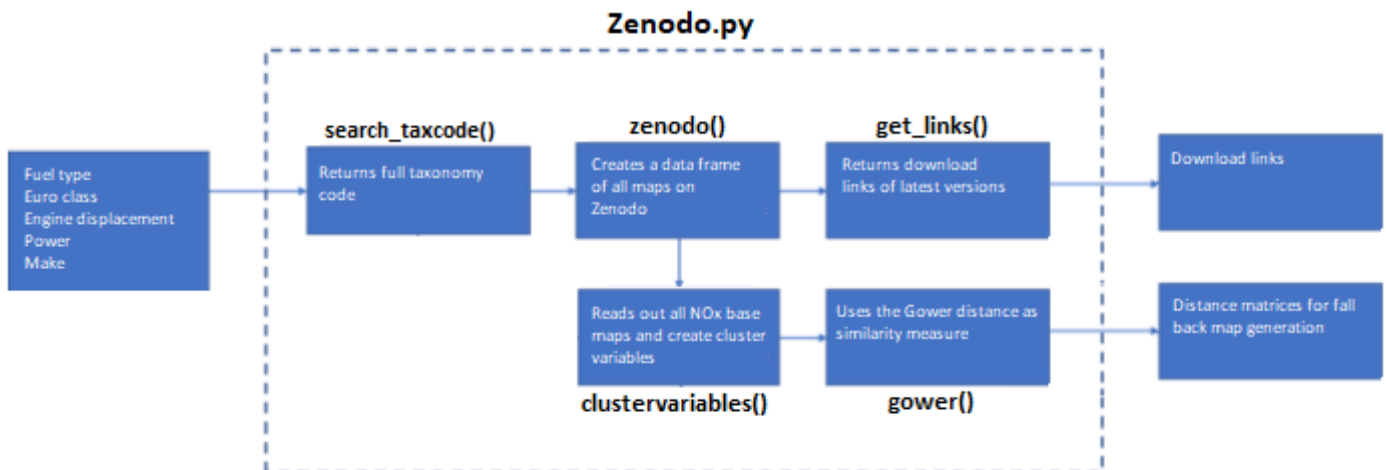


**Figure 10.1. Schematic illustration of AEM selection tool.**

One must have an access token to make use of the script. This access token can simply be achieved by creating a profile on Zenodo and following the steps: ‘profile’ → ‘applications’ → ‘new token’. This token is personal and should not be shared; one must paste the code into the python script as the variable ‘ACCESS\_TOKEN’. The input consists of the fuel type, Euro class, engine displacement, power, and make of the requested engine. The ‘search\_taxcode()’ function searches for the corresponding alliance by making use of the alliance code generation Excel file (Alliance\_code\_vx.xlsx). The ‘zenodo()’ function returns a data frame of all the maps uploaded to Zenodo. This data frame is used by the function ‘get\_links()’, which returns the download link of the latest version of all available maps (base+ augmentation) of the requested engine.

An additional function ‘clustervariables()’ is added which can be used as a selection procedure for generating fallback maps. An example where this could be necessary is given in Figure 10.2: the high emitting Euro 6dT diesel map (left) will be combined with the relatively lower-emitting diesel map on the right. The function reads the data of all NO<sub>x</sub> base maps and creates cluster variables, representative for the NO<sub>x</sub> distribution within the map. These variables will be used in the ‘gower()’ function, which provides a clustering method that is used to find similar NO<sub>x</sub> base maps. The function returns a distance matrix of all base maps, these distances are based on the Gower distance with 0 (identical) and 1 (maximally dissimilar).

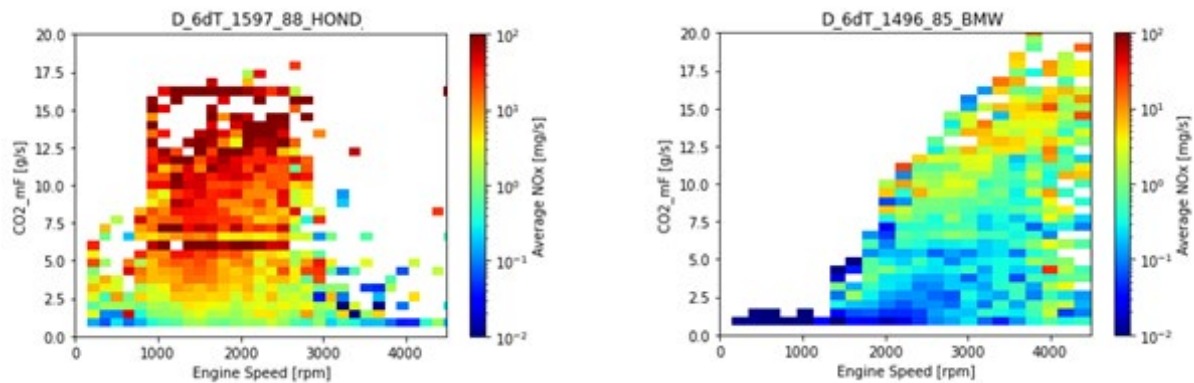


**Figure 10.2. AEMs of two different 6d-Temp diesel vehicles (left) a high emitter, (right) a high emitter.**

Furthermore, the results can be visualized in a dendrogram by using a linkage method, see Figure 10.3. Here, Ward's linkage is chosen; this method analyses the variance of clusters where the distance between two clusters is how much the sum of squares will increase when merged. This distance is shown on the horizontal axis of the dendrogram. The dendrograms show that Euro-class is more important for diesel engines than for petrol engines. Furthermore, similar engine sizes seem to cluster for petrol engines. The information retrieved from the cluster method can also be used during fallback map generation and map combination. For more in-depth analyses and argumentation, see also 'Emission map selection tool and driver classification' [49].

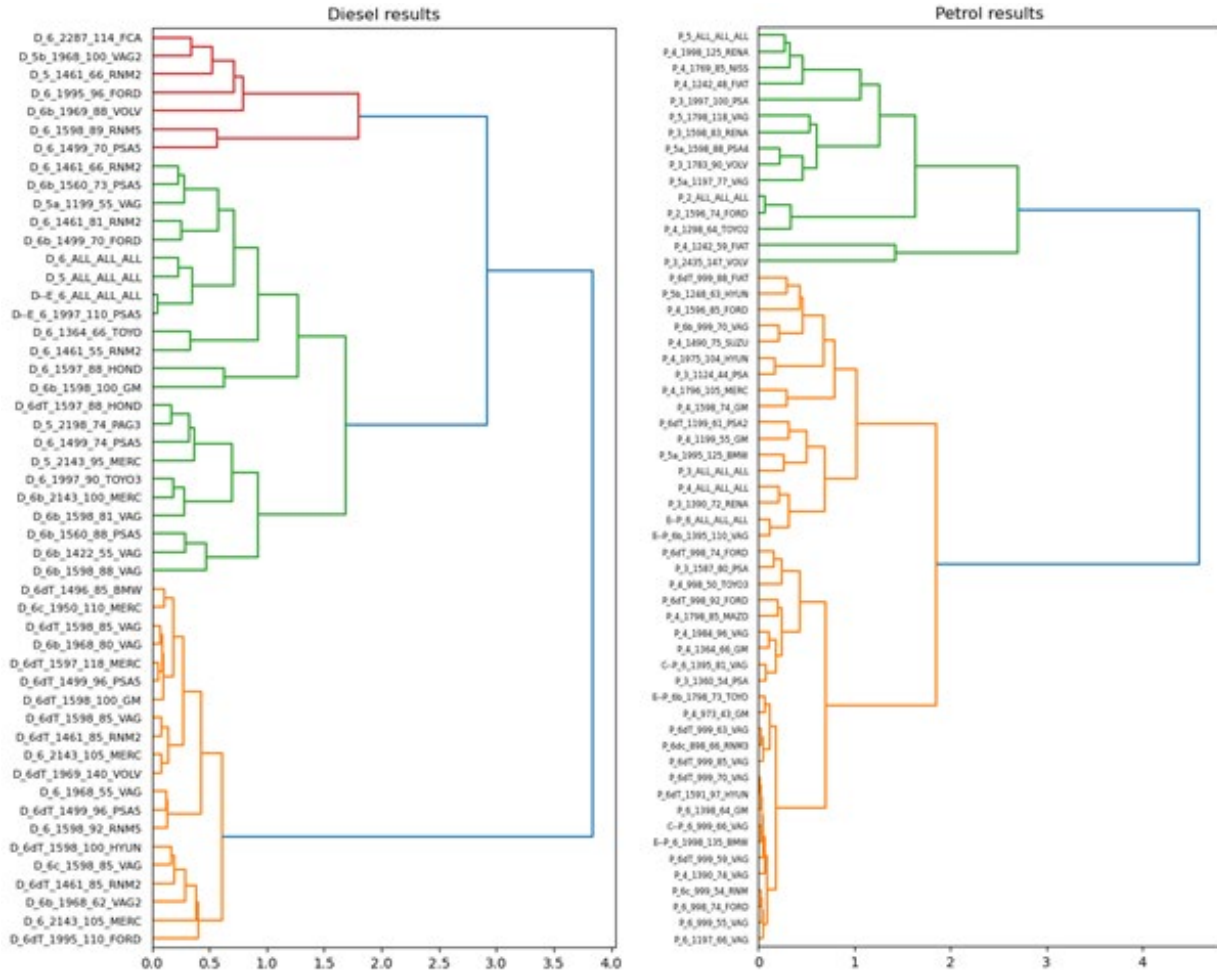


**Figure 10.3. Clusters of similar NO<sub>x</sub> base maps, for several diesel and petrol vehicles**

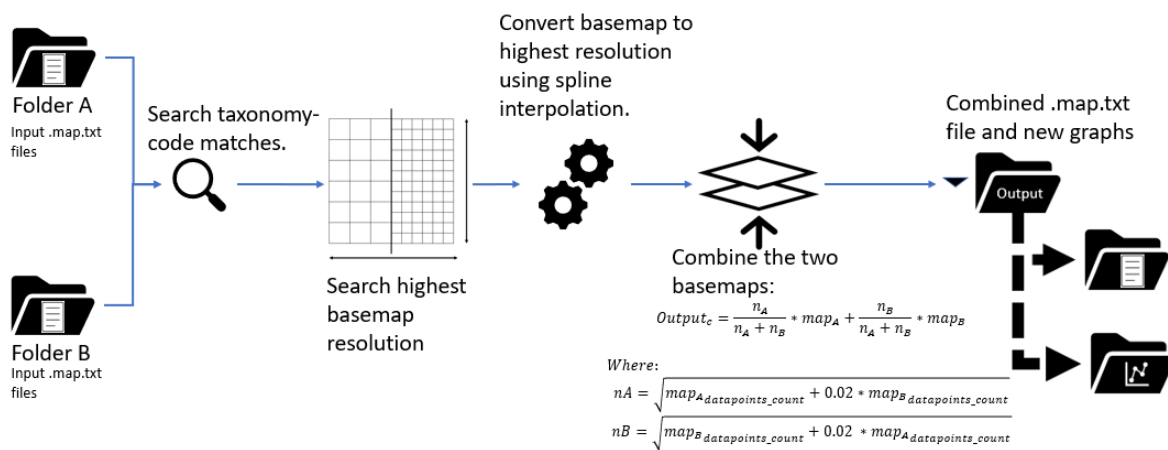
## 10.2 Combining a base map

### Combining emission maps

Emission base maps of a certain vehicle may come from different sources such as SEMS data and remote sensing data. If there are multiple base maps from different sources that have the same uCARE taxonomy code, the base maps can be combined for a more complete dataset. For example: there are currently 2 base map text files with taxonomy code P\_6b\_999\_70\_VAG which are generated from chassis dynamometer data and SEMS. The SEMS base map can be combined with the chassis dyno base map to create a new combined base map. This script is available via <https://github.com/Project-uCARE/>.

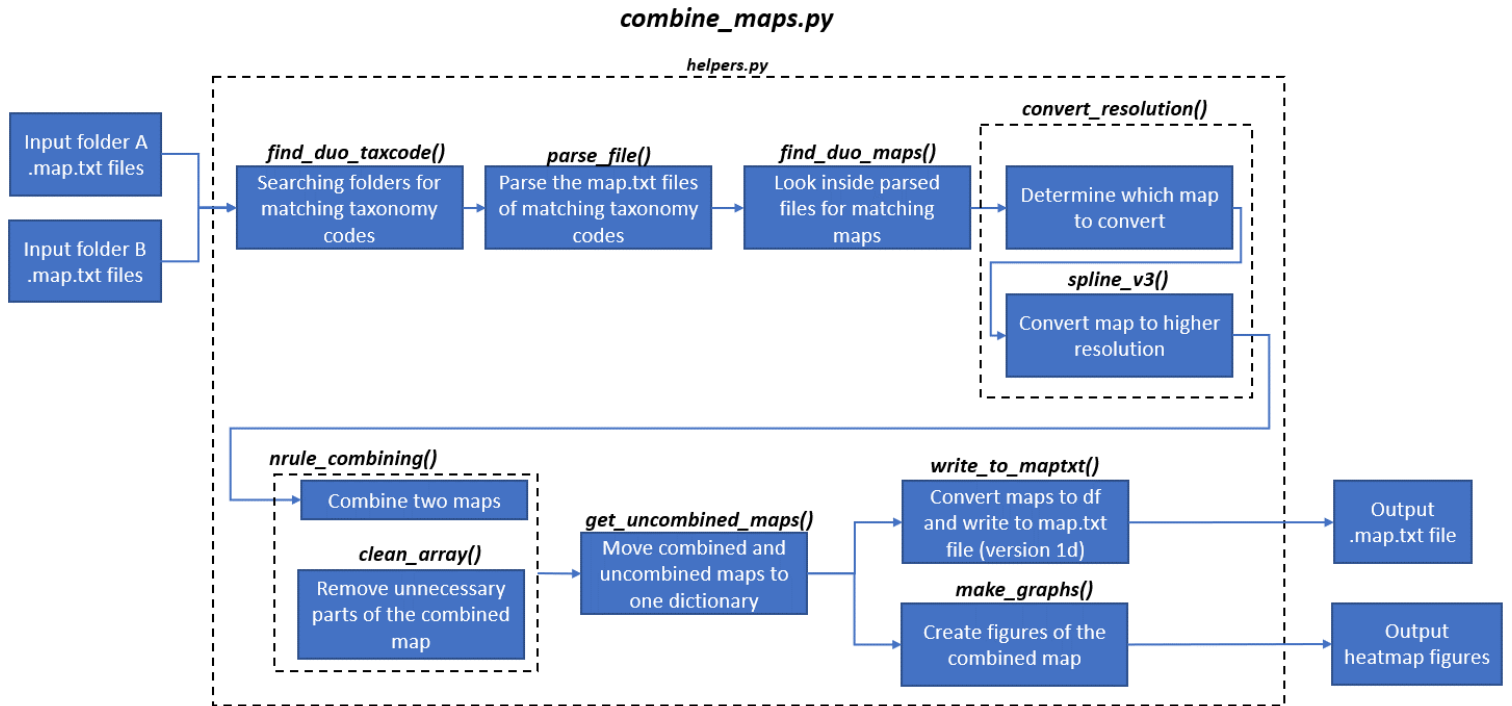
#### Process

The combining script works as shown in Figure 10.4 below. The factor 0.02 ensures that with a very skewed distribution of data, one map based on much more data than the other, the minimum weighing is  $1:0.02^{1/2}$  or 14% of the map with little data. An independent measurement set, however small, is valuable data and letting it count for 14% of the overall result is appropriate. At first, two input folders are scanned for matches of taxonomy codes in the .map.txt filenames. The number of columns and rows of an emission base map represent the resolution, the larger the amount, the higher the resolution is. For each match the .map.txt file is parsed, and the highest resolution of the base maps is determined. Next, the lowest resolution base map is converted to the higher resolution using spline interpolation. This interpolation method will be described in more detail later. Now the two base maps have identical resolutions, the combining can start. The maps are combined using a weigh factor which is based on the square root of the total number of datapoints within the map. The multiplication of both maps with the weigh factor will result in a new base map. This new base map will be processed to create a new .map.txt file and new graphs. The new .map.txt file contains the combined base map(s) and uncombined base map(s) of both sources.



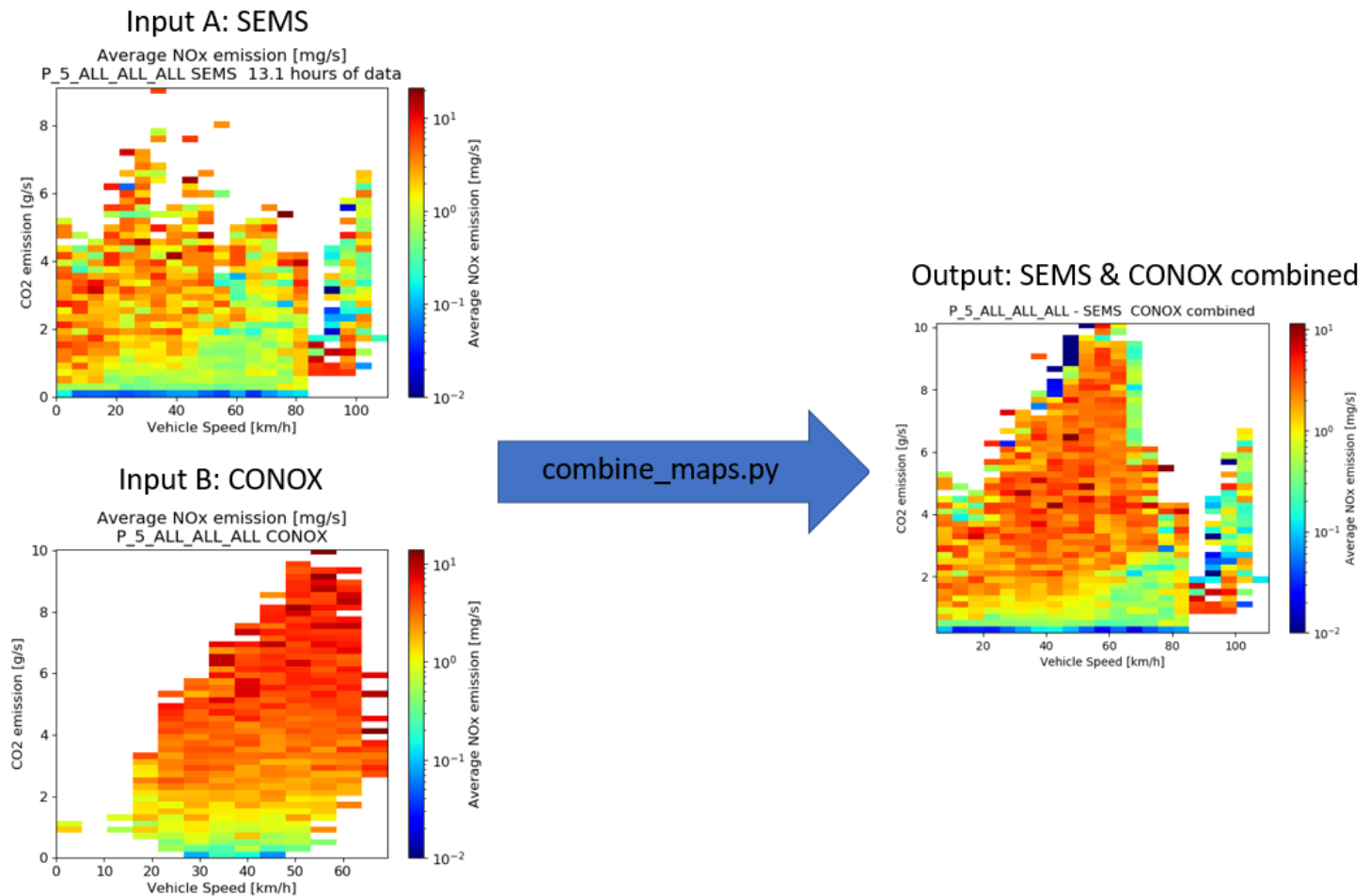
**Figure 10.4. Illustration of the combining-script process.**

Figure 10.5 below shows which (sub)functions of the *combine\_maps.py* script are responsible for the different steps during a combining iteration. The input folders A and B are in the same directory as the main script and are named 'source\_A' and 'source\_B'. The .map.txt output and the graphs are saved in the folder 'combined\_maps' which can also be found in the same directory as where *combine\_maps.py* is located.



**Figure 10.5. Schematic overview of the script to combine two emission maps.**

Figure 10.6 shows a graphical overview of what the inputs and output are of the *combine\_maps.py*. The inputs in folder 'source\_A' and 'source\_B' are emission maps in the .map.txt format but for illustration purposes the graphs of these emission maps are shown. In this example the fallback maps for Euro 5 petrol cars from SEMS and CONOX data is used as input. As expected, the combined map now has bins over a greater range in the x- and in the y-axis in comparison to the individual inputs.



**Figure 10.6. A graphic illustration of the input data and output data of combining\_maps.py. The inputs which are shown as graphs are representative of the .map.txt files of the emission maps in the combining process.**

### Interpolation

Interpolation is used to convert a low-resolution map to a higher resolution. An example of such a conversion is shown in Figure 10.7. Interpolation will distribute a bin value to its surrounding bins, in a circle with radius  $RR$  using weighted interpolation. When a base map matrix is converted to a higher resolution, an empty matrix of the desired resolution is created. Next, the values for each bin in the empty matrix are determined based on the low-resolution map. As shown in Figure 10.8, a fictive circle is drawn around the concerning bin (red). The radius of this circle is currently set to 1.5 and is called the 'circle of confusion'. At the centre of the circle the weighing factor is highest. The amount of the weighing factor varies from high (red) in the centre, to low (green) on the border of the circle. The weighing factors are multiplied by the corresponding values in the low-resolution matrix. The sum of this outcome divided by the sum of the weighing factors will result in the value that will be assigned to the selected bin in the high-resolution matrix. This process repeats over all the bins in the high-resolution matrix.

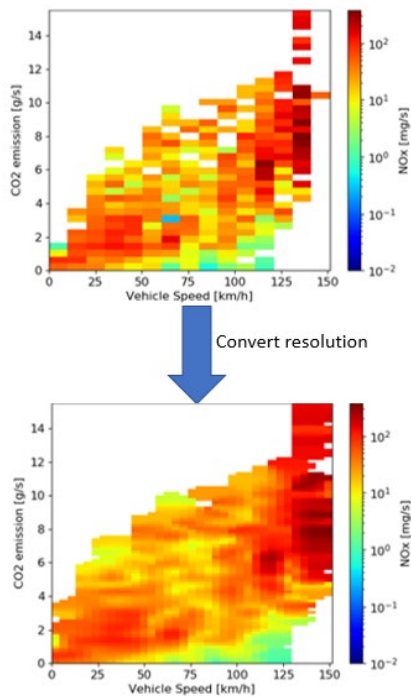


**Figure 10.7. Example of a conversion of the resolution of an emission base map**

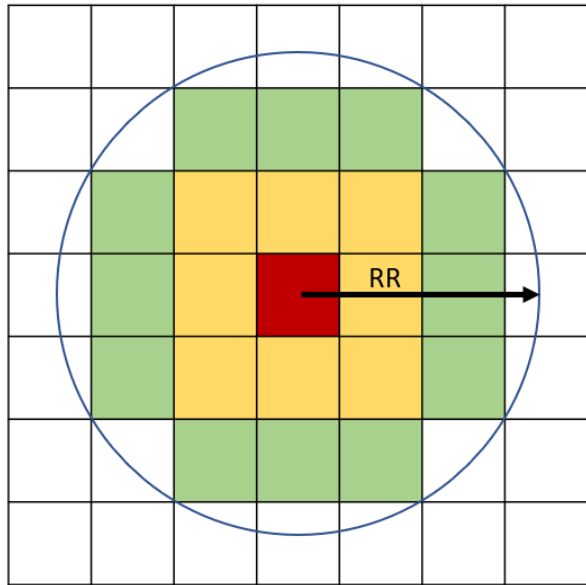


**Figure 10.8. Indicative illustration of different weighing factors in a circle around a selected bin in red. The radius of the circle is RR.**

## 10.3 Pseudocode cold start model

To assist with implementation of the cold start model, we include two sections of pseudocode. One for the implementation of the model, and one for the generation of the augmentation itself. References are made to the relevant equations in Chapter 3.3.

### 10.3.1 Main model

#### **Set input specifications:**

Set dt, nzyk and  $t_{stop}$  //Define time stamp trip data, list of trip segments and stop time between trip segments

#### **Load data:**

Load  $f_0, f_1, f_2, m$  //Load vehicle data: rolling resistance coefficients and vehicle mass

Load  $W_p, W_n, W_0, Q_{W0}, n_0, q_1, q_2, t_{1\_CO}, t_{2\_CO}, t_{3\_CO}, t_{1\_HC}, t_{2\_HC}, t_{3\_HC}, t_{1\_NOx}, t_{2\_NOx}, t_{3\_NOx}, t_{1\_PN}, t_{2\_PN}, t_{3\_PN}, m_{1\_CO}, m_{2\_CO}, m_{3\_CO}, m_{1\_HC}, m_{2\_HC}, m_{3\_HC}, m_{1\_NOx}, m_{2\_NOx}, m_{3\_NOx}, m_{4\_NOx}, m_{3\_PN}, m_{2\_PN}, m_{3\_PN}$  //Load model parameters (specific/optimized/average)

Load  $T_{amb}, v, n, \alpha$  //Load trip data for all trip segments

For each nzyk //For-loop over trip segments

#### **Model cool down during parking:**

Function COOLDOWN //Calculate initial engine temperature based on cool down curves with Eq. 5.1

#### **Model hot running engine:**

Calculate  $P(t)$  //Calculate traction power delivered to the wheels with Eq. 5.2

Calculate  $P_{pos}(t)$  //Calculate positive wheel power

Function WILLANS //Apply Willans model for hot running engine with Eqs. 5.3, 5.4 and 5.5

Calculate  $Q_{h\_hot}(t)$  //Calculate heating power with Eq. 5.6

#### **Model heating power during cold start:**

Function EXTRAHEAT //Calculate extra heat from fuel during cold start with Eq. 5.8

Calculate  $Q_h(t)$  //Calculate total heating power during cold start with Eq. 5.9

#### **Model engine warm-up during trip segment:**

Calculate  $T_e(t)$  //Calculate engine temperature warm-up during trip segment with Eq. 5.10 (only required for trip sequences)

Determine  $T_{e\_end}=T_e(end)$

#### **Model cold start duration:**

Function COLDSTARTDURATION //Calculate cold start duration with Eqs. 5.11 and 5.12

#### **Model cold start extra emissions:**

Calculate  $m_{\text{exh}}(t)$  //Calculate exhaust mass flow with Eqs. 5.15 and 5.16

Function EXTRAEMISSIONS //Calculate the cold start extra emissions with Eqs. 5.13 and 5.14

Calculate CSEE\_X //Calculate the cold start extra emissions of all pollutants as the maximum (or end in case of NOx) of the cumulated cold start extra emissions

Endfor

#### FUNCTION COOLDOWN:

If  $t_{\text{stop}} < 10\text{h}$  //If parking time below 10 hours

    Calculate  $T_{e0}$  //Calculate initial engine temperature with Eq. 5.1

elseif  $t_{\text{stop}} > 10\text{h}$  //If parking time above 10 hours

    Set  $T_{e0} = T_{\text{amb}}(0)$  //Set initial engine temperature to the ambient temperature at trip segment start

Endif

#### FUNCTION WILLANS:

Calculate  $Q_{\text{in\_hot}}(t)$  //Calculate the input power during hot running with Eq. 5.3

Correct  $Q_{\text{in\_hot}}(t)$  for motoring and idle //Apply motoring and idle corrections according to Eqs. 5.4 and 5.5

#### FUNCTION EXTRAHEAT:

Calculate  $\Delta Q_{\text{in}}(t)$  //Calculate extra heat from fuel during cold start with Eq. 5.8. Note: The integrals can be treated as a cumulative function in time

#### FUNCTION COLDSTARTDURATION:

Calculate  $Q_x$  //Calculate the integrated heating power over the cold start period for each pollutant with Eq. 5.11

Calculate  $Q_{\text{diff}}(t)$  //Calculate for each pollutant the difference between the integral of the heating power and the integrated heating power over the cold start with Eq. 5.12.

Calculate  $t_{\text{end\_x}}$  //Calculate the cold start duration for each pollutant by minimizing  $Q_{\text{diff}}$

#### FUNCTION EXTRAEMISSIONS:

Calculate  $dm_x(t)$  //Calculate the cold start extra emissions for each pollutant with Eqs. 5.13 and 5.14

### 10.3.2 Generating the augmentation

#### **Set input specifications:**

Set dt and nzyk //Define time stamp and list of cycles for model parametrization

#### **Load data:**

Load f0, f1, f2, m //Load vehicle data: rolling resistance coefficients and vehicle mass

Load  $T_{amb}$ , v, n,  $\alpha$  //Load trip data for all cycles

Load mX, mFlow //Load pollutants mass emission rates (X=CO, HC, NO<sub>x</sub>, PN) and exhaust flow data for all cycles

#### **Parametrize model for hot running engine:**

Define ind\_hot //Define hot part of cycles (e.g. bag 3 from IUFC)

Calculate  $Q_{in}(t)$  //Calculate measured heating power with Eq. 5.17

Calculate P(t) //Calculate traction power delivered to the wheels with Eq. 5.2

Calculate  $P_{pos}(t)$  //Calculate positive wheel power

Determine  $W_p$ ,  $W_n$ ,  $W_0$ ,  $Q_{w0}$  and  $n_0$  //Fit parameters in Eqs. 5.3-5.4-5.5 with least-squares optimization method by minimizing the difference between the measured and fitted heating power. Note: only hot parts of the cycles are used here.

#### **Parametrize model for heating power during cold start:**

Calculate  $Q_{in\_hot}(t)$  //Apply Willans model for hot running engine with Eqs. 5.3, 5.4 and 5.5 using the model parameters determined above.

Calculate  $\Delta Q_{in}(t) = Q_{in}(t) - Q_{in\_hot}(t)$  //Calculate measured cold start extra heating power.

Calculate  $Q_{h\_hot}(t)$  //Calculate heating power with Eq. 5.6.

Determine  $q_1$  and  $q_2$  //Fit parameters in Eq. 5.8 with least-squares optimization method by minimizing the difference between the measured and fitted cold start extra heating power. Note: at least two test cycles with different initial temperatures are required.

Calculate  $Q_h(t)$  //Calculate total heating power during cold start with Eq. 5.9 and model parameters determined above.

#### **Parametrize model for cold start duration (for X=CO, HC, NO<sub>x</sub>, PN):**

Calculate  $m_{hotX}(t)$  //Calculate hot emissions for each pollutant and cycle as the average emissions in the hot sub-cycles. Note:  $m_{hotX}$  is a time series with the length of a sub-cycle.

Calculate $dmX(t) = mX(t) - m_{hot}X(t)$	<i>//Calculate the cold start extra emissions for each pollutant by subtracting the corresponding average hot emissions from the measured emissions over the whole cycle.</i>
Calculate $cum(dmX(t))$	<i>//Calculate the cumulative of the measured extra emissions.</i>
Fit $cum(dmX(t))$	<i>//Fit the hot part of the cumulative of the measured extra emissions with a linear function.</i>
Determine $t_{end\_X}$	<i>//Determine the measured end of the cold start for each pollutant and cycle as the intersection between the cumulative of the measured extra emissions and the linear fit.</i>
Determine $t_{1\_X}, t_{2\_X}, t_{3\_X}$	<i>//Fit parameters in Eq. 5.11 with least-squares optimization method by minimizing the difference between the integrated (or cumulated) measured and fitted heating power until the end of the cold start. Note: at least two test cycles with different initial temperatures are required.</i>

**Parametrize model for cold start extra emissions (for X=CO, HC, NOx, PN):**

Determine $m_{1\_X}, m_{2\_X}, m_{3\_X}$ (and $m_{4\_X}$ for NOx)	<i>//Fit parameters in Eqs. 5.13 and 5.14 with least squares optimization method by minimizing the difference between the integrated (or cumulated) measured and fitted cold start extra emissions. Note: at least two test cycles with different initial temperatures are required.</i>
----------------------------------------------------------------------	------------------------------------------------------------------------------------------------------------------------------------------------------------------------------------------------------------------------------------------------------------------------------------------

## 10.4 Generating a base map

A Python script is created to generate base maps from different measurement devices such as TNO's SEMS (Smart Emission Monitoring Services), PEMS (Portable Emission Monitoring Systems), remote sensing data, and chassis dyno measurements. This script is available via <https://github.com/Project-uCARE/>.

### 10.4.1 Input Requirement

#### *Input CSV File*

An input CSV file containing the measurement data with minimum requirement of 1 parameter in each category: x-axis variable, y-axis variable, and the associated emission variable is required.

The current possibilities for the listed variables are as follows:

- X-axis variable: 'velocity', 'RPM'
- Y-axis variable: 'CO2'
- Emission variable: 'NOx', 'NH3', 'CH4' and others listed in the main script

For the x-axis, the 'velocity' column refers to vehicle speed in [km/h] and 'RPM' which refers to measured engine speed in [RPM]. For the y-axis, the 'CO2' column refers to measured CO2 mass flows in [g/s]. For the emission variable, the 'NOx', 'NH3', 'CH4' columns refer to measured emission mass flows in [mg/s].

An example of input CSV file that satisfies the minimum input requirements is shown in Figure 10.9.

	A	B	C	D	E	F	G	H
1	velocity	CO2	NOx					
2	0	0.005662	0.12982					
3	0	0.01488	0.068846					
4	0.046111	0.077484	0.058352					
5	0.323232	0.109563	0.044643					
6	0.858863	0.139472	0.033866					
7	1.458613	0.16565	0.024667					
8	2.174207	0.219996	0.016619					
9	3.582678	0.306484	0.00981					
10	5.671367	0.563914	0					
11	7.387172	0.565064	0					
12	8.067693	0.695741	0					
13	8.054319	0.596813	0					
14	8.003461	0.575285	0					
15	8.495806	0.625687	0					
16	9.747859	2.015991	0					
17	11.13746	2.241788	0					
18	11.88439	0.725778	0					
19	12.07426	0.310037	0					
20	12.28885	0.271293	0					

**Figure 10.9. Example of input CSV file that satisfy minimum input requirements**

With this example, the output file will contain a base map of NOx emission as a function of velocity and CO<sub>2</sub>.

Another example input CSV that contains more parameters is shown in Figure 10.10.

	velocity	RPM	CO2	NOx	NH3				
2	0	841	0.005662436	0.129820125	0.008737212				
3	0	811	0.014879915	0.068845673	0.004299638				
4	0.046111434	801	0.077483794	0.058352137	0.005950199				
5	0.323232113	801	0.109562921	0.044643042	0.006247597				
6	0.858863136	796	0.139471641	0.033865512	0.006352695				
7	1.458613163	786	0.165650385	0.02466694	0.006213601				
8	2.174206867	803	0.219996084	0.016619002	0.00713552				
9	3.582677612	783	0.306484034	0.009809664	0.008931249				
10	5.671367358	862	0.563914324	0	0.009976357				
11	7.38717232	938	0.565064488	0	0				
12	8.067692702	1109	0.695741455	0	0				
13	8.054318879	997	0.596812748	0	0				
14	8.00346068	958	0.575285184	0	0				
15	8.495805724	1067	0.625687301	0	0.000721968				
16	9.747859251	1434	2.015990991	0	0				
17	11.13745595	1670	2.241788353	0	0				
18	11.88439338	861	0.725777951	0	0.015117468				
19	12.07426399	799	0.310037265	0	0.007866073				
20	12.28884792	800	0.271293408	0	0.009676545				
21	12.93629163	859	0.500276547	0	0.012740171				
22	13.93932835	925	0.84329196	0	0				
23	15.09501501	967	0.843027994	0	0				

**Figure 10.10. Input CSV file with more parameters and emission signals**

With this example file, the resulting output file will contain 4 base maps:

- NOx as a function of velocity and CO2
- NOx as a function of RPM and CO2
- NH3 as a function of velocity and CO2
- NH3 as a function of RPM and CO2

*Input parameters in the main script*

In the main script (currently name `main_UCARE.py`), several input parameters are required to be used as the header of the output text file. The required parameters need to be filled manually:

- **datafile [string]**: contains the path location of the input CSV file
- **engine\_taxonomy\_code [string]**: contains the engine taxonomy code of the input file. The format of the engine taxonomy code to be used is described in D1.2
- **available\_pollutants [list]**: a list containing string variables of emission data inside input CSV file, for example, ['NOx', 'NH3']. This parameter has to match the column name inside the CSV file.
- **veh\_cnt [integer]**: the number of vehicles that are used to generate the measurement data in the input CSV file
- **method [string]**: describes method which is used to gather the data (for example: 'chassis dynamometer', 'PEMS')
- **DOI [string]**: Digital Object Identifier of this document
- **start\_mileage [float]** : average start mileage [km] of the vehicles used in measurement program. If not applicable or unknown, this parameter must be filled with "N/A"
- **BIN\_THRESHOLD [int]** : minimum number of data per bin required to be processed. Insufficient number of data per bin will be ignored from processing.
- **org\_name [string]** : organisation name that is generating the basemap
- **version\_ctrl [string]**: version control for basemap generation

## 10.4.2 Expected Output

*Text File Output*

An example of the text file output from the example data shown in Figure 10.10 is shown in Figure 10.11.

```
#####
# START META
#
# ID: D_6_2143_105_MERC
# TOTAL KM: 494.8
# TOTAL TIME [h]: 10.4 hours of data
# NUMBER OF VEHICLES: 1
# AVERAGE MILEAGE OF VEHICLES [km]: n/a
# REFERENCE DOI: 10.5281/zenodo.4268034
# AVAILBLE MAPS: VEHICLE SPEED - CO2 - MEAN NOx - STD - Q25 - Q75 - COUNT, VEHICLE SPEED - CO2 - MEAN NH3 - STD - Q25 - Q75 - COUNT, ENGINE
SPEED - CO2 - MEAN NOx - STD - Q25 - Q75 - COUNT, ENGINE SPEED - CO2 - MEAN NH3 - STD - Q25 - Q75 - COUNT
# END META
#####
# START VEHICLE SPEED - CO2 - MEAN NOx - STD - Q25 - Q75 - COUNT
#
# NOTES: [SEMS]
# XLABEL: Vehicle Speed upper bin limit [km/h]
# YLABEL: CO2 upper bin limit [g/s]
# Z1LABEL: Average NOx emissions [mg/s]
# Z2LABEL: Standard deviation NOx emissions [mg/s]
# Z3LABEL: 0.25 quantile NOx emissions [mg/s]
# Z4LABEL: 0.75 quantile NOx emissions [mg/s]
# Z5LABEL: Count per bin [#]
# START DATA VEHICLE SPEED - CO2 - MEAN NOx - STD - Q25 - Q75 - COUNT
X,Y,Z1,Z2,Z3,Z4,Z5
7.607222222222223,0.28630245391665177,0.0519090077683688,0.1952464927547179,0.0,0.0407856211033848,279.0
7.607222222222223,0.5726049078333035,0.09083134512178857,0.6205220006527493,0.0,0.0273891375140062,253.0
7.607222222222223,0.8589073617499553,0.1268816424506605,0.5664335653010335,0.0,0.0409775289696852,453.0
7.607222222222223,1.145209815666607,0.7358359793996823,2.009248595972766,0.0,0.30034339404063154,252.0
7.607222222222223,1.431512269583259,0.4852284428853211,1.0036446974791750,0.0,0.15541809752389998,130.0
7.607222222222223,1.7178147234999106,0.31702105068625663,0.9312419377533774,0.0,0.16714361416798101,43.0
7.607222222222223,2.0041171774165623,1.0097805978327528,1.9403197967681585,0.0,1.2137206884187246,15.0
```

**Figure 10.11. Example output text file based on input CSV file shown in Figure 10.10.**

The format of the output text file can be found in Chapter 9.

*Figure Files*

The figure file visualizes the emission base map data. Figure 10.12 shows an example of visualizing the average NO<sub>x</sub> emission as a function of CO<sub>2</sub> emission and velocity/vehicle speed.

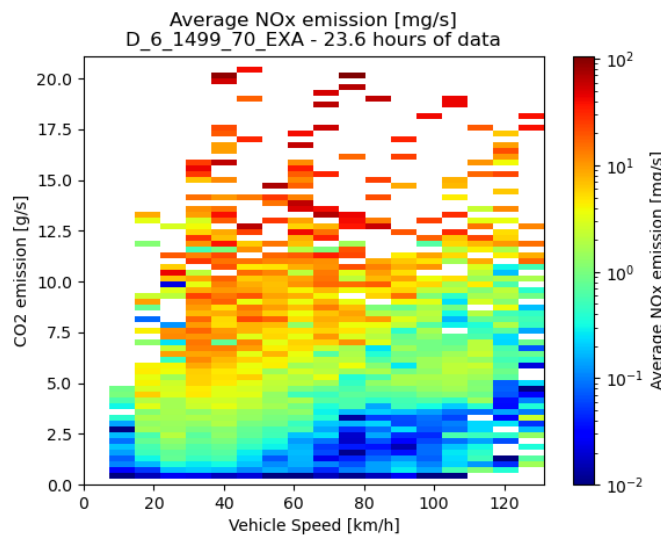


**Figure 10.12. Example of visualisation results of the emission base map, based on input CSV file shown in Figure 10.10**

The figure file serves as an overview of the distribution of the emission data from the input file.

**10.4.3 Script Flowchart**

The working procedure of the script can be visualised in Figure 10.13.

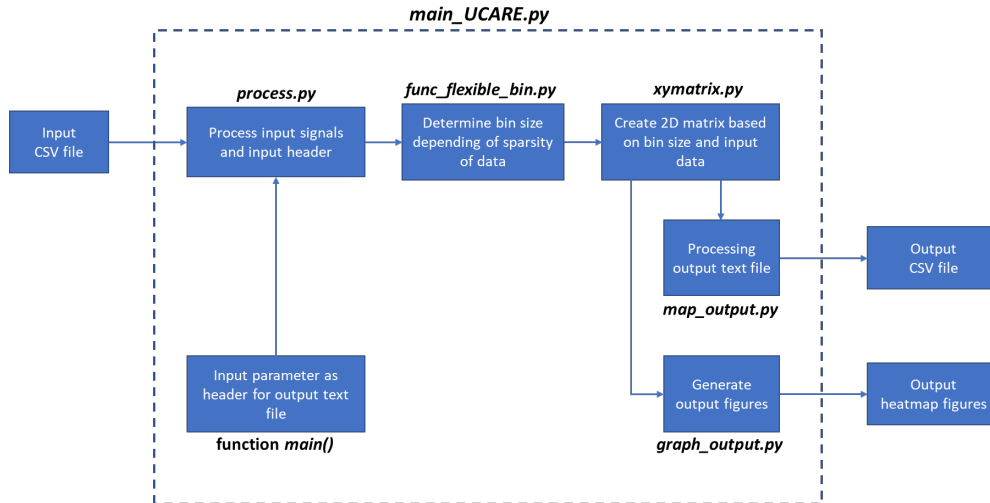


**Figure 10.13. Flow chart of the script to generate emission base map**

The blue blocks are named according to the script names or function names and contains the summary of the processes that are happening. For example, the script *func\_flexible\_bin.py* is used to determine the bin size depending of the sparsity of input measurement data.

#### 10.4.4 Description of flexible bin size algorithm

The algorithm used to determine the bin size is formulated by calculating the ratio of the maximum area of the island of pixels in the emission map, and the total count of non-zero pixels<sup>16</sup> (will be referred as coverage ratio). In other words

$$coverage\ ratio = \frac{Area_{island\ with\ maximum\ area}}{\sum Area_{all\ islands}}$$

An island of pixels is defined as a cluster of contiguous non-zero numbers in a sparsely populated matrix. For example, assuming that the emission map is an image that has the dimension of 4 x 4 pixels, and the bin size is set as 1x1 pixel (denoted by the black-dashed square), the emission map can be simplified as a 4x4 matrix as follows:

$$\begin{bmatrix} 1 & 0 & 1 & 0 \\ 0 & 0 & 1 & 1 \\ 0 & 0 & 0 & 0 \\ 1 & 1 & 0 & 0 \end{bmatrix}$$

Note that the ones represent the *existence* of data in the pixel and not the *amount* of data in each pixel.

In this example, the maximum area of the island of the pixels is 3, shown by the red bracket and the total area of non-zero pixels (or the total area of all the islands) is 6. The coverage ratio is  $\frac{3}{6}$ , or 50%. If the threshold of the acceptable coverage ratio is set to 90%, this case would not meet the threshold. The bin size of the emission map would then be enlarged and the emission map regenerated.

Assuming the bin-size is increased to 2x2 pixels, as denoted by the black-dashed square, the matrix above will be divided into 4 bins. The matrix can therefore be reduced into a 2x2 matrix to note the existence of data in the enlarged pixel, shown by the right matrix.

<sup>16</sup> Note that this means that a pixel is counted as covered if it has at least one data point.

$$\begin{bmatrix} \boxed{1} & \boxed{0} & 1 & 0 \\ 0 & \boxed{0} & 1 & 1 \\ 0 & \boxed{0} & 0 & 0 \\ 1 & 1 & 0 & 0 \end{bmatrix} \rightarrow \begin{bmatrix} 1 & 1 \\ 1 & 0 \end{bmatrix}$$

The maximum area of the island of the pixels in the right matrix is 3, shown by the red bracket. The total area of non-zero pixels is also 3, so the new coverage ratio is  $\frac{3}{3}$ , or 100%. The 2x2 pixels (as indicated by the black dashed line) will be the final bin size to be used to plot the emission map.

#### 10.4.4.1 Implementation of algorithm to emission map

The algorithm above is implemented to the two emission maps of NO<sub>x</sub> emissions (one with engine speed and one with vehicle speed on the x-axis).

In the creation of each emission map, the algorithm will start with the smallest bin size: vehicle speed 5 km/h per bin, CO<sub>2</sub> emission 0.2 g/s per bin, and engine speed 50 RPM per bin. Currently, the threshold for the acceptable coverage ratio is set at 90%.

If the starting coverage ratio is equal or larger than 90% (i.e. sufficient measurement data to cover the emission map), the starting bin size is chosen. The algorithm will not try to decrease the bin size further than the starting values.

If the starting coverage ratio is smaller than 90%, the bin sizes are scaled by the square root of 2. For example, in the vehicle speed-based NO<sub>x</sub> map, the bin size for vehicle speed will be scaled from 5 km/h to 7.1 km/h (and further to 10 km/h if necessary) and the bin size for CO<sub>2</sub> emission will be scaled from 0.2 g/s to 0.28 g/s (and further to 0.4 g/s if necessary). The value square root of 2 is chosen to control the speed of the resolution change.

#### 10.4.4.2 Example case: Skoda Octavia with 11 hours of measurement data

Data from a Skoda Octavia was collected from RDE (Real Driving Emissions) tests. Note that this is still Level 1 in paragraph 8.1. Using the algorithm above, the starting coverage ratio is calculated to be 64.4%, which is below the threshold value.

The algorithm increases the engine speed resolution incrementally from 50 RPM to 141 RPM and CO<sub>2</sub> emission resolution from 0.2 g/s to 0.57 g/s, where the final coverage ratio is calculated to be 97.1%. Figure 10.1 shows the comparison between the emission map with the starting smallest size (left figure) and the enlarged bin size (right figure).

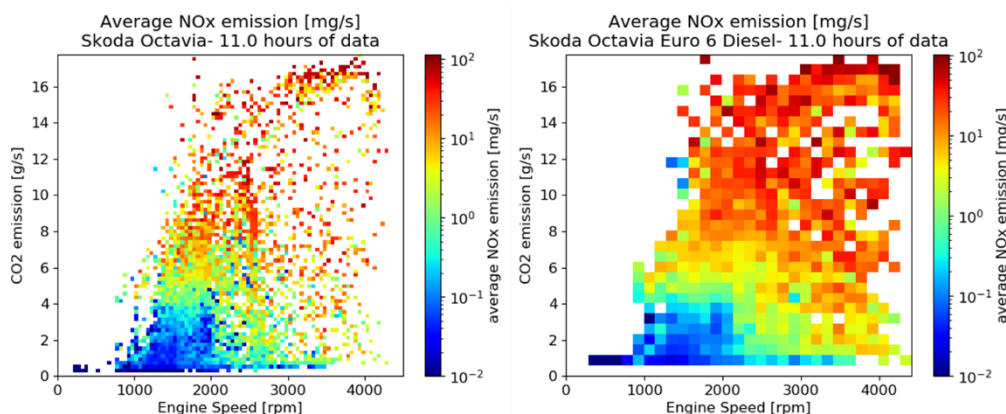


**Figure 10.1 Comparison of NO<sub>x</sub> emission map with the smallest bin size (left figure) and enlarged bin size (right figure) after the algorithm is applied.**

The flexible bin size algorithm will affect the resolution of the emission map. As a result, if the generated emission map is directly used as a tool for predicting the NO<sub>x</sub> emission of the vehicle, the accuracy of the prediction can be affected.

As an example case, the maps generated from Figure 10.1 are directly used to build a 2D lookup table for predicting NO<sub>x</sub> emission from the same vehicle. Any empty bins are directly filled with 0s for simplicity. Any further processing or aggregation are left to the end users to apply for their own intended purpose and is not discussed in this section.

When calculating the Root Mean Square Error (RMSE) between the measurement data and the prediction models, the NO<sub>x</sub> prediction using the smallest bin size is 4.17 mg/s while using the enlarged bin size is 4.32 mg/s. However, looking at the second by second data shown in Figure 10.2, the difference between the predicted and measured NO<sub>x</sub> value is more stable in the case of the enlarged bin size, as shown in Figure 10.3.

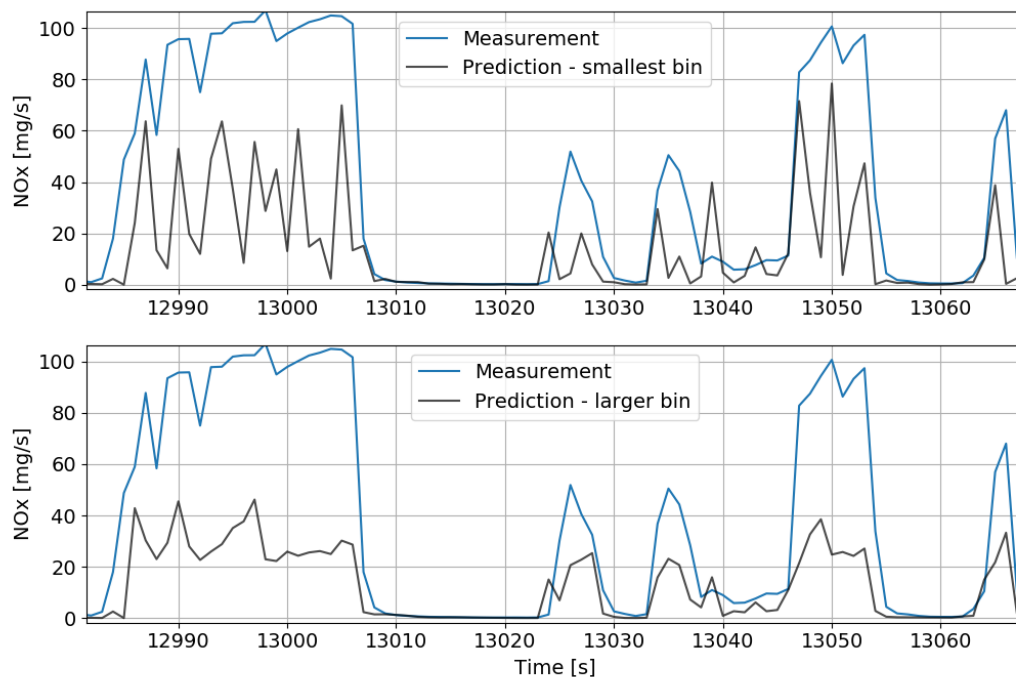


**Figure 10.2** Example case on directly predicting NO<sub>x</sub> with the emission map with smallest bin size (top figure) vs enlarged bin size (lower figure).

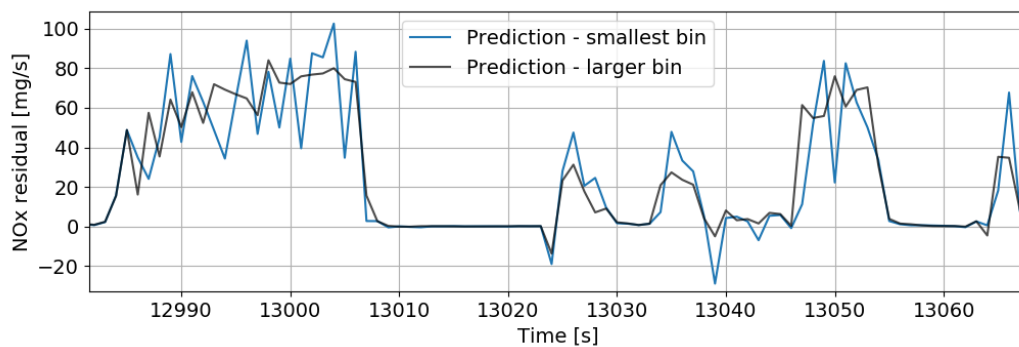


**Figure 10.3** Plot of NO<sub>x</sub> residuals from Figure 10.2.

## 11A formal explanation of the augmented emission map data exchange format

A data file structure has been developed to facilitate the exchange of map data among partners, simplify versioning, and enable the implementation of the emission maps in multiple tools. In this chapter we outline this file structure as well as provide the relevant syntax in Backus-Naur format.<sup>17</sup>

### 11.1 Metadata

In order to share data, the emission data format is standardized. The data exchange format contains all data that is applicable for a specific engine taxonomy code. The standardized emission map has a ".map.txt" extension and is also human readable. As shown in Figure 11.1, the file starts with metadata which contains information about:

- the engine taxonomy code
- total driven kilometres over which the data was gathered
- total time in hours over which the data was gathered
- the number of vehicles which were tested to create the emission map
- the average age of the vehicles, expressed in km driven, over which the data was gathered
- the DOI (Digital Object Identifier) reference, which references a document like this one, or an earlier version, providing the explanation how the data can be used.
- Which emission maps are available in the file. In Figure 11.1, two maps are mentioned.

```
#####
# START META
#
# ID: D_5a_1199_55_VAG
# TOTAL KM: 26649.3
# TOTAL TIME [h]: 345.9
# NUMBER OF VEHICLES: 1
# REFERENCE DOI: 10.5281/zenodo.3669986
# AVAILABLE MAPS: VEHICLE SPEED - CO2 - MEAN NOX - STD - Q25 - Q75 - COUNT, ENGINE SPEED - CO2 -
MEAN NOX - STD - Q25 - Q75 - COUNT
# END META
#####
```

**Figure 11.1. Screenshot of Metadata**

The formal description consists of a syntax description in Backus-Naur form with additional syntactical requirements in text. The root is the <AEM file>, i.e. the file with the ".map.txt" extension.

```
<AEM file> ::= <meta> <map list>
<map list> ::= <map> | <map> <map list>
<map> ::= <base map> | <cold start> | <deterioration>
```

The syntax for <meta> is elaborated below, each with a set of requirements.

<sup>17</sup> For an explanation of the Backus-Naur format see, for example, [https://en.wikipedia.org/wiki/Backus-Naur\\_form](https://en.wikipedia.org/wiki/Backus-Naur_form).

## Formal syntax definition <meta>

```

<meta> ::= "START META" <taxonomy id> <map notes> <total km>
        <total time> <nr vehicles> <vehicle age>
        <reference doi> <available maps> "END META"
<taxonomy id> ::= "ID:" <taxonomy identifier>
<taxonomy identifier> ::= <identifier>
<map notes> ::= "" | <map note> <map notes>
<map note> ::= "NOTES:" "[" <notes text> "]"
<total km> ::= "" | "TOTAL KM:" <km>
<km> ::= <real number> | "n/a"
<total time> ::= "" | "TOTAL TIME [h]:" <time>
<time> ::= <real number> | "n/a"
<nr vehicles> ::= "" | "NUMBER OF VEHICLES:" <nr>
<nr> ::= <integer> | "n/a"
<vehicle age> ::= "AVERAGE MILEAGE OF VEHICLES [km]:" <age> | ""
<age> ::= <integer> | "n/a"
<real number> ::= <integer> | "-" <integer> | <decimal> | <exponent>
<decimal> ::= <integer> "." <integer> | "-" <integer> "." <integer>
<exponent> ::= <decimal> "E+" <integer> | <decimal> "E-" <integer>
<reference doi> ::= "REFERENCE DOI:" <doi identifier>
<doi identifier> ::= <identifier>
<available maps> ::= <base maps> <cold start formulae>
                  <deterioration tables>
<base maps> ::= "" | "AVAILABLE MAPS:" <full map id lists>
<full map id lists> ::= <full map id list> |
                    <full map id list> "," <full map id lists>
<full map id list> ::= <map id list>
<map id list> ::= <map id> | <map id> "-" <map id list>
<map id> ::= <identifier>
<cold start formulae> ::= "" | "AVAILABLE COLD START:" <pollutant list>
<pollutant list> ::= <pollutant> | <pollutant> "," <pollutant list>
<pollutant> ::= "CO" | "HC" | "NOX" | "NOx" | "PN"
<deterioration tables> ::= "" | "AVAILABLE DETERIORATION:" <pollutant list>

```

## Requirements <meta>

- The <taxonomy\_identifier> should be formed according to Section 2.3.1 of this document.
- A <notes text> should not contain a "]" (ASCII 93) and can contain any character allowed in an identifier and spaces.
- The <doi identifier> should be formed according to ISO 26324 and should refer to this document or an earlier version of it.
- If <total km> is the empty string, that is equivalent to "TOTAL KM: n/a", i.e. the total number of kilometers driven for the collection of data is not available.
- If <total time> is the empty string, that is equivalent to "TOTAL TIME [h]: n/a", i.e. the total number of hours for the collection of data is not available.
- If <nr vehicles> is the empty string, that is equivalent to "NUMBER OF VEHICLES: n/a", i.e. the total number of vehicles for the collection of data is not available.
- If <vehicle age> is the empty string, that is equivalent to "AVERAGE MILAGE OF VEHICLES [km]: n/a", i.e. the average mileage is not available.
- For each <full map id list> in the <base map> there should be a <base map> in the <map list> with the same <full map id list>.
- The first <map id> in a <full map id list> should not be "COLD START".
- The first <map id> in a <full map id list> should not be "DETERIORATION".
- For each <pollutant> in the <pollutant list> of the <cold start formulae> there should be a <cold start> in the <map list> as follows.
  - <pollutant> == "CO" requires a <cold start> with <CO parameters>
  - <pollutant> == "HC" requires a <cold start> with <HC parameters>
  - <pollutant> == "PN" requires a <cold start> with <PN parameters>
  - <pollutant> == "NOX" or <pollutant> == "NOx" requires a <cold start> with <NOX parameters>
- If in the <deterioration tables> a <pollutant> occurs in the <pollutant list>, then <deterioration> should contain a <pollutant deterioration> with the same <pollutant>.
- In an <identifier> only the ASCII characters 32- 34 and 36-126 can be used; an <identifier> should not be equal to a key word.
- The ASCII characters 9 (Horizontal tab), 10 (Line Feed) and 35 (#) are all considered equivalent to a space (ASCII 32) and used to separate key words from <identifier>s, <real number>s, etc.
- In a <real number> there should be no spaces.
- An <integer> is a sequence of digits (ASCII 48-57) without spaces.

## 11.2 Emission base map data

The emission base map data follows the metadata. As shown in Figure 11.2, the map starts with the name of the map, followed by notes in which the measurement method can be mentioned. Next the labels are explained. The map in Figure 11.2 consists of:

- vehicle speed[km/h]
- CO2 upper bin limit [g/s]
- average emission within a bin [mg/s]. This could be any pollutant emission.
- standard deviation of the emission within a bin [mg/s]. This could also be followed by the 25<sup>th</sup> and 75<sup>th</sup> quartile.
- count of datapoint within a bin [#]

Figure 11.2 and Figure 11.3 show that each map starts and ends with "START" and "END".

```
#####
# START VEHICLE SPEED - CO2 - NOX - STD - COUNT
#
# NOTES: [SEMS monitoring]
# XLABEL: Vehicle Speed upper bin limit [km/h]
# YLABEL: CO2 upper bin limit [g/s]
# Z1LABEL: Avg NOx emissions [mg/s]
# Z2LABEL: Standard deviation NOx emissions [mg/s]
# Z3LABEL: Count per bin [#]
# START DATA VEHICLE SPEED - CO2 - NOX - STD NOX - COUNT
X,Y,Z1,Z2,Z3
5.359042631017666,0.0,0.0,0.0,0.0
5.359042631017666,0.20270030165953629,0.7469680521073303,0.023834804273464114,306.0
5.359042631017666,0.40540060331907257,20.23617307916325,0.07984795620023198,2398.0
5.359042631017666,0.6081009049786088,66.90430484277235,0.1188222323504034,3422.0
```

**Figure 11.2. Screenshot of emission base map data with START heading, indicating the start of map data**

```
144.69415103747698,18.04052004709075,0.0,0.0,0.0
144.69415103747698,18.243027149358266,0.0,0.0,0.0
144.69415103747698,18.445727451017802,0.0,0.0,0.0
# END VEHICLE SPEED - CO2 - NOX - STD NOX - COUNT
```

**Figure 11.3 Screenshot of emission map data with END heading, indicating the end of the map data**

The syntax for <base map> (which is a <map> as defined in 11.1) is elaborated below, with a set of requirements.

**Formal syntax definition <base map>**

```
<base map> ::= "START" <full map id list> <map notes> <map labels>
            "START DATA" <full map id list> <csv data>
            "END" <full map id list>

<map labels> ::= "XLABEL:" <label text> "YLABEL:" <label text>
               <zlabel list>

<zlabel list> ::= <zlabel keyword> <label text> |
                <zlabel keyword> <label text> <zlabel list>

<zlabel keyword> ::= "Z1LABEL" | "Z2LABEL" | "Z3LABEL" |
                   "Z4LABEL" | "Z5LABEL" | "Z6LABEL" | "Z7LABEL" |
                   "Z8LABEL" | "Z9LABEL"
```

### Requirements <base map>

- The three <full map id list>s in a <base map> should be identical.
- The <full map id list> in a <base map> should also occur in the <base maps> as defined in 11.1.
- A <map id> should contain at least three (3) <map id text>s.
- A <label text> can contain any character allowed in an identifier and spaces, but should not contain "XLABEL", "YLABEL" or any of the keywords in <Zlabel keyword>.
- The number of <map id>s in the <full map id list> should be identical to the number of <label text>s in the <map labels>.
- All <Zlabel keyword>s in the <Zlabel list> should be different.  
For human readability the use of consecutive numbers is recommended.
- The <csv data> in the <base map> should be formatted according to RFC 4180 and the number of columns in the csv data should be identical to the number of <label text>s in the <map labels>.

This makes the exchange format readable for both human and computers. The emission maps will be published on an Open research Data platform (Zenodo) so model developers can use it as input for their models. Qualified parties will be able to update an emission map when there is new and/or additional data for that specific engine taxonomy code available.

### 11.3 Cold start

The cold start augmentations are structured in a similar manner. The cold start meta data includes the taxonomy identifier (or engine code), the list of pollutants for which the cold start model parameters are available, as well as a brief description of the measurements used to parametrize the model (Figure 11.4). The cold start formulae parameters follow the meta data. Formal description of cold start data provides the parameters for the formulae in Section 3.5, used to calculate the cold start extra emissions. In the screenshots in Figure 11.5 and Figure 11.6 the cold start begins with "START COLD START", followed by the vehicle and the model parameters. After all parameters have been listed, it ends with "END COLD START".

```
#####
# START META
#
# ID: P_6c_1498_110_VAG
#
# AVAILABLE COLD START: CO, HC, NOx, PN
#
# NOTES: [Data source: IUFC -7°C and IUFC 23°C measurements from a VW Golf Variant]
#
# END META
#####
```

**Figure 11.4.: Screenshot of the meta data of a cold start AEM**

```
#####
# START COLD START
#
# START VEHICLE PARAMETERS
m[kg],f0[N],f1[N/(km/h)],f2[N/(km/h)^2]
1452,94.997,0.468,0.030
# END VEHICLE PARAMETERS
#
# START ENGINE MODEL PARAMETERS
wp[-], wn[W/rpm], w0[W], Qw0[W], n0[rpm], q1[1/K], q2[K/J]
3.218,17.828,-13672.085,4540.33,530.547,2.246E-03,2.645E-06
# END ENGINE MODEL PARAMETERS
#
# START CO MODEL PARAMETERS
```

**Figure 11.5.: Screenshot of the beginning of the cold start AEM section with START COLD START**

```
# START PN MODEL PARAMETERS
t1_PN[J/K], t2_PN[J], t3_PN[1/K], m1_PN[-], m2_PN[1/°C], m3_PN[(1/J)^(1/2)]
1.000E+05,1.568E+00,1.050E-01,1.516E+03,3.699E+01,1.890E-03
# END PN MODEL PARAMETERS
#
# END COLD START
#####
```

**Figure 11.6.: Screenshot of cold start AEM section with END heading, indicating the end of the cold start formulae parameters**

### Formal syntax definition <cold start> in cold start augmentations

The syntax for <cold start> (which is a <map> as defined in 11.1) is elaborated below, with a set of requirements.

```
<cold start> ::= "START COLD START" <map notes> <vehicle parameters>
               <engine model> <pollutant model list>
               "END COLD START"
<vehicle parameters> ::= "START VEHICLE PARAMETERS"
                        "m[kg],f0[N],f1[N/(km/h)],f2[N/(km/h)^2]"
                        <4real list> "END VEHICLE PARAMETERS"
<engine model> ::= "START ENGINE MODEL PARAMETERS"
                  "wp[-], wn[W/rpm], w0[W], Qw0[W], n0[rpm], q1[1/K],
                  q2[K/J]"
                  <7real list> "END ENGINE MODEL PARAMETERS"
<pollutant model list> ::= <pollutant model> |
                          <pollutant model> <pollutant model list>
<pollutant model> ::= <CO parameters> | <HC parameters> |
                     <NOx parameters> | <PN parameters>
<CO parameters> ::= "START CO MODEL PARAMETERS"
                   "t1_CO[J/K], t2_CO[J], t3_CO[1/K], m1_CO[-],
                   m2_CO[1/°C], m3_CO[(1/J)^(1/2)]"
                   <6real list> "END CO MODEL PARAMETERS"
<HC parameters> ::= "START HC MODEL PARAMETERS"
                   "t1_HC[J/K], t2_HC[J], t3_HC[1/K], m1_HC[-],
                   m2_HC[1/°C], m3_HC[(1/J)^(1/2)]"
                   <6real list> "END HC MODEL PARAMETERS"
<NOx parameters> ::= "START NOx MODEL PARAMETERS"
                    "t1_NOx[J/K], t2_NOx[J], t3_NOx[1/K], m1_NOx[-],
                    m2_NOx[1/°C], m3_NOx[(1/J)^(1/2)], m4_NOx[-]"
                    <7real list> "END NOx MODEL PARAMETERS"
```

```

<PN parameters> ::= "START PN MODEL PARAMETERS"
                  "t1_PN[J/K], t2_PN[J], t3_PN[1/K], m1_PN[-],
                  m2_PN[1/°C], m3_PN[(1/J)^(1/2)]"
                  <6real list> "END PN MODEL PARAMETERS"
<4real list> ::= <real number> "," <real number> "," <real number> ","
<real number>
<6real list> ::= <real number> "," <real number> "," <4real list>
<7real list> ::= <real number> "," <6real list>

```

### Requirements <cold start>

- If in the <available cold start> the <pollutant> "CO" occurs, then <CO parameters> must occur in <cold start>.
- If in the <available cold start> the <pollutant> "HC" occurs, then <HC parameters> must occur in <cold start>.
- If in the <available cold start> the <pollutant> "PN" occurs, then <PN parameters> must occur in <cold start>.
- If in the <available cold start> the <pollutant> "NOX" or "NOx" occurs, then <NOX parameters> must occur in <cold start>.
- The <pollutant model list> should contain at most one <CO parameters>, one <HC parameters>, one <PN parameters>, and one <NOX parameters>.

## 11.4 Deterioration

The deterioration table data follow the meta data. Formal description of deterioration provides the tables as defined in Chapter 3.8. In the screenshots in Figure 11.7 and Figure 11.8 the deterioration section begins with "START DETERIORATION", and allows for some notes, where e.g. the data source can be mentioned. After all tables have been listed, it ends with "END DETERIORATION".

```

# START DETERIORATION
#
# XLABEL: ACCUMULATED MILAGE [km]
# Y1LABEL: DETERIORATION FACTOR
# Y2LABEL: STD
# Y3LABEL: COUNT
#
# START DATA NOX
X, Y1
0.0,1.00
50000.0,1.00
100000.0,1.00
200000.0,1.03
300000.0,1.07
# END DATA NOX

```

**Figure 11.7. Screenshot of the start of deterioration table, with NOx emission as the first example**

```

# END DATA CO
#
# END DETERIORATION
#####

```

**Figure 11.8. Screenshot of the end of deterioration table for NOx emission**

The syntax for <deterioration> (which is a <map> as defined in 11.1) is elaborated below, with a set of requirements.

```
<deterioration> ::= "START DETERIORATION" <map notes>
                  <deterioration labels>
                  <pollutant deterioration list>
                  "END DETERIORATION"
<deterioration labels> ::= "XLABEL: ACCUMULATED MILAGE [km]"
                          "YLABEL: DETERIORATION FACTOR"
                          "Z1LABEL STD DETERIORATION FACTOR"
                          "Z2LABEL COUNT"
<pollutant deterioration list> ::= <pollutant deterioration> |
                                   <pollutant deterioration>
                                   <pollutant deterioration list>
<pollutant deterioration> ::= "START DATA" <pollutant> <csv file>
                              "END DATA" <pollutant>
```

### Requirements <deterioration>

- If a <pollutant> occurs in a <pollutant deterioration> then that <pollutant> should also occur in the <pollutant list> of the <deterioration tables> (see 11.1).
- The two <pollutant>s in a <pollutant deterioration> should be identical.
- The <csv data> in the <pollutant deterioration> should be formatted according to RFC 4180 and the number of columns in the csv data should be 4.

## 12 Engine and vehicle deterioration leads to increased emissions

Engine and vehicle components are subject to wear due to their continuous use. This applies to the aftertreatment devices and systems as well, which results in deterioration over the course of a vehicle's life. Data shows that, in most cases, an emissions increase is dependent on accumulated vehicle mileage and age. The main reasons behind the aftertreatment deterioration are the catalyst thermal ageing, the chemical poisoning and the mechanical wear, with the first mechanism being the dominant for most aftertreatment devices (this is discussed further in Section 12.1).

### 12.1 Deterioration leads to increased emissions via several different mechanisms

This section provides the background on the emissions deterioration, which is largely dependent on the aftertreatment device ageing. The description is separate for petrol and diesel vehicles. The relevant material has been integrated from literature, past data, as well as according to the experience and expertise of the consortium members. The relevant literature is summarised in the reference list. [9-16]

#### 12.1.1 Petrol

The following aftertreatment systems are usually installed in petrol vehicles:

- Three-Way Catalyst (TWC)
  - o A standard component of all vehicles powered by a petrol engine.
- Petrol Particle Filters (GPF)
  - o Applied in Petrol Direct Injection (GDI) engines.
  - o The current trend in petrol vehicles is towards GDI engines.
- DeNO<sub>x</sub> systems (LNT, SCR, TWNSC)
  - o Applied to GDI lean-burn engines.
  - o Are expected to have limited (if any at all) share in the future since lambda=1 engines are now being developed and are much more cost efficient in meeting current and future pollutant emission limits.

The main modes of petrol catalyst deactivation are outlined in Table 12.1.

**Table 12.1. Summary of petrol catalyst deactivation mechanisms**

Type	Mechanism	Definition/Brief Description	Relevant device
<b>Thermal/ Chemical</b>	Sintering	Thermally induced loss of catalytic surface area, change in washcoat structure and reduction of its surface, chemical transformations of catalytic phases to non-catalytic phases	TWC, catalytic GPF, LNT (NSC), SCR, TWNSC
<b>Chemical</b>	Poisoning	Strong chemisorption of species on catalytic sites, thereby blocking sites for catalytic reaction	As above
<b>Physical</b>	Fouling	Physical deposition of species from fluid phase onto the catalytic surface and in catalyst pores	As above

<b>Mechanical</b>	Degradation	Mechanical malfunction, improper operation of key components or physical damage	GPF (and TWC, loss of catalyst material due to fractures in the monolith)
-------------------	-------------	---------------------------------------------------------------------------------	---------------------------------------------------------------------------

From the analysis of the deactivation mechanisms of petrol engines pollution control devices, we conclude the following:

- Oxygen Storage Capacity (OSC) is reduced by a maximum of 12%, with a normal quantity of oil additive and 60h ageing, due to chemical ageing.
- With a 10 times higher concentration of oil additive, the maximum reduction of OSC is 50%.
- Comparatively, thermal ageing reduced OSC by 70-90%, after 60h.
- OSC is a critical parameter for the TWC. Lower OSC means that under rich conditions there will be less oxygen available to oxidize the extra CO and HC emissions. The petrol usually fluctuates around stoichiometry, and when in slightly lean conditions oxygen is stored in the Ce in the TWC, and when in slightly rich conditions this oxygen is released and used for the oxidation of CO and HC.
- Thermal ageing seems to have a greater effect on petrol engine catalysts than chemical ageing.

Poisoning can be limited with high quality fuels and a reduction in oil consumption in modern engines. Therefore, chemical poisoning is no longer the major cause for catalyst deactivation or malfunction. The industry standard theory assumes that all ageing is thermal, and that loss of catalytic activity depends on temperature and time. An explanation of thermal and chemical deactivation follows.

#### 12.1.1.1 Thermal deactivation

The thermal deactivation, sintering, is defined as the process of compacting and forming a solid mass of material by heat or pressure without melting it to the point of liquefaction. Thermal deactivation is caused by high temperatures (>500°C) and is also affected by:

- Catalytic species
  - o Rh is the most resistant to sintering
- Washcoat material
  - o Al<sub>2</sub>O<sub>3</sub> is the most common material, as it is more stable chemically and thermally. Another common material is Zeolite
- Oxygen concentration
  - o Higher O<sub>2</sub> concentration accelerates ageing

The four main mechanisms of thermal deactivation are described below.

#### Catalyst (precious metals, i.e. active material) sintering

- Atomic and crystallite migration of active precious metals due to sintering effects reduce catalysts activity to the point of almost total deactivation (Figure 12.1)
- Crystal growth leads to a decrease in catalytic surface area which means fewer catalytic sites available to the reactants (Figure 12.2)
- Active sites may also be buried within the crystal
- The experimental observations show that temperature is a dominant factor for sintering of active precious metals

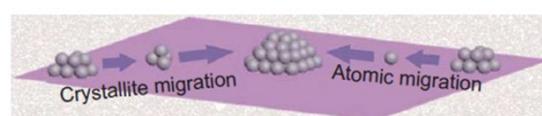


**Figure 12.1. Catalytic species sintering**

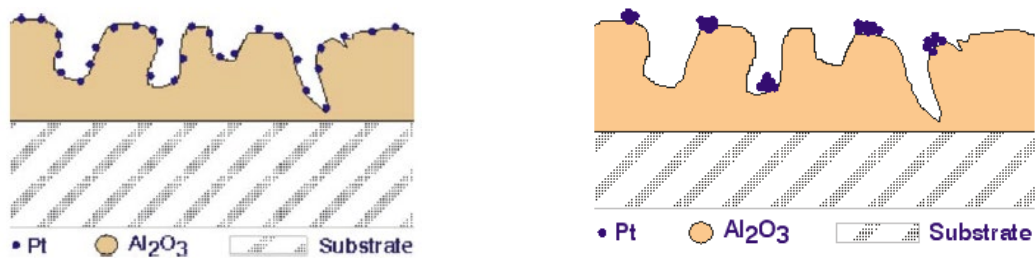


**Figure 12.2. Catalytic species in fresh (left) and aged (right) condition**

### Washcoat sintering – elimination of pores

- Washcoat sintering is defined as a loss of the internal pore structure leading to a decrease in the physical surface area of the carrier
- In extreme cases, leads to the encapsulation of catalyst particles
- Occurs at very high temperatures
- For  $\text{Al}_2\text{O}_3$ , sintering is accompanied by thermally induced phase transformation, e.g. from  $\gamma\text{-Al}_2\text{O}_3$  (100-200m<sup>2</sup>/g) to  $\delta\text{-Al}_2\text{O}_3$  (900<sup>o</sup>C) to  $\theta\text{-Al}_2\text{O}_3$  (1000<sup>o</sup>C) and to  $\alpha\text{-Al}_2\text{O}_3$  (1200<sup>o</sup>C, non-porous)

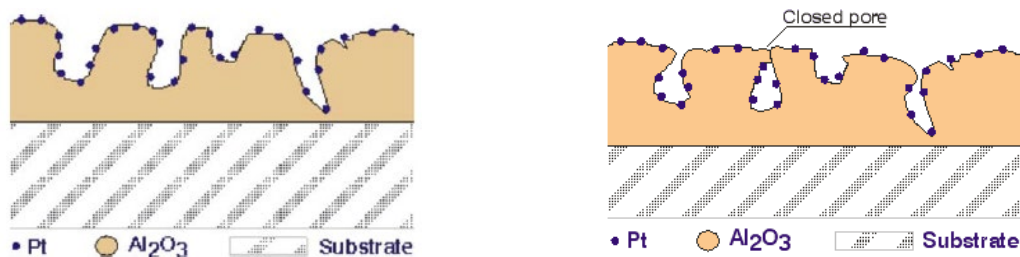


**Figure 12.3. Washcoat in fresh (left) and aged (right) condition**

### OSC (oxygen storage capacity) reduction

- OSC reduction only applies to TWC, LNT.
- Coalescence and growth of particles (Figure 12.4)
- Sintering of Ce sites:  $\text{CeO}_2$  sinters with growth of particles and loss of surface area
- Rapid reduction of the oxygen storage and release capacity

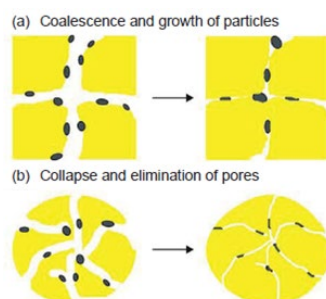


**Figure 12.4. OSC reduction mechanisms**

### Chemical interactions among active sites and between active site and washcoat

- Formation of Pt Pd alloy and Pt Ni alloy

#### 12.1.1.2 Chemical deactivation

- A catalyst poison is a substance which deposits on the surface of the catalyst, rendering it less active or inactive

- Poison usually comes from fuel or lubricant
- Fuel-bound poisons: S ( $\sim 5$ ppm), Mn, Pb (practically eliminated from modern petrol)
- Oil-bound poisons: Zn and P as lubricity enhancers, Ca, S
- Phosphorus (P) is accumulated in the washcoat, leading to poisoning
- LNT sensitive to S (BaO poisoning), but catalyst conditions is reversible following a desulphation process (applying rich operation at high temperature,  $\sim 700^\circ\text{C}$ )

Chemical deactivation can occur via either selective or non-selective poisoning.

### Selective poisoning

- a poison reacts directly with an active site, decreasing its activity for a given reaction
- if the poison reacts chemically with the catalyst component, the poisoning can be either temporary (e.g. sulphur poisoning and formation of barium sulphates) or permanent (e.g. poisoning with elements of the lubricant)
- if poisoning result from adsorption, then it can be (partially) reversible

### Nonselective poisoning (fouling or masking)

- masking of active sites and pores occurs due to a deposition of fouling agents on the washcoat
- decreasing the available catalytic surface area and blocking access to the pores

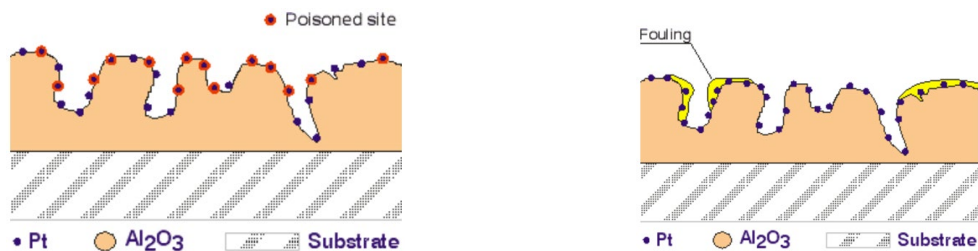


**Figure 12.5. Selective (left) and nonselective (right) poisoning**

For GPF another important degradation mechanism is ash deposition. Ash derives from typically mineral and metal additives in the lubricant. Layer ash improves (interception and impaction) filtration, while plug ash leads to a reduction in (diffusion) filtration. Ash deposition affects the pressure drop across the filter. The first effect of ash deposition is a decrease in the effective soot storage volume. The second effect is that ash reduces the active volume of the filter, this means that the gas velocity (space velocity) increases, exhaust gas residence time decreases, and so catalytic activity deteriorates (for catalytic GPF). A major challenge for GPFs is high exhaust mass flow with high PM concentration. This leads to fast PM loading and if there is enough heat in high temperature fuel-cut conditions then the GPF can be damaged due to thermal shock

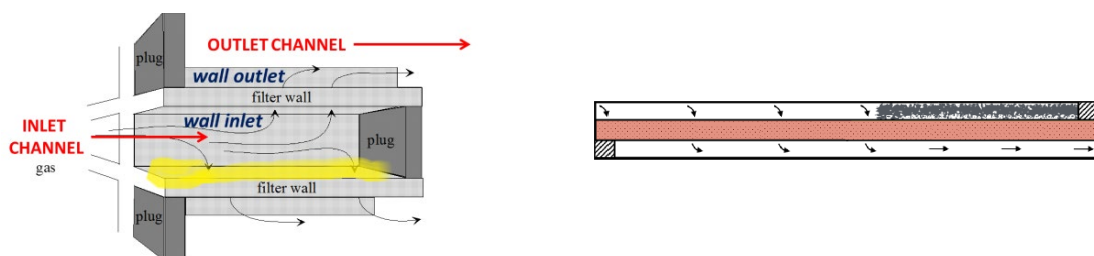


**Figure 12.6. Layer (left) and plug (right) ash**

### 12.1.2 Diesel

The following aftertreatment systems are usually applied within diesel vehicles:

- Diesel Oxidation Catalyst (DOC)
  - o for oxidation of CO and HC
- Diesel Particle Filter (DPF) or Catalysed Diesel Particle Filter (cDPF)
  - o for particles
- DeNO<sub>x</sub> systems (LNT/SCR/PNA)
  - o for the reduction of NO<sub>x</sub>
- Ammonia Slip Catalyst (ASC)
  - o used in combination with SCR, in order to minimize NH<sub>3</sub> emission

As mentioned above, the main modes of catalyst deactivation are thermal or chemical. However, investigation into these modes of deactivation are complicated by the fact that contrary to the petrol case, it is unclear if hydrothermal ageing effectively replicates the typical "on-road" ageing conditions (primarily with regards to the SCR).

#### SCR thermal ageing

SCR suffers from thermal ageing which leads to a decrease of active sites. High temperature from DPF regeneration affects SCR, and so thermal durability is required. Zeolite based base metal (e.g. Cu, Fe) catalysts are deactivated during high-temperature DPF regeneration. The front of the SCR is exposed to higher temperatures than the rear, it is therefore expected that the front of the SCR catalyst will be more degraded than the rear. Hydrothermal ageing at high temperatures (700 °C) leads to complete collapse of the zeolite structure. When ageing at 750 °C, washcoat cracking and the beginning of delamination from the cordierite is visible. The damage to the washcoat is more prominent in the front section of the catalyst than the rear.

#### SCR poisoning

Base metal (Fe, Cu)/zeolite SCRs are sensitive to sulphur poisoning. Even with the use of ultra-low sulphur fuel, sulphur poisoning is still a durability issue for base metal/zeolite SCR catalysts. The impact of sulphur poisoning is affected by the thermal ageing status. The most thermally durable SCR catalyst is not necessarily the most durable to sulphur poisoning. Two major sulphation modes are most likely involved: formation of (NH<sub>4</sub>)<sub>2</sub>SO<sub>4</sub> (ammonium sulphate) or (NH<sub>4</sub>)HSO<sub>4</sub> (Ammonium bisulphate, ammonium hydrogen sulphate), and formation of CuSO<sub>4</sub> (copper sulphate). NO<sub>x</sub> activity of Cu/zeolites is significantly reduced for samples poisoned by SO<sub>3</sub> compared to those poisoned by SO<sub>2</sub>. Sulphur poisoning can be an important ageing mechanism for SCR systems. Platinum (contained in DOC) contamination in the front section of the SCR catalysts is responsible for the severe decrease in NO<sub>x</sub> reduction performance. The precious metal is volatilized and deposits on the cooler SCR – Pt deposits lead to NH<sub>3</sub> oxidation.

Exposure of metal-exchanged-zeolites based SCR catalysts to temperatures higher than 500°C and water vapor causes irreversible modifications of catalysts properties, leading to permanent deactivation. Destruction of the zeolite structure occurs due to delamination, while isolated metallic species aggregate to form inactive metal oxide particles

#### LNT ageing

Accumulation of sulphur in the LNT leads to significant reductions in NH<sub>3</sub> production from the LNT, which is important in combined LNT-SCR systems. Although most effects are reversible (following a desulphation process), in cases of poisoning with high sulphur concentrations the system may not recover fully.

#### Combined LNT-SCR systems

Combined LNT-SCR systems are used to increase NO<sub>x</sub> conversion: the NH<sub>3</sub> produced in the LNT is used in the SCR. There are significant effects observed due to hydrothermal ageing

(Figure 12.7)– the Pt particles grow (sintering) and the reaction activity is reduced. Furthermore, sulphur poisoning was significant at high sulphur concentrations and desulfation did not restore fully the system.

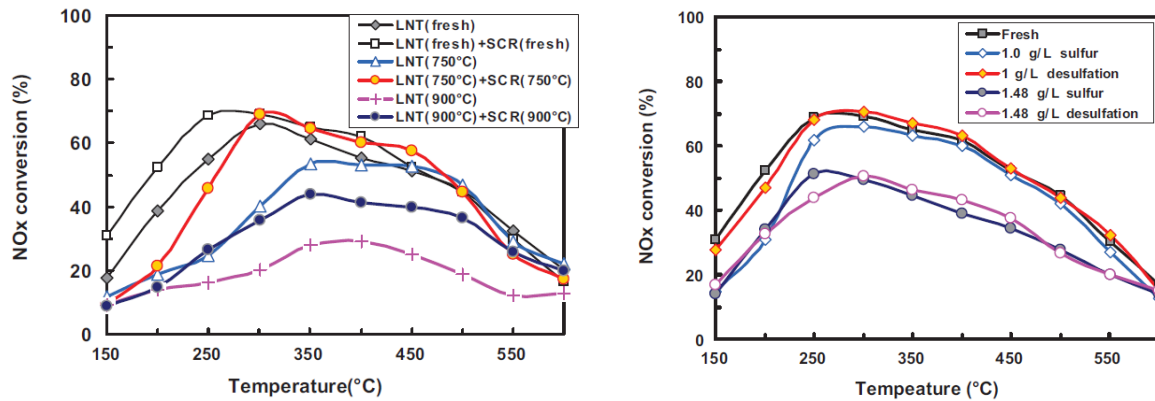


**Figure 12.7. Thermal ageing (left) and chemical poisoning (right) of a combined LNT-SCR system**

## 12.2 Deterioration influences cold start emissions

Catalyst ageing has the following impacts on the performance of the aftertreatment system:

- Reduction in the conversion efficiency of the catalyst – in elevated temperatures high conversion efficiency can be still achieved though
- Increase of the light-off (LOFF) temperature of the catalyst (LOFF is the temperature at which the conversion efficiency of the catalyst is 50%)
- Reduction in oxygen storage capacity (OSC, applicable for TWC)

During the cold-start period, when the catalyst temperature is below the LOFF value, the conversion efficiency is (very) low, and the catalyst ageing reduces it even further. As a result, when a fresh and an aged catalyst are exposed to the same increasing temperature profile, then the LOFF is achieved later in the aged catalyst (i.e. at higher temperatures). Independently of the catalyst ageing level, the time until LOFF varies for the different positions within the catalyst (LOFF is achieved first at the inlet position of the catalyst and progressively at the centre and outlet positions).

Indicatively, Figure 12.8 shows the change of the conversion efficiency for different modes of catalyst deactivation (thermal ageing, chemical poisoning).

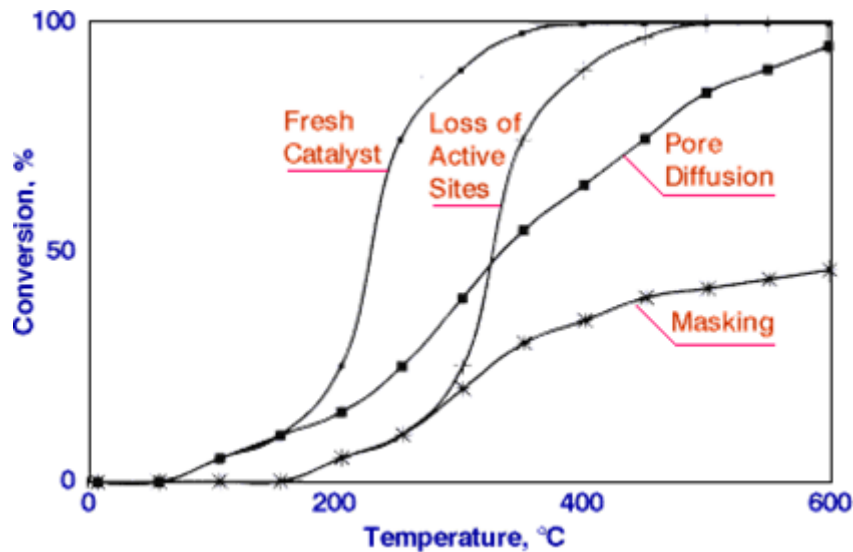


**Figure 12.8. Effect of catalyst ageing (deterioration) on conversion efficiency [50]**

The target of the methodology is to combine the ageing effect with cold start augmentation. The former is implemented with the deterioration factors (DF) described in Section 3.8 (and in this Chapter), while the latter is simulated with the model presented in Section 3.5. Before combining the augmentations, it should be considered that passenger cars spend most of their operational time in warm/hot conditions. In addition, the DFs have been determined using remote sensing (RS) data, which mostly correspond to warm/hot conditions of the vehicle (only the vehicles parked very close to the RS equipment will be measured while being still in the cold start phase). Thus, the DFs largely depict the 'hot' emissions of the vehicle. This means that for an aged vehicle (i.e. aged catalyst), the DF should be first applied on the base (hot) emission map and then the cold start augmentation should be implemented. In a more detailed approach, the catalyst ageing effect on the LOFF temperature can be incorporated.

The steps of the proposed methodology are as follows:

1. **Step 1:** Apply the DF due to ageing on the base hot emission map
2. **Step 2:** Add the cold start extra emissions, as calculated with the cold start model
3. **Step 3:** For additional detail: incorporate the effect of catalyst ageing on the cold start phase

While Steps 1 and 2 are clear, some further detail is provided for Step 3. The target of that step is to describe the increase of the light-off (LOFF) temperature of the catalyst and incorporate its effect of the tailpipe emissions of the vehicle. The result would be that as the catalyst gets aged, the LOFF is achieved later after cold start, as a higher temperature must be achieved. To quantify this effect, the following steps are taken:

- **Step 3A:** Quantify the effect of ageing on the LOFF temperature
- **Step 3B:** Define the exhaust gas temperature profile to which the catalyst is exposed
- **Step 3C:** Estimate the time difference until the LOFF between the fresh (LOFF@fresh) and the aged (LOFF@aged) catalyst

For the application of the above steps, very detailed and precise data is required (generated via testing in dedicated experimental facilities following specific testing protocols), which is scarce (if available at all). An example of the application of Steps 3A, 3B and 3C is described below for a TWC.

### **Step 3A – Ageing effect on LOFF**

The first step is to quantify the effect of ageing on the LOFF temperature. Figure 12.9 and Figure 12.10 indicate the conversion efficiency (as a function of temperature) of CO and HC, respectively, in the fresh and aged TWC. As clearly illustrated in these figures, when the catalyst is aged the conversion efficiency curve is shifted to higher temperatures and has a lower slope. This means that the LOFF temperature is strongly affected. The relevant increase is quantified in Figure 12.11. It is underlined here that the LOFF temperature is a function of temperature and depends on the catalyst characteristics and ageing level.

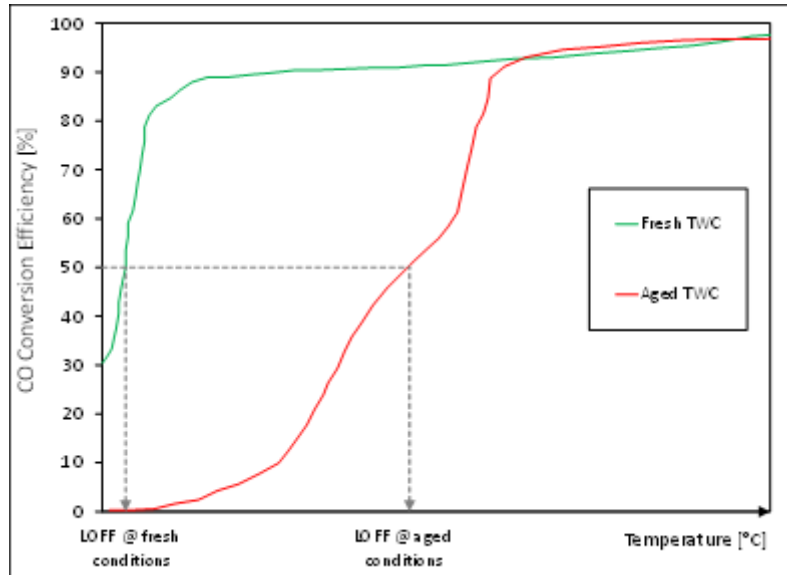


**Figure 12.9 CO conversion efficiency for the fresh and aged TWC**

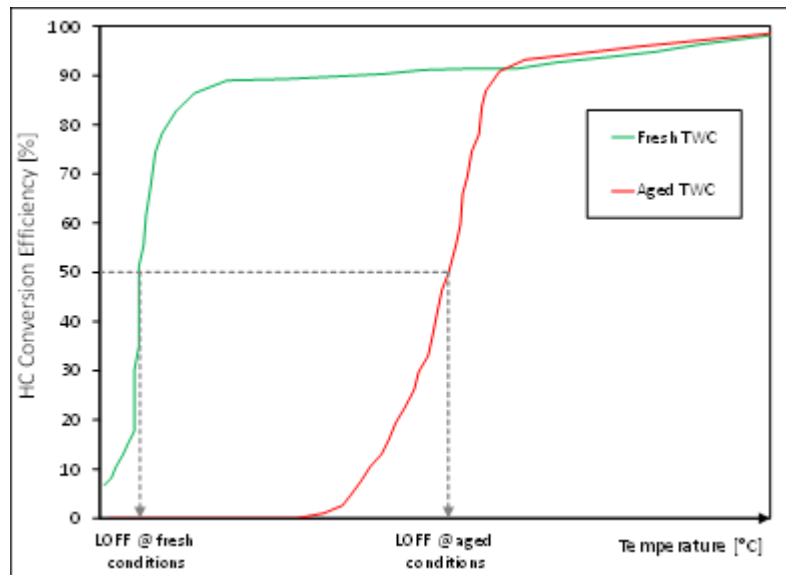


**Figure 12.10. HC conversion efficiency for the fresh and aged TWC**

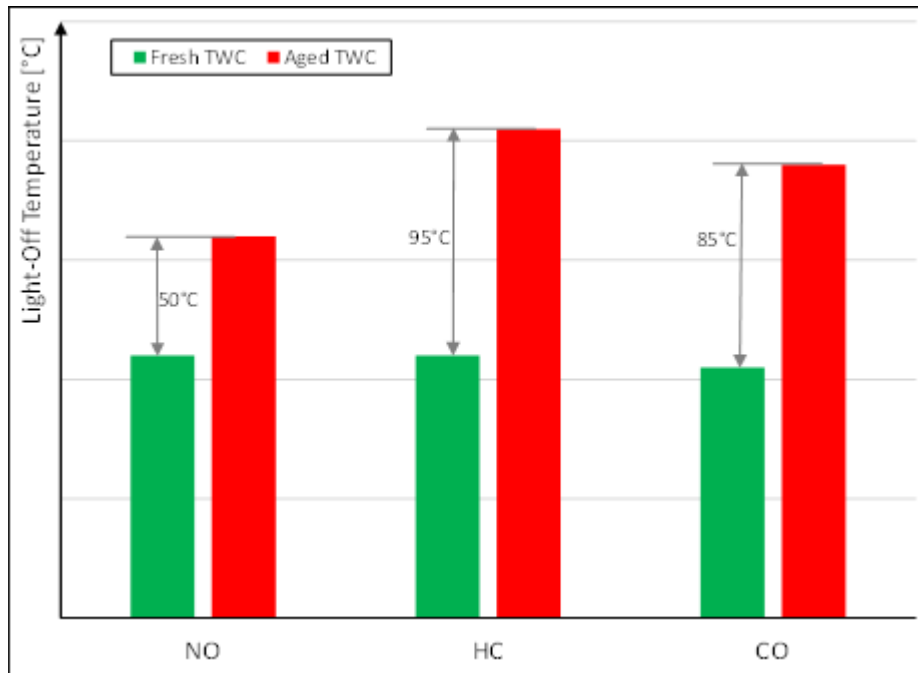


**Figure 12.11. LOFF temperature increase in the aged catalyst**

### **Step 3B – Exhaust gas temperature profile**

As mentioned before, the most critical parameter that affects conversion efficiency is the temperature to which the catalyst is exposed. The temperature is strongly affected by several parameters.

The first critical parameter is the driving conditions. Figure 12.12 shows the exhaust gas temperature of a petrol vehicle equipped with a TWC during on-road driving with varying dynamics: the same trip has been repeated with different driving behaviour. The temperature is shown at two positions, i.e. at the inlet of the catalyst and at the tailpipe. As clearly shown in the diagram, more dynamic driving behaviour (i.e. abrupt accelerations, “delayed” shifting to higher gear etc.) results in higher exhaust gas temperatures, affecting the warm-up phase of the catalyst.

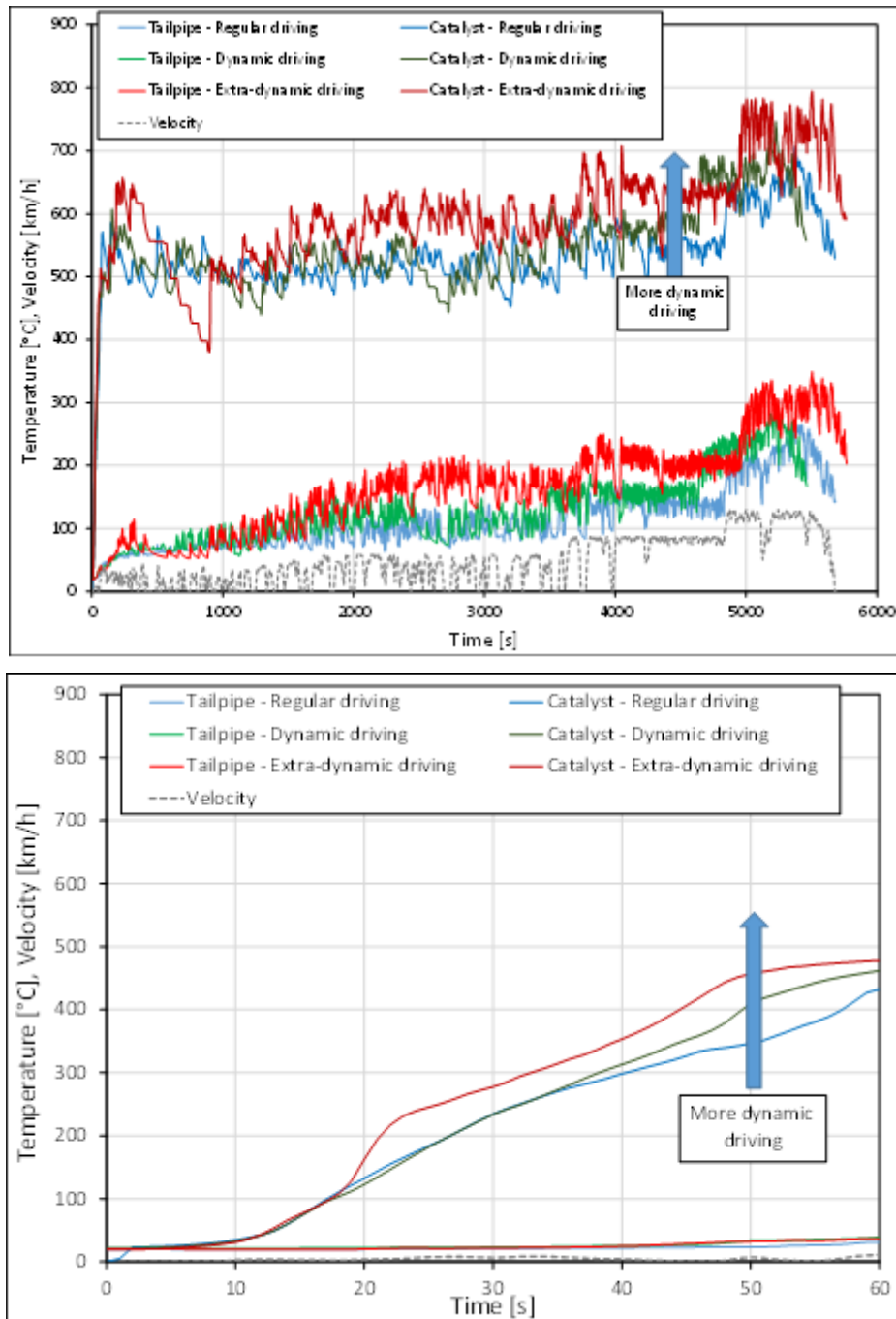


**Figure 12.12. Exhaust gas temperature of a petrol vehicle during on-road driving with varying dynamics**

The second critical parameter that affects exhaust gas temperature is the type of the powertrain. While in a conventional vehicle equipped with a thermal engine, there is always exhaust gas flow when the vehicle moves, in hybrid vehicles the engine operation is intermittent, strongly depending on the state of charge (SoC) of the high-voltage (HV) battery, as well as on the selected driving mode (hybrid, electric etc.). Figure 12.13 shows the exhaust gas temperature profile of a PHEV under the same trip, with full (top) and empty (bottom) battery. In the case of full battery (Figure 12.13, top), the vehicle is driven electrically for a large part of the trip, corresponding to urban and rural driving. The combustion engine turns on only when the vehicle goes onto the motorway and reaches high speeds. Under such driving conditions, both the exhaust gas temperature and flow are high, transferring high amount of heat to the TWC, resulting in faster heating (i.e. shorter duration until LOFF). On the other hand, when the battery is empty (Figure 12.13,

bottom), the combustion engine starts at the very beginning of the trip, where the vehicle moves at low speeds. Under such operating conditions, the exhaust gas flow and temperature are low, resulting in a longer warm-up phase of the TWC, i.e. more time is needed until LOFF. From these observations, it is made clear that the driving conditions under which the cold start occurs play a significant role in the catalyst warm-up.

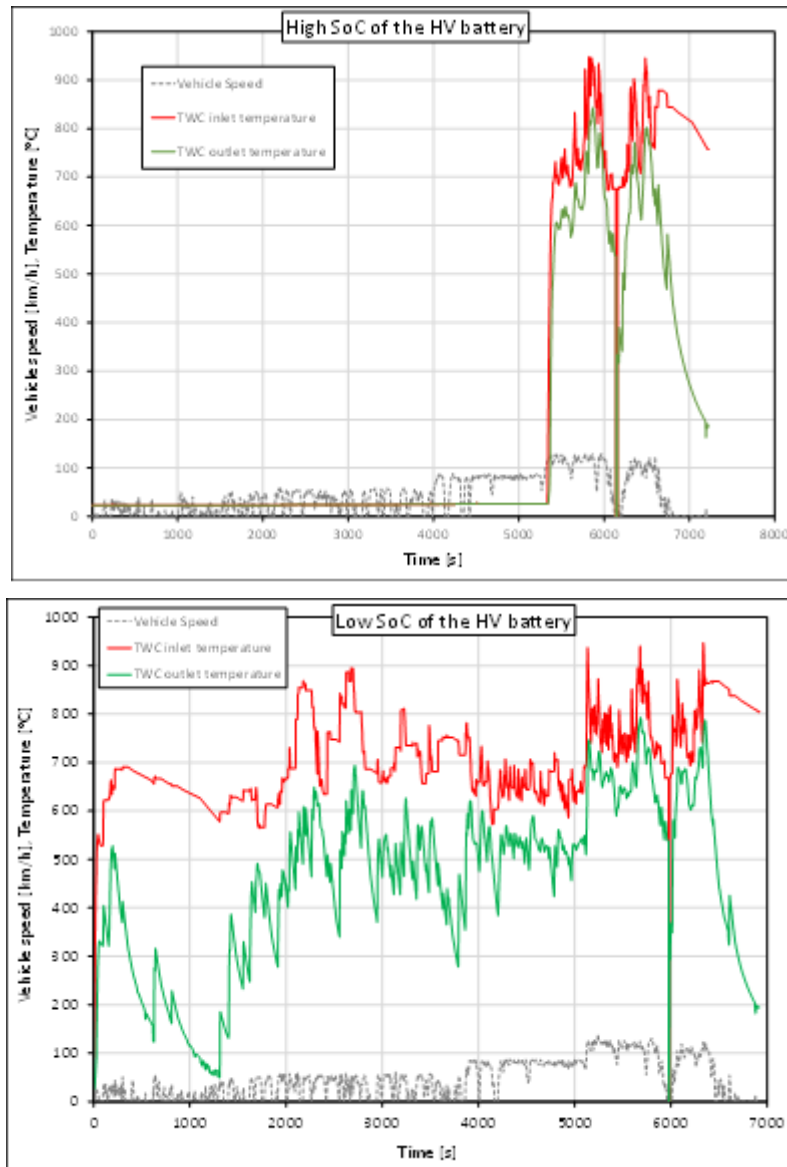


**Figure 12.13. Exhaust gas temperature of a petrol PHEV during on-road driving with varying SoC of the HV battery – top: full battery, bottom: empty battery**

The third parameter that affects the exhaust gas temperature is the exhaust line configuration and the overall calibration of the engine (particularly as concerns the engine internal measures for fast catalyst heating). Figure 12.14 shows the exhaust gas temperature profile of two different petrol vehicles driven over the same route. It is clearly shown that vehicle A reaches higher exhaust gas temperature than vehicle B, meaning that its TWC can reach LOFF faster, depending on its position (how close/far from the engine it is placed).

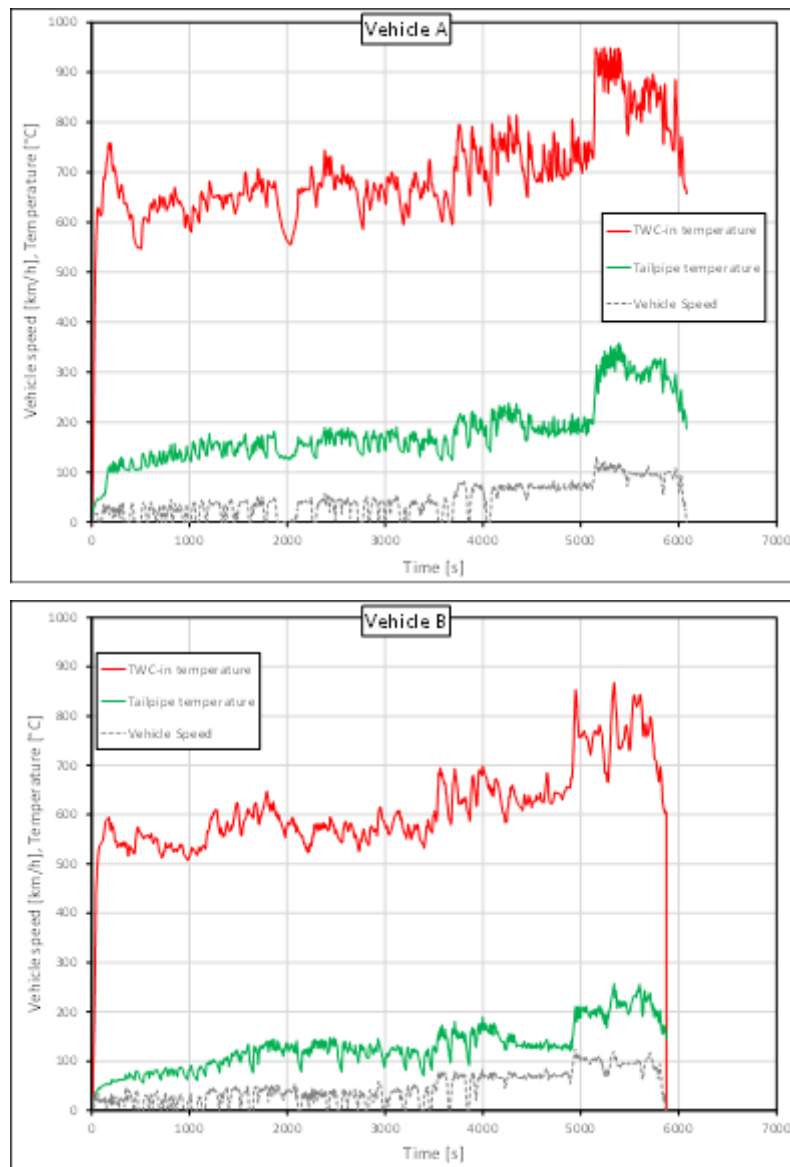


**Figure 12.14. Exhaust gas temperature of two different petrol vehicles equipped with TWC under the same trip**

### **Step 3C – Time to reach LOFF**

Summarizing the two previous steps, it is concluded that:

- From Step 3A: Conversion efficiency and LOFF of a TWC are a function of temperature and depend on the catalyst characteristics and ageing level.
- From Step 3B: The temperature to which the TWC is exposed depends on the driving conditions, the type of the powertrain (conventional, hybrid) and the position of the TWC, together with the engine calibration.

From the two points above, it is concluded that **a generic conclusion** applicable to different powertrains, driving conditions, exhaust line architectures and engine calibration **cannot be made**. On the other hand, experimental data covering all the different combinations are almost impossible to collect. In order to demonstrate the effect of the catalyst ageing to the prolongation of the time until LOFF, Figure 12.15 shows the temperature evolution at different positions of a TWC, during the cold-start phase of an on-road trip with a petrol vehicle, while Table 12.1 quantifies the time required until the LOFF is achieved at different positions in the catalyst. As shown by this data, the aged catalyst needs an extra 3 – 6 seconds (depending on the species) to reach LOFF at the

inlet position. When the middle position is examined, then LOFF is achieved 6 – 11 seconds later in the aged catalyst, as compared to its fresh counterpart.

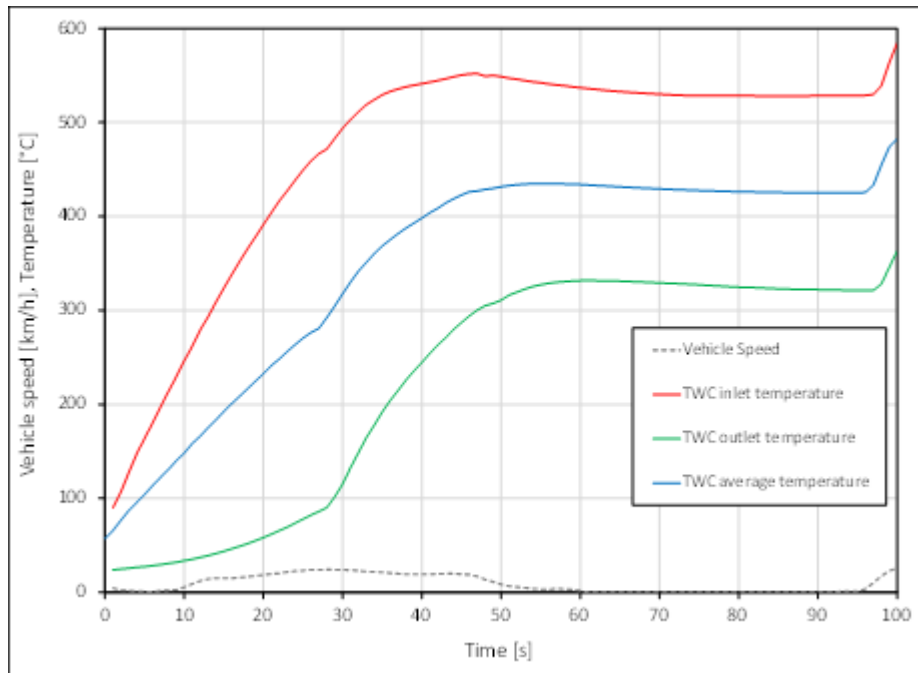


**Figure 12.15. Temperature at the inlet and outlet positions of a TWC during the cold-start phase of an on-road trip. The average value approximates the temperature at the middle position of the TWC.**

**Table 12.1. Time to LOFF for the fresh and aged TWC**

Parameter	Ageing level	Species		
		NO	HC	CO
LOFF [°C]	Fresh	215	215	210
	Aged	265	310	295
Time to LOFF [s] Inlet position (TWC-in)	Fresh	8	8	8
	Aged	11	14	13
$\Delta t$ to LOFF [s] (TWC-in)	Aged	3	6	5
Time to LOFF [s] Middle position (TWC-avg)	Fresh	18	18	17
	Aged	24	29	28
$\Delta t$ to LOFF [s] (TWC-avg)	Aged	6	11	11

The above steps describe the methodology to combine the deterioration due to catalyst ageing and cold start augmentations, the former applied with the DFs and the latter

simulated with a dedicated model. Beginning with the fresh vehicle, the base hot emission map is first multiplied with the DF. Secondly, the cold start extra emissions are calculated with the respective model. If more detail needs to be included in the calculation, then the effect of catalyst ageing on the cold start phase can be also incorporated. However, this needs detailed experimental data to cover all the different applications and operating conditions. This kind of data is very scarcely available.

### 12.3 Comparison of data used to derive the applied tabulated deterioration factors

This section presents the comparison among the different sources used for the determination of the deterioration factors. The relevant data have been retrieved from three databases that have accumulated emission deterioration data, namely the HBEFA handbook, the CONOX database and the COPERT database. The remote sensing data included in these databases is primarily from the same underlying source, however it has been amended and included via different approaches. For example, in some cases, the existing durability factors (DF) in the legislation, allowing an increase in emissions over time of the emissions during in-service conformity testing, was also used to inform the deterioration factors.

The following figures (Figure 12.16 to Figure 12.21) illustrate the deterioration factors as determined by the analysis of the databases. Figure 12.16 to Figure 12.18 refers to petrol (gasoline) cars, while Figure 12.19 to Figure 12.21 refers to diesel cars, covering in both cases NO<sub>x</sub>, CO and HC emissions. The deterioration factors are calculated for Euro 3, 4, 5 and 6 vehicles. Currently, the COPERT database includes data up to Euro 4 vehicles.

As observed in the following figures, in many cases the HBEFA and the CONOX data have a close agreement, e.g. petrol CO or diesel NO<sub>x</sub>, while in others there is a strong deviation, e.g. Euro 6 petrol NO<sub>x</sub>. As the latest HBEFA update includes the CONOX data, it was deemed preferable to use the HBEFA database for the determination of the deterioration factors.

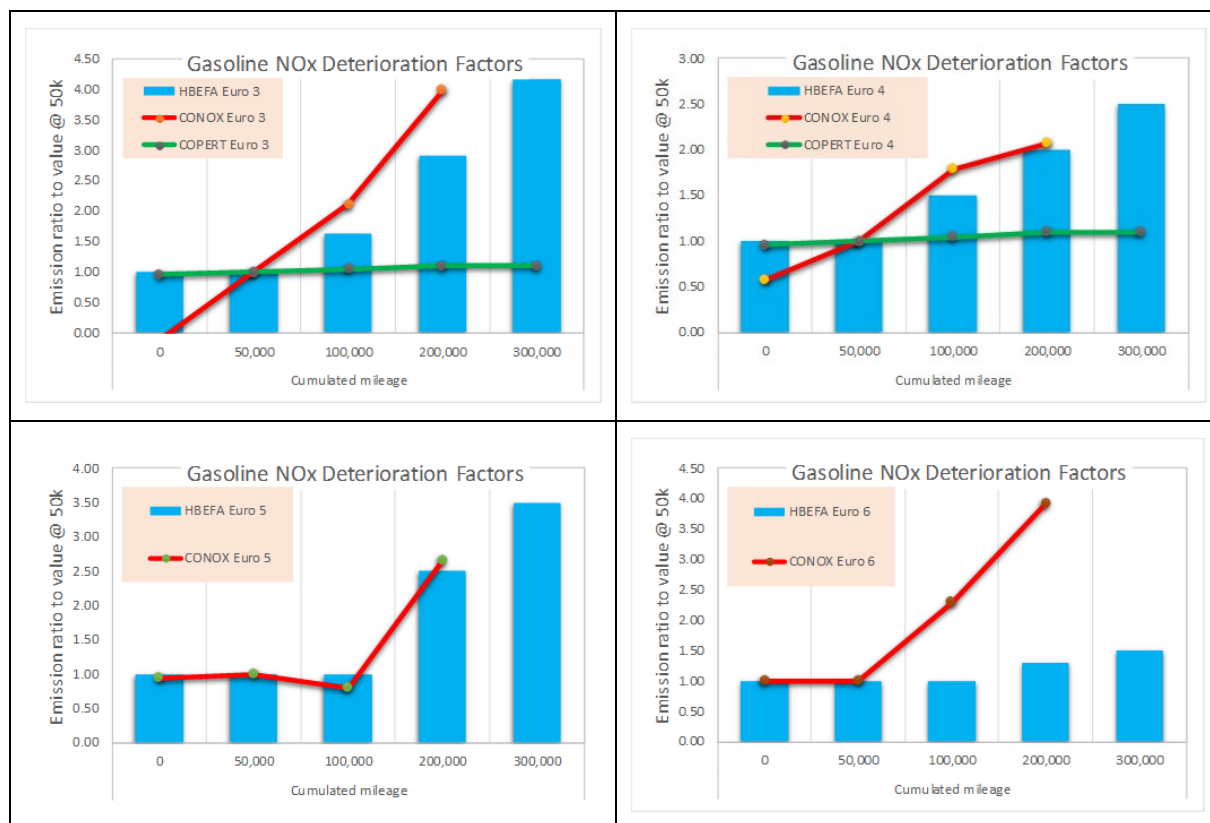


Figure 12.16. Deterioration factors for petrol NO<sub>x</sub> emissions

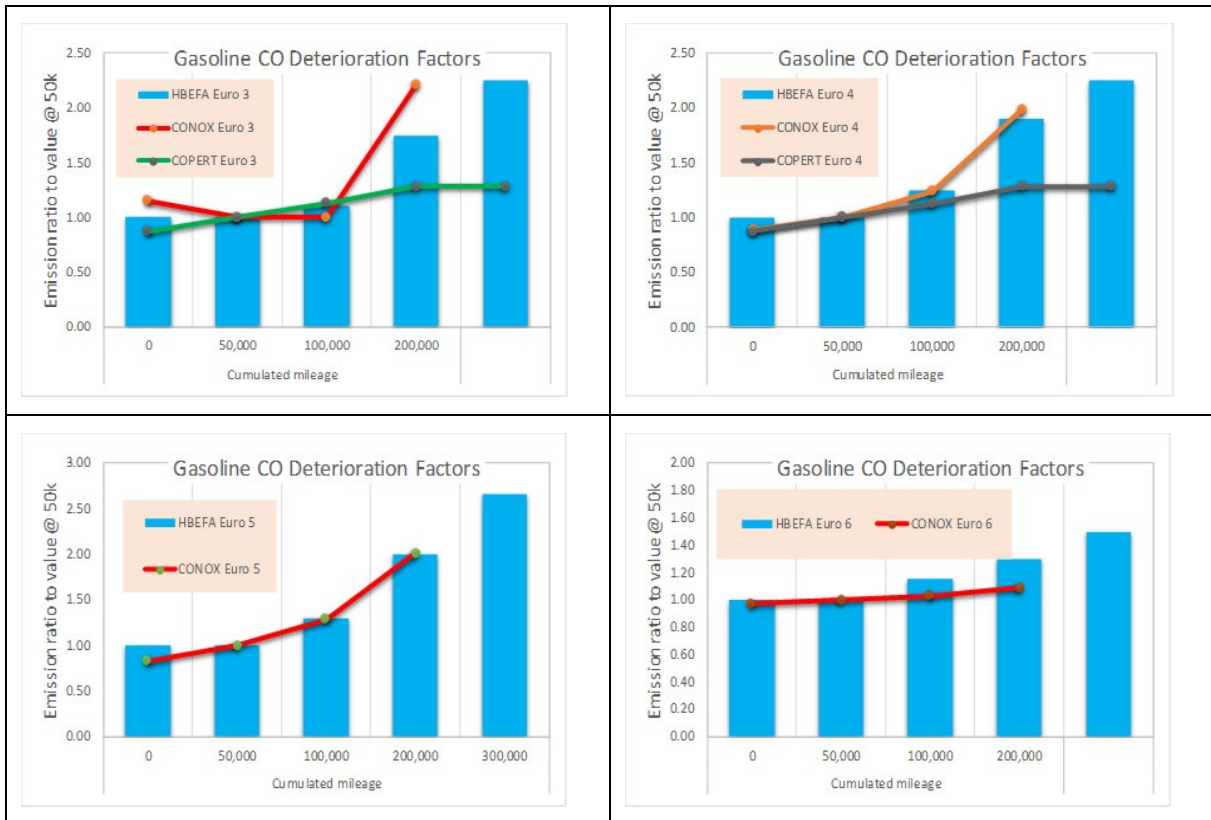


Figure 12.17. Deterioration factors for petrol CO emissions

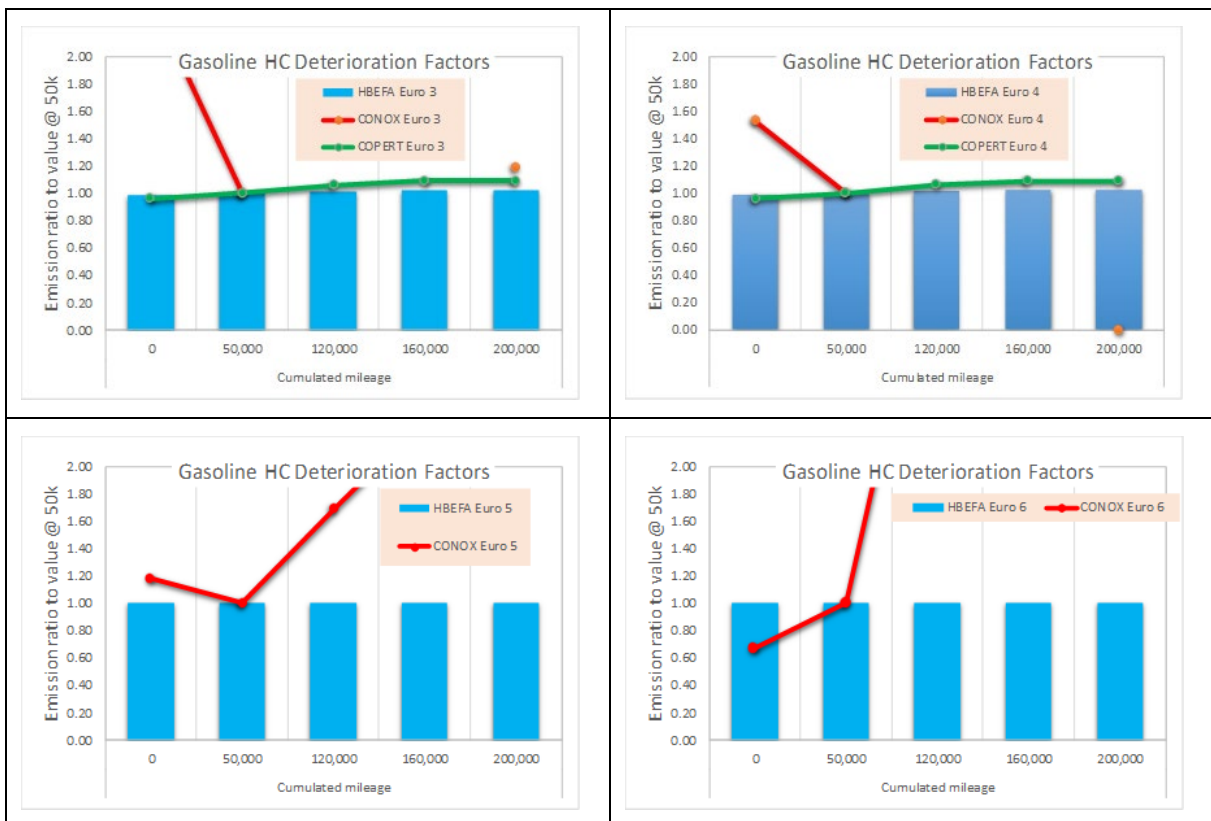
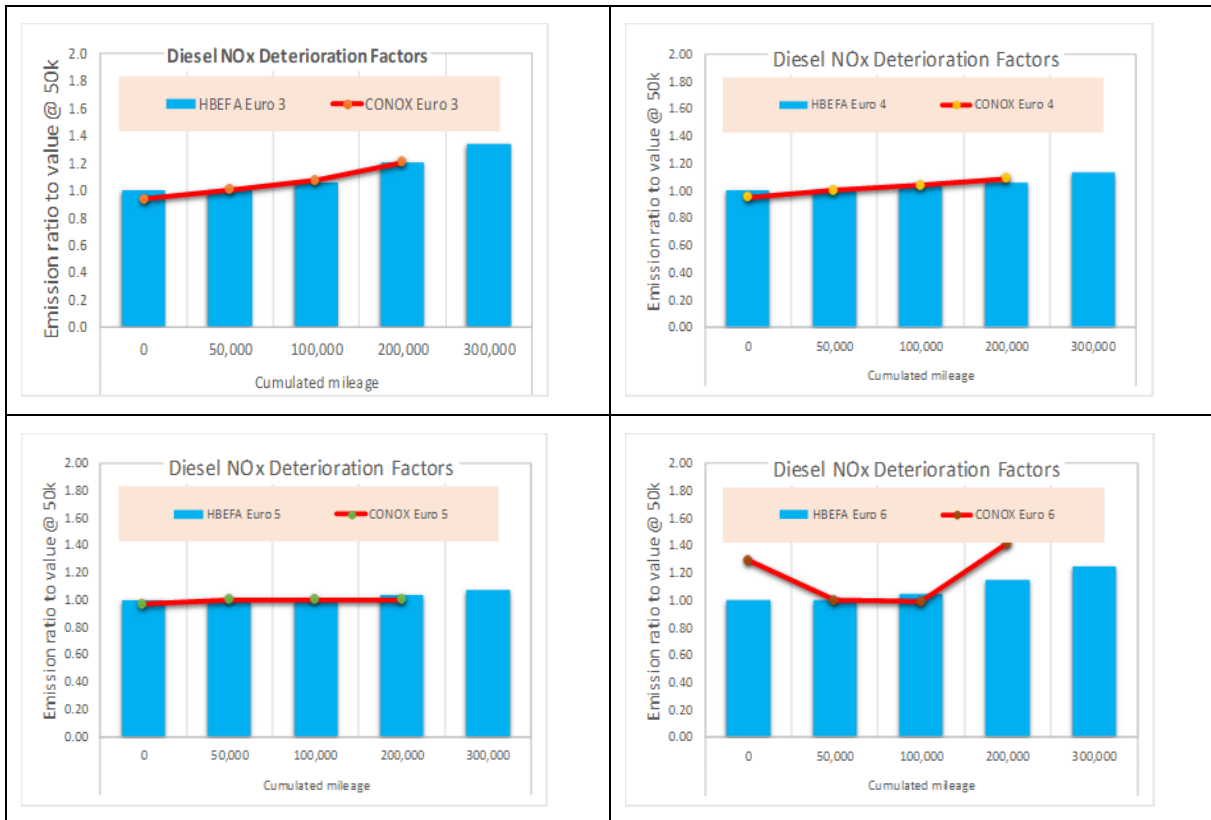
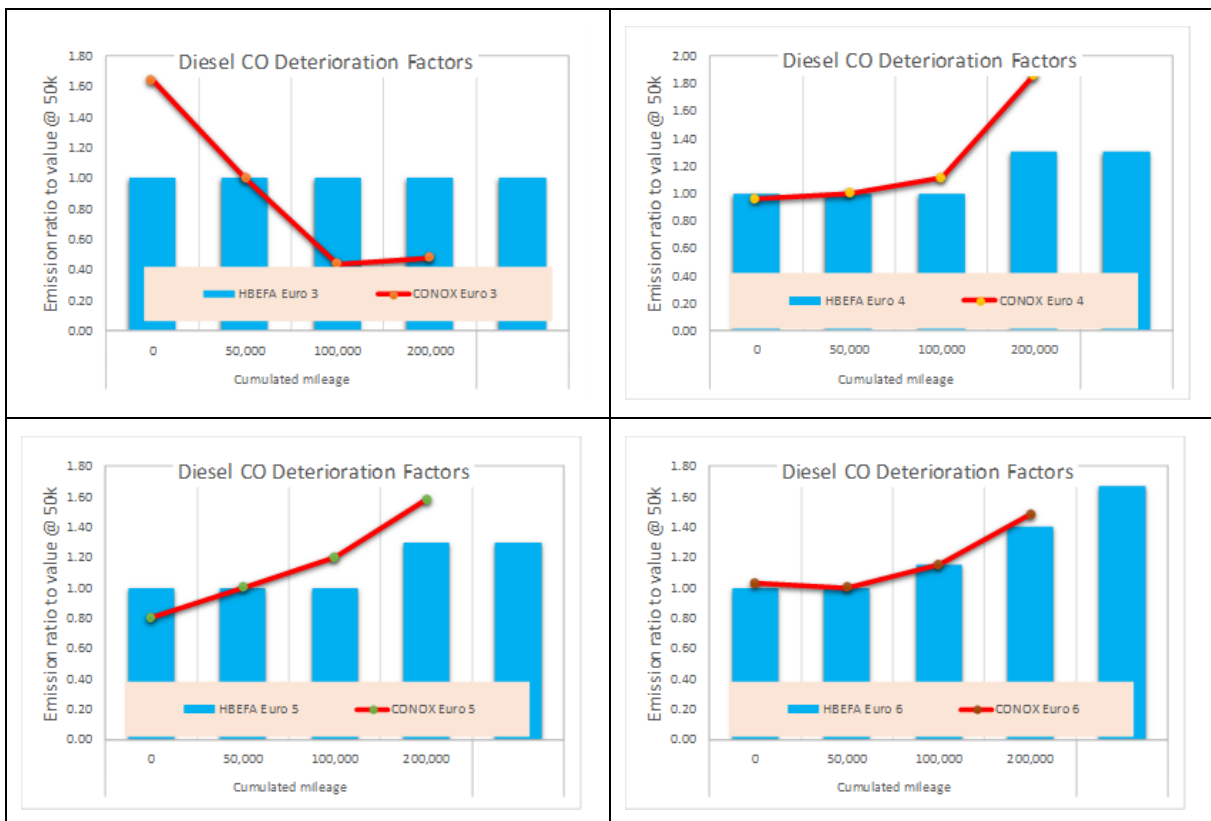


Figure 12.18. Deterioration factors for petrol HC emissions



**Figure 12.19. Deterioration factors for diesel NO<sub>x</sub> emissions**



**Figure 12.20. Deterioration factors for diesel CO emissions**

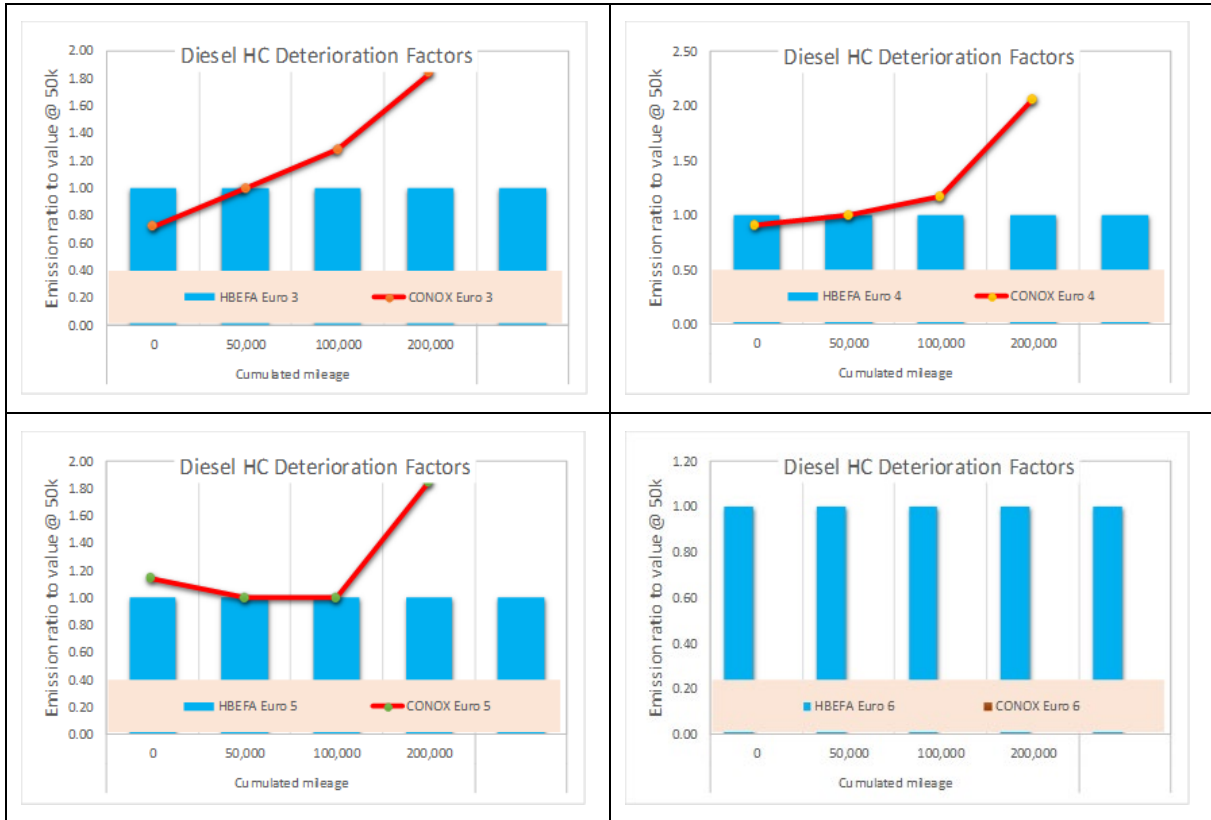


**Figure 12.21. Deterioration factors for diesel HC emissions**

## 12.4 Investigation of the deterioration factors for NH<sub>3</sub>

Remote sensing data for NH<sub>3</sub>, originating in the CONOX database, have been also assessed, in order to examine if they can be used for the determination of the respective deterioration factors.

The figures in this section present the relevant data for petrol and diesel cars, respectively, from Euro 1 to Euro 6. In the case of petrol cars, with exception of Euro 6, the trend appears to fluctuate. Even the Euro 6 values which appear to display a somehow consistent trend, have limited values as they correspond to only 5 years of data, with the fifth year exhibiting large dispersion. For the diesel cars, the respective values have either a negative value or present a peculiar trend. For those reasons, at this stage no deterioration factors for NH<sub>3</sub> are calculated. Further analysis of the available data will be conducted.

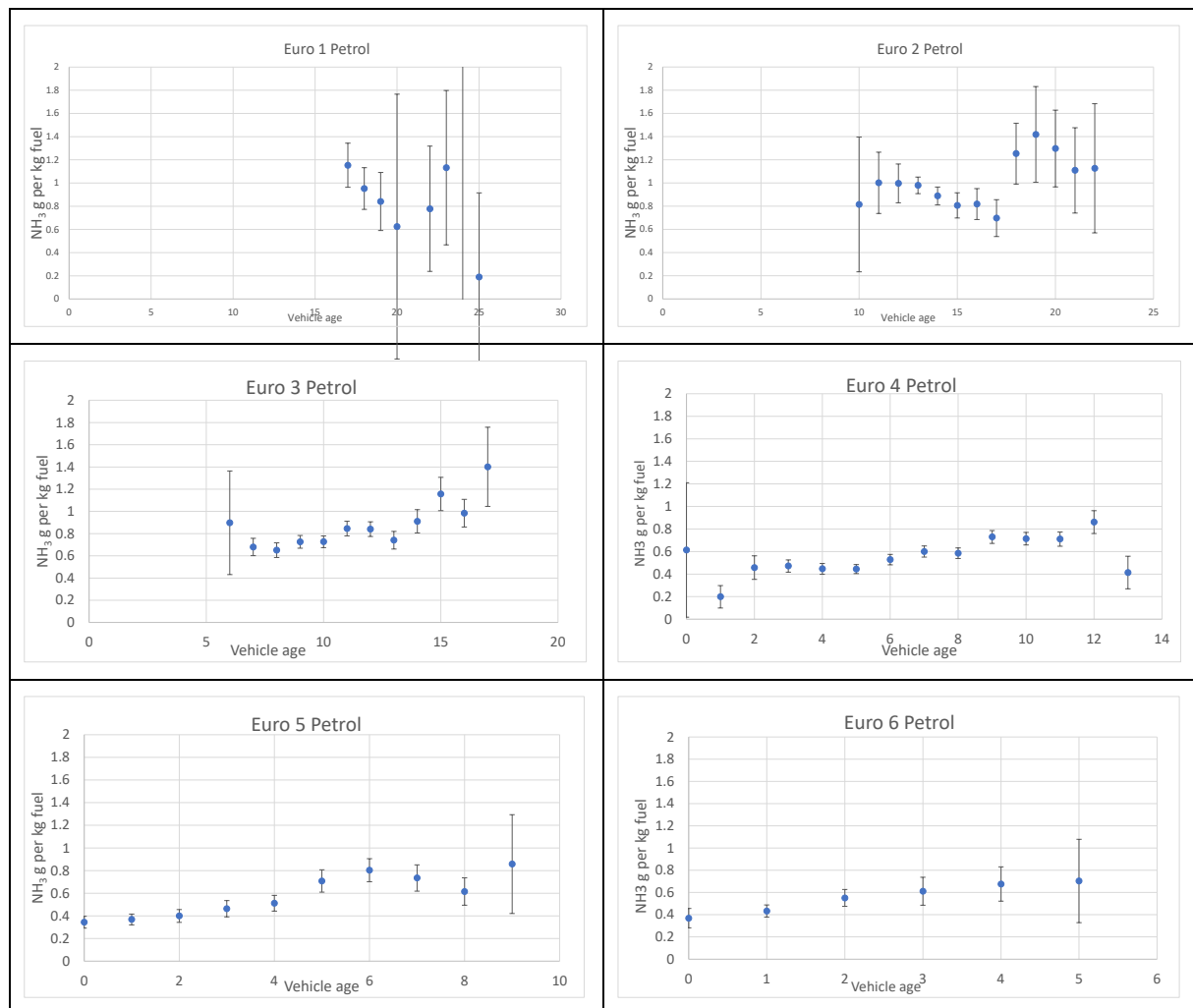


**Figure 12.22. NH<sub>3</sub> emission data for petrol cars**

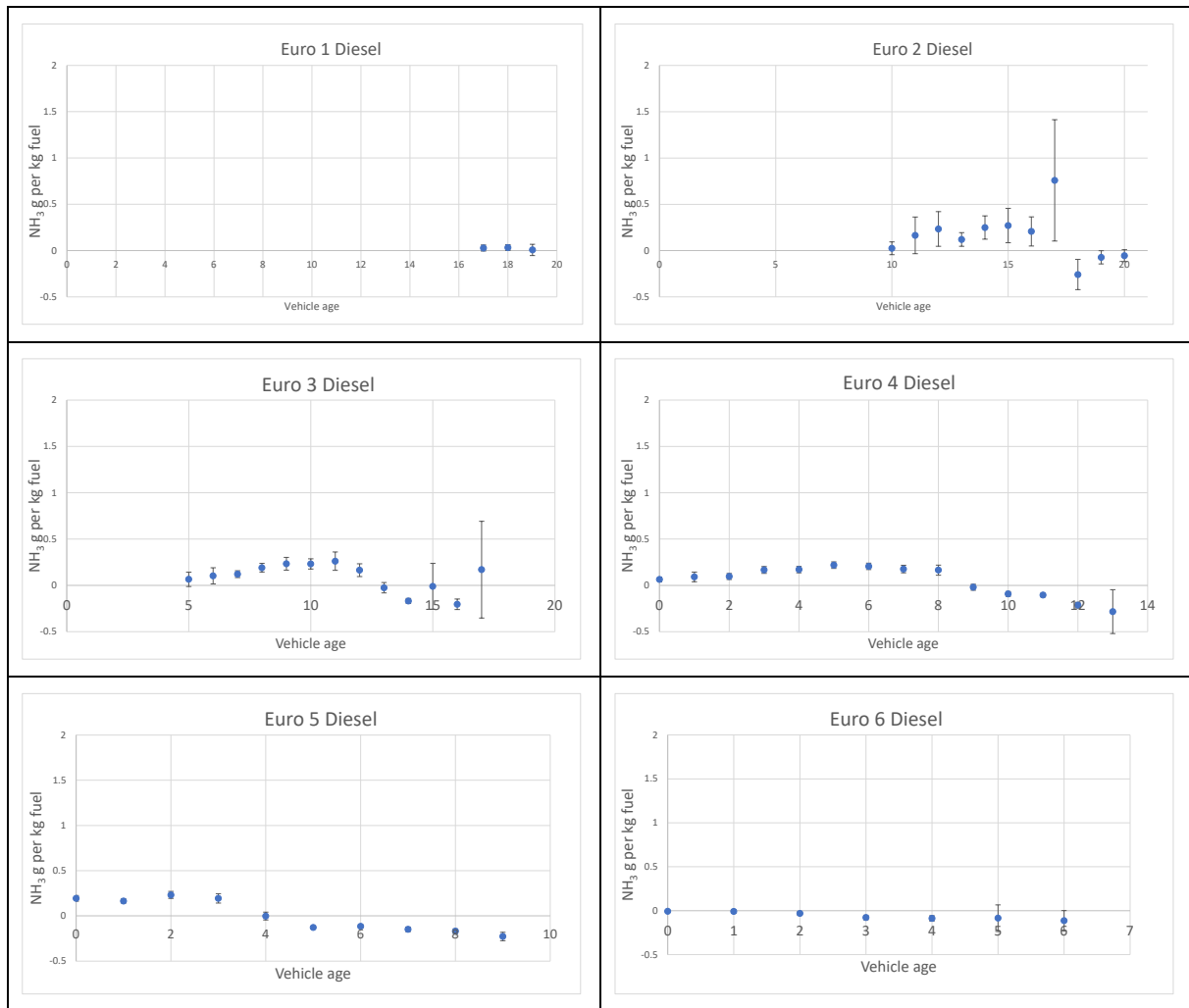


**Figure 12.23. NH<sub>3</sub> emission data for diesel cars**

## 12.5 Discussion on polynomial fits for vehicle mileage

Deterioration factors are a function of vehicle mileage, which in some cases is not available. In such cases, an approximation is made based on vehicle age. Here an analysis of the correlation between vehicle age and mileage is presented.

For this analysis, the following data sources have been used:

- CONOX – The CONOX Report UK and Switzerland/Sweden database. Reference [6]
- RICARDO – AEA - Improvements to the definition of lifetime mileage of light duty vehicles - Ricardo-AEA reference: ED59296- Issue Number 1. Reference [7]
- TRL – Emission factors 2009: Report 6 – deterioration factors and other modelling assumptions for road vehicles – Published project report PPR359. Reference [8]
- APR – Caserini S., Pastorello C., Gaifami P., Ntziachristos L. Impact of the dropping activity with vehicle age on air pollutant emissions. Atmospheric Pollution Research, 4, 282-289, 2013. Reference [9]

RICARDO, TRL and APR describe polynomial equations that correlate vehicle and mileage both for petrol and diesel vehicles. However, for CONOX the actual equation is not included in the paper and it has been extracted from the graph. The method used in each source are as follows:

CONOX combines two separate entries, the UK and the Switzerland/Sweden database. The UK mileage data is from the information collected from recent remote sensing campaigns

rather than being derived from national statistics as for Sweden and Switzerland. There are 75,235 records available with vehicle mileage information; approximately 14% of the measurements come from Sweden and 86% from the UK. These were made from 2017 onwards.

The focus of RICARDO was on the UK's periodic technical inspection (MOT) vehicle database where utilisation of anonymous vehicle identification numbers within the database allowed for vehicles to be tracked from one year to the next. Drawing on this data, two new databases were created in the data processing task, the Lifetime Mileage database and Annual Mileage database.

The Lifetime Mileage database contained all relevant vehicles that passed their MOT periodic technical inspection test in year  $i$  but were missing from the MOT database in year  $i+1$ ; or failed their MOT in year  $i$  and were missing from the MOT database in year  $i+1$ . Both criteria made it likely that a vehicle had been removed from the road and was therefore assumed to be at end of life. This database contained vehicles from MOT databases dating back to 2006. The total sample size of the Lifetime Mileage database is 328.344 for petrol cars and 107.755 for diesel cars.

The Annual Mileage database contained all relevant vehicles that passed their MOT in year  $i$  and had a subsequent pass in year  $i+1$ . These criteria allowed an annual mileage figure to be calculated for each vehicle as the mileage in year  $i$  and year  $i+1$  was now known. This database contained vehicles only from the 2012 and 2013 MOT databases. The total sample size of the Annual Mileage database is 75.713 for petrol cars and 50.838 for diesel cars.

TRL established relationships between vehicle age and mileage using data supplied by VOSA (Vehicle and Operator Services Agency) for in-service emission tests (MOT) conducted between November 2006 and November 2007. Contains about 33 million cars.

APR collected real-world data on passenger car mileage by visiting 32,950 individual second-hand passenger car sales on the internet. The collection and analysis of the data took place in the period between June and September 2010. The final dataset consisted of 18,652 petrol cars registered in the period from 1994 to 2010 and 14,298 diesel cars, registered between 1996 and 2010.

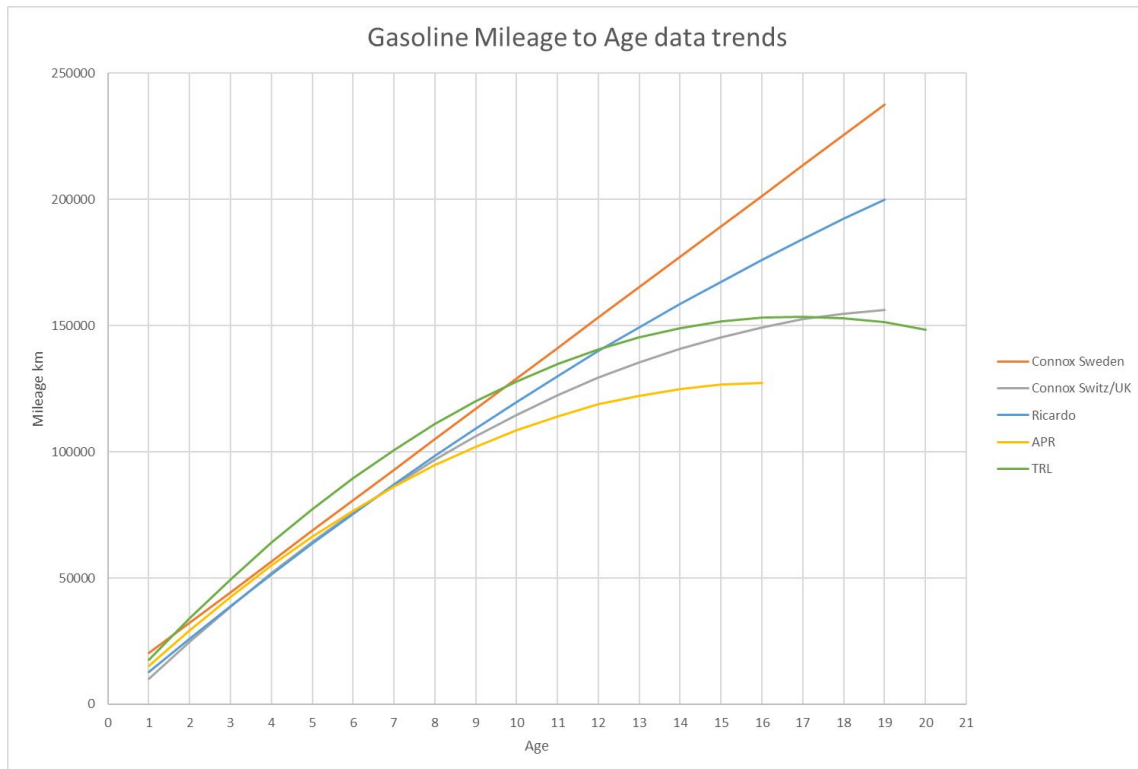


**Figure 12.24. Vehicle age-mileage correlation for petrol cars**

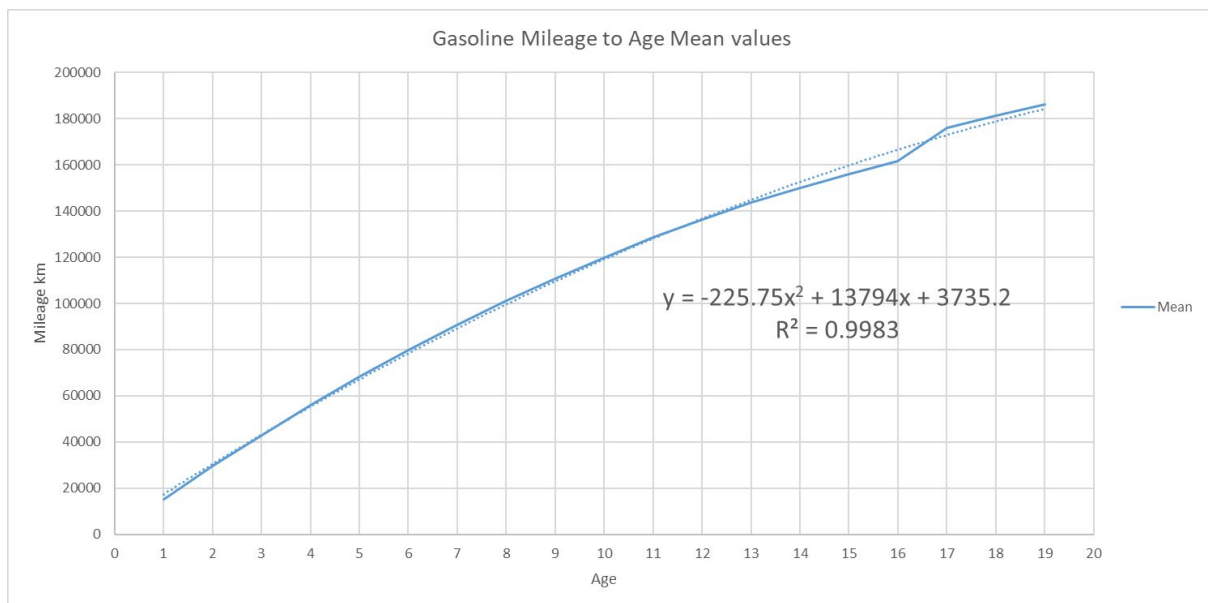


**Figure 12.25. Mean values of vehicle age-mileage correlation for petrol cars**

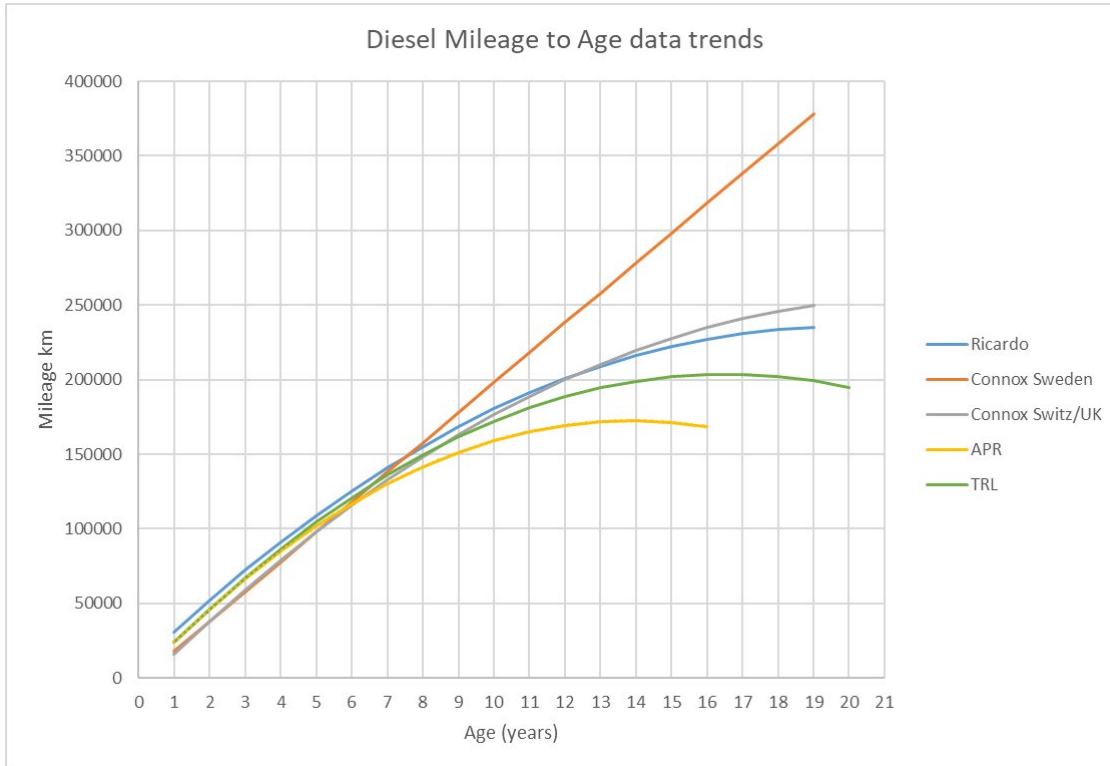


**Figure 12.26. Vehicle age-mileage correlation for diesel cars**

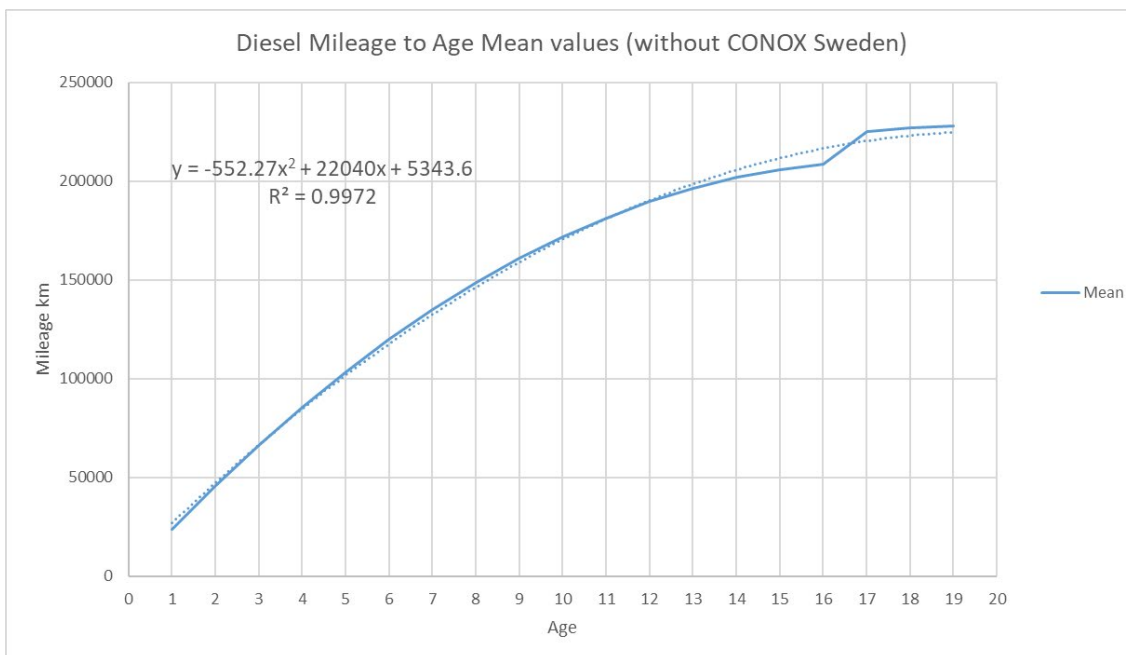


**Figure 12.27. Mean values of vehicle age-mileage correlation for diesel cars, without the CONOX Sweden database**

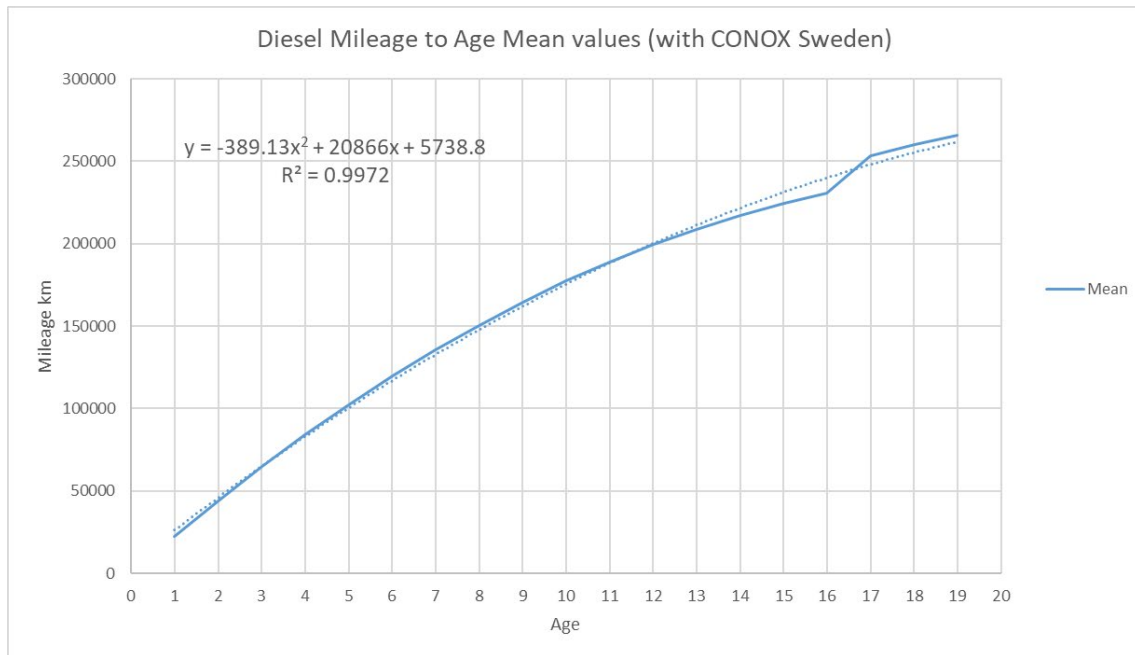


**Figure 12.28. Mean values of vehicle age-mileage correlation for diesel cars, with the CONOX Sweden database**

## 12.6 Alternative approach for the implementation of the deterioration factors

The implemented deterioration factors data contain information for 0, 50,000, 100,000, 200,000, 300,000 km only<sup>18</sup> and for that reason piecewise first-order functions can be created to extract the intermediate factors' value for any mileage value. The table below summarises the correlation functions for NO<sub>x</sub>, CO and HC deterioration factors, for petrol and diesel, while corresponding figures follow the table.

**Table 12.1. Equations for an alternative determination of deterioration factors.  $x$  is the mileage in 10<sup>3</sup> km, and  $y$  the deterioration factor.**

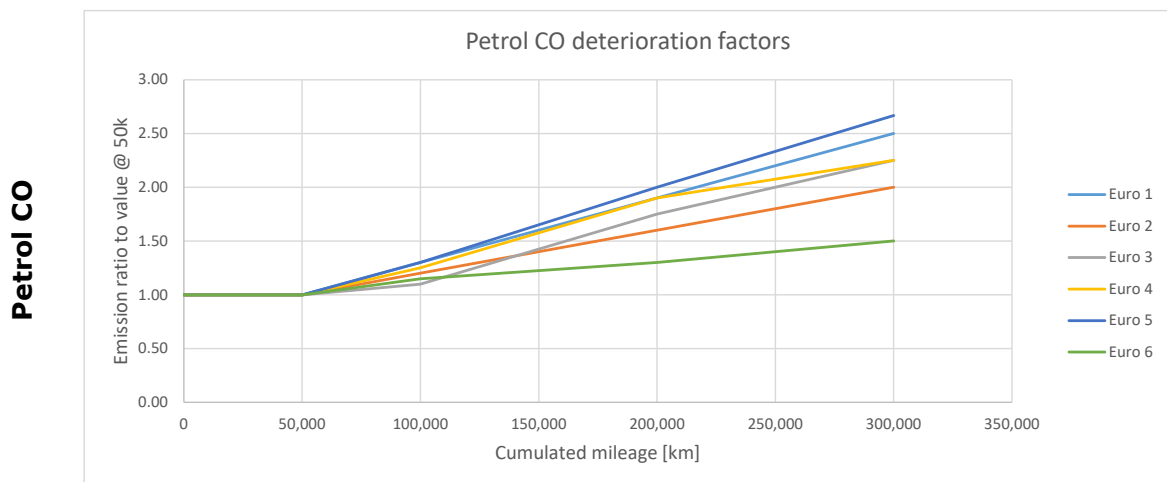
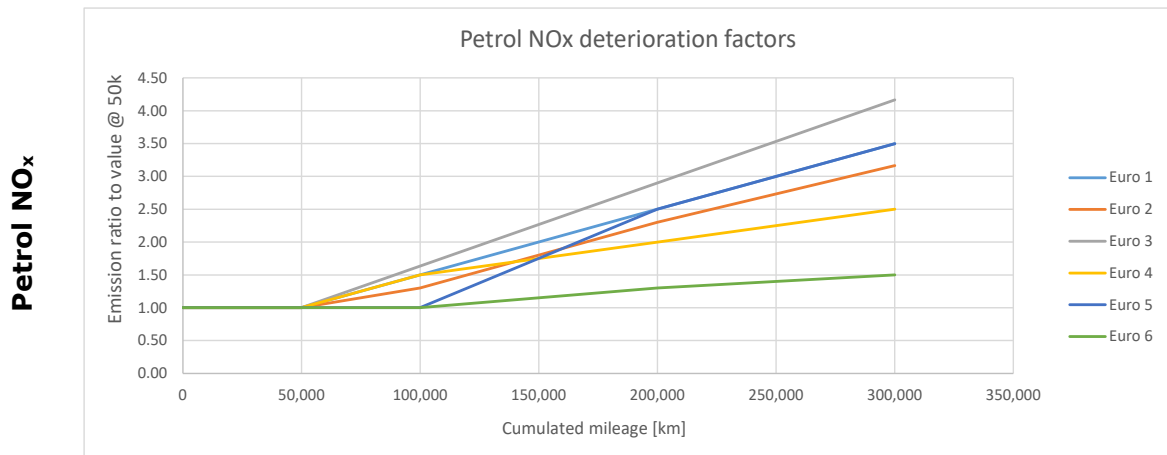
Fuel	Pollutant	Euro class	Equation
Petrol	NO <sub>x</sub>	Euro 1	$y = \begin{cases} 1, & x \leq 50 \\ (1 \times 10^{-5})x + 0.5, & x \geq 50 \end{cases}$
		Euro 2	$y = \begin{cases} 1, & x \leq 50 \\ (6 \times 10^{-6})x + 0.7, & 50 \leq x \leq 100 \\ (1 \times 10^{-5})x + 0.3, & 100 \leq x \leq 200 \\ (9 \times 10^{-6})x + 0.5667, & 200 \leq x \leq 300 \end{cases}$
		Euro 3	$y = \begin{cases} 1, & x \leq 50 \\ (1 \times 10^{-5})x + 0.3667, & 50 \leq x \end{cases}$
		Euro 4	$y = \begin{cases} 1, & x \leq 50 \\ (1 \times 10^{-5})x + 0.5, & 50 \leq x \leq 100 \\ (5 \times 10^{-6})x + 1, & 100 \leq x \leq 300 \end{cases}$
		Euro 5	$y = \begin{cases} 1, & x \leq 100 \\ (2 \times 10^{-5})x - 0.5, & 100 \leq x \leq 200 \\ (1 \times 10^{-5})x + 0.5, & 200 \leq x \leq 300 \end{cases}$
		Euro 6	$y = \begin{cases} 1, & x \leq 100 \\ (3 \times 10^{-6})x + 0.7, & 100 \leq x \leq 200 \\ (2 \times 10^{-6})x + 0.9, & 200 \leq x \leq 300 \end{cases}$
Petrol	CO	Euro 1	$y = \begin{cases} 1, & x \leq 50 \\ (6 \times 10^{-6})x + 0.7, & x \geq 50 \end{cases}$
		Euro 2	$y = \begin{cases} 1, & x \leq 50 \\ (4 \times 10^{-6})x + 0.8, & x \geq 50 \end{cases}$
		Euro 3	$y = \begin{cases} 1, & x \leq 50 \\ (2 \times 10^{-6})x + 0.9, & 50 \leq x \leq 100 \\ (7 \times 10^{-6})x + 0.45, & 100 \leq x \leq 200 \\ (5 \times 10^{-6})x + 0.75, & 200 \leq x \leq 300 \end{cases}$
		Euro 4	$y = \begin{cases} 1, & x \leq 50 \\ (5 \times 10^{-6})x + 0.75, & 50 \leq x \leq 100 \\ (7 \times 10^{-6})x + 0.6, & 100 \leq x \leq 200 \\ (3 \times 10^{-6})x + 1.2, & 200 \leq x \leq 300 \end{cases}$

<sup>18</sup> Petrol HC factors are the exception with reference points in 0, 50 000, 120 000, 160 000 and 200 000 km.

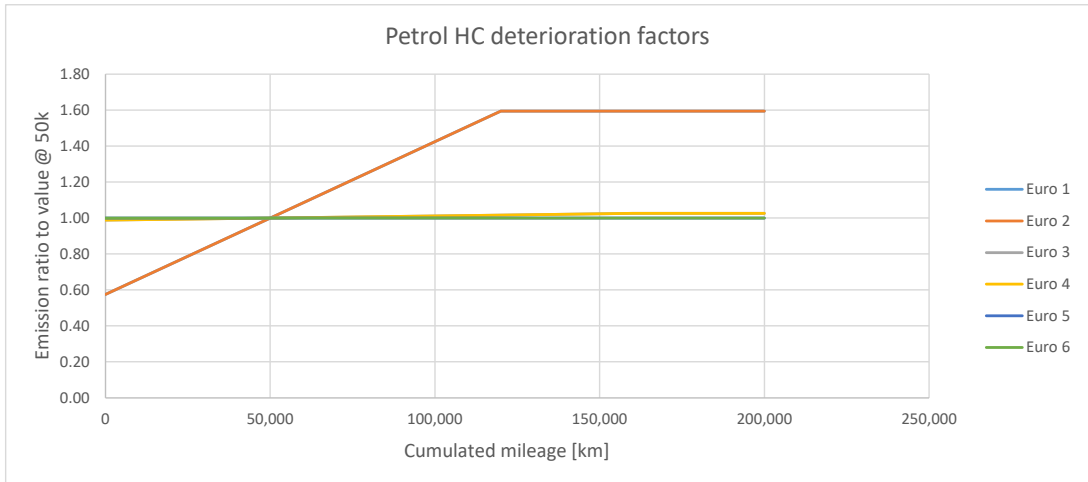
		Euro 5	$y = \begin{cases} 1, & x \leq 50 \\ (3 \times 10^{-6})x + 1.2, & 50 \leq x \leq 100 \\ (7 \times 10^{-6})x + 0.6, & 100 \leq x \leq 200 \\ (7 \times 10^{-6})x + 0.6667, & 200 \leq x \leq 300 \end{cases}$
		Euro 6	$y = \begin{cases} 1, & x \leq 50 \\ (3 \times 10^{-6})x + 0.85, & 50 \leq x \leq 100 \\ (2 \times 10^{-6})x + 1, & 100 \leq x \leq 200 \\ (2 \times 10^{-6})x + 0.9, & 200 \leq x \leq 300 \end{cases}$
<b>Petrol</b>	HC	Euro 1	$y = \begin{cases} (8 \times 10^{-6})x + 0.575, & x \leq 120 \\ 1.5944, & x \geq 120 \end{cases}$
		Euro 2	$y = \begin{cases} (8 \times 10^{-6})x + 0.575, & x \leq 120 \\ 1.5944, & x \geq 120 \end{cases}$
		Euro 3	$y = \begin{cases} (2 \times 10^{-7})x + 0.9883, & x \leq 160 \\ 1.025587, & x \geq 160 \end{cases}$
		Euro 4	$y = \begin{cases} (2 \times 10^{-7})x + 0.9883, & x \leq 160 \\ 1.025587, & x \geq 160 \end{cases}$
		Euro 5 & 6	$y = 1$
<b>Diesel</b>	NO <sub>x</sub>	Euro 1	$y = 1$
		Euro 2	$y = \begin{cases} 1, & x \leq 100 \\ (3 \times 10^{-6})x + 0.75, & 100 \leq x \leq 200 \\ 1.25, & 200 \leq x \leq 300 \end{cases}$
		Euro 3	$y = \begin{cases} 1, & x \leq 50 \\ (1 \times 10^{-6})x + 0.95, & 50 \leq x \leq 100 \\ (2 \times 10^{-6})x + 0.9, & 100 \leq x \leq 200 \\ (1 \times 10^{-6})x + 0.9333, & 200 \leq x \leq 300 \end{cases}$
		Euro 4	$y = \begin{cases} 1, & x \leq 50 \\ (6 \times 10^{-7})x + 0.97, & 50 \leq x \leq 100 \\ (3 \times 10^{-7})x + 1, & 100 \leq x \leq 200 \\ (7 \times 10^{-7})x + 0.92, & 200 \leq x \leq 300 \end{cases}$
		Euro 5	$y = \begin{cases} 1, & x \leq 100 \\ (3 \times 10^{-7})x + 0.97, & 100 \leq x \leq 200 \\ (4 \times 10^{-7})x + 0.95, & 200 \leq x \leq 300 \end{cases}$
		Euro 6	$y = \begin{cases} 1, & x \leq 50 \\ (1 \times 10^{-6})x + 0.95, & x \geq 50 \end{cases}$
<b>Diesel</b>	CO	Euro 1 - 3	$y = 1$
		Euro 4 & 5	$y = \begin{cases} 1, & x \leq 100 \\ (3 \times 10^{-6})x + 0.7, & 100 \leq x \leq 200 \\ 1.25, & 200 \leq x \leq 300 \end{cases}$

		Euro 6	$y = \begin{cases} 1, & x \leq 50 \\ (3 \times 10^{-6})x + 0.85, & 50 \leq x \leq 100 \\ (3 \times 10^{-6})x + 0.9, & 100 \leq x \leq 200 \\ (3 \times 10^{-6})x + 0.8667, & 200 \leq x \leq 300 \end{cases}$
<b>Diesel</b>	HC	Euro 1 - 6	$y = 1$

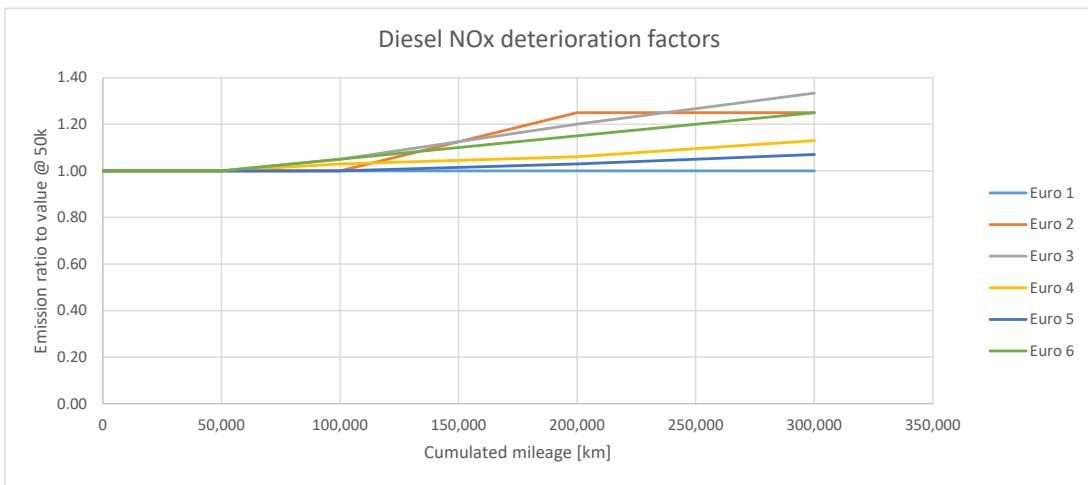
**Table 12.2. Pictorial representations of the equations suggested for an alternative determination of deterioration factors**



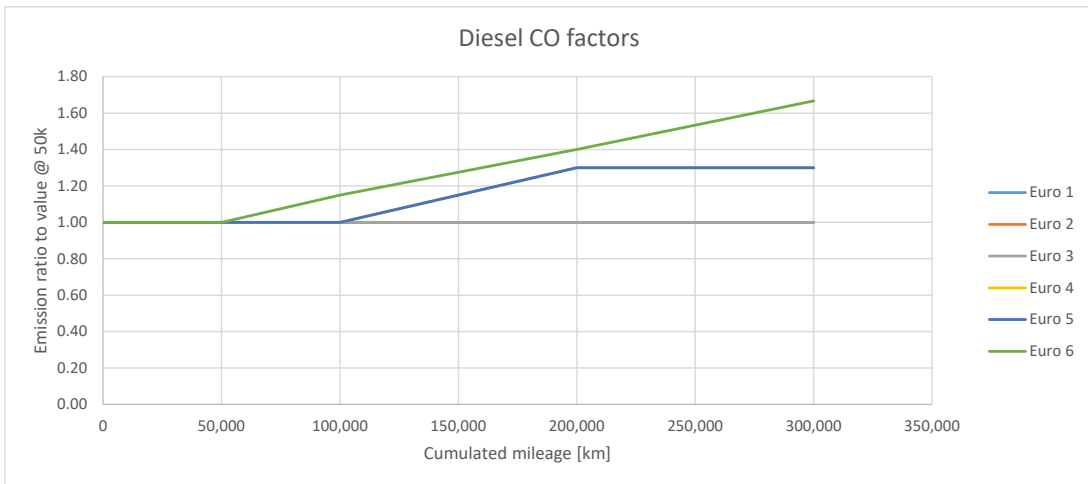
**Petrol HC**



**Diesel NO<sub>x</sub>**



**Diesel CO**



## 13 Background and project introduction

### 13.1 Background uCARE

With four million people dying annually due to outdoor pollution, improvement of air quality has become one of society's main challenges. In Europe, traffic and transport have a large effect on air quality, specifically passenger cars and commercial vehicles, and to a lesser extent non-road mobile machinery. While technical improvements and more stringent legislation have had a significant impact, traffic and transport emissions are still too high and air quality is still poor. Although the use of electric and other zero-emission propulsion technologies may drastically reduce the pollutant exhaust emissions from traffic, the slow introduction of such vehicles as well as the trend of increasing vehicle lifetimes means that vehicles with internal combustion engines are expected to dominate the fleet beyond 2030. This project is the first opportunity to improve emissions of vehicles, not by improving vehicle technology, but by actively involving vehicle users and enabling their contribution to clean driving.

So far, expertise on pollutant emissions has mainly been used to advise European policy makers on limited effectiveness of emission legislation (through real-world emission factors such as VERSIT, HBEFA and COPERT) and how to reduce traffic and transport pollutant emissions. The numerous mitigation methods are rarely extended to include the perspectives of users, thus uCARE enables a next essential step: providing user targeted emission reduction measures. These measures will be implemented and evaluated in real-life pilot projects.

The aim of uCARE is *to reduce the overall pollutant emissions of the existing combustion engine vehicle fleet by providing vehicle users with simple and effective tools to decrease their individual emissions and to support stakeholders with an interest in local air quality in selecting feasible intervention strategies that lead to the desired user behaviour*. The overall aim is accompanied by the following objectives:

1. To identify **user-influenced vehicle emission aspects** (such as driving behaviour and vehicle component choice).
2. To determine the **emission reduction potential** of each vehicle emission aspect with help of the uCARE model developed within a toolbox.
3. To develop a **toolbox**, containing models and emission reduction measures, that enables stakeholders to identify the most appropriate intervention strategies that reflect the specific users and their motivation.
4. **Support policy makers** and other **stakeholders with an interest in air quality**, such as municipalities and branch organizations, **in identifying intervention strategies** that translate the measures into desired behaviour of the user.
5. **To test and evaluate** intervention strategies in a set of pilot projects conducted with various target user groups in at least four European countries. The pilot projects illustrate effectiveness and feasibility of the toolbox and intervention strategies developed on its basis.
6. Perform an **impact assessment** of the intervention strategies effectiveness, in terms of cost, penetration, achieved emission reduction and lasting effects.
7. **Actively feed** European cities and international parties with uCARE learning and results, via awareness raising campaigns, communication tools, interactive web application and other dissemination activities. Open access to the broad public to the toolbox, data and developed tools.
8. Summarise the findings **in blueprints for rolling out** different user-oriented emission reduction programmes, based on successful pilots.

This document is part of WP1 and describes the Augmented Emission Maps, which are part of the collection of standardized data in the uCARE toolbox.

## 13.2 Purpose of the document

For a range of car models and makes uCARE will produce and publish emission maps, using the clustering of the uCARE Taxonomy as described in deliverable D1.1. The objective of this document is to provide the metadata to correctly interpret and use the emission maps.

## 13.3 Document Structure

The document is structured as follows.

### *Part 1*

Chapter 1 describes the context of why Augmented Emission Maps (AEM) are necessary. It also outlines possible use cases, for scientific purposes as well as for tool builders.

Chapter 2 describes and explains the AEM concept. An AEM can be made for each node in the uCARE Taxonomy<sup>19</sup> (D1.1) and it is explained how the AEMs and the taxonomy are linked. The file name conventions for AEMs are also defined in Section 2.3.1.

Chapter 3 outlines the three current AEM layers (base maps, the cold start augmentation and the deterioration augmentation) using a similar structure. First a brief introduction is given of how a tool builder may interpret the data supplied, followed by an outline of how to use the AEM layer, and concluded with several examples.

Chapter 4 shows a number of examples of how AEMs can give researchers or policy makers added insight into the relationship between driver behaviour and emissions.

Chapter 5 gives instructions on how organisations can contribute to the future of AEMs by generating their own AEMs and uploading them into the uCARE community.

Chapter 6 draws conclusions regarding the status of the AEMs as a standard for emission data exchange. Such standards are never static and may be refined and expanded.

### *Part 2*

Part 2 contains reference information that may be consulted when needed. This includes the experiments performed investigating non-tailpipe emissions, a discussion on the accuracy of the different layers, manuals for the different tools, and a formal explanation of the AEM data exchange format.

## 13.4 Deviations from original Description of Work (DoW)

### 13.4.1 Description of work related to deliverable as given in DoW

"This document provides a description of the functionality of augmented emission maps and a reference to the open-source website containing the augmented emission maps information for the relevant vehicle groups and technologies in the taxonomy."

### 13.4.2 Time deviations from original DoW

The document was planned to be delivered end of January 2020. The submission of version 1.0 was slightly delayed after agreement with the Project Officer to allow for production of a first batch of AEMs in parallel to this document.

The timing of subsequent versions, based on progressing insights in the project, was not included in the project plan.

---

<sup>19</sup> The vehicle taxonomy is a controlled vocabulary and vehicle classification system for all passenger cars on the road

### **13.4.3 Content deviations from original DoW**

None

This version [version 3.0] includes the following additions:

- recommendations and experiments on non-tailpipe emissions
- concrete examples of how AEMs can give extra insight into the relationship between driver behaviour and emissions
- a guide to how organisations can contribute by sharing their measurement data in the Zenodo uCARE community
- an extended discussion on uncertainties
- manuals for the supplied tools

## References

- [1] Gustafsson, M., Blomqvist, G., Gudmundsson, A., Dahl, A., Jonsson, P. and Swietlicki, E. (2009). Factors influencing PM10 emissions from road pavement wear. *Atmospheric Environment*. 43, 4699-4702,.  
<https://doi.org/10.1016/j.atmosenv.2008.04.028>.
- [2] Kupiainen, K.J. and Pirjola, L. (2011). Vehicle non-exhaust emissions from the tyre-road interface – effect of stud properties, traction sanding and resuspension. *Atmospheric Environment*. 45, 25, 4141-4146.  
<https://doi.org/10.1016/j.atmosenv.2011.05.027>.
- [3] Bridgestone: <https://www.bridgestonetire.com/tread-and-trend/drivers-ed/driving-winter-tire-year-round#>. Accessed: 2021-03-31.
- [4] Continental: <https://www.continental-tire.com/car/tire-knowledge/tire-change-fitting/changing-tire/winter-tire-in-summer>. Accessed: 2021-03-31.
- [5] Weilenmann, M., Soltic, P. and Hausberger, S. (2013). The cold start emissions of light-duty-vehicle fleets: A simplified physics-based model for the estimation of CO2 and pollutants. *Science of the Total Environment*. 444, 161-176,.
- [6] *The CONOX report UK and Switzerland/Sweden database*.
- [7] RICARDO – AEA *Improvements to the definition of lifetime mileage of light duty vehicles*. Report: Ricardo-AEA reference: ED59296-Issue Number 1.
- [8] TRL *Emission factors 2009: Report 6 – deterioration factors and other modelling assumptions for road vehicles*. Report: Published project report PPR359.
- [9] S. Caserini, C. Pastorello, P. Gaifami, and L. Ntziachristos (2013). Impact of the dropping activity with vehicle age on air pollutant emissions. *Atmospheric Pollution Research*. 4, 282-289,.
- [10] Heijne, V.A.M., Ligterink, N.E. and Cuelenaere, R.F.A. (2016). *Nederlandse wagenparksamenstelling 2016*. Report: TNO 2016 R11872. TNO.  
<https://repository.tudelft.nl/view/tno/uuid:5d4339e7-b2e5-470f-a18b-40e79f58ed25>.
- [11] Spreen, J.S., Kadijk, G., Vermeulen, R.J., et al. (2016). *Assessment of road vehicle emissions: methodology of the Dutch in-service testing programmes*. Report: TNO 2016 R11178v2. TNO.
- [12] Bernard, Y., Tietge, U., German, J. and Muncrief, R. (2018). *Determination of real-world emissions from passenger vehicles using remote sensing data*.  
[https://www.theicct.org/sites/default/files/publications/TRUE\\_Remote\\_sensing\\_data\\_20180604.pdf](https://www.theicct.org/sites/default/files/publications/TRUE_Remote_sensing_data_20180604.pdf).
- [13] Michal Vojtišek-Lom, Miroslav Vaculík, Martin Pechout, et al. (2021). Effects of Braking Conditions on Nanoparticle Emissions from Passenger Car Friction Brakes. *Science of the Total Environment*. Accepted.
- [14] Grigoratos, T. and Martini, G. (2015). Brake wear particle emissions: a review. *Environmental Science and Pollution Research*. 22, 4, 2491-2504.
- [15] Hinds, W.C. (1999). *Aerosol Technology: Properties, Behavior, and Measurement of Airborne Particles*. John Wiley & Sons.

- [16] Kukutschová, J., Moravec, P., Tomášek, V., et al. (2011). On airborne nano/micro-sized wear particles released from low-metallic automotive brakes. *Environmental Pollution*. 159, 4, 998–1006.
- [17] Zum Hagen, F.H.F., Mathissen, M., Grabiec, T., et al. (2019). Study of Brake Wear Particle Emissions: Impact of Braking and Cruising Conditions. *Environmental Science & Technology*. 53, 9, 5143–5150. <https://doi.org/10.1021/acs.est.8b07142>.
- [18] Mathissen, M., Grochowicz, J., Schmidt, C., et al. (2018). A novel real-world braking cycle for studying brake wear particle emissions. *Wear*. 414–415, 219–226. <https://doi.org/10.1016/j.wear.2018.07.020>.
- [19] Baensch-Baltruschat, B., Kocher, B., Stock, F. and Reifferscheid, G. (2020). Tyre and road wear particles (TRWP) - A review of generation, properties, emissions, human health risk, ecotoxicity, and fate in the environment. *Science of The Total Environment*. 733, 137823,. <https://doi.org/10.1016/j.scitotenv.2020.137823>.
- [20] Andersson-Sköld, Y., Johannesson, M., Gustafsson, M., et al. (2020). *Microplastics from tyre and road wear: a literature review*. Report: 03476030 (ISSN). Statens väg- och transportforskningsinstitut. <http://urn.kb.se/resolve?urn=urn:nbn:se:vti:diva-15243>.
- [21] Verschoor, A., Poorter, L., Dröge, R., Kuenen, J. and Valk, E. (2016). *Emission of microplastics and potential mitigation measures*. National Institute for Public Health. <https://ia802807.us.archive.org/4/items/blg-777944/blg-777944.pdf>.
- [22] Kole, P.J., Löhr, A.J., Van Belleghem, F.G.A.J. and Ragas, A.M.J. (2017). Wear and tear of tyres: A stealthy source of microplastics in the environment. *Int. J. Environ. Res. Public Health*. 14. <https://doi.org/10.3390/ijerph14101265>.
- [23] Pohrt, R. (2019). wear particle hot spots – Review of influencing factors. *Facta Univ. Ser. Mech. Eng.* 17, 17-27,. <https://doi.org/10.22190/FUME190104013P>.
- [24] Lowne, R.W. (1970). The effect of road surface texture on tyre wear. *Wear*. 15, 57-70,. [https://doi.org/10.1016/0043-1648\(70\)90186-9](https://doi.org/10.1016/0043-1648(70)90186-9).
- [25] Steyn, W.J. and Haw, M. (2005). Effect of road surfacing condition on tyre life. *SATC 2005: The 24th Annual Southern African Transport Conference and Exhibition, Pretoria, South Africa (2005)*, 1–10.
- [26] Wu, Y.P., Zhou, Y., Li, J.L., Zhou, H.D., Chen, J.M. and Zhao, H.C. (2016). A comparative study on wear behavior and mechanism of styrene butadiene rubber under dry and wet conditions. *Wear*. 356–357, 1-8,. <https://doi.org/10.1016/j.wear.2016.01.025>.
- [27] Blok, J. (2005). Environmental exposure of road borders to zinc. *Science of the Total Environment*. 348, 173-190,.
- [28] Klein, J., Hulskotte, J., Ligterink, N., Dellaert, S., Molnár, H. and Geilenkirchen, G. (2017). *Methods for calculating the emissions of transport in the Netherlands, Task Force on Transportation of the Dutch Pollutant Release and Transfer Register*.
- [29] Amato, F. (2018). *Non-Exhaust Emissions. An Urban Air Quality Problem for Public Health. Impact and Mitigation Measures*. Academic Press.

- [30] Grigoratos, T. and Martini, G. (2014). *Non-exhaust traffic related emissions - Brake and tyre wear PM: literature review*. European Commission. Joint Research Centre. Institute for Energy and Transport.
- [31] Gipser, M. (2007). - The tire simulation model for all applications related to vehicle dynamics. *Vehicle System Dynamics*. 45, 139-151,.
- [32] Farroni, F. (2016). T.R.I.C.K.-/Road Interaction Characterization & Knowledge - A tool for the evaluation of tire and vehicle performances in outdoor test sessions. *Mechanical Systems and Signal Processing*. 72-73, 808-831,.  
<https://doi.org/10.1016/j.ymssp.2015.11.019>.
- [33] Wang, C., Huang, H., Chen, X. and Liu, J. (2017). The influence of the contact features on the tyre wear in steady-state conditions. *Proc. Inst. Mech. Eng. Part D J. Automob. Eng.* 231, 1326-1339,.
- [34] Li, Y., Zuo, S., Lei, L., Yang, X. and Wu, X. (2011). Analysis of impact factors of tire wear. *Journal of Vibration and Control*. 18, 833-840.
- [35] Kwak, J.H., Kim, H., Lee, J. and Lee, S. (2013). Characterization of non-exhaust coarse and fine particles from on-road driving and laboratory measurements. *Science of the Total Environment*. 458-460, 273-282,.
- [36] Tonegawa, Y. and Sasaki, S. (2021). Development of -Wear Particle Emission Measurements for Passenger Vehicles. *Emission Control Science and Technology*. 7, 1, 56-62. <https://doi.org/10.1007/s40825-020-00181-z>.
- [37] Simons, A. (2016). Road transport: new life cycle inventories for fossil-fuelled passenger cars and non-exhaust emissions in ecoinvent v3. *Int. J. Life Cycle Assess.* 21, 1299-1313,.
- [38] Ntziachristos, L. and Boulter, P. (2019). *EMEP EEA air pollutant emission inventory guidebook, 1.A.3.b.vi Road transport: Automotive tyre and brake wear, 1A.3.b.vii Road transport: Automobile road abrasion*.
- [39] Luhana, L., Sokhi, R., Warner, L., et al. (2004). *Measurement of non-exhaust particulate matter. Deliverable 8 from EU project PARTICULATES - Characterisation of Exhaust Particulate Emissions from Road Vehicles*. Report: Deliverable 8 from EU project PARTICULATES-Characterisation of Exhaust Particulate Emissions from Road Vehicles, European Commission 5th Framework Programme.
- [40] Gustafsson, M. and Svensson, N. (2020). Influence of speed, inflation pressure and load on PM emissions from tyres - Tests in VTI road simulator. VTI Memo.
- [41] Grigoratos, T., Gustafsson, M., Eriksson, O. and Martini, G. (2018). Experimental investigation of tread wear and particle emission from tyres with different treadwear marking. *Atmospheric Environment*. 182, 200-212,.
- [42] Salminen, H. (2014). *Parametrizing tyre wear using a brush tyre model*. Kungliga Tekniska Högskola.
- [43] O.E.C.D. (2020). *Non-exhaust Particulate Emissions from Road Transport: An Ignored Environmental Policy Challenge*. OECD Publishing.  
<https://doi.org/10.1787/4a4dc6ca-en>.
- [44] Argonne National Laboratory (2019). *GREET vehicle-cycle model Series 2*.

- [45] Notter, B., Keller, M., Althaus, H.-J., et al. (2019). *HBEFA 4.1 Development Report*. INFRAS. [https://www.hbefa.net/e/documents/HBEFA41\\_Development\\_Report.pdf](https://www.hbefa.net/e/documents/HBEFA41_Development_Report.pdf).
- [46] Hulskotte, J.H.J., Roskam, G.D. and Denier van der Gon, H.A.C. (2014). Elemental composition of current automotive braking materials and derived air emission factors. *Atmospheric Environment*. 99, 436–445. <https://doi.org/10.1016/j.atmosenv.2014.10.007>.
- [47] Gerben Geilenkirchen, Katie Roth, Michel Sijstermans, et al. (2020). *Methods for calculating the emissions of transport in The Netherlands*. Report: PBL Report 4139. PBL Netherlands Environmental Assessment Agency.
- [48] Niels Hooftman (2019). *uCARE Deliverable D1.3 Tampering*. uCARE. <https://www.project-ucare.eu/wp-content/uploads/2020/01/D1.3-Tampering-.pdf>.
- [49] Nooij, S. (2021). *Emission map selection tool and driver classification*. Master's Thesis. Eindhoven University of Technology.
- [50] Catalyst Fundamentals: (2000). [https://dieselnet.com/tech/cat\\_fund.php](https://dieselnet.com/tech/cat_fund.php). Accessed: 2021-05-18.

## Definitions & Abbreviations

AEM	.....	Augmented Emission Map
ASCII	.....	American Standard Code for Information Interchange
CADC	.....	Common Artemis Driving Cycle
CAN	.....	Controller Area Network
cm <sup>3</sup>	.....	Cubic centimetre
CO	.....	Carbon monoxide
CO <sub>2</sub>	.....	Carbon dioxide
COPERT	.....	COmputer Program to calculate Emissions from Road Transport
DGR	.....	Directorate-General Research
DOI	.....	Digital Object Identifier
DoW	.....	Description of Work
EC	.....	European Commission
ECU	.....	Engine control unit
e.g.	.....	Example given
EGR	.....	Exhaust Gas Recirculation
ERMES	.....	European Research Group on Mobile Emission Sources
etc.	.....	Et cetera
FTIR	.....	Fourier-transform Infrared Spectroscopy
HBEFA	.....	Handbook Emission Factors for Road Transport
HC	.....	Hydrocarbon
ICE	.....	Internal Combustion Engine
i.e.	.....	Id est
ISO	.....	International Organization for Standardization.
IUFC	.....	Inrets urbain fluide court (a driving cycle to measure cold start emissions)
LNG	.....	Liquified natural gas
LPG	.....	Liquified petroleum gas
NEDC	.....	New European Driving Cycle
NH <sub>3</sub>	.....	Ammonia

---

NO	.....	Nitrogen monoxide
NO <sub>2</sub>	.....	Nitrogen dioxide
NO <sub>x</sub>	.....	Nitrogen oxide
OBD	.....	Onboard Diagnostics
PAH	.....	Polycyclic aromatic hydrocarbons
PEMS	.....	Portable Emissions Measurement System
PHEM	.....	Passenger Car and Heavy Duty Emission Model
PM	.....	Particle Mass
PN	.....	Particle Number
RDE	.....	Real Driving Emissions
RFC	.....	Request for Comments
RMSE	.....	Root-mean-square error
RPM	.....	Revolutions per minute
SCR	.....	Selective Catalytic Reduction
SEMS	.....	Simplified emission measurement system
VERSIT	.....	Dutch Vehicle Emission Model
WLTP	.....	Worldwide Light Duty Test Procedure
WP	.....	Work Package

